# The Role of Autophagy in Anti-*Wolbachia* Antibiotic Therapy

Thesis submitted in accordance with the requirements of the Liverpool School of Tropical Medicine

for the degree of Doctor in Philosophy

by

Anfal Yousef

May 2019

# Declaration

I certify that this thesis is an original work and no part or portion has been previously submitted in support of an application or degree in Liverpool School of Tropical Medicine or any other University or institute of learning.

# Contents

# List of Figures

# List of Tables

# List of Abbreviations

| | | | |
|---|---|---|---|
| ADLA | Acute dermatolymphangioadenitis | Eis | Enhanced intracellular survival |
| AFL | Acute filarial lymphangitis | ER | Endoplasmic reticulum |
| Akt/PKB | Protein kinase B | FITC | Fluorescein isothiocyanate |
| AL | Lysis buffer | FIP200 | Focal adhesion kinase family interacting protein of 200 kD |
| Ambra1 | Activating molecule in Beclin 1-regulated autophagy protein 1 | FKBP12 | FK506-binding protein 12 kDa |
| AMP | Adenosine monophosphate | g | Gravitational force |
| AMPK | AMP-activated protein kinase | GABARAP | γ-aminobutyric type A ($GABA_A$)-receptor associated protein |
| ANOVA | One-way analysis of variance | GPELF | Global Programme to Eliminate Lymphatic Filariasis |
| Atg | Autophagy-related proteins | *gst* | Glutathione S-transferase |
| ATL | Tissue lysis buffer | IDA | Ivermectin, diethylcarbamazine (DEC) and albendazole |
| A-WOL | Anti-*Wolbachia* consortium | IF | Immunofluorescence |
| Bif-1 | Endophilin B1 | JNK | JUN N-terminal kinase |
| Bm | *Brugia malayi* | LC3 | Microtubule associated protein 1 light chain 3 |
| BP1 | Phox/Bem 1p | LECs | human lymphatic endothelial cells |
| BSA | Bovine serum albumin | LF | Lymphatic filariasis |
| Ct | Cycle threshold | LIR | LC3 interacting region |
| C6/36*Wp* | *Wolbachia*-infected mosquito cell line | LPS | Lipopolysaccharides |
| DAPI | 4',6-diamidino-2-phenylindole | LSTM | Liverpool School of Tropical Medicine |
| DEC | Diethylcarbamazine | Ly294002 | 2-(4-morpholinyl)-8-phenylchromo |
| DMSO | Dimethyl sulfoxide | L-15 | Leibovitz 15 |
| EC50 | 50% effective concentration | MDA | Mass drug administration |
| ECACC | European Collection of Authenticated Cell Cultures | MDCK | Madin-Darby Canine Kidney cell line |
| EHNA | Erythro-9-[3-2-hydroxynonyl] adenine | Mf | Microfilariae |

| | | | |
|---|---|---|---|
| mTOR/TOR | Mechanistic target of rapamycin | RPM | Revolutions per minutes |
| mTORC1/TORC1 | Mechanistic target of rapamycin complex 1 | Rubicon | RUN domain protein as Beclin 1 interactingand cysteine-rich containing |
| mTORC2/TORC2 | Mechanistic target of rapamycin complex 2 | SD | Standard deviation |
| NADPH | Nicotinamide adenine dinucleotide phosphate oxidase | SDS-PAGE | Sodium dodecyl sulphate-polyacrylamide gel electrophoresis |
| NBR1 | Neighbour of Brca1 gene | SF9 | *Spodoptera frugiperda 9 cell line* |
| NDP52 | Nuclear dot protein 52 | SLRs | Sequestosome-1 like receptors |
| NOX2 | NADPH oxidase complex 2 | SNARE | N-ethylmaleimide-sensitive factor attachment protein receptor |
| OPTN | Optineurin | Spp. | Species |
| PAS | Pre-autophagosome structure | SQSTM 1 | Sequestosome 1 |
| PBS | Phosphate-buffered saline | TBS-T | Tris buffered saline – containing 0.1% Tween 20 |
| PBS-T | Phosphate-buffered saline with Triton x100 | TRITC | Tetramethylrhodamine |
| PE | Phosphatidylethanolamine | ULK1 | Unc-51-like kinase 1 |
| PI | Phosphatidylinositol | UK | United Kingdom |
| PI3k | Phosphotidylinositol 3-kinases | UVRAG | UV irradiation resistance-associated gene |
| PI3P | phosphatidylinositol triphosphate | Vps | Vacuolar protein sorting |
| $PI(3,4,5)P_3$ | PI 4,5-biphosphate to phosphatidylinositol 3,4,5-triphosphate | wAlbB | Wolbachia from Aedes albopictus |
| PK/PD | Pharmacokinetic-pharmacodynamic | WIPI | WD repeat domain phosphoinositide-interacting |
| qPCR | Quantitative polymerase chain reaction | WHO | World health organisation |
| Raptor | Regulatory associated protein of mTOR | *wsp* | *Wolbachia* surface proteins |
| RNA | Ribonucleic acid | 3-ma | 3-methyleadenine |
| ROS | Reactive oxygen species | | |

# Acknowledgements

First and foremost, I would like to thank my supervisor Professor Mark Taylor and secondary supervisor Dr Joseph Turner, for their boundless support, wisdom, encouragement and guidance throughout my study period. I am both grateful and lucky that I had this opportunity to learn from their experience and expertise in the field of parasitology.

This research could not have been possible without the help and support from all the members of the A-WOL team at the Liverpool School of Tropical Medicine. In particular, I would like to extend my gratitude and thanks to Dr Rachel Clare and Dr Kelly Johnston for all the help they have provided me in the course of my studies, both in my experimental work and learning process. Special thanks go to Andrew Steven, Amy Marriott, Shannon Quek, John Archer, Julio Furlong-Silva, Amber Fanthome, Dr Ghaith Aljayyoussi, Dr Shaun Pennington, Dr Nicolas Pionnier, Dr Armelle Forrer, Dr Yang Wu and Dr David Hong for their support and help in this research project.

My gratitude also goes to the progress assessment panel (PAP) members Professor Giancarlo Biagini, Professor Paul O'Neill and Dr Edwards Geoffrey, for their wise counsel and support, especially in a difficult period during my studies where their guidance was of tremendous help and value. Also, I would like to thank the excellent postgraduate team at LSTM, in particular Professor Martin Donnelly and Richard Madden.

In Kuwait I would like to thank Kuwait University for funding my project, as well as their supportive staff for believing in me: Professor Ali Dashti, Professor Suad Alfadhli, Professor Saud Alobaidi, Dr Khalifa Behbehani, Prof Adel Ayed, Mr Fahad Albader and my dear aunt Dr Sheikha Alzarban.

Last but not least, I could not have completed this project without the support and encouragement of my family and friends. I am blessed to have my parents who supported me with endless love and encouraged me throughout my life. To my sister, two brothers and my niece a sincere thanks for always being there for me. To my love, Fayez which I am forever grateful to have beside me, without his support I could not achieve this. We have been through a lot together during the period of my studies and this made us more determined and stronger than ever.

**Dedication:** To Taibah, who has sadly left us but will always be in our hearts and thoughts.

# Abstract

Lymphatic filariasis (LF) and onchocerciasis are significant global public health issues with more than 900 million individuals at risk and over 60 million people currently living with symptomatic manifestations caused by filarial diseases. Current drug treatments (albendazole, diethylcarbamazine citrate, ivermectin), which form the mass drug administration (MDA) of the World Health Organisation (WHO), only have a microfilaricidal properties and have a partial or ineffective efficacy against adult worms. The WHO has recognised that its target of achieving LF elimination by 2020 is not currently attainable through current MDA and has highlighted the importance of finding alternative drug regiments. Due to the importance of *Wolbachia,* an essential mutualistic intracellular bacterium, in the survival of filarial nematodes, anti-*Wolbachia* therapy has been validated as a safe macrofilaricidal treatment for LF and onchocerciasis. The A-WOL consortium was established with the goals of refining existing (repurposed) anti-*Wolbachia* antibiotics, as well as developing new drugs in a course of 7 days or less. Autophagy was chosen as a potential target in anti-*Wolbachia* drug efficacy due to previous research highlighting its role in the regulation of *Wolbachia* populations. In this study, we investigated the role of autophagy in the mode-of-action and efficacy of the portfolio of anti-*Wolbachia* drugs. This research has identified a range of concentrations for two autophagy inhibitors, wortmannin and l-asparagine, that suppressed autophagy and did not negatively impact cell growth, viability and toxicity in mosquito C6/36 cells and nematodes. By testing autophagic activity, this work has demonstrated a consistent increase in autophagy in four broad-spectrum anti-*Wolbachia* antibiotics from different classes (doxycycline, rifampicin, moxifloxacin and sparfloxacin) exposed to two different insect cell lines (C6/36 and SF9 cells) and in *B. malayi* microfilariae (mf). This activation was also observed for selected-candidates from the A-WOL consortium (TylAMac$^{TM}$, AWZ1066S and fusidic acid). Antibiotic-induced autophagy was observed in the absence of *Wolbachia*, indicating its effect independent of the bacteria. In this work, the activation of autophagy was not observed in mammalian cells indicating that autophagy activation by anti-*Wolbachia* drugs is restricted to insect cells and nematodes. Through concentration-dependency testing of anti-*Wolbachia* antibiotics, this study has demonstrated that only concentrations that induced autophagy resulted in effective *Wolbachia* depletion (of >90%), the empirical threshold of delivering the desired macrofilaricidal activity. In this work, the contribution of autophagy in the efficacy of anti-*Wolbachia* drugs and their ability to reduce bacterial viability was demonstrated in *B. malayi* mf and adult worms when autophagy was inhibited during anti-*Wolbachia* drug exposure. Moreover, a partial role for autophagy was observed in the continued decline in *Wolbachia* post-drug exposure. The findings of this research could be used in developing high-throughput screening of additional drug libraries and in the lead optimisation of existing 'hits' identified by the A-WOL consortium. Autophagy can become an important target for anti-*Wolbachia* drug research and provide future solutions in drug therapy. The outcomes of the study may help future work in improving the understanding of selective autophagy and the development of treatments against filarial diseases and other infectious diseases.

# Chapter 1 Introduction

## 1.1 Human filarial diseases: Epidemiology and causative agents

### 1.1.1 Lymphatic filariasis (overview)

Lymphatic filariasis (LF) is caused by parasitic filarial nematodes *Wuchereria bancrofti, Brugia malayi*, and *Brugia timori* (1). All three nematodes belong to the family of Onchocercidae and under the subfamily of Onchocercinae (2). The vast majority (over 90%) of human cases are caused by *W. bancrofti,* with most of the remaining cases of LF caused by *B. malayi* (1). LF caused by *Brugia* species (spp.) occurs predominantly in Asia (3). According to the World Health Organisation (WHO), LF is endemic in 72 countries worldwide, with 52 of them requiring preventive drug therapy for their populations (4). From a global perspective (see Figure 1.1), more than 880 million individuals are at risk of contracting LF, resulting in an estimated annual economic burden of over 1 billion USD for endemic countries (1, 5). LF is considered to be a significant global public health issue, particularly in tropical countries, where in 2000 an estimated 120 million cases were infected. Global burden estimates in 2018 (6) now account for 64.6 million cases as a result of the impact of the Global Programme for the Elimination of LF. Moreover, approximately 40 million individuals are currently living with symptomatic manifestations caused by the disease, including disability and disfigurement (1, 7).

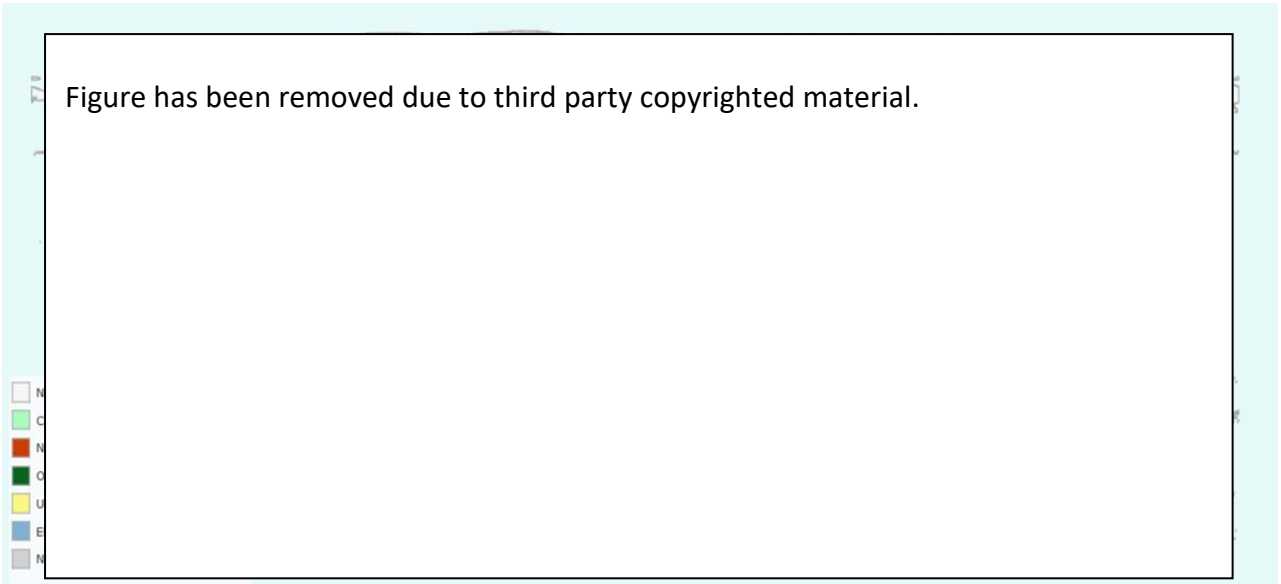


Figure 1. 1 Geographic distribution of lymphatic filariasis - 2018.

Figure source: (8).

While infections with *W. bancrofti* are exclusive to human hosts, *Brugia* spp. may naturally infect primates and carnivores (9). Transmission of LF requires mosquito vectors from the *Anopheles, Aedes, Culex*, *Mansonia* and *Coquillettidia* genera (9). For *W. bancrofti* there is evidence to suggest that transmission via *Culex* species generally occurs in urban settings, while rural transmission mainly occurs with *Anopheles* as vectors (1).

The life cycle of *W. bancrofti* is presented in Figure 1.2. The mosquito vector transmits the third stage filarial larvae (L3) as it feeds on a human host. Within the human host, the larvae continue to mature into adult worms and may survive for approximately ten years in the lymphatic system. Female adult worms release sheathed microfilariae (mf) into the blood of the host, thereby continuing the life cycle via subsequent blood feeding by mosquito vectors. Within the mosquito, mf start to exsheath in the midgut and haemocoel and later migrate towards the thoracic muscles and develop into the first larval stage (L1). Moulting of L1 occurs producing the second larval stage (L2), which moult again to produce infective L3. The L3 larvae migrate towards the head and the proboscis of the mosquito and the cycle is repeated when the infected mosquito initiates a blood feed on a human host (2, 10).

LF in the human host can present with acute, as well as serious chronic clinical manifestations. Despite the fact that the majority of LF cases are asymptomatic, approximately 40% of these individuals may present with subclinical evidence of impaired kidney function, such as haematuria, and all infected individuals present with (5). Furthermore, asymptomatic individuals are the principal sub-clinical lymphatic damage contributors to ongoing transmission of the nematode due to the presence of the mf in their blood (asymptomatic microfilaraemia) (11). Acute LF illness is generally characterised by the presence of fever and can be divided into two distinct syndromes: acute filarial lymphangitis (AFL) and acute dermatolymphangioadenitis (ADLA). AFL occurs when an adult worm dies resulting in inflammation and lymphangitis, while ADLA arises from secondary bacterial infections that cause additional lymphangitis and cellulitis. Acute illness can further develop into chronic LF, particularly in repeated acute episodes of the disease. Individuals suffering from chronic LF generally present with lymphoedema, commonly referred to as elephantiasis, affecting the extremities, as well as the breasts and male sexual organs. It is worth noting that the presentation of hydrocoele in males is restricted to infection with *W. bancrofti*, due to the absence of this particular symptom in chronic LF caused by *B. malayi* (1, 11). The symptoms associated with chronic LF may result in lifelong disfigurement, which can cause social stigma and socioeconomic disadvantages, on the individual and the community, as well as a negative impact on their mental health status (1).

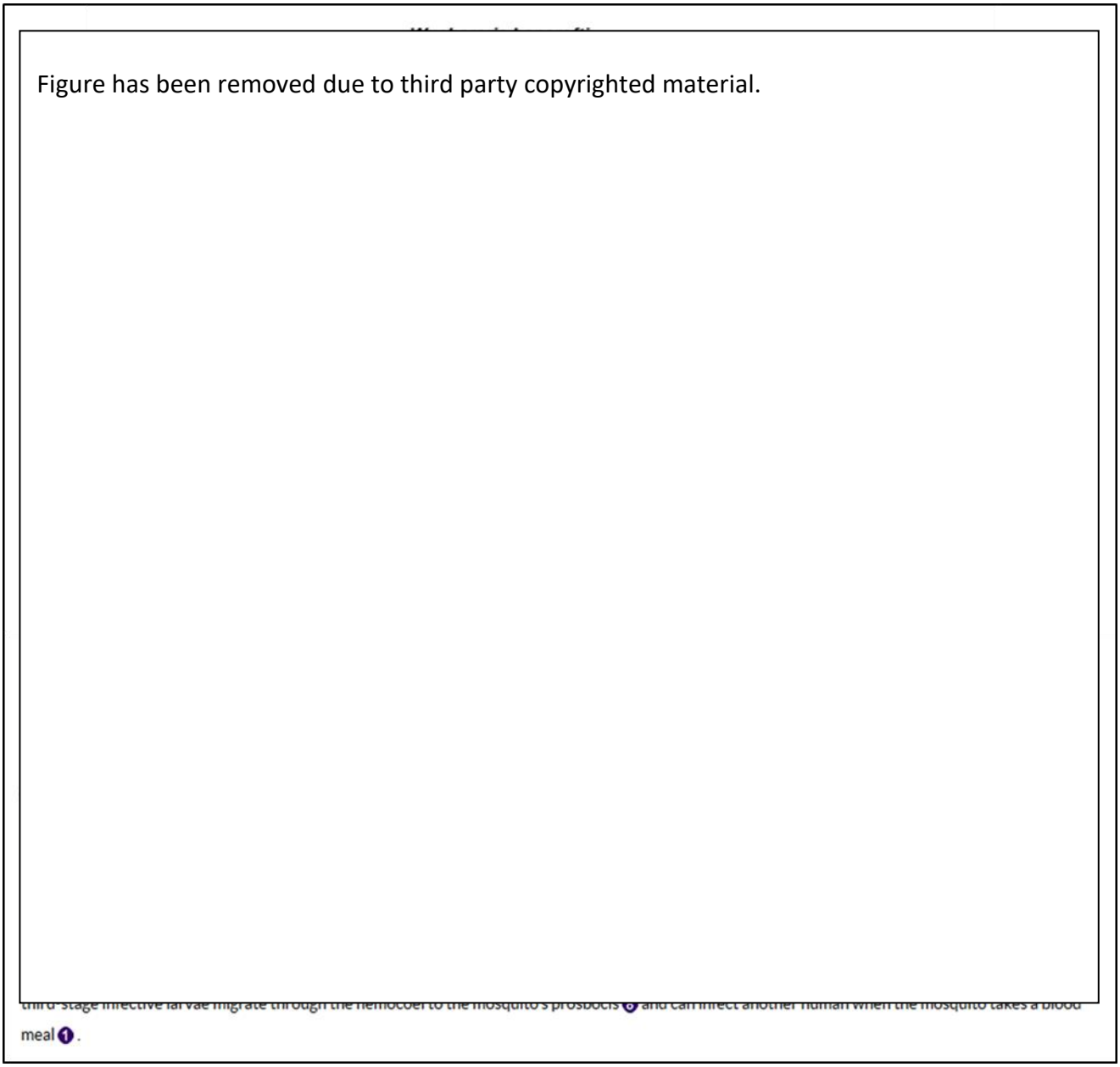


Figure 1. 2 The life cycle of *Wuchereria bancrofti*.

Figure source: (10).

### 1.1.2 Onchocerciasis (overview)

While the experiments in thesis have focused on *B. malayi*, it is important to discuss the causative parasite of onchocerciasis, *Onchocerca volvulus*, due to its significance as a human filarial disease and its relevance to anti-*Wolbachia* treatment (12). Onchocerciasis is of important public health relevance in the African continent (see Figure 1.3), which accounts for the vast majority (over 99%) of global cases. The remainder of cases occur in certain parts of South America, as well as in Yemen in the Middle East (13). *O. volvulus* is transmitted to a human host by the *Simulium* genus of blackflies that naturally occur near fast flowing rivers in endemic areas, hence the term "river blindness" is used to describe the disease (14). According to a recent estimate by the WHO, around 21 million people were infected with onchocerciasis in 2017, with approximately 70% of them presenting with dermatological conditions and 5% suffering from visual impairment due to the parasite (13).

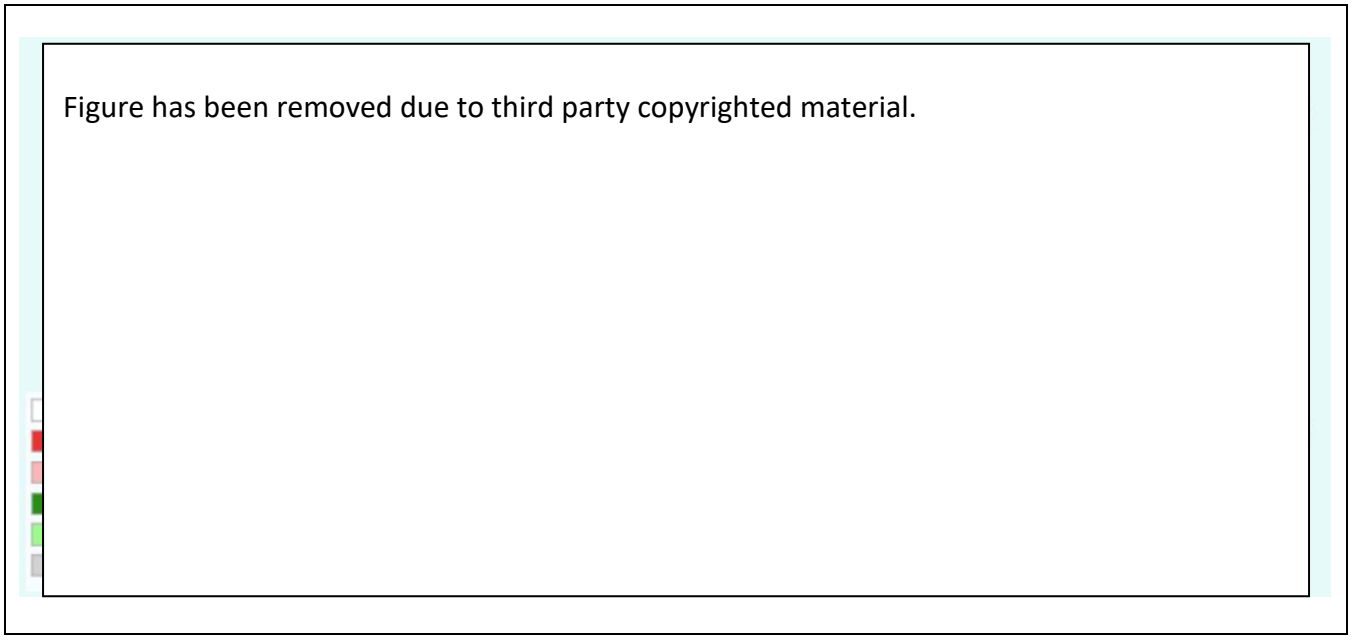


Figure 1. 3 Geographic distribution of onchocerciasis – 2018

Figure source: (15).

The life cycle for *O. volvulus* in the human host and infected blackflies is presented in Figure 1.4. When the L3 larvae enters the human host from an infected blackfly bite, they migrate to the subcutaneous tissue where they continue to develop to adult worms (16). This results in the formation of nodules, referred to as onchocercomas, which occur in subcutaneous sites and in deeper tissues (9). Adult female worms remain in the nodules for up to 15 years, where they produce millions of mf for approximately 9-11 years, which migrate to the skin for transmission to the blackfly vector (9, 16).

Severe itching is the commonest symptom in onchocerciasis infection. This occurs due to mf death, resulting in an inflammatory response from the human host (13). Moreover, dermal onchocerciasis may cause depigmentation (commonly named leopard skin) and lichenified onchodermatitis. One of the most important symptoms of onchocerciasis is the occurrence of ocular lesions caused by the migration of mf to the eye, potentially leading to optical atrophy and blindness (11, 13). Hence, onchocerciasis carries a huge socioeconomic burden due to the risk of visual impairment or blindness and the physical, psychological and social impact of dermatological symptoms (12).

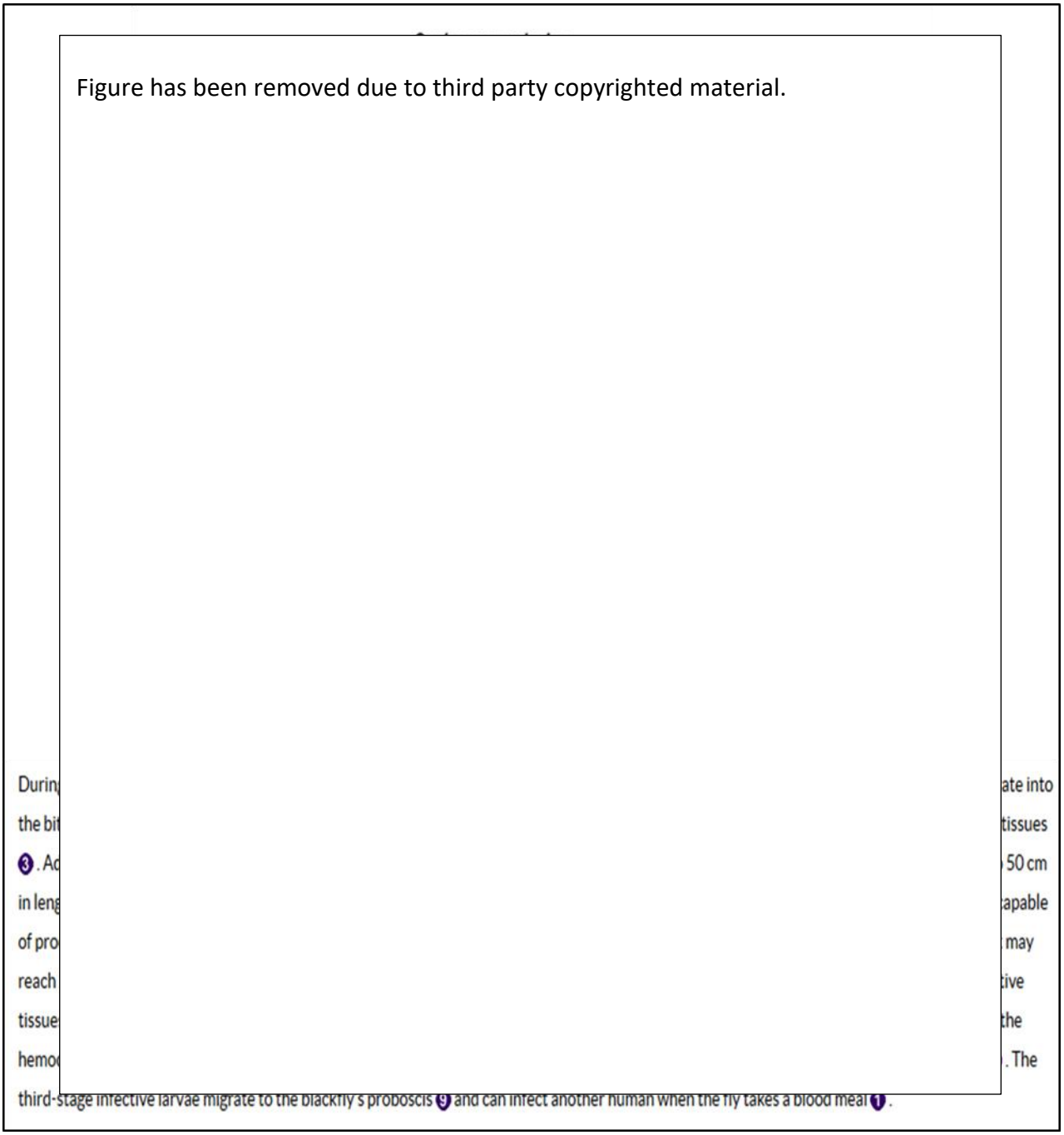


Figure 1. 4 The life cycle of *Onchocerca volvulus*.

Figure source: (16).

## 1.2 Current treatments for filarial diseases

In 2000, the WHO established its Global Programme to Eliminate Lymphatic Filariasis (GPELF) with the goal of preventing the transmission of LF and eliminating it as a global public health problem by 2020 (17, 18). The focus of the GPELF includes 1) preventive treatment through annual mass drug administration (MDA) (Table 1.1) in endemic areas using double combinations of three donated anthelminthic drugs; albendazole, diethylcarbamazine citrate (DEC) and ivermectin, and 2) morbidity management and disability prevention in patients with clinical disease (hydrocoele and lymphoedema) (1). The aim of MDA is to block transmission of infection by suppression of circulating microfilaraemia. All three agents used in MDA (albendazole, DEC and ivermectin) exhibit microfilaricidal or transient embryogenesis blocking properties, although they have only a partial efficacy or are ineffective against adult worms. Hence, suppression of transmission requires prolonged repeated annual doses, which may last for several years to cover the reproductive life-span of the adult worms (17). A total effective coverage for MDA of at least 65% of the population at risk is required for adequate control of LF in endemic areas (18).

| Anthelminthic | Annual Dose | Combination | Administration |
|---|---|---|---|
| **Albendazole** | 400 mg (twice/year) | N/A | Regions co-endemic with loiasis |
| **Ivermectin** | 200 mcg/kg | Albendazole 400 mg | Regions with onchocerciasis infections |
| **Diethylcarbamazine citrate (DEC)** | 6 mg/kg | Albendazole 400 mg | Regions with no onchocerciasis infections |

Table 1. 1 WHO recommendations for MDA of lymphatic filariasis in endemic areas.
Data source: (1).

Since the start of the GPELF, approximately 900 million individuals have received more than 7 billion administrations of MDA in 68 endemic countries (1). Despite this, only 20 out of a total of 72 countries have effectively reached the recommended WHO targets for LF elimination and no longer require MDA. Furthermore, more than 40% of endemic countries have not implemented adequate MDA coverage based on the WHO recommendations (17). The situation appears to be more complicated in the African region, where MDA coverage is often less than 60% and several endemic countries (South Sudan, Gabon and Equatorial Guinea) have not started MDA (18).

It is important to note that the three agents used for MDA are not eligible for use in the entire population. For example, ivermectin and DEC are contraindicated during pregnancy, and albendazole cannot be administered in the first trimester. Moreover, children below 2 years cannot receive DEC or two annual doses of albendazole. All three agents are contraindicated in children that are less than 90 cm in height and in the presence of severe illness (17). As MDA requires annual administration, the potential of long-term non-compliance has to be considered. Additionally, political, cultural and social acceptance change over time. Many of the countries that are considered endemic with LF are also developing nations and face numerous economic burdens, as well as the potential of conflict, famine and natural disasters. In the case of ivermectin, the emergence of drug resistance has been reported for *O. volvulus* (19, 20). All these factors can negatively impact on MDA and LF elimination (17).

In its recent guidelines on eliminating LF, the WHO has recognised that its previous target of achieving LF elimination by 2020 is not currently attainable, due to the previously mentioned issues and the multiple annual rounds required for MDA (17). In the same report, the WHO highlighted the importance of finding alternative drug regiments. One example that has been recommended is administering ivermectin, DEC and albendazole together, referred to as IDA, which received approval by the WHO in four countries in 2018 (18).

Due to the numerous limitations and issues associated with current MDA guidelines and available anthelminthic drugs, there is a need to develop and administer new agents for treating filarial diseases. This is also important due to the fact that current anti-filarial drugs

are not effective against adult worms and a macrofilaricidal drug treatment would provide many benefits towards the elimination of LF and onchocerciasis. One example of macrofilaricidal therapy has come from targeting *Wolbachia*, an essential intracellular bacterium with a mutualistic association with the filarial nematodes causing LF and onchocerciasis.

## 1.3 *Wolbachia*: filarial symbiosis and importance in potential treatment

*Wolbachia* are intracellular gram-negative bacteria with an approximate size of 0.2-4µm, that reside in vacuoles derived from its host (21). *Wolbachia* belong to alphaproteobacteria of the order Rickettsiales, under the Anaplasmatacea family. Currently, *Wolbachia pipientis* is the only recognised species within the *Wolbachia* genus (21-23). However, differences exist in *Wolbachia* supergroups (A to Q) in different host organisms, which will be discussed below (23). Hertig and Wolbach first discovered *Wolbachia* in the mosquito *Culex pipiens* (24). *Wolbachia* are now known to be widespread in other insects, where it is estimated up to 65% of species host the bacterium, as well as other arthropods, including certain types of spiders, mites and crustacea (25-27).

Since the 1970s, scientists have observed intracellular bacteria within filarial nematodes (26, 28-30). While earlier studies concluded they were a form of *Rickettsia*-like species, it was later confirmed that these intracellular bacteria were in fact *Wolbachia* (26, 31-33). *Wolbachia* are present in all life stages of filarial nematodes of humans, with the exception of *Loa loa*, the causative agent of loiasis (22, 34). Filarial nematodes responsible for onchocerciasis and LF contain *Wolbachia* from supergroups C and D, respectively (23, 35). Supergroup F of *Wolbachia* is also relevant to human filarial diseases as it is present in *Mansonella ozzardi*, the causative agent of mansonellosis (23, 36). In contrast, *Wolbachia* supergroups A and B are associated with arthropods (23).

From an evolutionary perspective, it is not fully understood how *Wolbachia* first infected Onchocercidae, the family that comprises numerous filarial nematodes, including the causative agents of LF and onchocerciasis (22, 37). *Wolbachia* may have been transmitted from arthropods to filarial nematodes (or the opposite) approximately 100 million years ago

through a single event (26, 35). Following this event, filarial nematodes were infected with *Wolbachia* vertically from female adult worms to their offspring. However, recent analysis of supergroup F has suggested the possibility of horizontal transmission, due to its presence in both insects and nematodes (23, 26, 35). The exact reason for the lack of *Wolbachia* in certain Onchocercidae nematodes is not known, although research has suggested that their ancestors may have been previously infected but have lost the bacteria. This theory was proposed due to the presence of genes acquired through lateral gene transfer with homology to *Wolbachia* in the host genome of nematodes that lack the bacteria, for example *Acanthocheilonema viteae*, *Onchocerca flexuosa* and *Loa loa* (22, 35, 38).

The complex relationship between filarial nematodes and *Wolbachia* is described as an obligate mutualistic symbiosis, due to the inability of nematodes to mature, reproduce, and obtain essential nutrients for survival without the presence of these bacteria (26, 37). Much of our understanding of the basis for this relationship has been revealed through comparative genomics of *B. malayi* and its *Wolbachia* symbiont (*w*Bm) (39, 40). One biochemical pathway provided by the endosymbiont is haem biosynthesis, which is crucial for filarial nematodes viability and motility and other processes involved in their maturity and energy metabolism (23, 40-43). Nematodes cannot synthesise haem in the absence of *Wolbachia* due to essential haem biosynthetic genes that are only present in the bacteria (22, 40-43). Similarly, synthesis of riboflavin and flavin adenine dinucleotide (FAD), are also derived from *Wolbachia* (22, 23, 40, 41). Conversely, there is evidence that *Wolbachia* also benefit from the filarial hosts, for example they provide essential amino acids needed for bacterial growth, as well as biotin, ubiquinone and coenzyme A, that the bacteria cannot synthesise alone (23, 44-46).

*Wolbachia* are located in the lateral cords of both male and female adult worms. In adult females, *Wolbachia* can be found throughout the reproductive system, including the ovaries and oocytes and developing embryos in the uterus (26). The reproductive system of adult male filarial nematodes is devoid of *Wolbachia* (47, 48). Antibiotic treatment results in a block of embryogenesis, indicating a critical role of the bacteria in embryo development (49).

*Wolbachia* also plays a crucial role in larval development. When the L3 larvae enters the mammalian host, *Wolbachia* populations dramatically expands and continues to growth throughout fourth-stage larval (L4) development (49). Antibiotic treatment of developing larvae leads to an arrested development at the early L4 stage. The consequence of *Wolbachia* removal following antibiotic treatment leads to extensive apoptosis in the adult germline and somatic cells of larvae and embryos (50).

*Wolbachia* can drive inflammatory responses that contribute to symptomatic presentations in onchocerciasis and LF. One example of this is observed in onchocerciasis infection of the cornea, where *Wolbachia* from mf are detected by Toll-like receptors (TLR2 and TLR6), resulting in inflammation and corneal oedema due to localised neutrophil recruitment and activation (12, 22). There is evidence to suggest that the adverse reactions following the administration of anti-filarial drugs DEC and/or ivermectin are linked to *Wolbachia*. These adverse reactions, include fever, neurological symptoms and enlarged lymph nodes, and are associated with the release of *Wolbachia* following nematode death, where the human host's innate and acquired immune system are activated through a neutrophil mediated response (9, 12). The severity of these adverse reactions appears to be linked to *Wolbachia* load in the patient's blood following anti-filarial treatment (9). Landmann *et al.* (47) have established that even viable adult worms may release *Wolbachia* through their secretory/excretory canal and initiate an immune response in the human host. The molecular drivers of *Wolbachia* mediated inflammation are derived from bacteria lipoproteins and principally the Peptidoglycan Associated Lipoprotein, PAL (51).

## 1.4 Anti-*Wolbachia* treatment: current situation and future potential

Due to the importance of *Wolbachia* in the survival of filarial nematodes, and the previously mentioned limitations of drugs used in MDA, anti-*Wolbachia* therapy has been validated as a safe macrofilaricidal treatment for LF and onchocerciasis (52, 53).

**Doxycycline and rifampicin as anti-*Wolbachia* agents:**

One of the first drugs that has been used for its anti-*Wolbachia* properties is doxycycline. Since its discovery in 1967, doxycycline, a derivative of tetracycline, has been widely used as a broad spectrum anti-bacterial drug and prophylaxis treatment for malaria (11, 54). The mechanism of action of doxycycline as a bacteriostatic agent is achieved through its targeting of the 30s ribosomal subunit in *Wolbachia* leading to inhibition of protein synthesis by blocking aminoacyl-tRNA attachment to ribosomes (22). In 1999, Hoerauf *et al.* (55) described the infertility and growth inhibiting effect of tetracycline on rodent filarial nematodes (*Litomosoides sigmodontis*) to be linked with *Wolbachia*. The same study also conducted experiments on filarial species *Acanthocheilonema viteae*, which lack *Wolbachia* and is unaffected by tetracycline treatment (55). Other research groups in the late 1990s have also described similar anti-*Wolbachia* properties using tetracycline against *Dirofilaria immitis* and *Brugia pahangi* (56). In terms of early *in vitro* studies on causative agents of human LF, *B. malayi* treated with doxycycline and tetracycline reduced *Wolbachia* load, leading to impairment of essential processes, including mf release and embryogenesis (57, 58).

Due to its importance in treating infections of *Mycobacterium tuberculosis* and leprosy, rifampicin is included in the WHO “model list of essential medicines” (59). The mechanism of action of rifampicin is achieved by disrupting nucleic acid production through its blocking of RNA polymerase (22, 60). Rifampicin is widely recognised to have potent anti-*Wolbachia* properties (61-64). Numerous *in vitro* (57, 58, 60, 63) and *in vivo* (61, 62) studies have demonstrated the ability of rifampicin to decrease *Wolbachia* load in filarial nematodes, including the causative agents of LF and onchocerciasis.

Following administration of anti-*Wolbachia* agents, adult worms slowly die after approximately 12 months and 18-27 months, for LF and onchocerciasis, respectively (65).

The anti-*Wolbachia* activity of rifampicin have been shown to be more potent than doxycycline (61). However, this observation was not replicated in human subjects when treated with the standard dose of rifampicin (61, 66, 67). Turner *et al.* (61) have shown this to be due to the pharmacokinetics of rifampicin, and PK/PD modelling and empirical studies in pre-clinical models (64) suggest higher doses of the drug would be required to achieve macrofilaricidal activity.

**Human clinical trials using anti-*Wolbachia* drugs:**

Optimisation of doxycycline regimens targeting *Wolbachia* have been tested in clinical trials. Initial trials on LF using doxycycline alone at 200mg per day, showed a sustained amicrofilaraemia, as well as potent macrofilaricidal properties with treatment periods for 6 or 8 weeks (68, 69). In a double-blind randomised control trial conducted by Supali *et al.* (70) on patients infected with *B. malayi* administered with doxycycline alone at 100mg per day for 6 weeks, recorded a 77% reduction in prevalence of LF after a year post-treatment. More recent trials have observed a complete elimination of adult worms after 18 months, following administration of doxycycline for 4 weeks (200mg/day) (67). In terms of onchocerciasis infections, successful macrofilaricidal effect and disruption of embryogenesis following treatment with doxycycline alone (100mg/day) for 5 weeks was achieved when patients were examined two years post-treatment (71).

Trials of a 3-week course of doxycycline produced only partial macrofilaricidal activity, although blockage of embryogenesis and reduced adverse events to subsequent antifilarial drugs remained intact (72). However, another study on bancroftian filariasis produced a macrofilaricidal effect and a significant reduction of hydrocoele when combining doxycycline (for 3 weeks) and DEC (after 4 months) (73). Other human trials on LF (68, 70) and onchocerciasis (74, 75) have produced the desired results when combining doxycycline with other drugs used in MDA, although these required longer treatment with doxycycline for 6 continuous weeks.

Rifampicin is another anti-*Wolbachia* antibiotic that has been examined in human clinical trials, however it did not exhibit the desired macrofilaricidal activity when administered alone. In onchocerciasis patients treated with rifampicin (at 10mg/kg/day) for 2 or 4 weeks,

Specht *et al.* (66) did not observe macrofilaricidal properties for both treatment periods, despite higher mf clearance and reduction in embryogenesis in the longer treatment period. Furthermore, the same study observed higher clearance of mf and more prominent impairment embryogenesis in 6-week treatment of doxycycline compared to rifampicin treatment for 2 or 4 weeks. A single clinical trial was found that combined both doxycycline (200mg/day) and rifampicin (10mg/kg/day) for 2 weeks and their effect was compared to doxycycline treatment at the same dose in a 4-week period. While macrofilaricidal activities were observed when combining both anti-*Wolbachia* drugs, this combination was not as potent as doxycycline alone for 4 weeks in eliminating adult worms (67).

A recent study by Aljayyoussi *et al.* (64) predicted through pharmacokinetic-pharmacodynamic (PK/PD) modelling that a higher dose of rifampicin (35mg/kg) may be required to produce a better macrofilaricidal outcome. *In vivo* studies on mice and gerbils infected with *B. malayi* testing this higher dose of rifampicin have been successful in producing a macrofilaricidal effect following a 7-day treatment combined with albendazole (61).

While other anti-*Wolbachia* agents have been examined in clinical trial on LF and onchocerciasis infected patients, the results of these did not provide the desired outcomes compared to doxycycline for 4 weeks. A newly repurposed agent, minocycline, has shown promise in onchocerciasis patients. Klarmann-Schulz *et al.* (76) have found that minocycline (at 200mg/day) for 3 weeks was more effective than doxycycline (200mg/day) in the same timeframe, however, it was not as effective as doxycycline for 4 weeks from a macrofilaricidal perspective.

**Anti-*Wolbachia* consortium (A-WOL):**

In 2007, the A-WOL consortium was established, through funding by the Bill and Melinda Gates Foundation, with the goals of refining existing (repurposed) anti-*Wolbachia* antibiotics, as well as developing new agents (52, 77). As the current anti-*Wolbachia* standard regimen of doxycycline for 4 to 6 weeks is a fairly long treatment period, the A-WOL consortium has targeted shorter oral treatment duration of ≤ 7 days (52, 78). Due to the length of current treatments, the risk of non-compliance and other individual barriers in

endemic areas must be considered. Additionally, despite its relative safety in adults, doxycycline is contraindicated in pregnancy, during breastfeeding and in children below the age of 8 years old (11, 52). Hence, new drugs should benefit these groups (79).

In order to achieve its objectives, the A-WOL consortium focuses on four different approaches:

A) Target identification: researchers in the A-WOL consortium identify important aspects associated with *Wolbachia* survival that could be used as potential targets for treatment (79). Examples of these include many of the previously mentioned metabolic pathways that provide the nematode with essential nutrients, such as haem (*Wolbachia* aminolevulinic acid dehydratase (ALAD), *w*ALAD) and lipoproteins (*Wolbachia* prolipoprotein signal peptidase II, LspA) biosynthesis (52, 79).

B) A-WOL assay development: the A-WOL screening funnel utilises cell-based high content screening assay (Operetta) to determine suitable drug hits that are effective against *Wolbachia* at 7 days or less (79, 80). At the time of writing, over 2 million chemical agents have been assessed for their anti-*Wolbachia* properties (81). Selected hits are tested on mf *in vitro* and larval and adult stages of *B. malayi in vivo* (79).

C) A-WOL library screening: drugs are selected from an extensive series of focused and diversity libraries, developed with the help of collaborators in the pharmaceutical industry (52).

D) Clinical field trials: these trials focused on optimising existing drugs with anti-*Wolbachia* properties to test the shortest regimen to obtain adequate macrofilaricidal activity (77).

Three newly identified (or repurposed) drug candidates have been selected by the A-WOL consortium through achieving potent anti-*Wolbachia* activity in a course of 7 days or less: TylAMac$^{TM}$, AWZ1066S and fusidic acid. The first drug TylAMac$^{TM}$ (ABBV-4083), a tylosin A analogue, was successfully tested *in vivo* in animals infected with *B. malayi*, *Litomosoides sigmodontis* and *Onchocerca ochengi* and demonstrated over 90% *Wolbachia* clearance following 1-week of treatment. Toxicology assessment provided a suitable safety profile (81). In comparison to doxycycline or minocycline for 3-4 weeks, TylAMac$^{TM}$ treatment for a

duration of 1 week showed higher efficacy. Currently, TylAMac$^{TM}$ has completed phase I trials and is progressing to phase II trials in Ghana.

The second pre-clinical candidate, AWZ1066S, synthesised from thienopyrimidine/quinazoline scaffold, is a highly potent macrofilaricidal with a high degree of specificity to *Wolbachia* (82). Through *in vitro* and *in vivo* experimentation, AWZ1066S has been shown to have higher anti-*Wolbachia* properties than doxycycline in *B. malayi*. Furthermore, it can also achieve its anti-*Wolbachia* properties through shorter treatment periods (1-day drug exposure) compared to doxycycline, rifampicin, moxifloxacin and minocycline in a time-kill assay. AWZ1066S, is currently undergoing pre-clinical development and lead optimisation studies (82).

Lastly, fusidic acid, a narrower spectrum antibiotic that principally targets gram-positive bacteria (83, 84), with utility in children and pregnancy (85), has been highlighted as a potential macrofilaricidal agent. *In vitro* and *in vivo* experiments have shown significant reduction of *Wolbachia* in *B. malayi* L3 and adult worms in animal models, for 14 and 7 days of treatment, respectively. PK/PD modelling has predicted promising outcomes for shorter regimens in human trials (86).

## 1.5 Autophagy: types and regulation

The rationale for studying the role of autophagy in anti-*Wolbachia* drug efficacy was driven by a study highlighting its role in the regulation of *Wolbachia* populations. The study by Voronin *et al*. (87) demonstrated that activating autophagy by chemical or genetic approaches reduced *Wolbachia* loads to the same magnitude as antibiotics. This stimulated us to investigate the role of autophagy in the mode-of-action and efficacy of the portfolio of anti-*Wolbachia* drugs.

In this section, we will start by describing the concept of autophagy, along with the different types and regulatory processes involved with this pathway.

From a general standpoint, autophagy can be defined as “the major intracellular degradation system by which cytoplasmic materials are delivered to and degraded in the

lysosome" (88). The process serves a crucial role in various cellular mechanisms, including homeostasis in response to stress stimuli and quality control of proteins and organelles (89). Autophagy may occur at low levels in the absence of stress and external stimuli, which is referred to as basal autophagy (90). It is believed that basal autophagy regulates the removal of damaged organelles and proteins in most types of cells under normal circumstances to maintain cellular homeostasis (91).

Autophagy occurs in all eukaryotic cells and can be divided broadly into three distinct types: macroautophagy, microautophagy and chaperone-mediated autophagy (92, 93). Prior to discussing macroautophagy (the form of autophagy we have examined in my thesis), we will briefly describe the other two types of autophagy. Microautophagy occurs when lysosomes directly engulf small cytoplasmic material via invaginations on the lysosomal membrane (93, 94). The second type of autophagy, chaperone-mediated autophagy, has only been observed in mammalian cells and involves specific targeting of cytosolic substrates that carry KFERQ-like pentapeptides (88, 93). This targeting is achieved through chaperone proteins in the cytoplasm, including heat shock cognate 70 (Hsc70) and other cochaperones, which transport the substrate to receptors on the lysosome called lysosomal-associated membrane protein 2A (LAMP2A), forming a multimeric complex (88, 93). Following the delivery of the substrate to the lumen of the lysosome for degradation, the LAMP2A reverts back to its monomeric form for subsequent substrate transportation (88, 93). Hence, chaperone-mediated autophagy does not result in structural changes to the lysosomal membrane (94). It is worth mentioning that this type of autophagy is absent in organisms that lack the LAMP2A homolog, for example *Drosophila* (95).

Macroautophagy is the most widely studied type of autophagy and the process examined in the experimental approaches used in this thesis. In contrast to the other two types of autophagy, macroautophagy requires the presence of specific double membraned vesicles called autophagosomes. The general pathway for macroautophagy is presented in Figure 1.3. This pathway is regulated by a series of autophagy-related (Atg) proteins and other non-autophagy-related proteins (96). Activation of the macroautophagy pathway can occur through various cellular stress conditions, for example microorganism infections, oxidative stress, endoplasmic reticulum (ER) stress and nutritional depletion of amino acids, growth factors and energy (88). These stress conditions result in autophagy induction through the

inhibition of target of rapamycin (TOR). There are two classes of TOR, both of which are involved in the macroautophagy pathway: TORC1 and TORC2, where the former is more sensitive to rapamycin (97). The inhibition of TOR causes the activation of Atg1-Atg13-Atg17-Atg31-Atg29 complex, which initiates the formation of the pre-autophagosome structure (PAS) (88, 93). It is still unknown if the formation of PAS occurs from the ER, although there is evidence that the mitochondria, plasma membrane and Golgi apparatus may play a role in their formation (88).

The formation of phagophores from PAS occurs through two steps: i) nucleation of the vesicles, followed by ii) vesicle elongation. This formation takes place in close proximity of the cytoplasmic material that initiated autophagy in order to completely engulf it at a later stage. Nucleation is mediated by phosphatidylinositol 3-phostphate (PI3P), which is generated by phosphatidylinositol 3-phostphate kinase class 3 (PI3KC3) complex. The PI3KC3 complex contains Atg6 (mammalian: BECN1), an important autophagy marker, as well as vacuolar protein sorting 34 (Vps34), Vps15 and Atg14 (90, 93).

Following nucleation, phagophores expand through a process called elongation. This is achieved by two ubiquitin-like conjugation systems in yeast and mammalian cells: Atg12-Atg5-Atg16 related to phagophores; and Atg8- phosphatidylethanolamine (PE) (mammalian: LC3-PE) related to both phagophores and autophagosomes (98). The formation of the Atg12-Atg5-Atg16 complex involves two enzymes, Atg7 (E1 enzyme) and Atg10 (E2 conjugating enzyme) (93, 99). The second system requires Atg12-Atg5, which performs as an E3 ligase to form the Atg8-PE (LC3-PE) complex. Prior to the formation of this complex, Atg4 processes Atg8, which is later transferred to Atg7 (E1 enzyme) and Atg3 (E2-like enzyme), thereby forming Atg8-PE (93). Atg8 (LC3) is an important autophagy marker that we have used in the experimentation in this thesis and is described in more detail in Chapter 2 (99). LC3-I indicates the processed form of LC3, while LC3-II refers to the conjugated form of LC3 with PE (93). In addition to LC3, there are several forms of Atg8-like proteins in mammalian cells, including γ-aminobutyric type A ($GABA_A$)-receptor associated protein (GABARAP). There is evidence to suggest that Atg9 may play a role in both yeast and mammalian cells in the elongation process in macroautophagy by further developing the phagophore membrane, although its mechanism is not completely understood (93). At the end of

elongation process, the autophagosome formation is complete and the target material is engulfed within its structure.

Mature autophagosomes reach the lysosomes via microtubules and fuse to form autophagolysosomes. While the fusion process in macroautophagy is not fully understood, there are several proteins that may influence the fusion. Examples of these include Rab7, as well as N-ethylmaleimide-sensitive factor attachment protein receptor (SNARE) components in yeast, *Drosophila* and mammalians (93, 95, 100). Moreover, there is evidence that LAMP-2 may be involved in the fusion process in mammalian cells (99). Following the fusion process, a variety of acid hydrolases, including Atg15, Rab2 (in *Drosophila* and mammalians), and cathepsin B, D and L, will initiate the degradation of the engulfed material (95, 99). The degraded material is released and could provide the cell with amino acids for reuse (92). The exportation of recycled amino acids from the degraded autophagolysosomes to the cytosol is mediated by Atg22 and lysosomal amino acid transporter 1 (LYAAT-1), in yeast and mammalians, respectively (92).

Macroautophagy can be regulated either dependently or independently of mTOR. If macroautophagy is regulated through mTOR, it follows the same pathway described above from inhibition of mTOR (or activation of mTOR in the case of autophagy suppression) and until lysosomal degradation (100). There is evidence that mTORC1 regulates autophagy in nutrient and growth factor depletion, while mTORC2 activates the Protein kinase B (Akt) pathway, resulting in the activation of mTORC1 (93, 97). On the other hand, cAMP-dependent protein kinase A (PKA) may activate autophagy independently of mTORC1. PKA can be influenced by nutrients, for example glucose, causing an upregulation of PKA and inhibition of autophagy. Furthermore, PKA can directly activate mTORC1, or indirectly through inhibition of AMP-activated protein kinase (AMPK) (93). Manipulation of the autophagy pathway can be achieved experimentally, through chemical or genetic approaches, and the literature covering the inhibition and activation of autophagy is described in detail in Chapter 2 and Chapter 3.

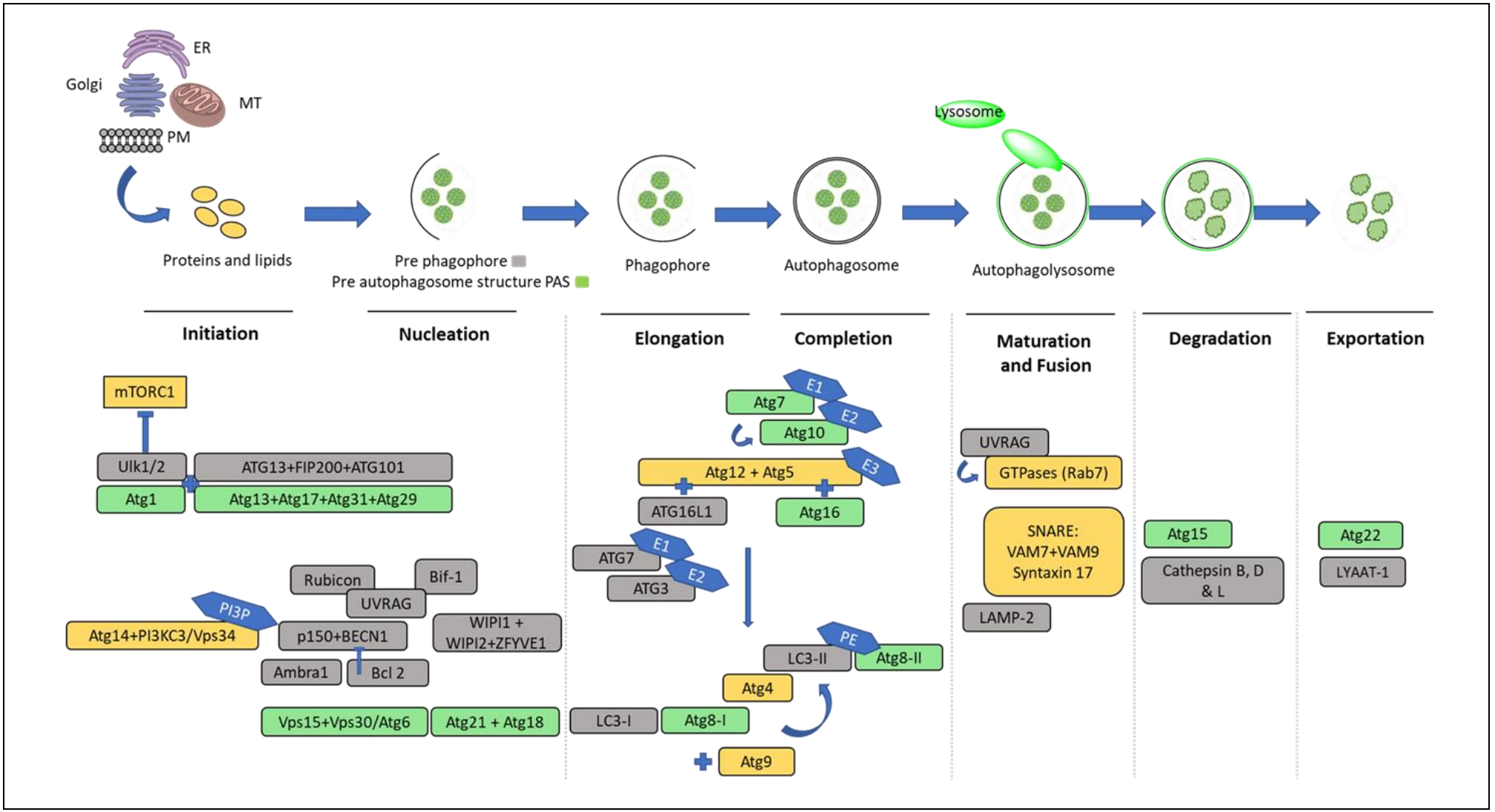


Figure 1. 5 Steps for the macroautophagy pathway.

The pathway is regulated through a series of autophagy-related (Atg) proteins (abbreviated as ATG for mammalian proteins) and other non-autophagy-related proteins. Green and grey boxes represent proteins in yeast and mammalian autophagy, respectively. Yellow boxes indicate shared proteins between yeast and mammalian cells.

Data source: modified from (92, 93).

Despite the fact that macroautophagy can engulf cytoplasmic materials for degradation in a non-selective manner, such as that observed in starvation, it can also achieve this by selective engulfing specific targets (93). An example of this is mitophagy, where damaged mitochondria are specifically targeted for degradation through the autophagic pathway. This occurs in response to ROS generation caused by mitochondrial damage, where deficiency of this type of autophagy can result in neurodegenerative conditions and pathological disorders associated with ageing (101, 102). Other types of selective autophagy with specific targets include lipophagy (targets lipid droplets), aggrephagy (protein aggregates), pexophagy (peroxisomes), reticulophagy (ER) and ferritinophagy (ferritin) (101).

One of the most important types of selective macroautophagy is xenophagy, where intracellular microorganisms are specifically targeted for degradation as a host immune response against infections (101). This is achieved by selective autophagy adaptors, referred to as sequestosome-1 like receptors (SLRs), targeting ubiquitinated effectors present in intracellular bacteria. Bacterial components are detected through pathogen recognition receptors (PRR), for example Toll-like receptors. The most important SLRs are Nuclear dot protein 52 (NDP52), TAX1 binding protein 1 (TAX1BP1), optineurin (OPTN), as well as p62 (mammalian: sequestosome-1), which was used extensively in the experimentation of our research and will be discussed in detail in Chapter 2 (103). The previously mentioned SLRs also play a role in host inflammatory responses. To achieve their selective autophagic properties, SLRs have the same three specific binding sites, these are: the ubiquitin-binding domain, LC3 interacting region, and multimerisation domain (103). An example of autophagy induced by bacteria is observed in *Mycobacterium tuberculosis*, where the bacteria is marked by ubiquitination, which enables its binding to the autophagic adaptors NDP52 and p62. In *Salmonella* infection, PRRs recognise bacterial effectors resulting in their ubiquitination and subsequently detection by p62 and OPTN (103). Conversely, bacteria, viruses and parasites may induce or suppress host autophagy for their own survival and growth (104). This concept of pathogen manipulated autophagy will be discussed in further detail in Chapter 2 and Chapter 3.

There is evidence that autophagy is involved in the regulation of *Wolbachia* populations in filarial nematodes (87, 105). While *Wolbachia* and the filarial nematode host share a mutual symbiotic relationship (as previously described in Section 1.4), *Wolbachia* may still be considered a foreign "pathogen" by the host immune system (105). Voronin *et al.* (87) have examined this relationship by chemically and genetically inducing and suppressing autophagy, which resulted in a decrease and increase of *Wolbachia* load respectively, in mosquito cell C6/36 infected with *Wolbachia* (C6/36*Wp*) as well as filarial nematodes of *B. malayi* . In this experiment the primary focus was on autophagy activation, which was achieved chemically using rapamycin, a known autophagy promoter, and genetically through gene silencing of TOR in *B. malayi* adult worms (bmTOR). Voronin *et al.* (87) evaluated the activation of autophagy by observing an increase in mature autophagosomes and autophagolysosomes in female adult worms. Additionally, the presence of degraded *Wolbachia* was observed within autophagolysosomes. *Wolbachia* elimination was also confirmed by an increase of apoptotic structures and impaired embryogenesis. Furthermore, the researchers described the observed bacterial elimination of *Wolbachia* from nematode autophagic activation to have a similar level as doxycycline treatment and carries a future potential in antibiotic treatment against filarial diseases (87, 105). Despite this, the mechanism of how *Wolbachia* harness or evade nematode host autophagy is still not understood.

While Voronin *et al.* (87) have examined the chemical inhibition of autophagy to have the opposite effect of autophagy activation by increasing *Wolbachia* load, this was only observed in mosquito cell line C6/36*Wp*. Hence, the impact of chemically inhibiting autophagy and its effect on *Wolbachia* populations in other cell lines and organisms, including *B. malayi*, is unknown. Moreover, cell/organism viability and toxicity of chemical inhibition of autophagy was not addressed. Despite the fact that autophagy inhibition was observed to increase *Wolbachia* number, this relationship was not examined further in the presence or absence of antibiotics with activity against *Wolbachia*. As anti-*Wolbachia* antibiotics are essential in the treatment of filarial diseases, the potential of understanding the role autophagy when combined with these drugs could further enhance current treatment regimen.

## 1.6. Project Aims:

This project will examine the role of autophagy in anti-*Wolbachia* therapy of antibiotics for treatment of lymphatic filariasis. The main aim of this thesis is to examine the role of autophagy in the anti-*Wolbachia* activity of diverse classes of antibiotics in different experimental conditions. This will be achieved experimentally through the following objectives:

1. Screening for optimum chemical autophagy inhibitors in mosquito cell line C6/36*Wp*.

2. Monitoring and measuring antibiotics-induced autophagy in different cell lines and nematodes.

3. Examining the contribution of autophagy in the activity of anti-*Wolbachia* drugs with different modes of action, during exposure and post-drug exposure to antibiotics.

# Chapter 2 Screening for optimum chemical autophagy inhibitors

## 2.1 Chapter overview

This chapter of the thesis will present and discuss the experimentation performed in order to determine suitable chemical autophagy inhibitors for the *Aedes albopictus* C6/36 cell line. It will start by presenting a brief literature review the concept of autophagy inhibition, previous studies conducted on different autophagy inhibitors (both chemical and genetic) and the methodology followed in monitoring autophagy inhibition. The concept of autophagy as a cellular process has previously been covered in detail (Chapter 1).

In order to examine the role of autophagy in antibacterial activity of selected antibiotics against *Wolbachia*, it is necessary to suppress autophagy in the presence of these antibiotics using autophagy inhibitors. The rationale of this is to determine the impact of suppressing autophagy on anti-*Wolbachia* activity to eliminate the symbiotic bacteria.

Four different experiments were done in this chapter using four pre-selected chemical autophagy inhibitors, namely: 3-methyladenine (3-ma), 2-(4-morpholinyl)-8-phenylchromo (ly294002), wortmannin and l-asparagine. These chemical inhibitors, which target different stages of the autophagy pathway, were evaluated in *Wolbachia*-infected mosquito cell line (C6/36*Wp*).

## 2.2 Background

### 2.2.1 Naturally occurring autophagy inhibition

Specific biological conditions can either activate or inactivate autophagy. For example, health conditions such as heart diseases and acute pancreatitis have been found to activate autophagy, whereas inflammatory bowel conditions, neurodegenerative diseases and some types of cancer may suppress the pathway. Additionally, certain infectious diseases can alter the autophagy process, in which pathogens can manipulate the pathway for the benefit of their survival and replication (106). *Mycobacterium tuberculosis* has been found to indirectly influence autophagy by inactivating the JUN N-terminal kinase (JNK), in turn preventing the

generation of reactive oxygen species (ROS) resulting in autophagy inhibition. This process is mediated by the mycobacterial enhanced intracellular survival protein (Eis) and its absence has been found to activate autophagy by increasing autophagosome production (107). A second example of an organism indirectly influencing autophagy is *Salmonella typhimurium*. In the initial hour of infection *S. typhimurium* activates autophagy, it then inhibits the process over the next four hours by normalising amino acid levels, leading to the activation of the mechanistic target of rapamycin (mTOR) causing the suppression of autophagy (108). As previously mentioned in Chapter 1, the inactivation of mTOR is a crucial step in the initiation of autophagy (107).

In certain circumstances, microorganisms can directly inhibit the autophagy pathway. For example, *Legionella pneumophila* can inhibit autophagy through targeting the C-terminal region of the lipidated form of the microtubule associated protein 1 light chain 3 (LC3) mediated by RavZ effector protein, thereby disabling the binding of LC3 to the membranes of pre-autophagosomal structures and preventing their maturity (109, 110). There is also evidence suggesting that *Shigella flexneri* may directly inhibit autophagy related genes (110, 111). Other microorganisms, such as *Staphylococcus aureus* (112)*, Anaplasma phagocytophilum* (113) and *Coxiella burnetii* (114, 115), can influence the autophagy pathway to their own benefit. In these microorganisms, this is achieved by replicating within the autophagic vacuoles (107, 110).

### 2.2.2 Autophagy inhibitors: chemical and genetic

From a broad perspective, autophagy inhibitors can be classified into two categories: chemical and genetic. Chemical autophagy inhibitors are compounds that can act on different stages of the autophagy pathway and comprise a broad range of chemical agents. Genetic autophagy inhibitors are genes (whether experimentally modified or naturally occurring) that are directly or indirectly involved in the autophagy pathway.

In the literature, genetic inhibition of autophagy has been achieved in using a gene silencing RNA interference technique by knocking down regulatory genes involved in autophagy pathway. The most commonly targeted genes include: Atg3, Atg5, Beclin1, Atg7, Atg9, Atg16L1, Focal adhesion kinase family interacting protein of 200 kD (FIP200) and Activating

molecule in Beclin 1-regulated autophagy protein 1 (Ambra1). One disadvantage of genetic inhibition is that many of these genes and other autophagy related genes are multi-functional and can be involved in other signalling pathways (106).

Experimental suppression of the autophagy pathway can be accomplished with the use of chemical compounds with a known inhibitory effect on the process. These chemical inhibitors are widely discussed in the literature and target different stages of the autophagy cascade. One group of widely used chemical inhibitors act on phosphatidylinositol 3-kinases (PI3ks). These enzymes act on the phosphorylation of the 3-hydroxyl group phosphatidylinositol (PI) located on the inositol ring of phospholipids (116). While there are three different classes of PI3ks, only two (class I and III) are known to be associated with autophagy. Class I PI3ks have been found to inhibit autophagy through the activation of beclin1 and protein kinase B mediated by the phosphorylation of PI 4,5-biphosphate to phosphatidylinositol 3,4,5-triphosphate ($PI(3,4,5)P_3$) (116, 117). Conversely, class III PI3ks activate autophagy and primarily act on stimulating the biogenesis of autophagosomes by the production of phosphatidylinositol triphosphate (PI3P). This in turn will recruit other autophagic components for the elongation process of the pre-autophagosome vesicles to form complete autophagosomes (117, 118). Hence, chemical autophagy inhibitors that act on PI3ks should ideally target class III of this pathway as the inhibition of this class will prevent the formation of autophagosomes (117, 118).

Three of the chemical inhibitors used in the experiments in this chapter, 3-ma, ly294002 and wortmannin, have been identified in the literature as PI3ks inhibitors, mainly acting on class III (119-121). Although 3-ma was the first of these to be discovered and one of the most commonly used inhibitors, it has recently been identified to have a dual function in acting on both class I and III PI3ks when using nutrient rich medium over an extended period of time (116-118). There is also evidence to suggest that class I PI3ks are inhibited by wortmannin and ly294002. However, in the case of wortmannin the inhibition of class I is short-acting and does not persist as in the case with 3-ma (117). With regards to ly294002, it appears to exhibit a link with calcium stores when inhibiting class I PI3ks, thereby increasing the generation of intracellular calcium levels (118).

Certain types of autophagy inhibitors act at a later stage of the autophagy cascade, for example preventing the delivery of mature autophagosomes to lysosomes. Examples of these include nocodazole and vinblastine, which alter microtubules to prevent the fusion of autophagosomes with lysosomes (106, 122, 123). Erythro-9-[3-2-hydroxynonyl] adenine (EHNA) also blocks the delivery of autophagosomes to lysosomes, although this is achieved by inactivating dynein ATPase (122). Autophagy inhibition can also occur by directly altering lysosomal pH levels, which prevents their fusion with mature autophagosomes. Two commonly used autophagy inhibitors that target lysosomes in this manner include bafilomycin A1 (a vacuolar ATPase inhibitor) and chloroquine (an alkaliser) (118, 124).

L-asparagine, an amino acid that has been examined in this chapter as a potential autophagy inhibitor, has a long history as a chemical inhibitor selectively blocking the delivery as well as the fusion of autophagosomes with lysosomes (123, 125, 126). There is evidence in the literature that different amino acids can play a role as autophagy inhibitors, and this may differ depending on the selected amino acid (127).

In situations where autophagy is highly activated, the degradation of the components of the autophagolysosomes results in the release of excessive amino acids. There is evidence to suggest that this amino acid influx will promote protein phosphorylation through mTOR class 1 (mTORC1) activation or by an mTOR independent manner, both of which affect the Unc-51-like kinase 1 (ULK1) complex (128, 129). As the ULK1 complex is inhibited, this facilitates the binding of beclin1 with bcl2 leading to sequestration of beclin1-UVRAG/Atg6 complex, thus resulting in the inhibition of autophagy (128). For the mTOR independent mechanism, inhibition can be achieved by the suppression of AMP-activated protein kinase (AMPK), causing an increase in ATP production by the release of 2-oxoglutarate. Other methods of AMPK inhibition involve phosphorylation of ribosomal protein S6 (8). It is important to note that inhibition of autophagy with amino acids is not fully understood, therefore the possibility of different actions on different cell types cannot be ruled out.

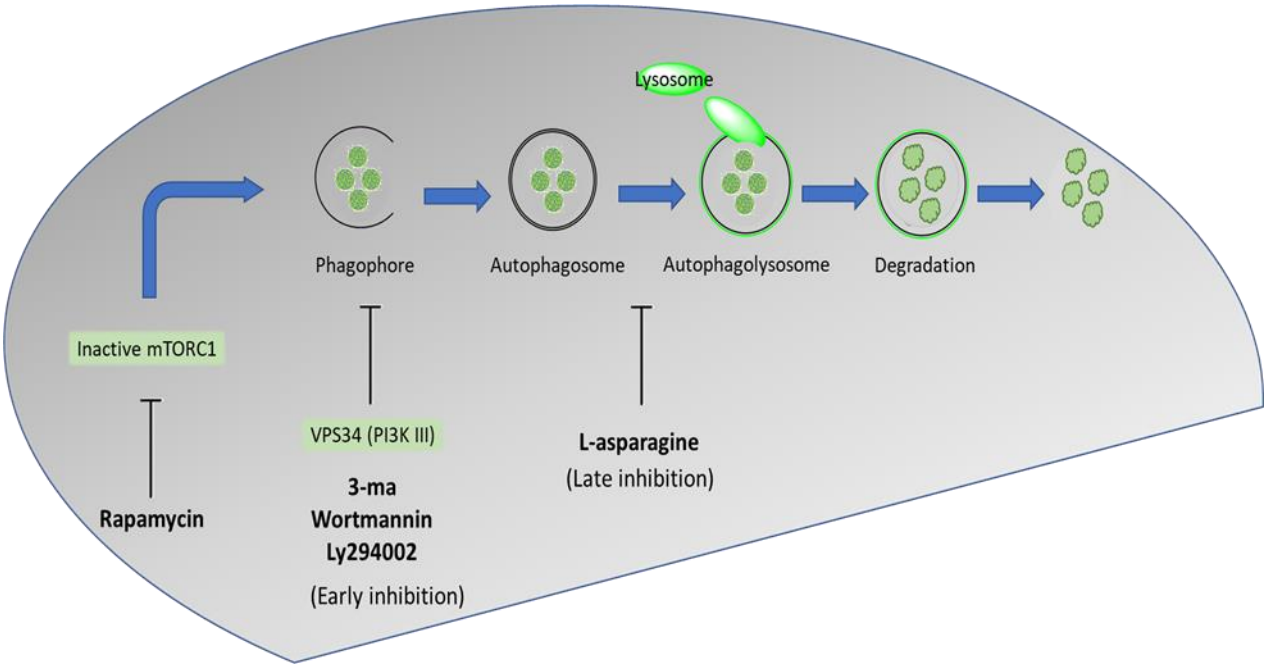


Figure 2. 1 Target sites of selected autophagy inhibitors in the autophagy pathway.

3-ma, ly294002 and wortmannin act at an early stage of the autophagy pathway by inhibiting PI3Ks class III, inhibiting autophagosome formation. L-asparagine inhibits a later stage, by blocking the delivery of autophagosomes to fuse with lysosomes thereby inhibiting autophagic degradation. Rapamycin inactivates mTOR class I, hence activating autophagy.

### 2.2.3 Available methods and assays to measure and monitor autophagy

Several experimental methods that have been developed to qualitatively and quantitively measure autophagic influx and inhibition. The first method focuses on monitoring the morphological features of autophagic vacuoles, such as autophagosomes and autophagolysosomes, as well as other cellular structures, including endoplasmic reticulum and mitochondria, using transmission electron microscopy (130, 131).

One of the most commonly used methods for studying autophagy is by performing immunofluorescence (IF) staining techniques to monitor autophagic activity and visualise intracellular pathogen (in xenophagy) or mitochondria (in the case of mitophagy) (types of autophagy previously mentioned in Chapter 1). These IF techniques can be performed using fluorescence microscopy, laser scanning confocal microscopy and flow cytometry. Fluorescent labelled antibodies are selected based on their ability to target specific markers

and cellular components involved in the autophagy cascade (131, 132). In both Chapter 2 and 3 of this thesis, laser scanning confocal microscopy was used to monitor autophagy inhibition and activation of specific targeted markers.

Flow cytometry can be utilised as a quantitative approach by measuring fluorescent intensity or the location of "live" individual cells within the autophagy cascade. Although flow cytometry analysis is considered faster and requires less cell material than confocal microscopy, its use is mainly with cells in suspension (133). While preparing adherent cells in suspension can be achieved, this can induce cellular stress, which in turn activates autophagy and may influence experimental outcomes. Also, a second limitation of using this approach is that flow cytometry can only evaluate the total LC3 expression in cells, rather than identifying its isoforms separately (131).

An example of an autophagy marker that was targeted in the experimentation performed in this chapter is LC3B using confocal microscopy, a mammalian homologue of the Atg8a protein previously described in Chapter 1, which will be referred to as LC3B in this thesis. Within the autophagy pathway, LC3 plays an important role in inducing autophagic elongation and promoting autophagosome growth when autophagy is activated. While there are three different types of LC3 (LC3A, LC3B and LC3C) only the LC3B/Atg8a component is associated with an increase in size or number of autophagosomes (93, 99, 130). LC3B is recruited by Atg7, the E1 ubiquitin activating enzyme, which is activated by Atg12, Atg5 and Atg16 complex. A cysteine protease known as Atg4 cleaves the C terminal of LC3 to produce the cytosolic form LC3B-I, which in turn will be transported by Atg3 to an E2 like ubiquitin transporter. This will be followed by lipid conjugation of phosphatidylethanolamine (PE) to the carboxyl terminal glycine of the cytosolic form generating the active membrane form LC3B-II (94, 98, 134-137). While other members of the LC3 family can be targeted in a similar manner, for example γ-aminobutyric type A ($GABA_A$)-receptor associated protein (GABARAP), little is known about them and they are not widely used as LC3B-II (94, 137).

A second commonly used marker is p62, which was also used as part of the experimentation for screening a suitable autophagy inhibitor in this chapter. As previously mentioned in Chapter 1, p62 is a human homologue of sequestosome 1 (SQSTM1) and Ref(2)p in

*Drosophila* species, which will be referred to as p62 in this thesis (138-140). P62 plays an important role as an adaptor in the selective autophagy pathway (141). This is achieved through two interactive domains present in the p62 gene. The first of these is ubiquitin binding domain (UBA), which facilitates the specific binding of p62 to other ubiquitinated proteins in the cytoplasm, including bacterial ubiquitin (141). The second domain is referred to as Phox/Bem 1p (BP1), which allows the accumulation of p62 genes resulting in a polymer structure, thereby stabilising its binding to selected targets (138).

P62 may interact with the previously discussed LC3 protein through what is referred to as the LC3 interacting region (LIR) (138, 142). Hence, in the case of xenophagy, pathogens will be recognised and targeted for autophagic degradation through LIR (143). For detection purposes, levels of p62 will be low in circumstances of induced autophagy due to high degradation levels of targeted material, as well as p62 degradation. On the other hand, when autophagy is suppressed, an increase in p62 levels is observed (138).

In addition to p62, other autophagy markers have recently gained prominence in the literature for selective autophagy. These include neighbour of Brca1 gene (NBR1), nuclear dot protein 52 (NDP52) and optineurin (OPTN) (143). These three selective autophagy adaptors share similar structural characteristics to p62, as they all have the UBA and LIR, which aid in targeting ubiquitinated material and attachment to LC3 on autophagosomal membranes (143-145). Despite the similarity between p62 and NBR1, one study has found they operate independently and can selectively target cargo for degradation in the absence of the other (146). It has been reported in the literature that NDP52 has an additional role in ensuring complete ubiquitinated microbial degradation autophagosome maturation (145).

Other autophagy proteins can also be used as markers using immunofluorescence staining and other experimental methods. Examples of these markers include Atg4, Atg5, Atg12 and beclin1 (130). However, their lack of specificity for xenophagy is not ideal for the experimental requirements in this thesis. (130).

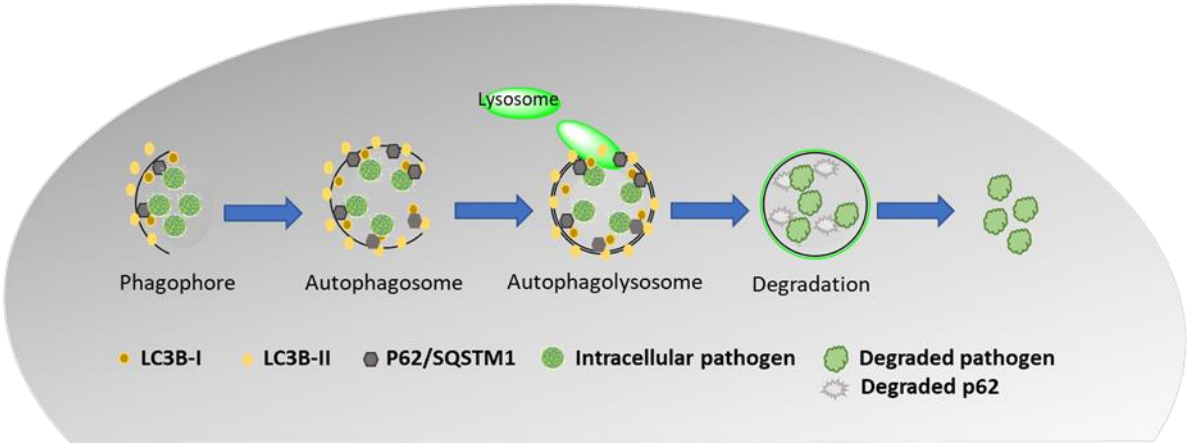


Figure 2. 2 The location of autophagic markers (LC3B-I, LC3B-II and p62) in the autophagy pathway.

LC3B-I/Atg8a-I is located in the cytoplasm and LC3B-II/Atg8a-II lipid conjugated form is located on the autophagosomal membrane. P62 is attached to both the ubiquitinated targeted pathogen and LC3B-II.

Immunoblotting analysis has an important role in monitoring autophagic flux. Many of the protein markers previously mentioned in the IF techniques, including LC3B and p62 used in this thesis, can also be used in measuring autophagy using western blot. One important difference with the use of LC3B in western blot is that it detects both of its isoforms (LC3B-I and LC3B-II), while most of the available antibodies used in IF techniques only detect LC3B-II. The protein LC3B has two isoforms: a cytosolic form LC3B-I, and a membrane form LC3B-II (98, 137, 147). This feature of detecting both isoforms of LC3B presents an added advantage over IF techniques, which measure the conversion of LC3B-I to LC3B-II. However, there are limitations to assessing this conversion, since expression of LC3B-I and LC3B-II varies in different cell lines and therefore need experimental validation (130).

An additional method used for measuring autophagy activity is by using transcriptome analysis. Autophagy related genes can be specifically targeted for deletion or silencing and can be quantified through measuring mRNA transcripts of selected genes using quantitative polymerase chain reaction (qPCR) (130-132).

### 2.2.4 Experimental justification

In this chapter, four chemical autophagy inhibitors were tested: 3-ma, ly294002, wortmannin and l-asparagine. These inhibitors and their concentrations were pre-selected based on their known role in inhibiting autophagy *in vitro*. 3-ma, ly294002 and wortmannin are known to affect an early step of autophagy by inhibiting class III PI3k enzymes thereby blocking autophagosome formation (116-118, 148). L-asparagine, has a later stage inhibitory effect in the autophagy process, in which it blocks the delivery of autophagosomes to lysosomes (123, 125, 129).

The first set of experiments in this chapter were performed to determine whether the selected chemical autophagy inhibitors affected cell viability/cytotoxicity. Different concentrations and incubation times were used for each chemical inhibitor on the mosquito cell line C6/36 using the high content imaging system (Operetta).

The second set of experiments were conducted to determine the overall autophagic inhibitory ability of the four chemical inhibitors, as well as the optimum concentration to achieve this. Two widely used markers for selective autophagy, p62 and LC3B, were selected as autophagy markers using immunofluorescence staining technique (confocal microscopy) and immunoblotting assay (western blot).

All experiments in this chapter were conducted on mosquito cell line C6/36*Wp*, a validated *in vitro* model developed by the A-WOL consortium for anti-*Wolbachia* drug screening. The use of this particular insect cell-based model was considered for carrying out a high throughput screening for suitable autophagy inhibiters based on its previous optimisation by the A-WOL consortium using Operetta (52). Due to the technical and economic issues related to the use of *B. malayi* nematodes, primary screening of autophagy inhibitors was carried on C6/36*Wp* cells and the suitable inhibitors in terms of favourable outcomes of viability and toxicity will be further tested on nematodes (Chapter 4).

## 2.3 Materials and methods

For more details on the materials used in the experimentation performed in this chapter, please refer to the Appendix B section of this thesis (Table B.1).

### 2.3.1 *In vitro* culture of the mosquito cell line C6/36 infected with *Wolbachia*

In the experiments performed in this chapter, the *Wolbachia* infected mosquito cell line, *Aedes albopictus* clone (C6/36*Wp*) was used. C6/36 cells were retrieved from a cryopreserved culture vial (with a cell density of 4 x $10^6$ cells/ml) stored at Liverpool School of Tropical Medicine (LSTM), United Kingdom (UK). These cells were originally purchased from European Collection of Authenticated Cell Cultures (ECACC) (clone C6/36, 89051705) and transfected by Dr Kelly Johnston (Department of Tropical Disease Biology, LSTM, UK). Cells were infected with *Wolbachia pipientis w*AlbB strain derived from Aa23 cells using the procedure and methodology described by O'Neill *et al*. (149) and Turner *et al*. (150) and cryopreserved and stored in liquid nitrogen.

Leibovits-15 (L-15) (Gibco, Thermo Fisher Scientific) medium used in C6/36*Wp* cell culture was supplemented with 20% heat inactivated hyclone fetal bovine serum (FBS) (Thermo Fisher Scientific), 2% tryptone phosphate broth (Sigma Aldrich) and 1% non-essential amino acids (Sigma Aldrich), all were filtered using 1 L filter with 0.22 µM pores.

Immediately after thawing, L-15 medium lowered to room temperature was used to wash the C6/36*Wp* cells. Cells were centrifuged at 400 g (gravitational force) for 5 minutes to pellet them. The obtained pellet was resuspended in 13 ml media, cultured in a closed cap 75- $cm^2$ tissue culture flask (Nunc™, Thermo Fisher Scientific) and incubated at 26˚C. C6/36*Wp* cells were sub-cultured and kept at a dilution of 1:4 (split ratio) every 7 days to reach confluency of approximately 80%. Under sterile conditions, cells were detached using cell scrapers (Nunc, Thermo Fisher Scientific), and resuspended in fresh media.

### 2.3.2 High content screening imaging system: Operetta/harmony software for C6/36*Wp* cells – Growth dynamics

Cell based screening assay was optimised following the protocol described by Clare *et al*. (80) using Operetta (PerkinElmer). All Operetta assays in this chapter were done on C6/36*Wp* at a confluency level of ~80% at day 7 of culture.

The Operetta assays were carried out using 384-well Cell Carrier plate (PerkinElmer) at a density of 2000 cells/well with 100 µl final volume diluted in L-15 medium. Attached cells were dislodged using sterile cell scrapers in spent media. Total viable cell count was calculated using an automated cell counter (Biorad). 10 µl of cell suspension and 0.4% trypan blue (Sigma Aldrich) were mixed and added to a cell counter slide (Biorad) for the total number of live cells per ml.

C6/36*Wp* cells were incubated with different autophagy inhibitors at different concentrations, as follows: 3-ma (between 1 to 5 mM), ly294002 (between 1-20 µM), wortmannin (between 1-20 µM), and l-asparagine (between 1-20 mM), along with 1% Dimethyl sulfoxide (DMSO) treated cells as a vehicle control, for 8 days at 26°C. All chemical autophagy inhibitors and DMSO were purchased from Sigma Aldrich.

All concentrations of the four tested autophagy inhibitors were prepared in DMSO for a working stock and diluted in culture medium with four biological repeats for each concentration. On day 0, 2, 4, 6 and 8, cells were stained for 30 minutes with Syto11 (Life Technologies, Thermo Fisher Scientific), a nucleic acid green fluorescent stain to visualise cell nuclei and *Wolbachia* at 2 µl/ml and imaged using Operetta/Harmony software (with objective lens at 60x and fluorescein filter).

Harmony software was used to analyse the cell images of each well (5 fields and 4 stacks) to calculate the total number of cells during the 8-day period of treatment with autophagy inhibitors. Autophagy inhibitor concentrations were considered to have an impact on cell growth when we observed a reduction of 50% compared to control groups with no treatment.

### 2.3.3 High content screening imaging system: Operetta/Harmony software for C6/36*Wp* cells – Cell viability and cytotoxicity

The viability of C6/36*Wp* cells in the presence of autophagy inhibitors was determined using Live/Dead Viability/Cytotoxicity kit (Life Technologies, Thermo Fisher Scientific). This kit contained Calcein AM for staining live cells (green fluorescent) and Ethidium homodimer-1 for staining dead nuclei (red fluorescent), diluted at 2 µM and 4 µM respectively. The dilution was prepared as per manufacturer guidelines. The cells were counterstained with Hoechst 34442 (Life Technologies, Thermo Fisher Scientific) at 2 µg/ml to visualise the nuclei. Saponin (Sigma Aldrich) treated cells were used as a positive control for this experiment, in which 0.1% saponin was added to cells for a duration of 10 minutes.

Using Operetta under bright field, the following channels were utilised: i) fluorescin for calcein AM, ii) DSred for ethidium homodimer-1 and iii) Hoechst for Hoechst 34442.

Harmony software was used to analyse the cell images in each well (8 fields and 6 stacks per well) to calculate the total number of live and dead cells during the 8-day period of treatment with autophagy inhibitors.

### 2.3.4 Immunofluorescence staining assay: Confocal laser scanning microscopy and fluorometric assay:

C6/36*Wp* cells were treated for 7 days with the four autophagy inhibitors at different concentrations: 3-ma (at 1 mM), ly294002 (at 1 µM), wortmannin (at 1, 5, 10 and 20 µM) and l-asparagine (at 1, 5, 10 and 20 mM). In this experiment, DMSO was used as a vehicle control.

A known autophagy activator, rapamycin at 5 µM (Sigma Aldrich), was used as positive control. Additionally, rapamycin at 5 µM was also added to all tested concentrations of autophagy inhibitors to examine if the tested inhibitors can continue to suppress autophagy in rapamycin-induced autophagy groups.

**Confocal laser scanning microscopy:**

Microscopic localisation of two autophagy markers; LC3B-II and p62 was performed in cells treated with the four autophagy inhibitors. The expression of these markers and interpretation within the autophagic pathway are presented in Figure 2.3.

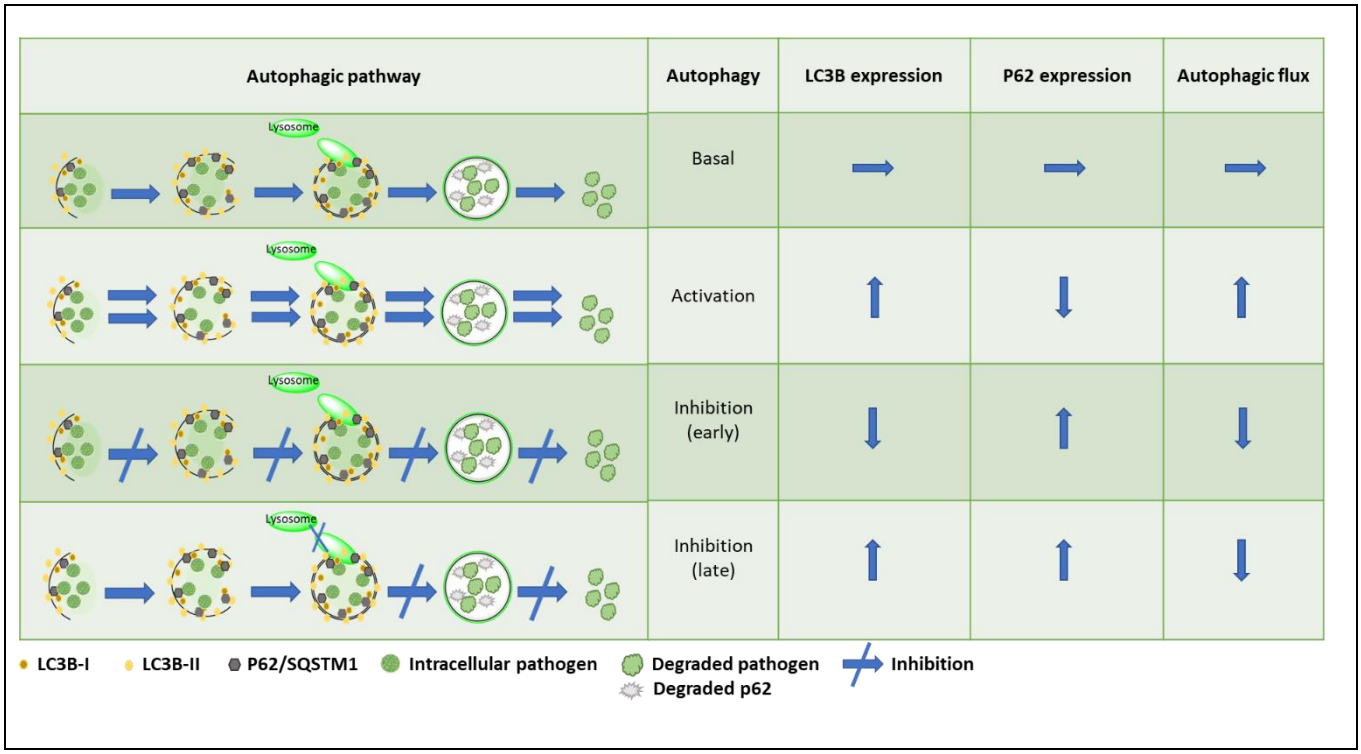


Figure 2. 3 Interpreting the expression of autophagic markers LC3B and p62 in the autophagy pathway.

Basal levels of autophagy represent naturally occurring autophagy. In autophagy activation (as seen with rapamycin, a known autophagy activator), expression of LC3B is increased (due to autophagosomes formation) and p62 levels decreased (due to autophagic degradation). Differences occur in terms of autophagy inhibition. For early inhibition (for example measuring autophagy using wortmannin), LC3B expression levels will decrease and p62 will increase in level due to inhibition of autophagosomes formation and autophagic degradation, respectively. Conversely, in late autophagy inhibition (as seen with l-asparagine), both markers will increase in level, due to autophagosomes accumulation (for LC3B) and blocking autophagic degradation (p62).

Data source: modified from (106).

50,000 cells were seeded in 2 ml L-15 media using shell vial tubes (Thermo Fisher Scientific) for confocal analysis. After cell suspensions were incubated between 14-16 hours at 26°C to allow cell attachment to the cover slips, the culture media was removed and replaced with prepared autophagy inhibitors diluted in L-15 media at the desired concentrations and cultured for 7 days in the incubator at 26°C. Media was removed and cells were fixed and permeabilised using 4% formaldehyde (Pierce, Thermo Fisher Scientific) diluted in phosphate-buffered saline (PBS) (Sigma Aldrich) containing Triton x100 (PBS-T) (Sigma Aldrich) for 30 minutes. Cells were then washed 3 times to remove excess fixative solution with PBS and blocked with 1% bovine serum albumin (BSA) (Sigma Aldrich) diluted in PBS for 15 minutes.

It is important to note that the LC3B-II and p62 markers were used separately in the immunofluorescence staining assay to avoid species mismatch. The primary antibodies used in this experiment, rabbit anti-LC3B-II (Invitrogen, Thermo Fisher Scientific) and rabbit anti-p62 (Cell Signaling), were diluted in 1% BSA blocking buffer at 1:400 and cells were incubated overnight at 4°C. Next, fluorescence-labelled secondary antibodies diluted at 1:500, goat anti-rabbit Fluorescein isothiocyanate Ds grade (FITC) (Invitrogen, Thermo Fisher Scientific) used to target LC3B-II and goat anti-rabbit tetramethylrhodamine (TRITC) (Sigma Aldrich) used to target p62, were added to cells for one hour at room temperature.

Cells were washed three times with PBS following each antibody incubation to remove unbound antibodies. Cover slips of each vial were removed and mounted on a microscopic slide with 4',6-diamidino-2-phenylindole (DAPI) mounting medium (Vectashield, Vector Laboratories) to view under confocal laser scanning microscope (Zeiss LSM 880) at 63x magnification using Z-stack 3D images. Fixed cells on slides were imaged and analysed across three different areas, in which each cell per area was selected using a graphic software (Zen software) to measure mean fluorescence intensity.

**Fluorometric assay:**

Quantitative analysis of fluorescence expression of autophagy markers was measured using fluorometric assay. Cells were seeded in 200 µl L-15 media of a 96-well plate, which were black walled with clear flat-bottom (PerkinElmer). Following the same protocol mentioned above for confocal immunostaining assay, at day 7 the intensity of LC3B-II-FITC and p62-TRITC fluorescence was measured at an excitation of 490 and 557, and emission of 525 and 576 for FITC and TRITC respectively, using Varioskan plate reader (Thermo Fisher Scientific). Wells without cells were also measured to exclude fluorescence background readings.

## 2.3.5 Western blot analysis

C6/36*Wp* cells were seeded into T-25 flasks (Thermo Fisher Scientific) at a density of $1x10^6$ cells per 5 ml L-15 media. Different concentrations were used for the three autophagy inhibitors: for ly294002 at 1 µM, wortmannin 1-20 µM and l-asparagine 1-20 mM. Additional treatment groups consisting of C6/36*Wp* cells treated with the three autophagy inhibitors (using the same concentrations mentioned above) combined with rapamycin were analysed using western blot. DMSO treated cells were used as a vehicle control and rapamycin as an autophagy inducer. All treatment groups were incubated at 26°C for 7 days.

At the end of treatment, cells were washed with cold PBS and lysed using 100 µl RIPA lysis buffer (Thermo Fisher Scientific) with an added protease inhibitor mix (GE Healthcare) at 10 µl/ml for 5 minutes and centrifuged to pellet the cell debris. The prepared whole cell lysates were used for protein measurements (in µg/µl), in which the total protein concentration of each sample was estimated using bicinchoninic acid protein assay kit (Pierce, Thermo Fisher Scientific).

Equal protein concentrations of 50 µg/40 µl were diluted in NuPAGE LDS sample loading buffer (Thermo Fisher Scientific) and loaded into gels along with 5 µl of molecular weight marker PageRuler Prestained Protein Ladder - 10 to 180 kDa, (Thermo Fisher Scientific). All lysates were reduced using NuPAGE reducing agent (Thermo Fisher Scientific) and heated at 70°C for 10 minutes before loading into gels. Loaded proteins were then separated using

sodium dodecyl sulphate-polyacrylamide gel electrophoresis (SDS-PAGE) in a precast of NuPAGE 6-12% Bis Tris Bolt plus polyacrylamide gel (Thermo Fisher Scientific) at a voltage of 130 v for 1 hour with NuPAGE MES running buffer (Thermo Fisher Scientific) containing NuPAGE antioxidant reagent (Thermo Fisher Scientific).

Proteins were then transferred into a nitrocellulose membrane with a pore size of 0.22 µM (Amersham, GE Healthcare). In a Mini Trans-Blot Electrophoretic Transfer Cell (Biorad), a gel-blot sandwich was assembled into a gel holder cassette and placed into the transfer cell and processed at 200 mA for 1 hour using Tris Glycine transfer buffer containing 20% methanol (self-prepared: see Appendix B Table B.2 for components). All components of the gel-blot sandwich including filter papers and filter pads were equilibrated by submerging them into the same transfer buffer for 10 minutes before transferring the blot. Transferred proteins were checked with Ponceau S staining (self-prepared: see Appendix B Table B.2 for components) to confirm transfer quality and an equal amount of loading volumes.

Membrane blots were blocked using 5% BSA diluted in Tris buffered saline with 0.1% Tween 20 (TBS-T) (Sigma Aldrich) for 2 hours with gentle agitation. All primary antibodies were added to the membranes as indicated in Table 2.1 and left overnight at 4°C with gentle agitation (~30rpm). Following this step, blots were washed three times with PBS-T, with each wash cycle lasting 5 minutes, to remove unbound primary antibodies. Secondary antibodies were then added to the membranes as presented in Table 2.1 and left for 1 hour at room temperature.

| Primary antibody | | | | | Secondary Antibody (HRP conjugated) | | | | |
|---|---|---|---|---|---|---|---|---|---|
| Target | Species | Dilution | Blocking buffer | Supplier | Target | Species | Dilution | Blocking buffer | Supplier |
| **LC3B** | Rabbit | 1:1000 | 5% non-fat milk in TBS-T | Novus | **Anti-rabbit** | Goat | 1:5000 | 5% non-fat milk in TBS-T | Cell Signaling |
| **P62** | Rabbit | 1:1000 | 5% BSA in TBS-T | Cell Signaling | **Anti-rabbit** | Monkey | 1:10000 | TBS-T | GE Healthcare |
| **Beta actin** | Mouse | 1:1000 | 5% BSA in TBS-T | Cell Signaling | **Anti-mouse** | Rabbit | 1:20000 | TBS-T | Sigma Aldrich |

Table 2. 1 Primary antibodies and secondary antibodies used in western blot analysis, along with their target, species, dilution, and type of blocking buffer.

Excess secondary antibodies were removed by washing the membranes again with PBS-T x3 for 10 minutes. SuperSignal Chemilluminscent substrate HRP system (Pierce, Thermo Fisher Scientific), was added to the membranes for 5 minutes, and then exposed to x-ray CL Xposure films (Thermo Fisher Scientific) and imaged using Photons Developer Instrument. For blots where the primary antibodies were of similar species (see Table 2.1), primary and secondary antibodies were stripped off using Restore Plus Western Blot Stripping Buffer (Thermo Fisher Scientific) for 15 minutes and washed 3 times with washing buffer TBS-T.

### 2.3.6 Statistical analysis

Statistical analysis for this chapter was performed for continuous variables in cell growth dynamic and confocal immunofluorescence assay using independent sample Student's t-test. One-way analysis of variance (ANOVA) was used for continuous variables with two or more independent variables for viability/cytotoxicity experiment. Statistical significance was at $p \leq 0.05$. GraphPad Prism version 7 was used for all sections of the statistical analysis in this chapter.

## 2.4 Results

The results section for this chapter is divided into four parts, where each section represents the different set of experiments conducted to determine an optimum autophagy inhibitor in C6/36*Wp* cells.

### 2.4.1 Cell growth dynamic of mosquito cell line C6/36*Wp*

The findings for total C6/36*Wp* cell number using the Operetta high throughput imaging system are presented in Figure 2.4, obtained at different time points during the 8-day treatment period with the four autophagy inhibitors at a range of concentrations. Each treatment group had four biological repeats, and the values presented as mean total cell count per group. The measured values for the percentage reduction in total number of cells for each treatment group are presented in the Appendix A (Table A1).

Each individual graph in Figure 2.4 presents the total number of C6/36*Wp* cells for different autophagy inhibitors: 3-ma (1-5 mM), ly294002 (1-20 µM), wortmannin (1-20 µM) and l-asparagine (1-20 mM). The cut-off for autophagy inhibitor effect on cell growth was taken at a 50% reduction of total cells compared to the control (DMSO treated cells) at day 8. This cut-off point was based on the threshold used previously for A-WOL drug screening (151). It should be noted that prior to day 4 of treatment, all autophagy inhibitors at all concentrations appeared similar in terms of cell growth effect.

For 3-ma (Figure 2.4 A) only the lowest concentration at 1 mM did not affect cell growth by more than 50%. This was also observed for ly294002, although the initially selected range of concentrations warranted further evaluation, which presented a suitable range between 1-2 µM (Figure 2.4 B and C). However, it is important to note that for ly294002 at 2 µM there was noticeable variability measured at day 8 (Figure 2.4 C).

In the case of wortmannin and l-asparagine (Figure 2.4 D and E), all the initially selected concentrations were suitable and did not hinder cell growth by more than 50%.

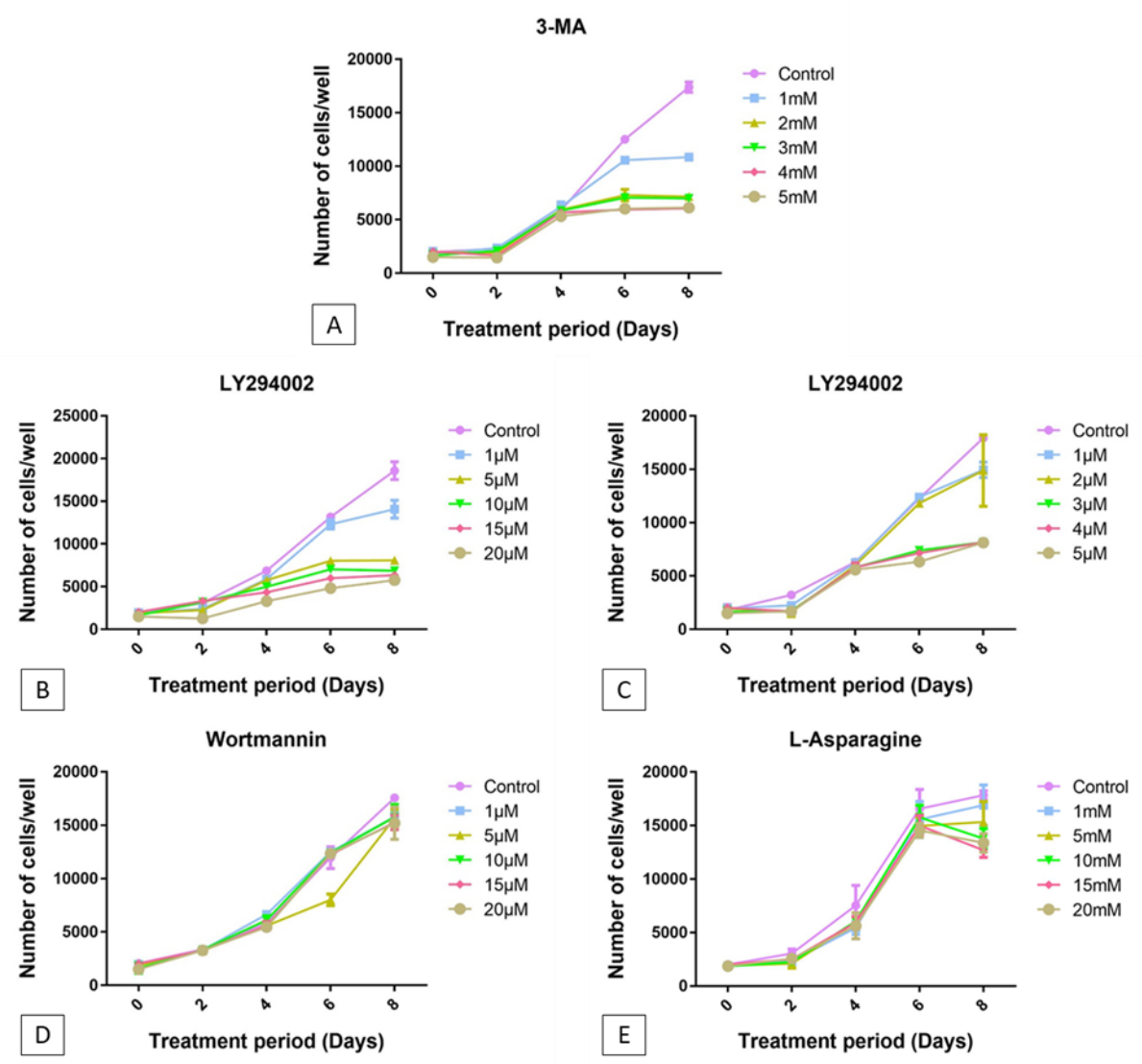


Figure 2. 4 C6/36*Wp* cell growth dynamics for autophagy inhibitors at different concentrations.

C6/36*Wp* cells infected with *w*AlbB were treated with four autophagy inhibitors for 8 days. Total number of cells/well were measured every two days (at day 0, 2, 4, 6 and 8) using Operetta. Graphs (mean with SD) represent the total number of cells/well in four biological repeats for every treatment group. Suitability of autophagy inhibitor concentration was considered if its effect on cell proliferation was less than 50% reduction compared to control (DMSO treated cells).

### 2.4.2 Cell viability and cytotoxicity

In the second experiment, viability of cells was assessed on C6/36*Wp* cells treated with the selected autophagy inhibitors (3-ma, ly294002, wortmannin and l-asparagine) at different concentrations for 8 days using the Operetta/Harmony high throughput imaging. This experiment was performed as a confirmatory step for the previous experiment (section 2.4.1), in which four chemical autophagy inhibitors were tested to determine their effect on reducing cell growth at 50% compared to a control.

Live cells were differentiated from dead with the use of two viability stains as mentioned in the method section 2.3.3. For all autophagy inhibitors, the same concentrations were used as experiment 2.4.1. The findings for cell viability and cytotoxicity are presented in Figure 2.5.

As in the previous experiment, there was a significant difference between 3-ma at 1 mM and all the other concentrations tested in terms of cell cytotoxicity. Moreover, there was a significant difference recorded between DMSO treated cells (control) and 3-ma at 1 mM, indicating a toxic effect even at the lowest concentration tested for this inhibitor.

In the case of ly294002, only the lowest concentration tested (1 µM) did not appear to have a toxic effect compared to the control. As expected, the effect on cell viability was concentration-dependent, where an increase in the concentration of ly294002 significantly increased cell toxicity compared to the control.

For both wortmannin and l-asparagine, all the tested concentrations presented a similar picture and did not appear to have a significant effect on cell toxicity/viability even at the highest concentration, as indicated in Figure 2.5.

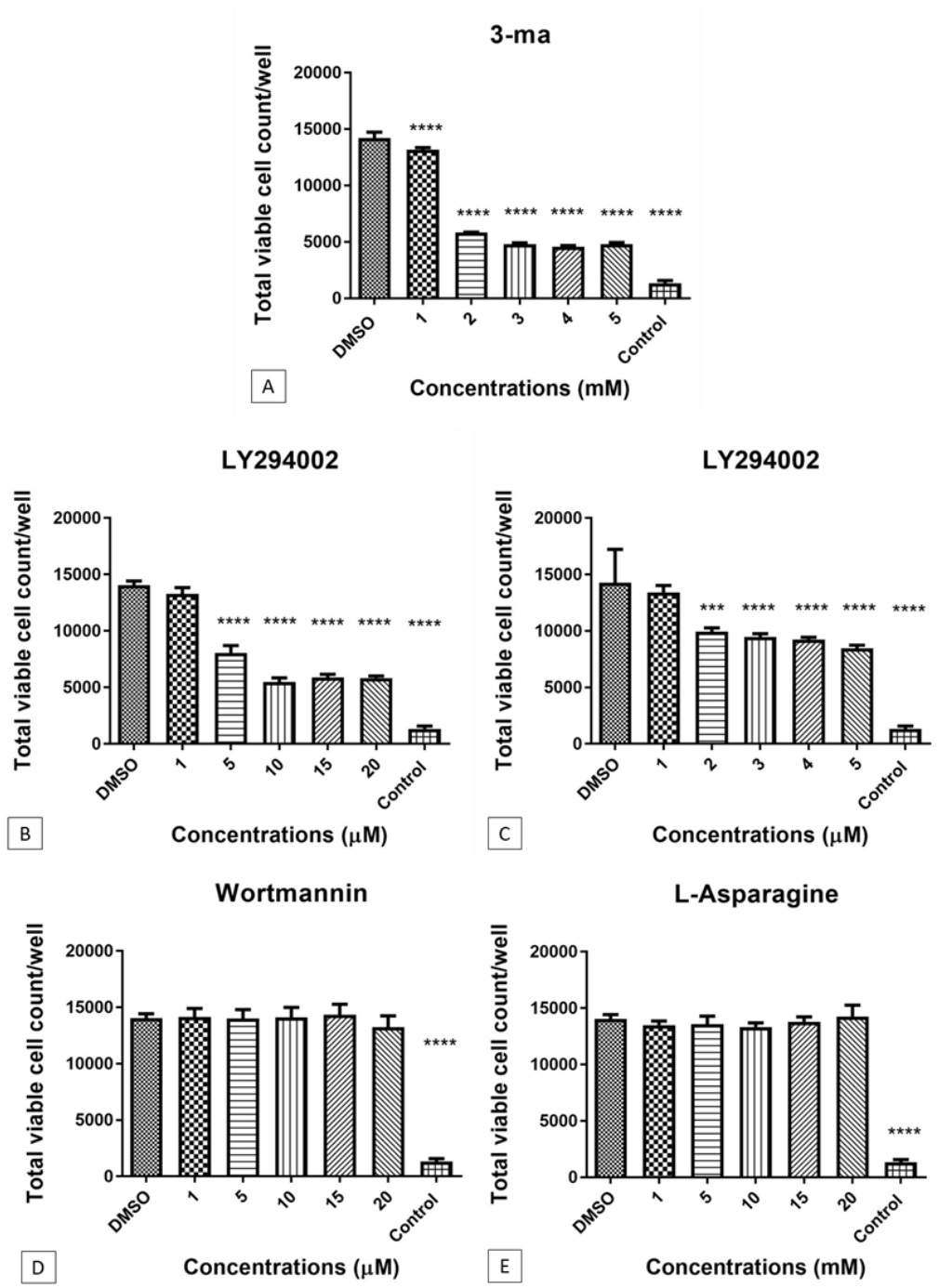


Figure 2. 5 C6/36*Wp* cell viability/cytotoxicity for autophagy inhibitors at different concentrations.

C6/36*Wp* cells were treated with four autophagy inhibitors for 8 days. Total number of viable cells were stained with calcein AM and measured at day 8 using Operetta. Saponin was used as a control, expressing the presence of dead cells. Graphs (mean with SD) represent total viable cell count/well in four biological repeats for every treatment group. Cell viability/cytotoxicity was assessed by comparing with DMSO control using one-way ANOVA Dunnett's test, where statistical significance was $p \leq 0.05$. For p-value * = 0.01 to 0.05, ** = 0.01 to 0.001, *** = 0.001 to 0.0001, and **** ≤ 0.0001.

### 2.4.3 Immunofluorescence staining assay

Based on the results obtained from the experiments on cell growth dynamic and cell viability/cytotoxicity (section 2.4.1 and 2.4.2), we selected suitable concentrations for the four autophagy inhibitors, and these were assessed using an immunofluorescence staining method at day 7 of treatment. Therefore, autophagy inhibitor concentrations that were deemed non-toxic and were evaluated for their autophagic inhibitory effect. These findings are presented in Figures 2.6-2.11, using two autophagy markers: LC3B-II (conjugated with FITC - green fluorescent puncta) and p62 (conjugated with TRITC - red fluorescent puncta), and cell nuclei (DAPI - blue fluorescent). It should be noted that for all PI3ks inhibitors (3-ma, ly294002 and wortmannin), inhibition of autophagy will present a decrease in LC3B-II green fluorescence expression indicating a blocking of autophagosome formation. Whereas, for l-asparagine inhibition of autophagy will present as an increase in green fluorescence intensity due to its late stage inhibition in the autophagy cascade indicating the accumulation of autophagosomes. While for p62, an increase of red fluorescence indicated a suppression of autophagy degradation for all inhibitors.

As previously described in the methods section, rapamycin was used a positive control for autophagy activation. The optimum concentration of rapamycin at 5 µM was determined through a separate cell growth dynamic and cell viability/cytotoxicity analysis. This is presented in Appendix A (Figure A1).

**Autophagy inhibitor: 3-ma**

While 3-ma was observed to be toxic even at the lowest tested concentration, it did not affect cell growth by more than 50% following an 8-day treatment. Due to this inconsistent finding we tested the inhibitory effect of 3-ma at 1 mM for 7 days. As presented in Figure 2.6, 3-ma at 1 mM did not significantly reduce LC3B-II (Figure 2.6 A and B) or increase p62 (Figure 2.6 C and D) compared to the DMSO control, indicating this concentration as not adequate for autophagy suppression. The addition of 3-ma to rapamycin-induced autophagy cells decreased LC3B-II fluorescence intensity when compared to rapamycin treated cells alone. This indicates that 3-ma at 1 mM suppressed autophagy effectively only in cells with

rapamycin-induced autophagy. This was further confirmed by the higher fluorescence intensity of p62 in rapamycin and 3-ma treated cells compared to rapamycin alone.

**Autophagy inhibitor: Ly294002**

In the case of ly294002 (Figure 2.7), only one concentration (1 µM) was observed to be suitable in terms of its lack of toxicity to carry out immunofluorescence staining analysis. However, ly294002 at 1 µM was not found to be an effective autophagy inhibitor at this concentration. Additionally, ly294002 combined with rapamycin was found to be ineffective when compared to rapamycin alone.

**Autophagy inhibitor: wortmannin**

For both wortmannin and l-asparagine, the findings in cell growth and cell viability/cytotoxicity presented a wide range of suitable concentrations to be tested. For wortmannin, apart from the lowest concentration tested at 1 µM, all concentrations presented a statistically significant difference compared to the control with a lower expression of LC3B-II (Figure 2.8) and a higher expression of p62 (Figure 2.9). This observation indicates that autophagy inhibition has occurred by the blocking of autophagosome biogenesis and p62 degradation. As expected, wortmannin combined with rapamycin significantly suppressed autophagy compared to the high LC3B-II fluorescence signal observed with rapamycin alone. The suppression of autophagy by wortmannin at the tested concentrations in rapamycin-induced autophagy cells measured by p62 fluorescence level was significant only at 10 µM and 20 µM compared to rapamycin alone.

**Autophagy inhibitor: L-asparagine**

For the four tested concentrations for l-asparagine, only the highest two concentrations (10 and 20 mM) achieved a statistically significant differences compared to the control. As previously mentioned, this was expressed differently compared to the other tested autophagy inhibitors due to the late stage autophagy inhibition of l-asparagine. Therefore, both LC3B-II (Figure 2.10) and p62 (Figure 2.11) expression increased for l-asparagine at 10 mM and 20 mM compared to the control, indicating the suppression of autophagosomes fusion with lysosomes. Interestingly, the combination of rapamycin with l-asparagine

treated cells did not present any significant differences in LC3B-II expression compared to rapamycin-induced autophagy treated cells. However, as with all other tested autophagy inhibitors, combining rapamycin with l-asparagine at the desired concentrations significantly increased p62 levels compared to l-asparagine alone.

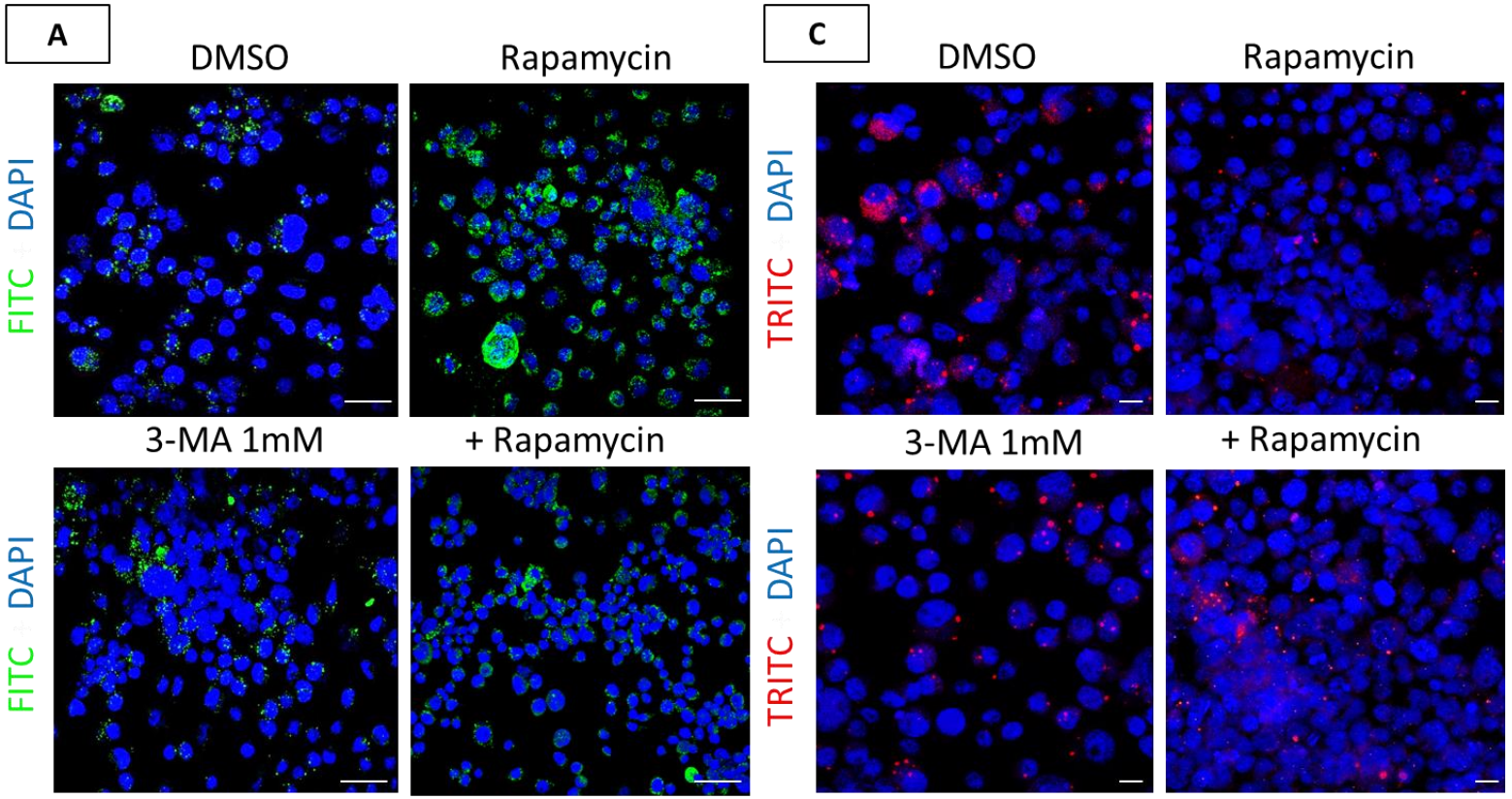
A
DMSO
Rapamycin
FITC + DAPI
3-MA 1mM
+ Rapamycin
FITC + DAPI
C
DMSO
Rapamycin
TRITC + DAPI
3-MA 1mM
+ Rapamycin
TRITC + DAPI

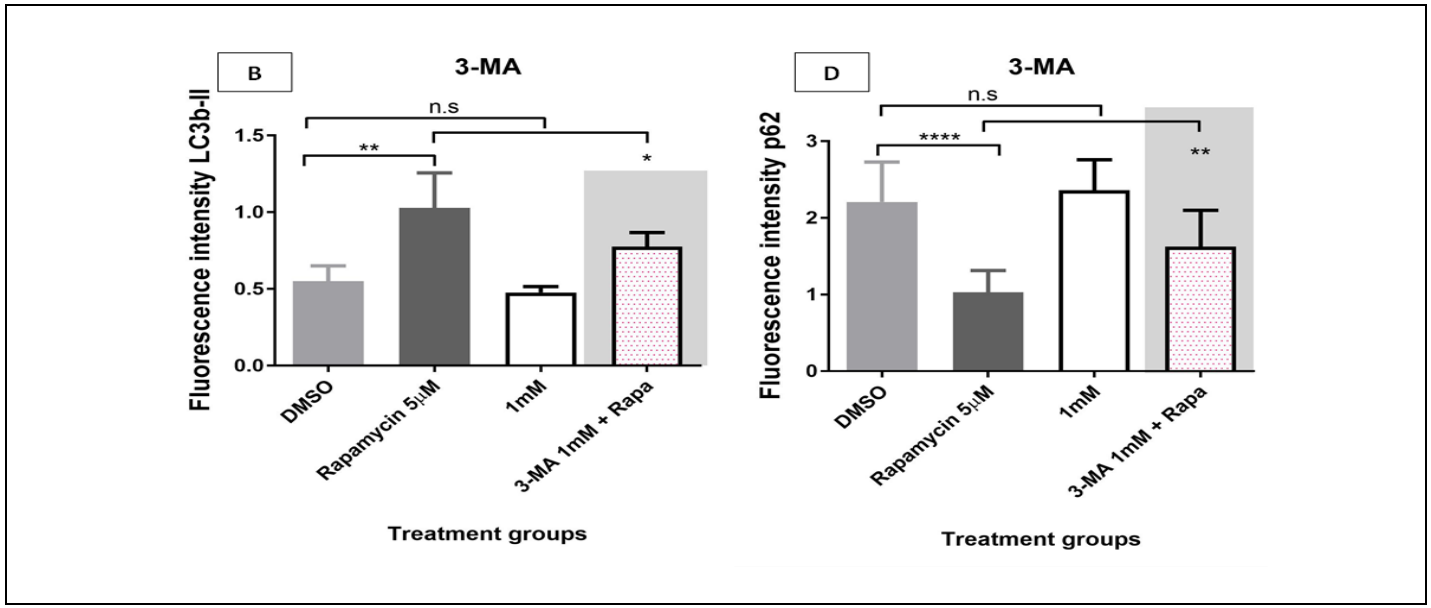


Figure 2. 6 Immunofluorescence staining for C6/36*Wp* cells treated with 3-ma.

Infected C6/36 cells with *w*AlbB were treated with autophagy inhibitor 3-ma at 1 mM, rapamycin at 5 µM (positive control), a combination of 3-ma and rapamycin and DMSO treated cells (vehicle control representing basal autophagy) for 7 days. Graphs (mean with SD) represent B) LC3BII or D) p62 fluorescence intensity in nine biological repeats per treatment group. Cells were fixed, permeabilized and incubated with primary and secondary antibodies. DAPI was used to counterstain cell nuclei (blue fluorescence). Autophagy inhibition is shown by a decrease in green puncta (decrease in LC3B-II) and an increase in red puncta (increase in p62). Scale bars in A are 50 µm and in C are 10 µm.

Statistical significance tested using Student's t-test, statistical significance was at $p \leq 0.05$. For p-value * = 0.01 to 0.05, ** = 0.01 to 0.001, *** = 0.001 to 0.0001, and **** ≤ 0.0001.

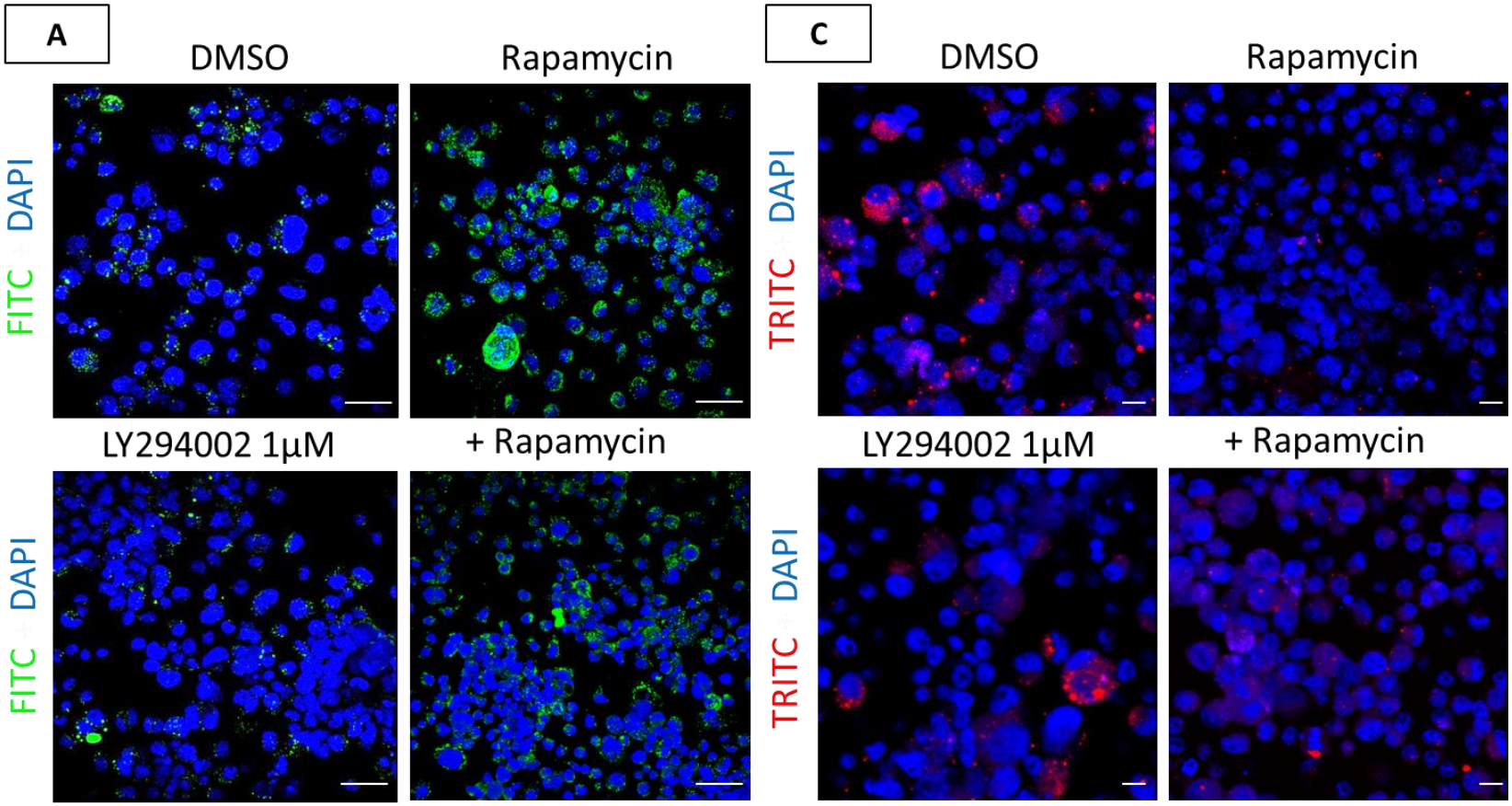
A
DMSO
Rapamycin
FITC + DAPI
LY294002 1μM
+ Rapamycin
FITC + DAPI
C
DMSO
Rapamycin
TRITC + DAPI
LY294002 1μM
+ Rapamycin
TRITC + DAPI

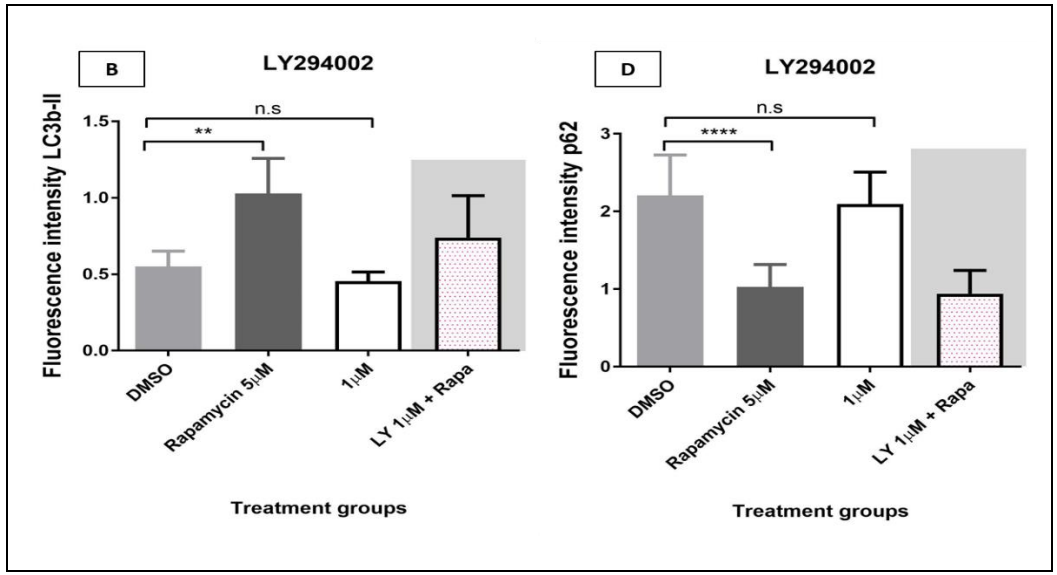


Figure 2. 7 Immunofluorescence staining for C6/36*Wp* cells treated with ly294002.

Infected C6/36 cells with *w*AlbB were treated with autophagy inhibitor ly294002 at 1 µM, rapamycin at 5 µM (positive control), a combination of ly294002 and rapamycin and DMSO treated cells (vehicle control representing basal autophagy) for 7 days. Graphs (mean with SD) represent B) LC3BII or D) p62 fluorescence intensity in nine biological repeats per treatment group. Cells were fixed, permeabilized and incubated with primary and secondary antibodies. DAPI was used to counterstain cell nuclei (blue fluorescence). Autophagy inhibition is shown by a decrease in green puncta (decrease in LC3B-II) and an increase in red puncta (increase in p62). Scale bars in A are 50 µm and in C are 10 µm.

Statistical significance tested using Student's t-test, statistical significance was at $p \leq 0.05$. For p-value * = 0.01 to 0.05, ** = 0.01 to 0.001, *** = 0.001 to 0.0001, and **** ≤ 0.0001.

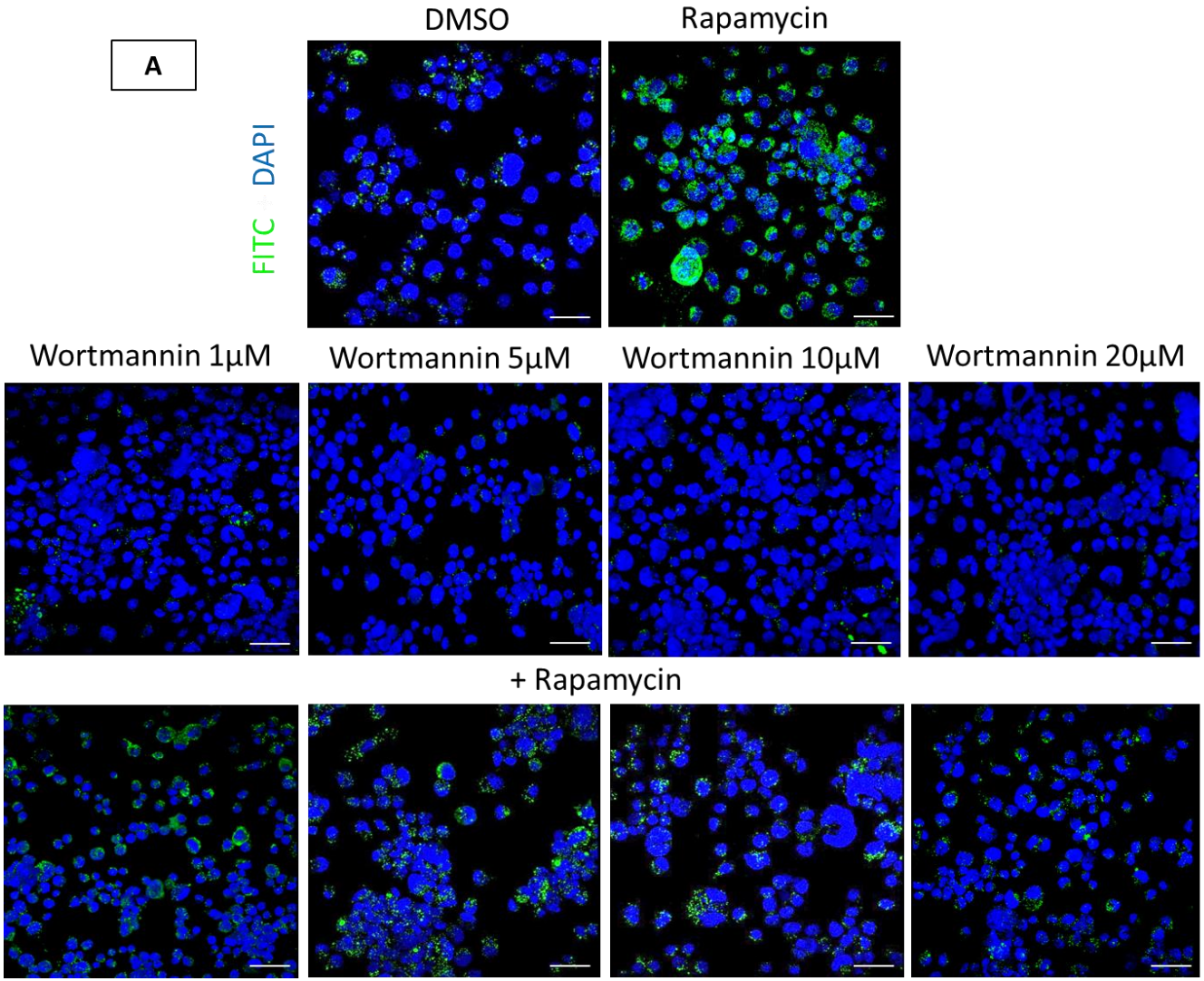
A
DMSO
Rapamycin
FITC DAPI
Wortmannin 1μM
Wortmannin 5μM
Wortmannin 10μM
Wortmannin 20μM
+ Rapamycin

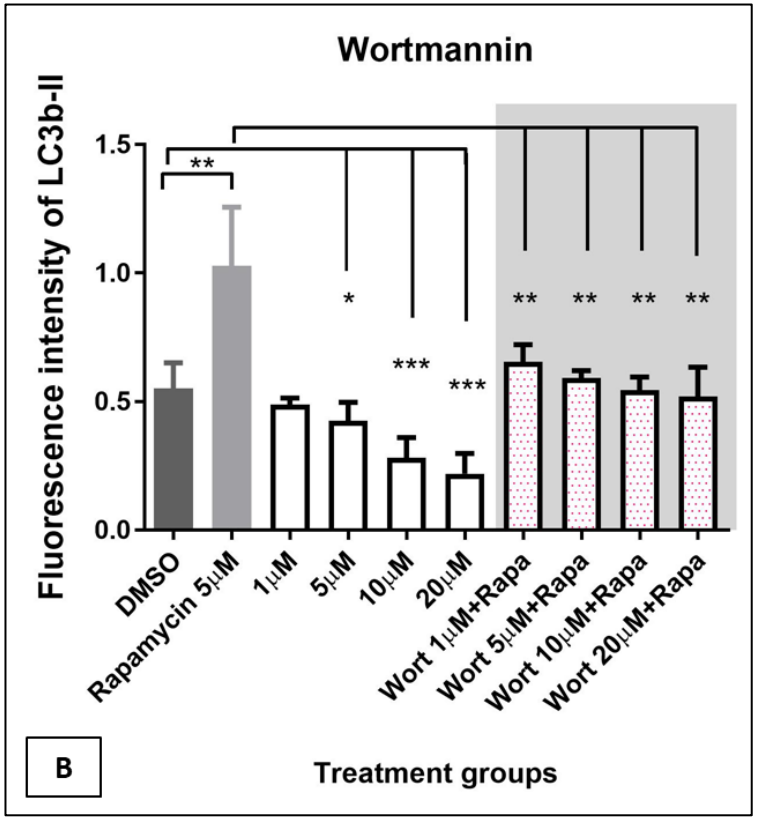


Figure 2. 8 LC3B-II Immunofluorescence staining for C6/36*W*p cells treated with wortmannin.

Infected C6/36 cells with *w*AlbB were treated with autophagy inhibitor wortmannin at 1-20 µM, rapamycin at 5 µM (positive control), a combination of wortmannin and rapamycin and DMSO treated cells (vehicle control representing basal autophagy) for 7 days. Graph (mean with SD) represents LC3BII fluorescence intensity in nine biological repeats per treatment group. Cells were fixed, permeabilized and incubated with primary and secondary antibodies. DAPI was used to counterstain cell nuclei (blue fluorescence). Autophagy inhibition is shown by a decrease in green puncta (decrease in LC3B-II due to suppression of autophagosomal formation). Scale bars in A are 50 µm.

Statistical significance tested using Student's t-test, statistical significance was at $p \leq 0.05$. For p-value * = 0.01 to 0.05, ** = 0.01 to 0.001, *** = 0.001 to 0.0001, and **** ≤ 0.0001.

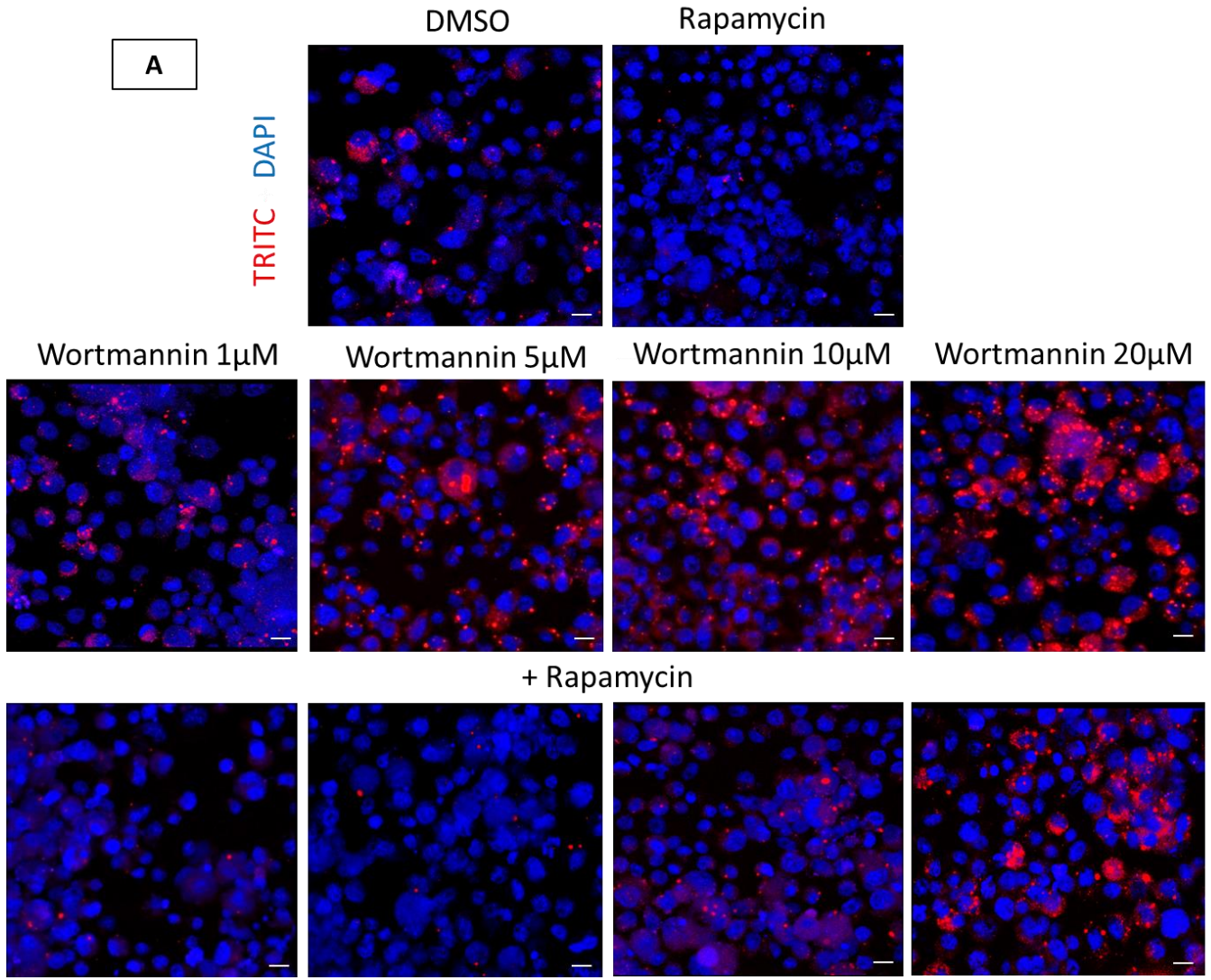
A
DMSO
Rapamycin
TRITC DAPI
Wortmannin 1μM
Wortmannin 5μM
Wortmannin 10μM
Wortmannin 20μM
+ Rapamycin

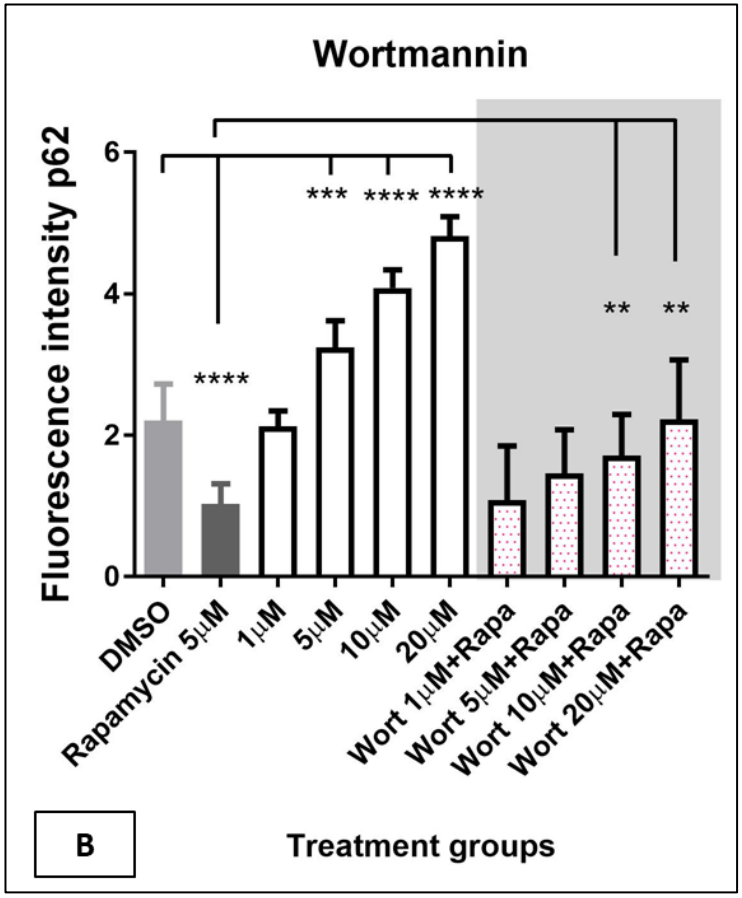


Figure 2. 9 P62 Immunofluorescence staining for C6/36*W*p cells treated with wortmannin.

Infected C6/36 cells with *w*AlbB were treated with autophagy inhibitor wortmannin at 1-20 µM, rapamycin at 5 µM (positive control), a combination of wortmannin and rapamycin and DMSO treated cells (vehicle control representing basal autophagy) for 7 days. Graph (mean with SD) represents p62 fluorescence intensity in nine biological repeats per treatment group. Cells were fixed, permeabilized and incubated with primary and secondary antibodies. DAPI was used to counterstain cell nuclei (blue fluorescence). Autophagy inhibition is shown by an increase in red puncta (increase in p62 due to the suppression of its autophagic degradation). Scale bars in A are 10 µm.

Statistical significance tested using Student's t-test, statistical significance was at $p \leq 0.05$. For p-value * = 0.01 to 0.05, ** = 0.01 to 0.001, *** = 0.001 to 0.0001, and **** ≤ 0.0001.

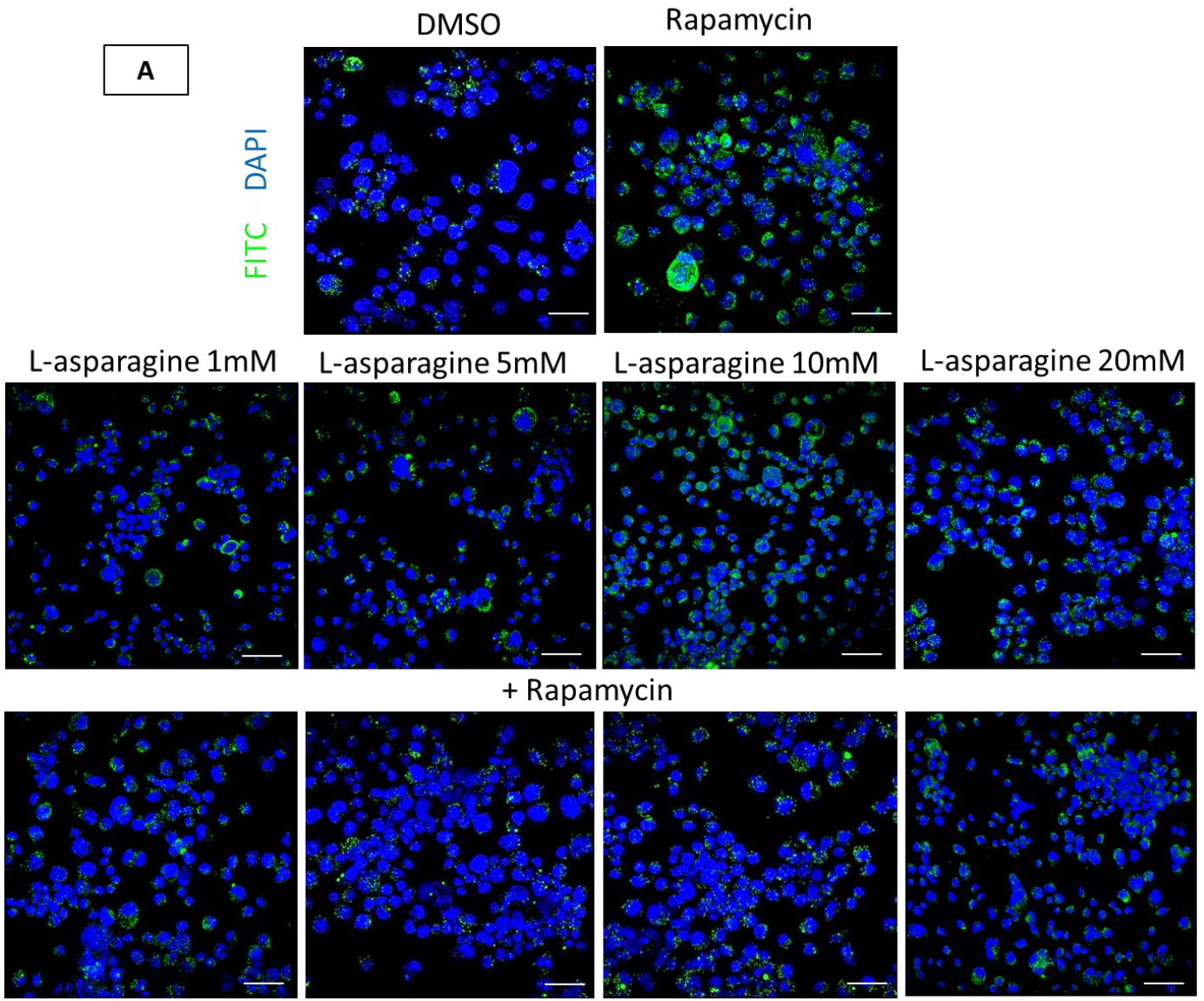
A
DMSO
Rapamycin
FITC + DAPI
L-asparagine 1mM
L-asparagine 5mM
L-asparagine 10mM
L-asparagine 20mM
+ Rapamycin

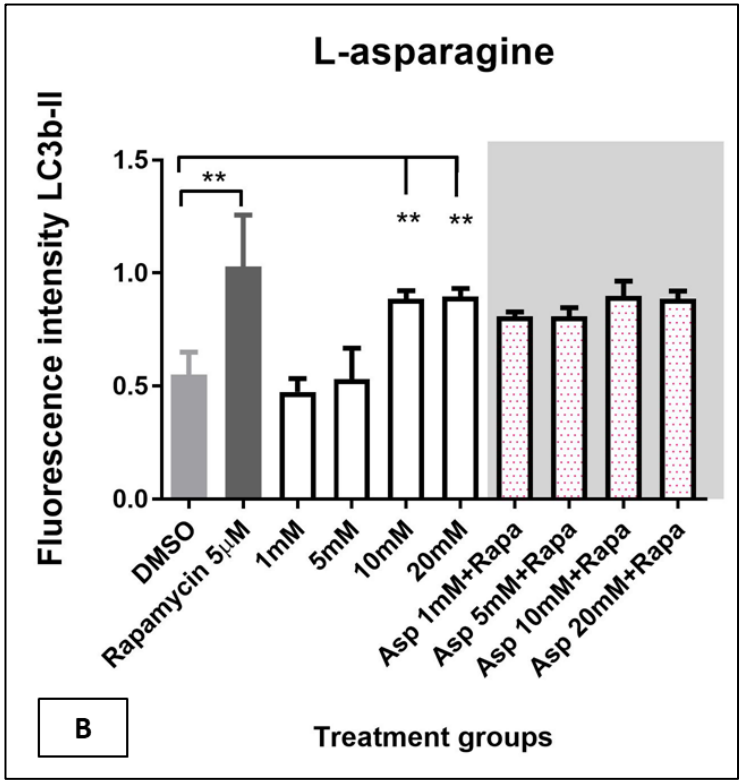


Figure 2. 10 LC3B-II Immunofluorescence staining for C6/36*W*p cells treated with l-asparagine.

Infected C6/36 cells with *w*AlbB were treated with autophagy inhibitor l-asparagine at 1-20 mM, rapamycin at 5 µM (positive control), a combination of l-asparagine and rapamycin and DMSO treated cells (vehicle control representing basal autophagy) for 7 days. Graph (mean with SD) represents LC3BII fluorescence intensity in nine biological repeats per treatment group. Cells were fixed, permeabilized and incubated with primary and secondary antibodies. DAPI was used to counterstain cell nuclei (blue fluorescence). Autophagy suppression with a late autophagy inhibitor is presented by an increase in green puncta (increase in LC3B-II due to blocking the fusion of autophagosomes with lysosomes causing autophagosome accumulation). Scale bars in A are 50 µm.

Statistical significance tested using Student's t-test, statistical significance was at $p \leq 0.05$. For p-value * = 0.01 to 0.05, ** = 0.01 to 0.001, *** = 0.001 to 0.0001, and **** ≤ 0.0001.

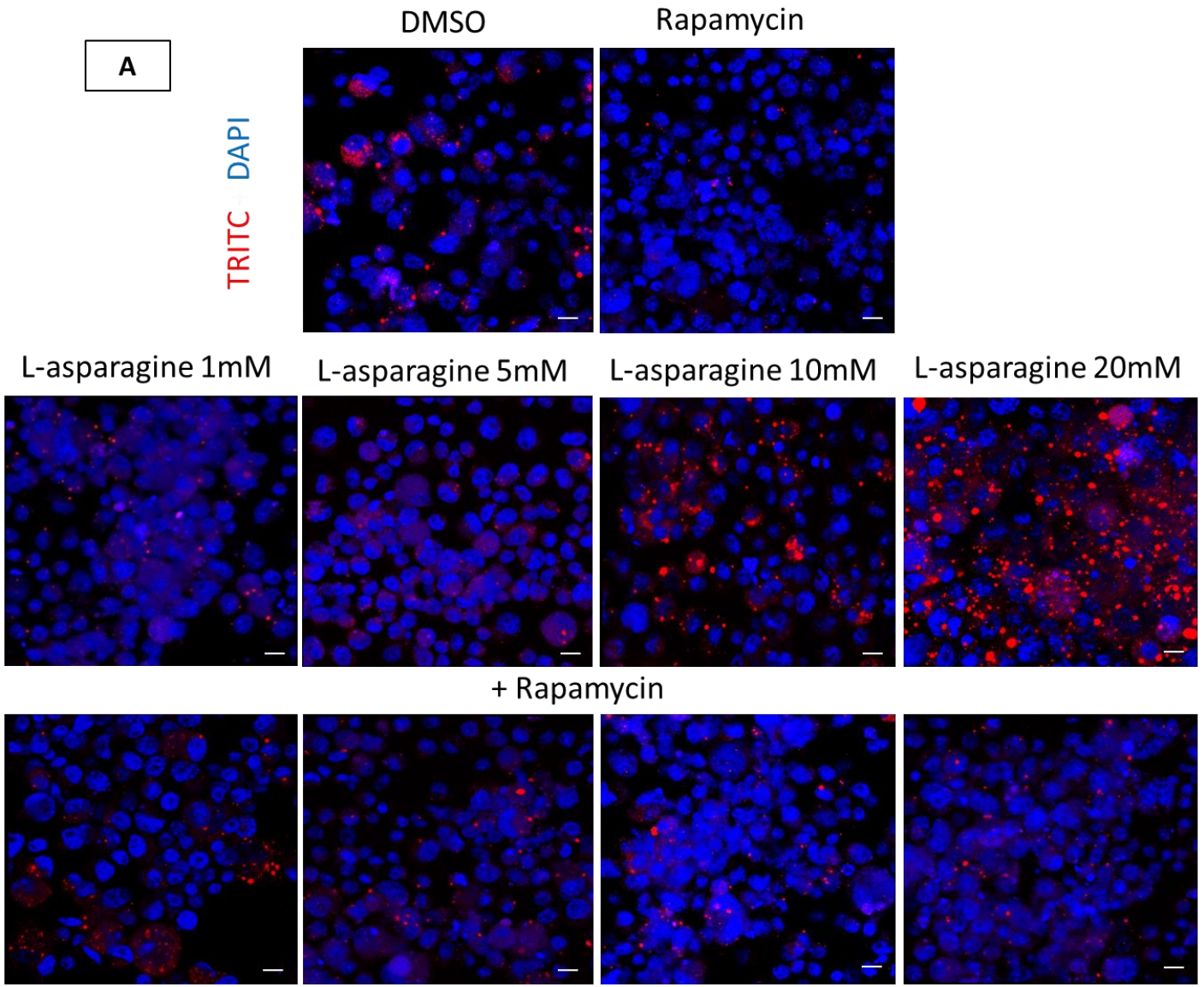
A
DMSO
Rapamycin
TRITC DAPI
L-asparagine 1mM
L-asparagine 5mM
L-asparagine 10mM
L-asparagine 20mM
+ Rapamycin

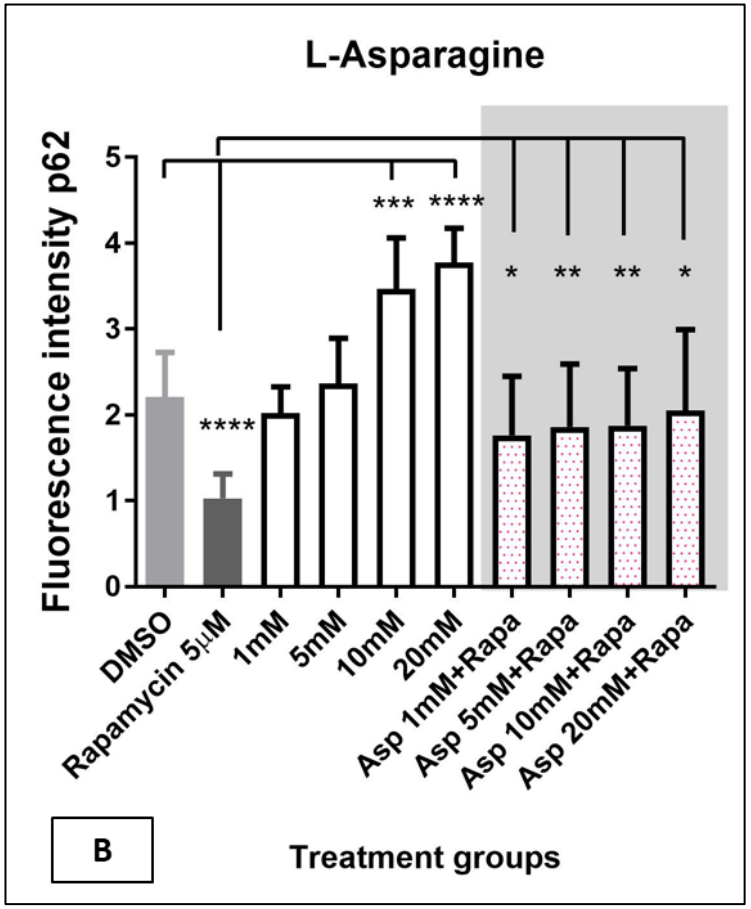


Figure 2. 11 P62 Immunofluorescence staining for C6/36*W*p cells treated with l-asparagine.

Infected C6/36 cells with *w*AlbB were treated with autophagy inhibitor l-asparagine at 1-20 mM, rapamycin at 5 µM (positive control), a combination of l-asparagine and rapamycin and DMSO treated cells (vehicle control representing basal autophagy) for 7 days. Graph (mean with SD) represents p62 fluorescence intensity in nine biological repeats per treatment group. Cells were fixed, permeabilized and incubated with primary and secondary antibodies. DAPI was used to counterstain cell nuclei (blue fluorescence). Autophagy inhibition is shown by an increase in red puncta (increase in p62 due to the suppression of its autophagic degradation). Scale bars in A are 10 µm.

Statistical significance tested using Student's t-test, statistical significance was at $p \leq 0.05$. For p-value * = 0.01 to 0.05, ** = 0.01 to 0.001, *** = 0.001 to 0.0001, and **** ≤ 0.0001.

### 2.4.4 Western blot

Three autophagy inhibitors (ly294002 at 1 µM, wortmannin at 1-20 µM and l-asparagine at 1-20 mM) were assessed in lysed C6/36*Wp* mosquito cell line using western blot analysis as a confirmatory step to validate the observations in the immunofluorescence staining method (section 2.4.3). 3-ma was not examined using western blot due its toxic effect in the viability/cytotoxicity experiment (section 2.4.2).

The results for the inhibitory activity of the chemical inhibitors using western blot are presented in Figure 2.12 using autophagy markers LC3B (Figure 2.12 A) and p62 (Figure 2.12 B). For the full gel of the antibody blotting membrane in this experiment please refer to Appendix A (Figure A2). In both immunoblots, DMSO used as a vehicle control, represented the basal level of autophagy in C6/36*Wp* cells. LC3B antibody was expressed in the immunoblot in two bands: LC3B-I at a protein molecular weight ~ 16 kDa and LC3B-II at ~14 kDa. Unlike LC3B-I, the second form LC3B-II is conjugated with lipids and theoretically should have a higher molecular weight, although it has been found to migrate at an apparent lower protein size due to its higher mobility during gel electrophoresis (130, 134). As the conversion of LC3B-I to LC3B-II indicates the occurrence of autophagic activity, the band intensity of LC3B-II expresses autophagosomal formation (136). The expression of LC3B-I was stable throughout the treatment groups (Figure 2.12) and its expression was not used to indicate autophagic activity, this was previously noted in other studies (147, 152-154).

P62 was represented by a single protein band at ~80 kDa. Previous studies on insect cells have found p62 to exhibit a similar molecular weight using western blot (98, 140, 155, 156). As shown in both blots, Beta-actin of a molecular size at ~ 40 kDa was used as a loading control to ensure that an equal amount of protein concentration was loaded per lane.

In a similar manner to the immunofluorescence staining experiment, rapamycin was used as a positive control and this is presented alone and combined with the three autophagy inhibitors. Due to rapamycin's autophagic promoting role, the expression of LC3B-II was more prominent (due to autophagosome production), while p62 appeared faint in the blot (representing higher autophagic degradation).

In the case of ly249002, the reduced band of LC3B-II was similar in intensity to the DMSO control. This suggests that at this concentration of 1 µM only basal autophagy is exhibited and there appeared to be no inhibitory effect by ly294002. Similarly, this was also observed for p62 degradation. As expected, combining ly294002 at 1 µM with rapamycin did not reduce autophagy activity showing no observable decrease in fluorescence intensity of LC3B-II compared to rapamycin and a reduced band of p62 expression appeared in the combination group.

At all tested concentrations of wortmannin, there were no observed bands for LC3B-II indicating its autophagic inhibitory role by blocking autophagosome generation. For p62, the lower concentration of wortmannin tested at 1 µM showed no difference from the control and there appeared to be a concentration-dependent increase of intensity with increasing concentrations of wortmannin. The findings in the rapamycin and wortmannin groups point to a similar conclusion, where autophagy was suppressed by a lower and higher expression of LC3B-II and p62, respectively.

For a late-stage autophagy inhibitor such as l-asparagine, the expression of LC3B-II should increase in autophagy inhibition, suggesting the blocking of autophagosomes transforming to autophagolysosomes (157). As shown in Figure 2.12 A, there appeared to be a gradually increase in intensity of the LC3B-II band with increasing concentrations of l-asparagine. It is important to note that compared to the control, there appeared to be no noticeable difference between the reduced intensity of the LC3B-II band at concentrations 1 mM and 5 mM for l-asparagine. Similar findings were also observed when immunoblotting p62 in l-asparagine, where only at 10 and 20 mM l-asparagine appeared to have an inhibitory role compared to the control. L-asparagine when combined with rapamycin did not present a noticeable difference in LC3B-II expression compared to rapamycin alone. Conversely, p62 expression was increased when l-asparagine was combined with rapamycin compared to rapamycin alone.

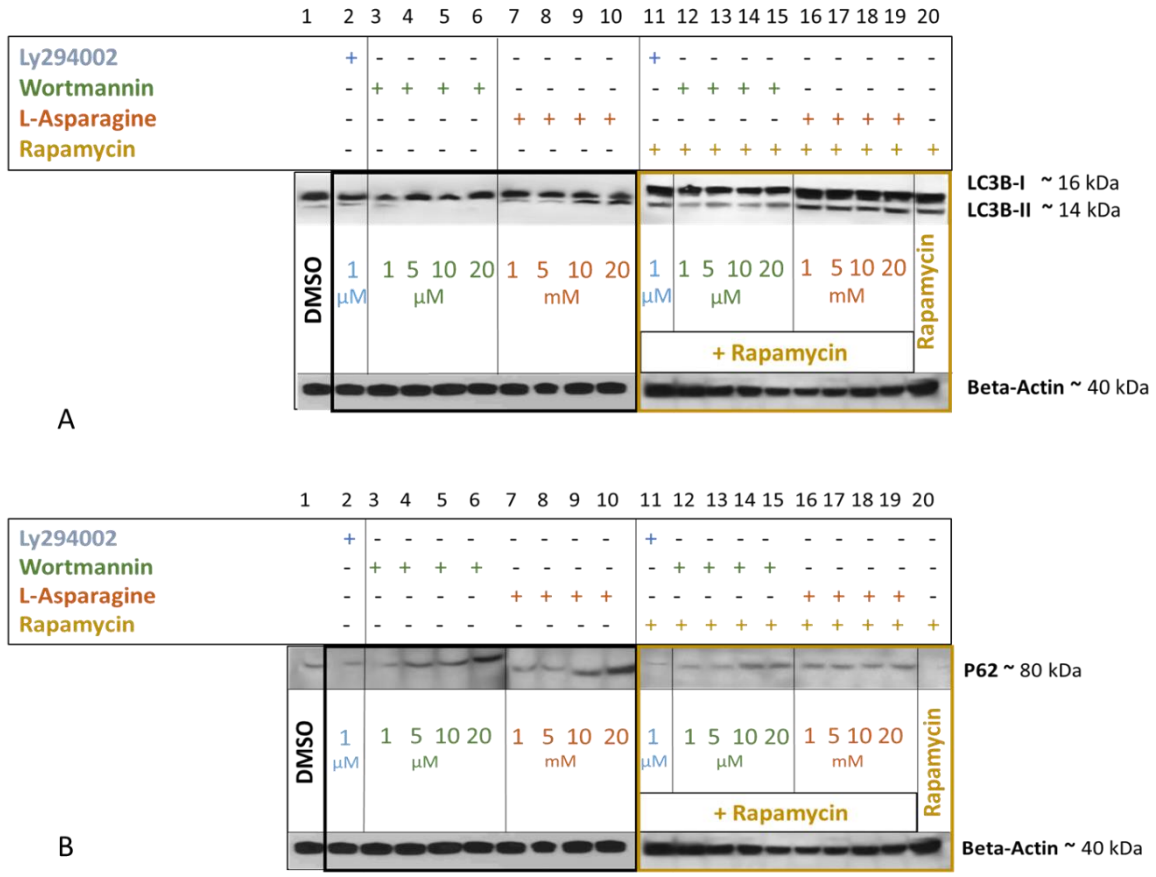


Figure 2. 12 Detection of LC3B and p62 expression for autophagy inhibitors in C6/36*Wp* cells using Western blot.

C6/36 mosquito cells infected with *Wolbachia w*AlbB were treated with: DMSO – vehicle control (lane 1), Ly294002 at 1 µM (lane 2), wortmannin from 1-20 µM (lane 3-6), and l-asparagine from 1-20 mM (lane 7-10) for 7 days. A combination of rapamycin with Ly294002 (lane 11), wortmannin (lane 12-15) and l-asparagine (lane 16-19) and rapamycin alone - positive control (lane 20) were also analysed. Reduced protein extracts of cells were loaded at 50 µg/40 µl per lane into 4-12% bis tris SDS-PAGE gels. Separated proteins were transferred into nitrocellulose membrane, blocked with 5% BSA-TBST and incubated with primary and secondary antibodies.

Western blot protein expression is presented in **A)** for rabbit anti-LC3B (LC3B-I at 16 kDa and LC3B-II at 14 kDa) and **B)** rabbit anti-p62 (at 80 kDa). A reference protein; mouse anti-beta actin was used as a control with a size of approximately 40 kDa. In autophagy inhibition: **A)** LC3B-II intensity decreased (for early autophagy inhibitors) and increased (for late autophagy inhibitor, l-asparagine) **B)** p62 intensity increased.

## 2.5 Discussion

The series of experiments performed in this chapter have successfully achieved their role in determining suitable concentrations of pre-selected chemical autophagy inhibitors by examining their suitability and inhibitory profile in mosquito cell line C6/36*Wp*. Furthermore, it has presented a methodology to determine optimum concentrations of autophagy inhibitors in C6/36*Wp* cells based on their impact on cell viability/cytotoxicity, as well as their impact on cell growth.

For the four tested autophagy inhibitors, the experiments conducted on C6/36*Wp* cells for cell growth effect and cell viability/cytotoxicity have produced consistent findings. The results have shown that 3-ma is not a suitable option for inhibiting autophagy in C6/36 cells. 3-ma has been shown to have a significant toxic effect over the 8-day culture period, even at the lowest tested concentration of 1 mM. While 3-ma did not impact cell growth over shorter treatment periods, this observation requires further experimentation and validation in other insect cells. Most of the previous research on 3-ma as an autophagy inhibitor was conducted on mammalian cells (116, 119, 158-161). However, concerns have been proposed with the use of 3-ma due to its effect on cell proliferation and other signalling pathways, including apoptosis, even within the commonly used concentrations for autophagy inhibition (162-166). Additionally, there is evidence to suggest that 3-ma has a dual role in the autophagy cascade, as it may inhibit and activate autophagy (117). Two of the conditions highlighted in the literature for 3-ma to promote autophagy were culturing cells in full nutrient medium and long experimentation time. In the same study, 3-ma did not activate autophagy in starved cells and culturing for less than 9 hours (117).

In this research, the results of immunofluorescence staining for autophagy protein markers LC3B-II and p62 for C6/36*Wp* cells treated with 3-ma at 1 mM (lowest concentration tested) did not inhibit autophagy. This indicates that a higher concentration of 3-ma would have been needed to suppress autophagy in C6/36 cells. Previous studies using 3-ma on C6/36 cell line (in both *Wolbachia* infected and uninfected cells) observed an effective concentration for autophagy inhibition at 5 mM, however this concentration was found to have a toxic effect in our study (87). Experiments performed on non-insect cells have found an optimum inhibitory concentration for 3-ma to be between 5-10 mM (127, 167, 168).

Therefore, further research is needed to enhance our understanding on using 3-ma on insect cells considering the findings of our study.

The results for ly294002 showed a lack of toxicity at 1 µM, while all the higher concentrations tested were toxic. This was further confirmed through analysing its effect on cell growth, where the same concentration at 1 µM did not hinder cell proliferation. However, ly294002 treated cells at 1 µM failed to achieve a significant autophagy inhibitory effect when analysed by immunofluorescence staining and western blot. Previous studies on ly294002 as an autophagy inhibitor have been mainly conducted on mammalian cells, with concentrations ranging between 1-100 µM (116, 121, 134, 169, 170). A single study has suggested that the autophagic effect of ly294002 was concentration-dependent and it was found to cause cell cycle arrest at 25 µM in mouse embryo fibroblast cells (171). This suggests that the concentration of ly294002 may operate differently according to the type of cells, both in terms of toxicity and inhibitory effect on autophagy. Recent studies have shown that ly294002 may not be suitable as a PI3Ks inhibitor as it can also inhibit mTOR through an ATP binding site, thereby activating autophagy (172). To conclude, based on our experimentation ly294002 was not a suitable chemical to evaluate autophagy on C6/36*Wp* cells.

Based on our results, both wortmannin and l-asparagine have been observed to be suitable autophagy inhibitors in C6/36 cells in terms of their lack of toxicity in all tested concentrations. Additionally, we were able to determine a suitable range of concentrations for both chemical compounds that successfully inhibited autophagy (wortmannin= 5-20 µM, l-asparagine= 10-20 mM).

In the case of wortmannin, the concentrations tested in our study were between 1-20 µM, and this range was higher than most of the previous research on wortmannin as an autophagy inhibitor, where concentrations ranged between 10 nM-1 µM (116, 120, 148, 161, 170, 173, 174). With regards to C6/36 cells, wortmannin has been previously used to inhibit autophagy at 10 µM and this was within the suitable concentration observed in our study (87). While little is known about the suitable upper limit of wortmannin concentration in insect cells, one study on Hela cells has suggested that 50 µM may induce cell death

(162). In conclusion, from the findings of this study wortmannin between 5-20 µM has been observed to be a suitable autophagy inhibitor for C6/36*Wp* cells.

From the results of this chapter, while l-asparagine has been found to be non-toxic in all tested concentrations, autophagy inhibition was only achieved between 10-20 mM. Other studies have also achieved successful autophagy suppression at similar concentrations using rat hepatocytes (123, 125). Moreover, previous research conducted on other amino acids (for example histidine, leucine and glutamine) acting as autophagy inhibitors, whether combined or alone, have also recorded their inhibitory effect through lysosomal dysfunction in higher concentrations (125, 175-177).

In this study, we used rapamycin as a control for autophagy activation, alone or combined with different autophagy inhibitors. The use of rapamycin is well documented as a promoter of autophagy and has been used in previous studies to assess autophagy inhibitors, including 3-ma and wortmannin (178-181). Voronin *et al.* (87) used rapamycin at 5 µM to activate autophagy in both *B. malayi* worms and C6/36 mosquito cells (infected and uninfected with *Wolbachia*). In addition, the same study assessed autophagy promotion through nutrient starvation, where serum deprivation in C6/36*Wp* cells activated autophagy. The potential of using other means of autophagic induction are described in more detail in Chapter 3.

An observation worth mentioning in our immunofluorescence experiment using LC3B-II for the inhibitory effect of l-asparagine when combined with rapamycin was that it did not provide a statistically significant result compared to rapamycin alone. Previous research has also found that levels of LC3B-II when analysing late stage autophagy inhibitors have presented similar findings to our observations (147). A proposed cause of this is due to the lack of generation of autophagosomes and autophagic degradation was inhibited by l-asparagine (a late stage autophagy inhibitor) (147). Conversely, the use of p62 in our study provided a more conclusive and expected result for l-asparagine combined with rapamycin.

While there are gaps in the current knowledge of the role of amino acids (such as l-asparagine) in the autophagy inhibition cascade, it has been found that rapamycin and amino acids influence mTORC1 in opposite directions. Meijer *et al.* (128) have proposed that

in addition to disrupting the delivery of autophagosomes to fuse with lysosomes, amino acids may also activate mTORC1.

The use of more than one method in this research to measure autophagic inhibition is the optimum approach and has been recommended in the literature. While there is no “gold standard” method to measure autophagic activity, the two methods used in this research, immunofluorescence and western blot, have been widely proposed as suitable and valid methods (98, 106, 133, 152).

There are two important points worth mentioning with regards to the protein markers (LC3B and p62) used for western blot in our study. First, in our interpretation of LC3B in western blot, only LC3B-II was used to analyse autophagic inhibition (blocking autophagasomal formation) while LC3B-I remained unchanged in all treatment groups. Previous studies have also commented on the unreliable role of LC3B-I in measuring autophagic activity in certain conditions or cell types (132, 147). Second, while p62 in mammalian cells has a protein molecular weight of 62 kDa, it has been observed to have a higher molecular weight in insect cells at 80-100 kDa (98, 154, 156). This correlates with our findings for the bands obtained in western blot for p62, which were observed at ~80 kDa.

An important limitation in our western blot experiments is that we were unable to quantify band intensity (densitometry). This was due to the occurrence of two bands expressed by the LC3B antibody, which were close in terms of their molecular weight on the SDS-PAGE gels (131). Therefore, attempting to quantify these bands using ImageJ software may present inaccurate results.

In conclusion, we were able to determine two autophagy inhibitors, wortmannin and l-asparagine, that have successfully inhibited autophagy in C6/36*Wp* cells without affecting cell viability and growth. In the upcoming chapters both wortmannin and l-asparagine will be used for their autophagic inhibitory roles in order to study the main aim and objectives of our research.

# Chapter 3 Monitoring and measuring antibiotic-induced autophagy

## 3.1 Chapter overview:

In this chapter I will present a series of experiments to examine autophagic induction by different classes of antibiotics on various cell lines (both insect and mammalian cells) and *B. malayi*. The chapter will start with a brief background section of the previous literature involving autophagy activation, through chemical, metabolic and physiological methods. This will be followed by a literature review of studies examining antibiotic-induced autophagy. As previously noted, autophagy as a concept was covered in detail in Chapter 1, while the chemical inhibition of autophagy was discussed in Chapter 2 of this thesis.

Four sets of experiments are presented in this chapter. In the first group of experiments, autophagy activation was monitored using eight different antibiotics from five diverse classes (doxycycline, rifampicin, moxifloxacin, sparfloxacin, levofloxacin, ciprofloxacin, amoxicillin and streptomycin) in four different cell lines and nematodes: *Aedes albopictus* C6/36 cells (and C6/36*Wp*), *Spodoptera frugiperda* (SF9) cells, *Brugia malayi* microfilariae, Human monocytic leukaemia (THP-1) cells and Madin-Darby Canine Kidney (MDCK) cells. In the second set of experiments, three highly specific anti-*Wolbachia* agents recently prioritised by the A-WOL consortium (TylAMac$^{TM}$, AWZ1066S and fusidic acid) were tested in C6/36 cells for their autophagy activation. The third and fourth group of experiments examined autophagic induction of the same eight antibiotics mentioned above to investigate concentration-dependency and the timeframe for activation.

## 3.2 Background

### 3.2.1 Autophagy induction: environmental, physiological, and chemical

Numerous factors ranging from environmental, physiological, and chemical sources may influence and induce autophagy in different cells and tissues. This upregulation can be measured using the same experimental techniques described in Chapter 2 for monitoring and measuring autophagy inhibition.

Basal autophagy has been observed to naturally occur at low levels in almost all species, including humans, and has been widely described in the literature. There is evidence to suggest that basal autophagy may provide a benefit to organisms through maintaining their internal homeostatic environment (106, 182, 183). An example of how this might be achieved is through its regulation of accumulated damaged proteins and eliminating dysfunctional cellular organelles (91, 184-186). In *Drosophila* species, basal autophagy can play a role in targeting damaged mitochondria to ensure the survival of the organism (187).

**Starvation and nutrient depletion**

Modification of environmental and physiological conditions can influence the induction of autophagy in various organisms. These environmental and physiological stimuli can be intracellular or extracellular in their origin (99, 188). One of the commonest stress stimuli that can induce macroautophagy is starvation, which can occur naturally or be achieved experimentally by energy or nutrient withdrawal (189). Examples of essential nutrients and elements that have been observed to induce autophagy when depleted include amino acids, nitrogen, growth factors, glucose, carbon, oxygen and sulphate (92, 190-192). Experiments have observed that depletion of amino acids result in the highest starvation-induced autophagy (88, 193, 194). Autophagy induction through nutrient starvation mostly occurs through an mTORC1 dependent manner, but can also occur independently of mTOR for certain nutrients, such as amino acids (92, 195-197).

**Environmental stimuli: Oxidative stress, hypoxia, acidic pH**

A second example of a stimuli that can activate autophagy is reactive oxygen species (ROS) formation. These are molecules that contain a reduced form of oxygen, such as peroxide compounds, superoxide and hydroxyl radicals (198). ROS are mainly generated intracellularly by mitochondria through certain conditions which include nutrient deficiency, resulting in an increase ATP consumption and hence ROS formation (199). Due to their link to mitochondria, it is believed that chronic damage to these organelles could potentially lead to an increase in ROS formation. This is referred to as mitophagy (200, 201). A lesser studied method of ROS formation, specifically superoxide production, is generated by nicotinamide adenine dinucleotide phosphate (NADPH) oxidase 2 (NOX2), occurring on the surface of macrophages and neutrophils following microbial infection. When autophagy is induced in this manner it is referred to as xenophagy (198, 202, 203).

Hypoxia is recognised as an important stimulus for autophagic induction, which can occur to due ROS accumulation (199). This can be achieved through ATP reduction in hypoxic conditions, in turn increasing AMP-activated protein kinase (AMPK), thereby inactivating mTORC1 and inducing autophagy. Hypoxia can also influence autophagic induction by activating hypoxia induced factor-1 alpha (HIF-1a). Activation of HIF-1a results in the inhibition of mTORC1 by the inhibitory effect of hypoxia responsive genes on Ras homolog enriched in brain (Rheb) guanosine triphosphate enzymes (GTPase), hence inducing autophagy (92, 99, 189, 204). Hypoxic conditions can also occur due to the presence of certain types of cancer, which could potentially lead to an increase in autophagic activity. In the presence of hypoxia, cancer cells could hijack the autophagy cascade in order to provide essential nutrients for tumour growth (205-208).

A final environmental factor that can influence autophagy induction is the occurrence of acidic pH conditions. Despite the evidence documenting the role of a low pH to be linked with other autophagy inducers, such as hypoxia, nutrient starvation and ROS, recent evidence has shown that acidic pH alone may induce autophagy (209-211). This was observed experimentally in osteoblastic cells, where acidic media directly promoted autophagy in the absence of other environmental stimuli (209). Moreover, exposing melanoma cells to acidic media induced autophagy in an mTOR dependent manner (210).

**Autophagy induction by microorganisms**

While certain microorganisms can inhibit autophagy, as previously discussed in Chapter 2, there are also several that can induce autophagy within a host. From a general perspective, intracellular bacteria may induce autophagy in order to seize nutrients from host cells produced through autophagy to ensure their own survival (104, 188). One example of this is observed in *Anaplasma phagocytophilum*, which can promote autophagosome formation by secreting the *Anaplasma* translocated substrate 1 (Ats-1) effector, resulting in an increase in autophagic influx (188, 212). Certain bacteria may also form intracellular vacuoles that accumulate autophagy specific markers, thereby promoting autophagy (188). Examples of such vacuole forming bacteria include *Yersinia* species, such as *Y. pseudotubeculosis* and *Y. pestis*, *Coxiella burnetii, Brucella abortus* and *Legionella pneumophila* (188, 213-219).

In the case of *Staphylococcus aureus* infection, there is evidence to suggest that toxins secreted by the bacteria may increase autophagic activity by influencing Atg5 and possibly participating in the completion of autophagosomes (188, 220, 221). Similarly, in parasitic infections, for example *Toxoplasma gondii,* autophagy can be induced through activating Atg5 in human cell lines (222).

With regards to viral infections, both RNA and DNA viruses have been found to upregulate the autophagic pathway. For instance the RNA viruses; poliovirus, dengue virus, coronavirus and rhinovirus and the DNA virus, Epstein-Barr virus, have been shown to influence autophagic induction in order to promote viral replication (223-225). .

Previous studies on *Wolbachia* have shown the induction of autophagic activity in *Brugia malayi wBm*, *Aedes albopictus wAlbB* and *Drosophila melanogaster wMelPop* (87), which is particularly upregulated during rapid population expansion and is a key regulator of *Wolbachia* populations. In arthropods, Le Clec'h *et al.* (226) observed that horizontal transfer of *Wolbachia* from *Armadillidium vulgare* transfected into another host, *Porcellio d. dilatatus,* can activate autophagy in the new host. This activation of autophagy resulted in disrupting the central nervous system of the new host.

**Chemical inducers of autophagy**

Chemical inducers may activate autophagy through inhibiting mTOR. An example of this is Torin1, which is defined as a "selective ATP-competitive small molecule mTOR inhibitor" (227). Torin1 affects both mTORC1 and mTORC2 (227, 228). A more recent discovery is that of Torin2, that has been shown to have similar but more efficient pharmacological properties than Torin1, as well as having an additional function of inhibiting phosphatidylinositol 3-kinases (PI3Ks). Hence, Torin2 produces a stronger autophagic induction than its predecessor (100).

Certain chemicals can induce autophagy by specifically inhibiting mTORC1 and not mTORC2, for example rottlerin, amiodarone and niclosamide. In the case of rottlerin, the inhibition of mTORC1 is achieved through the presence of tuberous sclerosis complex 2 (TSC2), while this has not been observed for the other two chemicals (229, 230).

Lithium, a chemical used therapeutically to treat bipolar disorder, is described in the literature as an mTOR-independent inducer of autophagy (231, 232). It activates autophagy by reducing inositol levels through the blocking of inositol monophosphatase (IMPase). Similar observations were also documented in other psychotropic drugs, such as sodium valproate and carbamazepine, where the former was found to decrease inositol 1,4,5-trisphosphate (IP3) in addition to its effect on inositol (229, 233).

Several agents belonging to L-type calcium channel blockers, including loperamide and verapamil, are presented in the literature as autophagy inducers. This induction is achieved by their ability in decreasing intracellular calcium concentrations thereby inhibiting calpains, a form of cysteine proteases specific to calcium (229, 234).

Other chemicals that have proven autophagic inducing properties include minoxidil, resveratrol, spermidine and trehalose (100).

**Antibiotic-induced autophagy**

Two antibiotics used in the treatment of *Mycobacteria tuberculosis*, isoniazid and pyrazinamide, were found to induce autophagy in macrophages infected with the bacteria. The proposed mechanism of this induction was believed to have occurred through the involvement of ROS production, as well as increase in calcium levels and AMPK activation (235). In a second study another anti-TB drug, rifampicin also activated autophagy by targeting mitochondria and initiating their degradation (236). Additionally, rifampin was also observed to initiate ROS accumulation in *M. tuberculosis*, an important inducer of autophagy (237).

With regards to the tetracycline class of antibiotics, three have been identified as possible autophagy inducers. The first of these to be recognised was tigecycline, which upregulated autophagy in an mTOR dependent manner in human gastric cancer cells (238). Similar autophagic inducing characteristics were also observed for minocycline, which enhances autophagy in a number of cell types, including cardiomyocytes (239), neurons (240) and vascular endothelial cells (241), but can also suppress autophagy in other systems (242, 243). Another tetracycline antibiotic, doxycycline, which was used in the experiments conducted in this chapter, was found in a previous study to induce autophagy, possibly through its known effect on mitochondria and ROS formation (244). Both doxycycline and minocycline cause mTOR inhibition in hepatocyte cell lines, which may contribute to tetracycline-induced hepatoxicity adverse effects (245).

Several other antibacterial agents have been described as potential autophagy inducers, including ohmyunsamycin, which activates autophagy by influencing AMPK pathway (246).

**Rapamycin**

One of the commonest used autophagy inducers is the macrolide and immunosuppressant agent rapamycin, sometimes referred to as sirolimus. Rapamycin acts by inhibiting mTORC1 through binding with FK506-binding protein 12 kDa (FKBP12), leading to the stability of regulatory associated protein of mTOR (Raptor) (100, 118, 227, 229). While rapamycin mainly inhibits mTORC1, there is evidence that prolonged exposure may also inhibit mTORC2 in certain cell lines (247). Due to its widespread use and autophagy inducing

characteristics in many different cell lines, rapamycin was selected as an autophagy inducing control (positive control) in the experimentation performed in this chapter (87, 178, 180, 181).

An analogue of rapamycin, CCI-779 (or temsirolimus), has shown to have a similar autophagic inducing effect. CCI-779 has gained prominence recently due to its potential use in the treatment of solid tumours (118, 248). Interestingly, while CCI-779 operates in the same manner as rapamycin by inhibiting mTORC1, it has been observed that in higher concentrations it may induce autophagy independently of FKBP12 (248). Recent studies have examined safer approaches in delivering rapamycin, referred to as small molecule enhancers of rapamycin (SMERs) in an mTOR-independent manner. SMERs possibly achieve their autophagic inducing role through Atg5. (118, 229, 249).

### 3.2.2 Experimental justification

For the experiments in this chapter of the thesis, eight antibacterial antibiotics were pre-selected: doxycycline, rifampicin, moxifloxacin, sparfloxacin, levofloxacin, ciprofloxacin, amoxicillin, and streptomycin. The choice of the four anti-*Wolbachia* drugs (doxycycline, rifampicin, moxifloxacin, and sparfloxacin) was based on their known role in eliminating *Wolbachia* (26, 67, 250-253). The remaining four antibiotics were pre-selected from different classes due to them not exhibiting efficacy against *Wolbachia* (55, 250, 252, 253). Rapamycin and wortmannin were used as controls in the experiments of this chapter due to their known effects in different cell lines as autophagy inducer and autophagy inhibitor, respectively (254-257).

In the first group of experiments, the eight previously mentioned antibiotics were examined in terms of their autophagy inducing effects on different insect and mammalian cell lines and the filarial nematode, *B. malayi*. All antibiotics were tested at 5 µM (the gold standard set by A-WOL consortium for the concentration of doxycycline *in vitro* testing) in all cell lines and nematodes. These group of experiments were performed using immunoblotting assay (western blot) and confocal microscopy (for C6/36 and C6/36*Wp* cells only). To further confirm our findings, concentrations of 1 µM and 10 µM of the eight antibiotics tested were assessed for autophagy activation in C6/36 and C6/36*Wp* cells using western blot assay.

The second group of experiments were performed on uninfected and infected mosquito cell line C6/36 with *Wolbachia* (*w*AlbB) treated with three anti-*Wolbachia* agents that have recently been candidate-selected by the A-WOL consortium: TylAMac$^{TM}$ (a newly discovered tylosin analogue), AWZ1066S ( a newly synthesised thienopyrimidine/quinazoline anti-*Wolbachia* agent), and fusidic acid (a repurposed antibiotic) (81, 82, 86). Autophagy activation for these agents was assessed using immunoblotting assay (western blot).

The third and fourth set of experiments were conducted on infected mosquito cell line C6/36*Wp* with *Wolbachia* (*w*AlbB), treated with the same eight pre-selected antibiotics (mentioned above) at different concentrations and time-points. The rationale of testing on different concentrations and time-points of antibiotics was to determine the effect it may

have on measurable autophagic activity (measured using confocal microscopy and western blot) as well as on *Wolbachia* load (quantified by qPCR).

In this chapter, we have monitored autophagic activity using two widely used autophagic markers (LC3B and p62). Previous research has recommended the use of more than one marker when examining autophagic influx (106, 131, 133).

## 3.3 Materials and methods:

For more details on the materials used in the experiments conducted in this chapter please refer to the Appendix B Table B.1 section of this thesis.

### 3.3.1 *In vitro* culture of cell lines and nematodes

**i) *Wolbachia*-free mosquito cell line C6/36:**

Mosquito cells (*Aedes albopictus* clone) were purchased from European Collection of Authenticated Cell Cultures (ECACC) (clone C6/36, 89051705).

For the maintenance of *Wolbachia*-free C6/36 cells, the same preparation and cell sub-culture procedures were followed as previously described in Chapter 2.3.1.

**ii) Mosquito cell line C6/36*Wp* cells with *w*AlbB:**

The materials and preparation used for mosquito cell line C6/36*Wp* infected with *w*AlbB were the same as previously described in Chapter 2.3.1.

**iii) *Brugia malayi* microfilariae (mf):**

*B. malayi* life cycle is maintained at Liverpool School of Tropical Medicine (LSTM), UK and were originally obtained from TRS Laboratories, United States (US). The mf stage of the parasite was extracted from the peritoneal cavity of gerbils, this was performed by Mr Andrew Steven and Mr John Archer, Department of Tropical Disease Biology at LSTM, UK following the same protocol and procedure as described by Griffiths *et al.* (258). Mf worms were cleaned and filtered using PD-10 Desalting columns (GE Healthcare) using RPMI 1640 culture media (Gibco, Thermo Fisher Scientific) containing 2 mM L-glutamine, 25 mM HEPES, 100 U/ml penicillin-streptomycin (Thermo Fisher Scientific) and 2.5 mg/ml amphotericin B (Thermo Fisher Scientific) at 37°C.

After filtration, mf were centrifuged at 400 g for 5 minutes to form a pellet. The pellets were resuspended in fresh RPMI 1640 culture media supplemented with L-glutamine, HEPES and antibiotics (as mentioned above), and 10% FBS (Thermo Fisher Scientific), which will be referred to as RPMI media in this chapter. Mf were counted using light microscopy, where

an average of three readings were taking per 10 µl of 1 ml media containing mf. 10,000 mf (for western blot) were cultured in 200 µl media containing antibiotics at the desired concentrations per well of 96-well plate with a clear flat-bottom (Thermo Fisher Scientific) and incubated at 37°C in 5% $CO_2$.

**iv) *Spodoptera frugiperda* derived cell line (SF9):**

Cryopreserved *Spodoptera frugiperda* (known as the fall armyworm) SF9 cells (Gibco® Sf9, Thermo Fisher Scientific) were obtained from Dr. Abdulwahab Khashab, Tropical Disease Biology Department, LSTM, UK. SF9 cells were defrosted and diluted in SF-900 II media (Gibco®, Thermo Fisher Scientific), centrifuged at 400 g for 5 minutes and resuspended in 13 ml Sf-900 II media and cultured in a 75- $cm^2$ flask (Thermo Fisher Scientific) at 2.3 $x10^6$ cells/ml.

The culture media used to maintain SF9 cells was supplemented with 20% FBS, 1% non-essential amino acids (Sigma Aldrich) and 2% Tryptone phosphate broth (Sigma Aldrich) and flasks were incubated at 26°C. Cells were sub-cultured weekly using cell scrapers (Nunc, Thermo Fisher Scientific) at a split ratio of 1:4.

**v) Human monocytic leukaemia cell line (THP-1):**

Cryopreserved THP-1 cells were provided by Professor Giancarlo Biagini's group, with the help of Dr Shaun Pennington and Mr. Julio Furlong-Silva, Tropical Disease Biology Department at LSTM, UK. Cryopreserved cells were dissolved in a water bath at 37°C, washed with RPMI 1640 media (2 mM L-glutamine, 10% FBS, 5% penicillin-streptomycin and amphotericin B) and centrifuged at 400 g for 5 minutes to form a pellet. Pellets were resuspended in media, cultured at 3 $x10^5$ cells/ml in suspension (vertical positioned) in a 75-$cm^2$ flask at 37°C with 5% $CO_2$. Cells were sub-cultured twice a week by removing 10 ml cell suspension and replacing it with fresh culture media.

**vi) Madine-Darby canine kidney epithelial cells (MDCK):**

Cryopreserved MDCK epithelial cells (ECACC) were supplied by Ms. Amy Marriott, Tropical Disease Biology Department at LSTM, UK. Cryopreservation media was removed by centrifugation of cells at 400 g for 5 minutes in Eagle's Minimum Essential Medium (EMEM)

media (Sigma Aldrich) supplemented with 10% FBS, 5% penicillin-streptomycin and amphotericin B. Cells were cultured at 1 x$10^5$ in 75-$cm^2$ flasks and incubated at 37°C in 5% $CO_2$. A split ratio of 1:4 was performed when cells reached a confluency of approximately 80%.

When MDCK cells were ready to sub-culture, they were washed once while cells were adhered at room temperature with phosphate-buffered saline (PBS) (Sigma Aldrich). After washing, 10 ml of trypsin/EDTA (Sigma Aldrich) was added to culture flasks for 5 minutes for cell detachment followed by the addition of an equal amount of fresh media in order to neutralise the trypsin/EDTA solution. Collected cells were later centrifuged and supernatant was removed and replaced with fresh media.

### 3.3.2 Western blot analysis

The western blot protocol followed for all tested cells and nematodes in this experiment was previously described in Chapter 2.3.5. Any differences for the experimentation in this chapter are mentioned below.

As in Chapter 2, we used two autophagic protein markers for immunoblotting assay to monitor autophagic activation: LC3B and p62. The method in which these two markers are expressed and their interpretation within the autophagic cascade is presented in Figure 3.1.

Three controls were used for western blot analysis: DMSO (as a vehicle control), rapamycin at 5 µM (as a positive control for autophagy activation) and wortmannin at 10 µM (as a negative control for autophagy inhibition). All three compounds were purchased from Sigma Aldrich.

**Protein sample preparation for different cell line/nematodes:**

**i) Insect cell lines: Mosquito cell line C6/36 cells (C6/36*Wp* and *Wolbachia*-free) and SF9 cells**

Following the same protocol mentioned in Chapter 2.3.5, cells were treated for three days with the following antibiotics at two different concentrations (1 and 10 µM for C6/36 cells - infected or uninfected with *w*AlbB) and at one concentration (5 µM for SF9 cells): doxycycline, rifampicin, moxifloxacin, sparfloxacin, levofloxacin, ciprofloxacin, amoxicillin and streptomycin (all from Sigma Aldrich).

All antibiotics and chemical agents used in this experiment were dissolved in DMSO. Protein expression of two autophagy markers LC3B (rabbit antibody from Novus) and p62 (rabbit antibody from Cell Signaling) diluted at 1:1000 in 5% non-fat milk/TBS-T and 5% BSA/TBS-T, respectively. Secondary antibodies conjugated with horseradish peroxidase (HRP) (goat anti-rabbit from Cell Signaling diluted at 1:5000 in 5% non-fat milk in TBS-T blocking buffer for LC3B, and monkey anti-rabbit from GE Healthcare diluted at 1:10,000 in PBS-T for p62) were added and measured against beta actin (loading control) (Cell Signaling).

**Pre-clinical candidates and re-purposed antibiotic from the A-WOL consortium**

Three drugs identified by the A-WOL consortium were also tested for their autophagy activation using mosquito cells C6/36 (infected and uninfected with *w*AlbB) for three days at their pre-determined 10x EC50 concentrations (concentrations that demonstrated 50% of the maximal response of drugs) in mosquito cells and nematodes against *Wolbachia*: TylAMac$^{TM}$ (at 7 nM), AWZ1066S (at 2390 nM) and Fusidic acid (at 2890 nM).

**ii) *B. malayi* mf larval worms**

The same treatment groups for the eight antibiotics mentioned above for insect cells were tested in mf at one concentration (5 µM) for three days.

Microfilariae (mf) were collected and filtered using PD-10 columns. 10,000 mf/well were cultured in flat-bottom 96-well plate in 200 µl RPMI 1640 media. At day 3, mf were pooled out of a total of 4 wells to yield the adequate amount of protein required for

immunoblotting assay. All worms were lysed with 50 µl Tissue Extraction Reagent (Invitrogen, Thermo Fisher Scientific). Tissue lysates were homogenised using a Pellet pestle motor (Kimble) and incubated for 5 minutes. All lysates were centrifuged at 13,000 g for 2 minutes, and supernatant were transferred to new tubes. Following this step, the rest of the western blot procedure is as described in Chapter 2.3.5.

The primary antibodies used for *B. malayi* worms were rabbit antibodies against LC3B and p62 (both from Cell Signaling) at a dilution of 1:1000 in 5% BSA in TBS-T and secondary monkey anti-rabbit conjugated with HRP (from GE Healthcare) diluted at 1:10,000 in PBS.

**iii) Mammalian cell lines: THP-1 cells and MDCK cells**

The same treatment groups for the eight antibiotics mentioned above for insect cells were tested at one concentration (5 µM) for two different time-points: day 3 and day 7 of treatment.

THP-1 cells were mixed manually prior to centrifugation at 400 g for 5 minutes. MDCK cells were detached using trypsin/EDTA solution in 25-$cm^2$ flasks prior to centrifugation. For both mammalian cells, the same primary and secondary antibodies as mf were used.

### 3.3.3 Immunofluorescence staining assay – Confocal laser scanning microscopy

For this experiment's C6/36 cell preparation, fixation/permeabilisation, primary and secondary antibody incubation/staining and slide mounting, the same procedure as that described in Chapter 2.3.4 was followed for the confocal microscopy.

C6/36 mosquito cells infected or uninfected with *Wolbachia* (*w*AlbB) were treated for 3 days with eight antibiotics at a range of selected concentrations: between 0.125-20 µM for rifampicin, moxifloxacin, sparfloxacin, levofloxacin, ciprofloxacin, amoxicillin and streptomycin and between 0.125-10 µM for doxycycline (previously determined to be toxic at 20 µM in C6/36*Wp* cells by A-WOL consortium). The range of concentrations for all antibiotics was selected where the upper limit did not exceed toxic concentrations in C6/36 cells, previously determined by members in the A-WOL consortium (unpublished data).

Starting from the highest concentration, 6 concentrations were titrated for each antibiotic, in order to determine the impact of concentration response on *Wolbachia* reduction and autophagy activation.

DMSO (as a vehicle control), rapamycin at 5 µM (positive control for autophagy activation) and wortmannin at 10 µM (negative control for autophagy inhibition) were used as controls for this experiment. All compounds were purchased from Sigma Aldrich and diluted in DMSO.

As in Section 3.3.2 for western blot, the same two autophagic markers were used for the confocal microscopy in this chapter: LC3B and p62 (both primary antibodies are generated in rabbit). For the expression of these markers and interpretation within the autophagic pathway please refer to Figure 2.3. In addition to autophagic antibodies, *Wolbachia* was stained with nucleic acid stain, syto11 and cell nuclei were counter-stained with DAPI. This was also used to confirm *Wolbachia* absence from uninfected C6/36 cells.

Quantification analysis for autophagy marker expression was determined by measuring the number of LC3B-II (Invitrogen) and p62 (Cell Signaling) puncta formation per cell. The total number of puncta/cell was then graphed and expressed as percentages, where an increase and decrease in percentage indicated autophagic activity for LC3B-II and p62 puncta, respectively. Using confocal microscopy/Zen software (Zeiss LSM 880), LC3B-II and p62 positive cells (representing autophagic marker presentation) were quantified across 3 different sections of the slides and compared to the DMSO control. Each area covered a minimum of ≥ 50 cells as a threshold for further analysis.

### 3.3.4 Quantitative polymerase chain reaction (qPCR) - C6/36 cells:

C6/36 cells were prepared as described in Section 3.3.1. In a 96-well plate, C6/36 cells (uninfected and infected with *w*AlbB) were seeded at 10,000 cells/ml for a total volume of 200 µl Leibovits-15 (L-15) media.

For antibiotic treatment prior to qPCR analysis, two methods were performed depending on the experimental variable, as described below:

**i) Concentration -based antibiotics experiment**

C6/36*Wp* cells were exposed to pre-selected antibiotics for 3 days at different concentrations: Between 0.125-10 µM for doxycycline, and between 0.125-20 µM for rifampicin, moxifloxacin, sparfloxacin, levofloxacin, ciprofloxacin, amoxicillin and streptomycin. DMSO was used as a vehicle control, while rapamycin at 5 µM (autophagy activator) and wortmannin at 10 µM (autophagy inhibitor) were used in this experiment to monitor the effect of autophagy activation or inhibition on *Wolbachia* titre. For every tested concentration in each compound, three biological repeats were performed. All compounds were diluted in DMSO.

**ii) Time-course experiment**

C6/36*Wp* were treated with the following antibiotics: doxycycline, rifampicin, moxifloxacin, sparfloxacin, levofloxacin, ciprofloxacin, amoxicillin and streptomycin at 5 µM for different time-points: Day 0, 1, 3, 5 and 7. DMSO (vehicle control), rapamycin at 5 µM (autophagy activator) and wortmannin at 10 µM (autophagy inhibitor) were used along the control. For every tested time-point for each compound, three biological repeats were performed.

At day 0, 1, 3, 5 and 7 samples were taken for DNA extraction and assessed for their *Wolbachia* titre using qPCR.

**iii) *Wolbachia* detection in C6/36 and SF9 cells**

qPCR technique was used to confirm the absence of *Wolbachia* in both insect cells: C6/36 and SF9 cells used in the experiments of this chapter. For SF9 cells, 10,000 cells/ml were seeded in a 96-well plate for a total volume of 200 µl SF9-II media.

**DNA lysis and extraction – C6/36 cells**

Using QIAmp mini DNA kit (Qiagen) to extract genomic DNA from cultured cells, the media was removed from 96-well plates and placed into 1.5 ml microtubes. 35 µl Proteinase K and 100 µl ATL tissue lysis buffer (supplemented with kit) were added to all microtubes and incubated overnight in a water bath set at 56°C. On the following day, microtubes were removed and 200 µl AL lysis buffer (supplemented with kit) was added. Next, all tubes were placed back in the water bath at 70°C for 10 minutes to allow for adequate cell lysis. 200 µl absolute ethanol (Sigma Aldrich) was added to tubes and incubated for 5 minutes at room temperature for DNA precipitation. All cell lysates were transferred to mini spin columns (provided by the DNA kit) and centrifuged at 5000 g for 1 minute. Following centrifugation, two washing steps were performed by adding 500 µl of AW1 followed by 500 µl of AW2 washing buffer (supplemented with kit). 100 µl AE elution buffer (supplemented with kit) was added into each mini spin column. Columns were centrifuged at 13,000 g for 5 minutes and purified eluted DNA was collected and stored at -20°C for qPCR analysis.

**qPCR Analysis:**

Extracted DNA was amplified using specific primers against the *16s* rRNA *Wolbachia* gene normalised to *Aedes albopictus 18s* rRNA gene (forward and reverse primers sequence were designed by Integrated DNA Technologies (UK) see Appendix B Table B.3). In a total volume of 10 µl per reaction, a master mix was added into tested wells of the 384 well-plate (Biorad). In each reaction well, the master mix (8 µl) contained the following: 5 µl Ssofast EvaGreen Supermix (Biorad), 1 µl of forward primer (200 nM), 1 µl of reverse primer (200 nM), 1 µl nuclease-free water (Thermo Fisher Scientific). Following this, 2 µl of the prepared extracted genomic DNA was added to the master mix.

*16s* and *18s* standards (Integrated DNA Technologies (UK) see Appendix B Table B.3) were diluted at 1:20 to form a stock of 5 x $10^8$/µl (top standard), followed by a serial dilution at 1:10 starting from 5 x $10^7$/µl to 5 x $10^0$/µl (standards). 1 µl of each prepared standard was added to 9 µl of master mix in duplicates into reaction wells in order to obtain the number of gene copies from unknown samples. Three technical repeats were performed for each biological sample.

Using CFX384 Real-Time System with C1000 Thermal Cycler (Biorad), the following cycling conditions were applied for this experiment: 15 minutes at 95°C, 40 cycles (and 35 cycles for uninfected cells) for 15 seconds at 94°C, 30 seconds at 55°C, 15 seconds at 72°C and a melting curve between 50-95°C. Gene copy numbers were normalised and expressed as a *16s:18s* ratio.

### 3.3.5 Statistical analysis

Statistical analysis in this chapter was performed for continuous variables for confocal immunofluorescence assay and qPCR using independent sample Student's t-test. Statistical significance was at $p \leq 0.05$. For all sections of the statistical analysis in this chapter, we used GraphPad Prism version 7.

## 3.4 Results

### 3.4.1 Measuring antibiotic-induced autophagy in different cell lines and nematodes using western blot

The results of the expression of two autophagic markers LC3B and p62 using western blot to examine autophagic induction of the eight tested antibiotics from diverse classes in different cell lines and nematodes are presented in Figures 3.2 to 3.5 (for the full immunoblots, please refer to the Appendix A Figure A3-A6).

For insect cells and mf, LC3B protein was expressed in two distinct bands: LC3B-I (~16 kDa) and LC3B-II (~14 kDa). The difference in molecular weight between LC3B-I and LC3B-II and its significance in protein expression was previously described in Chapter 2.4.4 in insect cells. Whereas for mammalian cells, due to the relatively close molecular weight between LC3B-I and LC3B-II, their protein expression is presented as two fused bands, due to the high rate of conversion of LC3B-I to LC3B-II, making the latter more intense (131).

In mammalian cells and mf, p62 protein expression was represented at ~62 kDa by a single band. As previously discussed in Chapter 2.4.4 and observed in previous studies on insect cells, p62 expression in C6/36 and SF9 cells was observed at ~80 kDa.

For all tested cells and nematodes, an increase in autophagic influx was indicated by an increase of expression of LC3B-II (indicating autophagosome formation) on the immunoblots. Conversely, a decrease in expression of p62 (increased autophagic degradation) indicated autophagy activation.

In all immunoblots, DMSO was used as a vehicle control, representing the basal level of autophagy for all tested cells and nematodes. Rapamycin, a known autophagic inducer was used as a positive control, hence LC3B-II appeared prominent and p62 showed a reduced or absent expression. On the other hand, wortmannin and l-asparagine, the autophagy inhibitors we have previously tested successfully in Chapter 2, were used as negative controls in all immunoblots. These were expressed as a reduced (wortmannin) and prominent (l-asparagine) band of LC3B-II and a high intensity of p62 band for both inhibitors. Beta-actin (loading control) was represented at molecular size ~40 kDa.

#### 3.4.1.1 Insect cells and nematodes

**i) C6/36*Wp* and C6/36 cells**

In C6/36*Wp* cells (Figure 3.2 A and B), all four anti-*Wolbachia* drugs tested at 1 µM (doxycycline, rifampicin, moxifloxacin and sparfloxacin), presented with a higher intensity of LC3B-II (Figure 3.2 A) and a reduced expression of p62 (Figure 3.2 B) compared to DMSO. When these antibiotics were tested at higher concentrations (10 µM), there appeared to be a concentration-dependent increase in intensity for rifampicin and moxifloxacin only. All four anti-*Wolbachia* agents appeared to express an increase in intensity of LC3B-II similar to that of rapamycin. In contrast, the antibiotics inactive against *Wolbachia* (levofloxacin, ciprofloxacin, amoxicillin and streptomycin) did not activate autophagy.

Interestingly, the results for C6/36 cells (Figure 3.2 C and D) presented a similar picture to C6/36*Wp* (Figure 3.2 A and B). In the absence of *Wolbachia*, all anti-*Wolbachia* agents activated autophagy (Figure 3.2 C and D). The absence of *Wolbachia* in C6/36 cells was confirmed using qPCR (this was tested in C6/36 and SF9 cells and is presented in the Appendix A Figure A7). Conversely, the other tested antibiotics did not show any evidence of autophagic induction compared to DMSO. The ability of antibiotics to activate autophagy directly was more clearly observed in uninfected C6/36 cells, as this removes the *Wolbachia* induced autophagy as demonstrated in the DMSO controls.

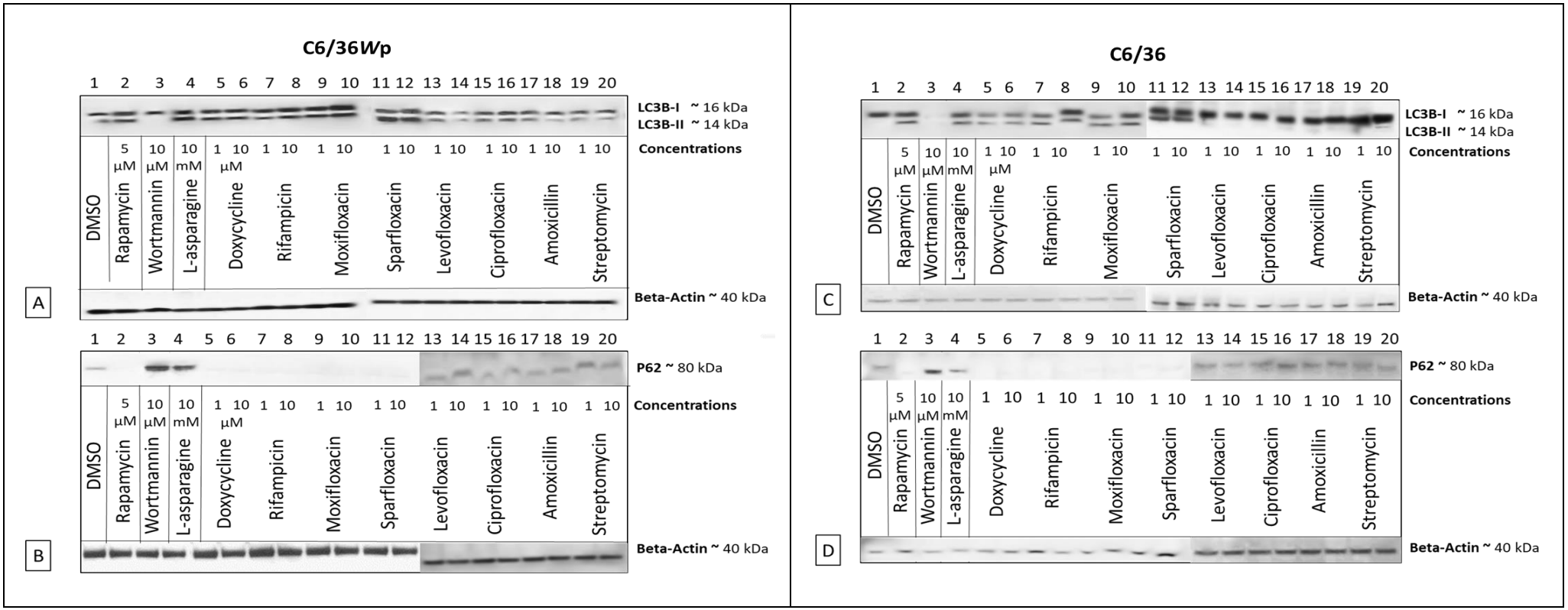


Figure 3. 1 Detection of LC3B and p62 expression for antibiotics from diverse classes in C6/36 cells using western blot.

C6/36 mosquito cells A and B) infected with *Wolbachia w*AlbB C and D) *Wolbachia*-free cells were treated with: DMSO – vehicle control (lane 1), rapamycin – positive control (lane 2), wortmannin – early autophagy inhibitor (lane 3), l-asparagine – late autophagy inhibitor (lane 4), four anti-*Wolbachia* antibiotics: doxycycline (lane 5-6), rifampicin (lane 7-8), moxifloxacin (lane 9-10), sparfloxacin (lane 11-12), and four different antibiotics: levofloxacin (lane 13-14), ciprofloxacin (lane 15-16), amoxicillin (lane 17-18), and streptomycin (lane 19-20) for 3 days. Reduced protein extracts of cells were loaded at 50 µg/40 ul per lane into 4-12% bis tris SDS-PAGE gels. Separated proteins were transferred into nitrocellulose membrane, blocked and incubated with primary and secondary antibodies. Western blot protein expression is presented in A and C) for rabbit anti-LC3B (LC3B-I at 16 kDa and LC3B-II at 14 kDa) and B and D) rabbit anti-p62 (at 80 kDa). A reference protein; mouse anti-beta actin was used as a control with a size of approximately 40 kDa.

**ii) Pre-clinical candidates and re-purposed antibiotic from the A-WOL consortium in C6/36*Wp* and C6/36 cells**

For all three tested agents, TylAMac™, fusidic acid and AWZ1066S, LC3B-II expression was prominent compared to the DMSO control (Figure 3.3 A). The autophagic inducing capabilities of these three agents were further confirmed by the reduced expression of p62, especially when compared to DMSO (Figure 3.3 B). These findings for both autophagic markers were observed in C6/36*Wp*, as well as non-infected C6/36 cells.

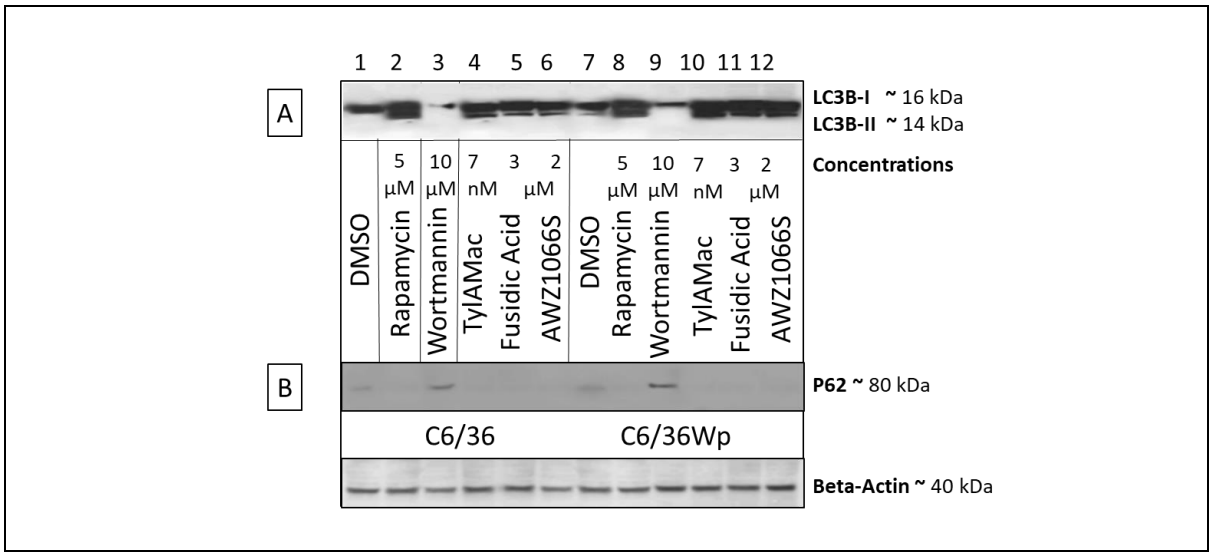


Figure 3. 2 Detection of LC3B and p62 expression for A-WOL selected candidates and repurposed anti-*Wolbachia* agents in C6/36 cells using western blot.

*Wolbachia*-free C6/36 (lane 1-6) and infected C6/36*Wp* cells (lane 7-12) were treated with: DMSO – vehicle control (lane 1 and 7), rapamycin – positive control (lane 2 and 8), wortmannin – autophagy inhibitor (lane 3 and 9), TylAMac™ (lane 4 and 10), fusidic acid (lane 5 and 11), and AWZ1066S (lane 6 and 12) for 3 days. Reduced protein extracts of cells were loaded at 50 µg/40 ul per lane into 4-12% bis tris SDS-PAGE gels. Separated proteins were transferred into nitrocellulose membrane, blocked and incubated with primary and secondary antibodies. Western blot protein expression is presented in A) for rabbit anti-LC3B (LC3B-I at 16 kDa and LC3B-II at 14 kDa) and B) rabbit anti-p62 (at 80 kDa). A reference protein; mouse anti-beta actin was used as a control with a size of approximately 40 kDa.

**iii) SF9 cells and *B. malayi* mf**

For both SF9 cells and *B. malayi* mf (Figure 3.4), a similar representation as C6/36 cells was observed with the induction of autophagy for all anti-*Wolbachia* drugs and an absence of activation for antibiotics that lack activity against *Wolbachia*.

In summary, for all the tested insect cells and nematodes, the anti-*Wolbachia* antibiotics showed evidence of autophagy induction, as presented by the higher expression and lower intensity of LC3B-II and p62, respectively. This was also observed for *Wolbachia*-free C6/36 and SF9 cells. In contrast, the antibiotics, which lack activity against *Wolbachia* (levofloxacin, ciprofloxacin, amoxicillin and streptomycin) did not activate autophagy.

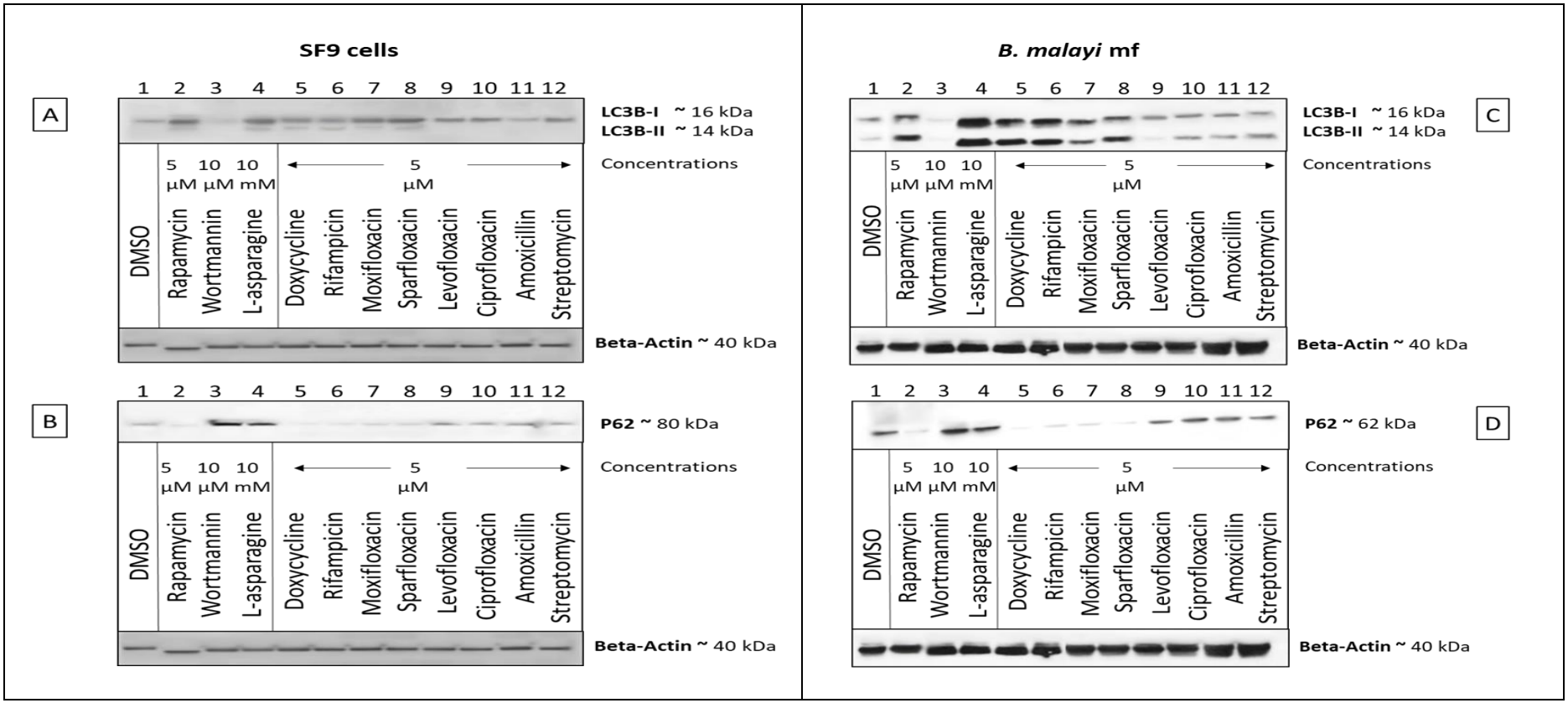


Figure 3. 3 Detection of LC3B and p62 expression for antibiotics from diverse classes in SF9 cells and *Brugia malayi* mf using western blot.

A and B) SF9 insect cells and C and D) *B. malayi* mf worms were treated with: DMSO – vehicle control (lane 1), rapamycin – positive control (lane 2), wortmannin – early autophagy inhibitor (lane 3), l-asparagine – late autophagy inhibitor (lane 4), four anti-*Wolbachia* agents: doxycycline (lane 5), rifampicin (lane 6), moxifloxacin (lane 7), sparfloxacin (lane 8), and four different antibiotics: levofloxacin (lane 9), ciprofloxacin (lane 10), amoxicillin (lane 11), and streptomycin (lane 12) for 3 days. Reduced protein extracts of cells were loaded at 50 µg/40 ul per lane into 4-12% bis tris SDS-PAGE gels. Separated proteins were transferred into nitrocellulose membrane, blocked and incubated with primary and secondary antibodies. Western blot protein expression is presented in A and C) for rabbit anti-LC3B (LC3B-I at 16 kDa and LC3B-II at 14 kDa) and B and D) rabbit anti-p62 (at 80 kDa for SF9 and 62 kDa for mf). A reference protein; mouse anti-beta actin was used as a control with a size of approximately 40 kDa.

#### 3.4.1.2 Mammalian cells: THP-1 and MDCK

In order to test whether the pattern of autophagy activation observed in insect cells and microfilariae was also a feature of mammalian cells, THP-1 and MDCK cells were exposed to the same antibiotics and autophagy marker expression was assessed at 3 days post-exposure.

For both THP-1 (Figure 3.5 A and B) and MDCK cells (Figure 3.5 C and D), LC3B expression showed a different pattern to that observed with insect cells and microfilariae. Due to the inconsistent pattern, we further tested both mammalian cells at 7 days post-exposure to confirm our findings in longer treatment periods.

For THP-1 cells exposed to doxycycline and rifampicin there was no evidence of autophagy activation at either day 3 or 7 post-exposure. THP-1 cells exposed to moxifloxacin and sparfloxacin, did appear to show an up-regulation of LC3B-I and LC3B-II at day 3, but this upregulation did not continue until day 7, as evident from its similar expression to DMSO. Antibiotics without an activity against *Wolbachia* showed a pattern similar to controls with no evidence of autophagy activation. However, the apparent activation of LC3B for moxifloxacin and sparfloxacin was not reproduced in the expression of p62, which remained similar to control levels for all tested antibiotics, suggesting a lack of autophagy activation.

With MDCK cells rifampicin, moxifloxacin and sparfloxacin induced the upregulation of LC3B at day 3 and 7, which was more intense for the fluroquinolones. Antibiotics lacking activity against *Wolbachia* showed expression levels similar to controls. As for THP-1 cells the expression of p62 did not replicate the patterns observed for LC3B and showed similar levels to controls for all tested antibiotics.

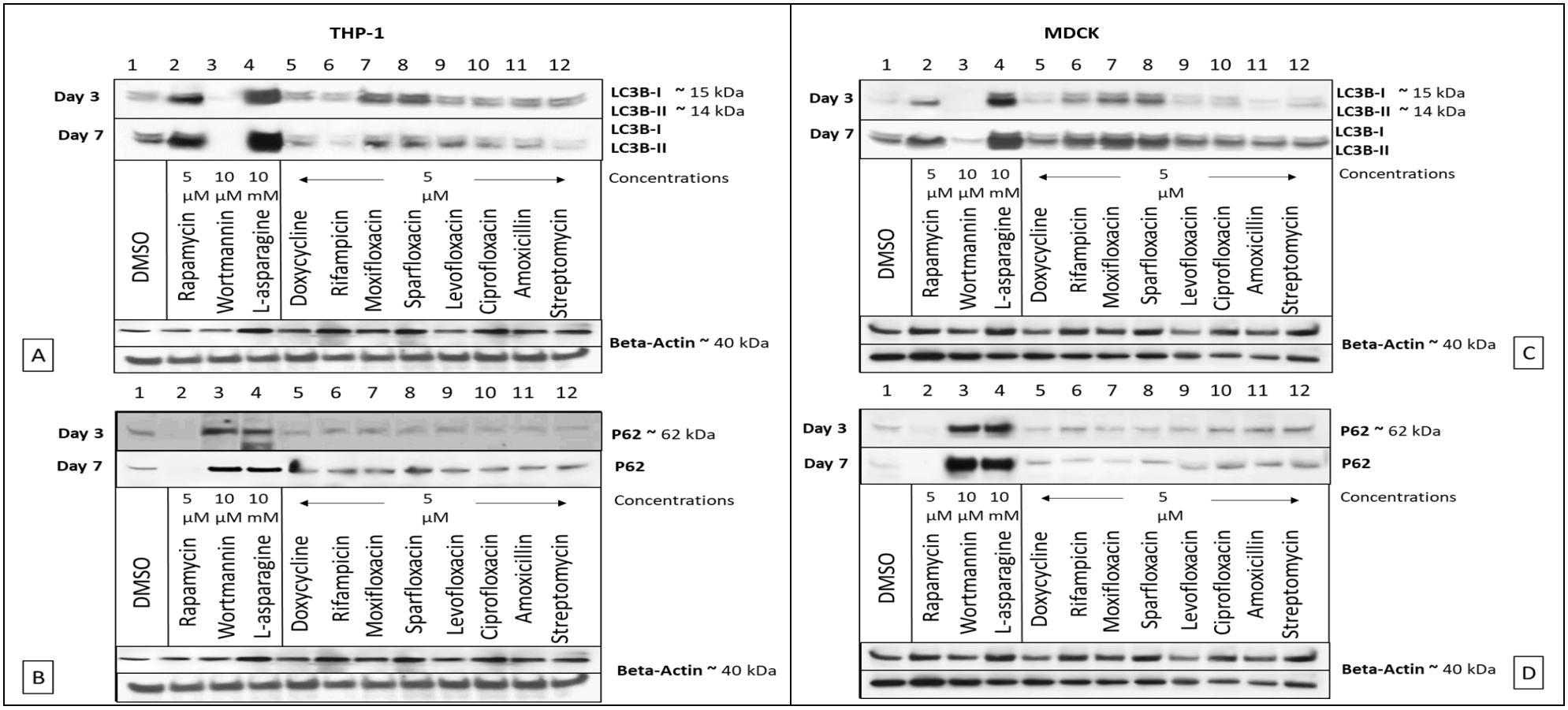


Figure 3. 4 Detection of LC3B and p62 expression for antibiotics from diverse classes in mammalian cells: THP-1 and MDCK using western blot.

A and B) THP-1 and C and D) MDCK cells were treated with: DMSO – vehicle control (lane 1), rapamycin – positive control (lane 2), wortmannin – early autophagy inhibitor (lane 3), l-asparagine – late autophagy inhibitor (lane 4), four anti-*Wolbachia* agents: doxycycline (lane 5), rifampicin (lane 6), moxifloxacin (lane 7), sparfloxacin (lane 8), and four different antibiotics: levofloxacin (lane 9), ciprofloxacin (lane 10), amoxicillin (lane 11), and streptomycin (lane 12) for 3 and 7 days. Reduced protein extracts of cells were loaded at 50 µg/40 ul per lane into 4-12% bis tris SDS-PAGE gels. Separated proteins were transferred into nitrocellulose membrane, blocked and incubated with primary and secondary antibodies. Western blot protein expression is presented in A and C) for rabbit anti-LC3B (LC3B-I at 15 kDa and LC3B-II at 14 kDa) and B and D) rabbit anti-p62 (at p62 kDa). A reference protein; mouse anti-beta actin was used as a control with a size of approximately 40 kDa.

### 3.4.2 Measuring antibiotic-induced autophagy in C6/36*Wp* and C6/36 cells using immunofluorescence staining assay

To further validate our findings in western blot analysis, we examined autophagic induction in the same eight antibiotics using immunofluorescence staining assay in C6/36*Wp* followed by those for *Wolbachia*-free C6/36 cells. Cell-based images are presented at one selected concentration (5 µM, which is the gold standard concentration used by the A-WOL consortium for *in vitro* testing) treated for 3 days. We quantified the percentage of cells with positive LC3B-II and p62 puncta for the tested antibiotics to determine their statistical significance compared to the DMSO control. Confocal images of cells treated with antibiotics presented in this section were performed using the same two autophagy gene markers LC3B-II (conjugated with TRITC – red fluorescent puncta) and p62 (conjugated with TRITC – yellow fluorescent puncta). Hence, the increase in red fluorescence puncta is indicative of autophagic activation (high LC3B-II). On the other hand, the presence of low yellow fluorescence puncta represents autophagy induction due to p62 protein degradation. Green and blue fluorescence staining represent *Wolbachia* and cell nuclei, respectively.

#### 3.4.2.1 C6/36 cells infected with *w*AlbB

All four anti-*Wolbachia* agents: doxycycline, rifampicin, moxifloxacin and sparfloxacin, appeared to show an increase in autophagic influx due to the increase in LC3B-II expression (Figure 3.6) and decrease in p62 fluorescence (Figure 3.7). This observation was similar to that of the positive control (rapamycin treated cells). Conversely, all the remaining antibiotic agents without anti-*Wolbachia* activity: levofloxacin, ciprofloxacin, amoxicillin and streptomycin, did not exhibit any observable difference in LC3B-II and p62 fluorescence compared to the DMSO control. There appears to be a noticeable difference in the confocal images between the tested anti-*Wolbachia* agents and other antibiotics in terms of *Wolbachia* number (green fluorescence).

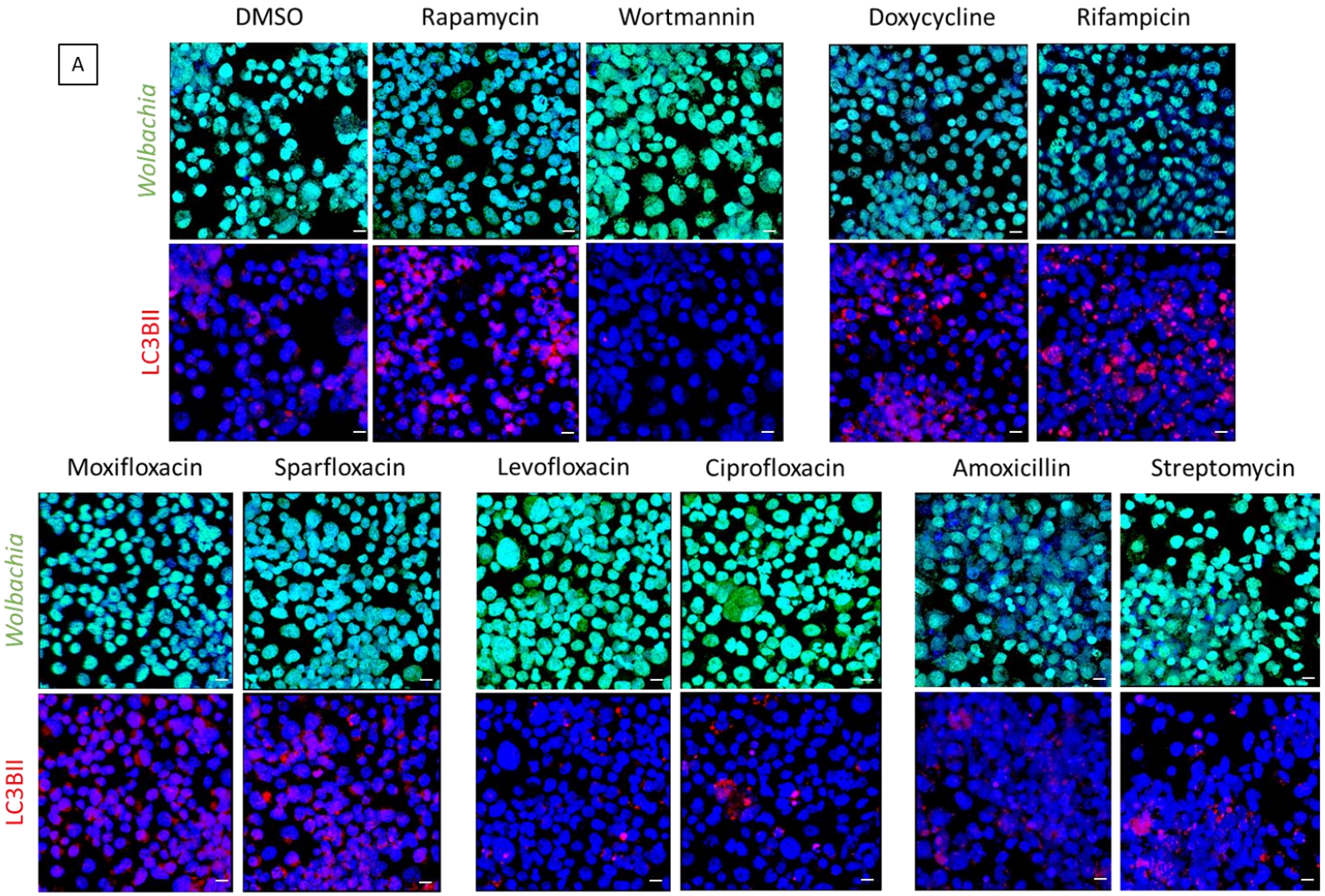
A
DMSO
Rapamycin
Wortmannin
Doxycycline
Rifampicin
Wolbachia
LC3BII
Moxifloxacin
Sparfloxacin
Levofloxacin
Ciprofloxacin
Amoxicillin
Streptomycin
Wolbachia
LC3BII

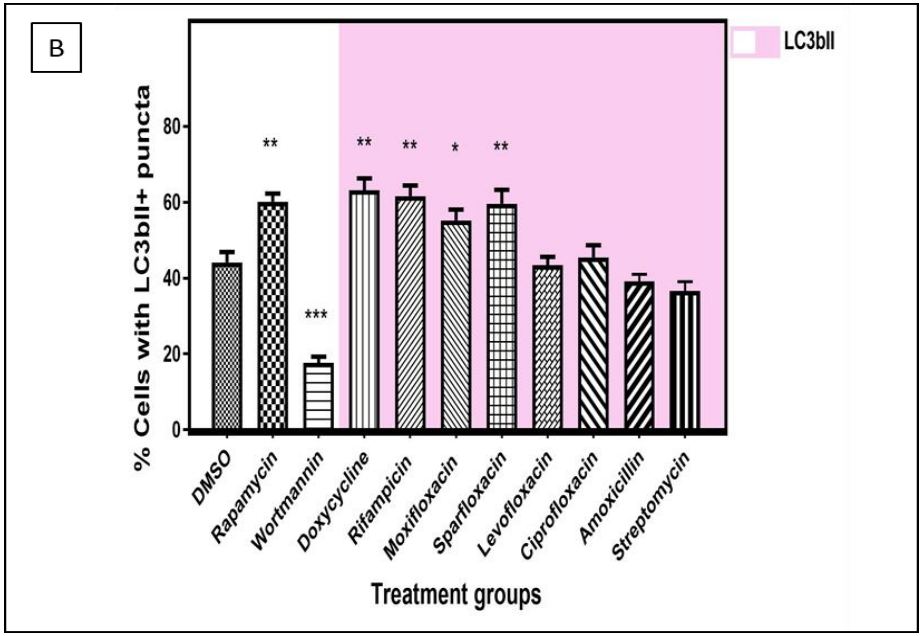


**Figure 3. 5 Immunofluorescence staining in C6/36*Wp* cells for different antibiotics using autophagic marker LC3B-II.**

C6/36 cells infected with *wAlbB* were treated with DMSO (vehicle control representing basal autophagy), rapamycin at 5 µM (positive control), wortmannin at 10 µM (negative control), four anti-*Wolbachia* agents: doxycycline, rifampicin, moxifloxacin and sparfloxacin, and four other antibiotics: levofloxacin, ciprofloxacin, amoxicillin and streptomycin, all at 5 µM for 3 days. Cells were fixed, permeabilised and incubated with autophagy primary and secondary antibodies. Syto11 and DAPI were used to stain *Wolbachia* and cell nuclei (green and blue fluorescence), respectively. Autophagy activation is shown by an increase in red puncta (increase in LC3B-II due to autophagosomes formation). Bar graph (mean with SD) represents % cells with LC3BII positive puncta for each treatment group with three different sections were imaged, where each section contained ≥50 cells. Scale bars in A are 10 µm.

Statistical analysis was performed to compare all treatment groups to DMSO. Statistical significance tested using Student's t-test, statistical significance was at $p \leq 0.05$. For p-value *= 0.01 to 0.05, ** = 0.01 to 0.001, *** = 0.001 to 0.0001, and **** ≤ 0.0001.

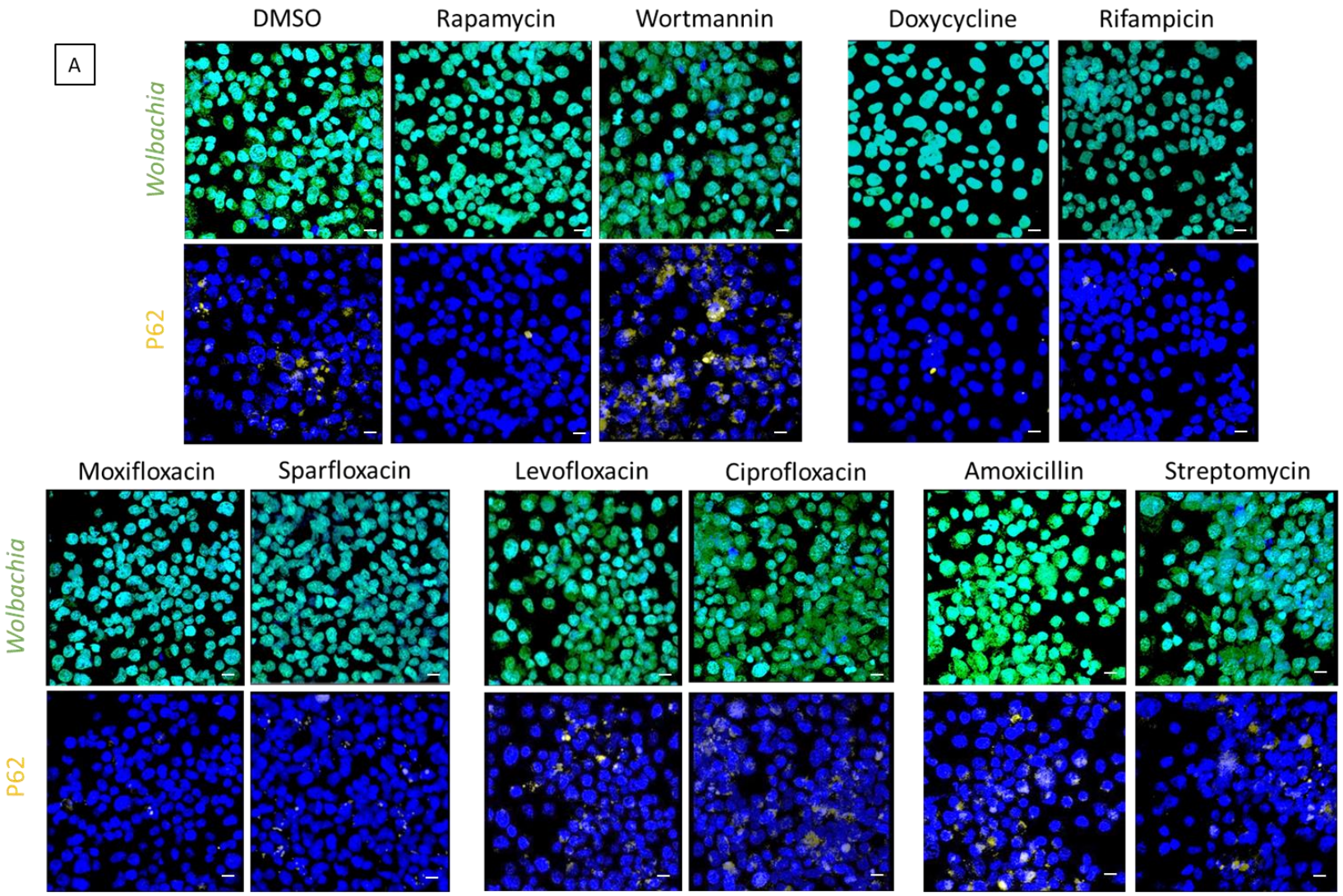
A
DMSO
Rapamycin
Wortmannin
Doxycycline
Rifampicin
Wolbachia
P62
Moxifloxacin
Sparfloxacin
Levofloxacin
Ciprofloxacin
Amoxicillin
Streptomycin
Wolbachia
P62

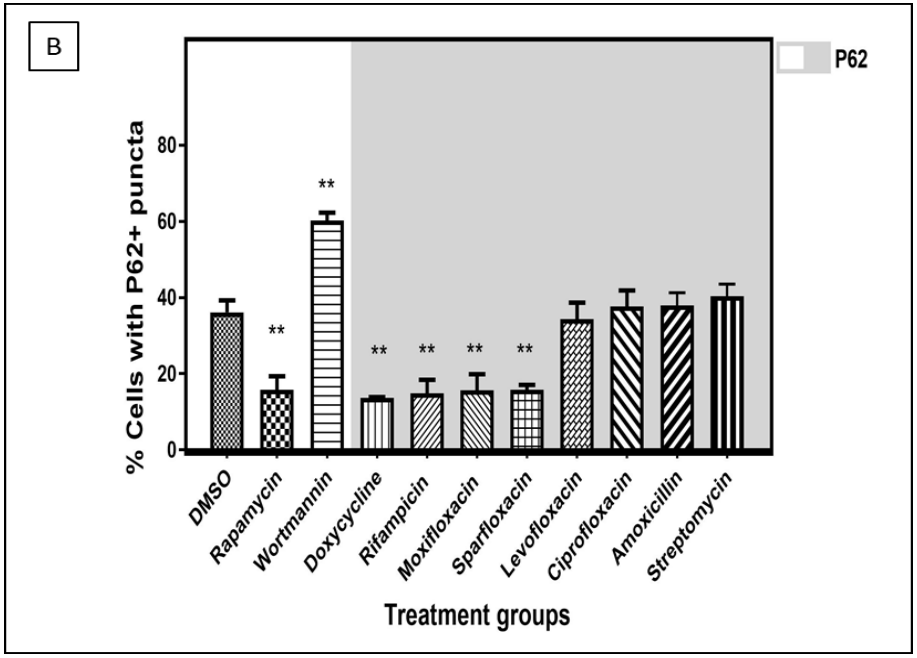


**Figure 3. 6 Immunofluorescence staining in C6/36*Wp* cells for different antibiotics using autophagic marker p62.**

C6/36 cells infected with *wAlbB* were treated with DMSO (vehicle control representing basal autophagy), rapamycin at 5 µM (positive control), wortmannin at 10 µM (negative control), four anti-*Wolbachia* agents: doxycycline, rifampicin, moxifloxacin and sparfloxacin, and four other antibiotics: levofloxacin, ciprofloxacin, amoxicillin and streptomycin, all at 5 µM for 3 days. Cells were fixed, permeabilised and incubated with autophagy primary and secondary antibodies. Syto11 and DAPI were used to stain *Wolbachia* and cell nuclei (green and blue fluorescence), respectively. Autophagy activation is shown by a decrease in yellow puncta (decrease in p62 due to autophagic degradation). Bar graph (mean with SD) represents % cells with p62 positive puncta for each treatment group with three different sections were imaged, where each section contained ≥50 cells. Scale bars in A are 10 µm.

Statistical analysis was performed to compare all treatment groups to DMSO. Statistical significance tested using Student's t-test, statistical significance was at $p \leq 0.05$. For p-value *= 0.01 to 0.05, ** = 0.01 to 0.001, *** = 0.001 to 0.0001, and **** ≤ 0.0001.

#### 3.4.2.2 *Wolbachia*-free C6/36 cells

Interestingly, the visual presentation for *Wolbachia*-free C6/36 was similar to that of C6/36*Wp*. All four anti-*Wolbachia* agents: doxycycline, rifampicin, moxifloxacin and sparfloxacin, presented with high red fluorescence and low yellow fluorescence representing LC3B-II (Figure 3.8) and p62 (Figure 3.9) expression, respectively. This indicated the presence of autophagic induction in these drugs. On the contrary, the confocal images for the remaining antibiotics, which lack activity against *Wolbachia*: levofloxacin, ciprofloxacin, amoxicillin and streptomycin, did not present any evidence of autophagic activation. An interesting observation was that when comparing the DMSO control between infected and uninfected C6/36 cells, there was evidence of higher autophagic influx in the presence of *Wolbachia*, indicated by high LC3B-II and low p62 expression. This difference in expression was significant for both autophagic markers (this is presented in the Appendix A Figure A8).

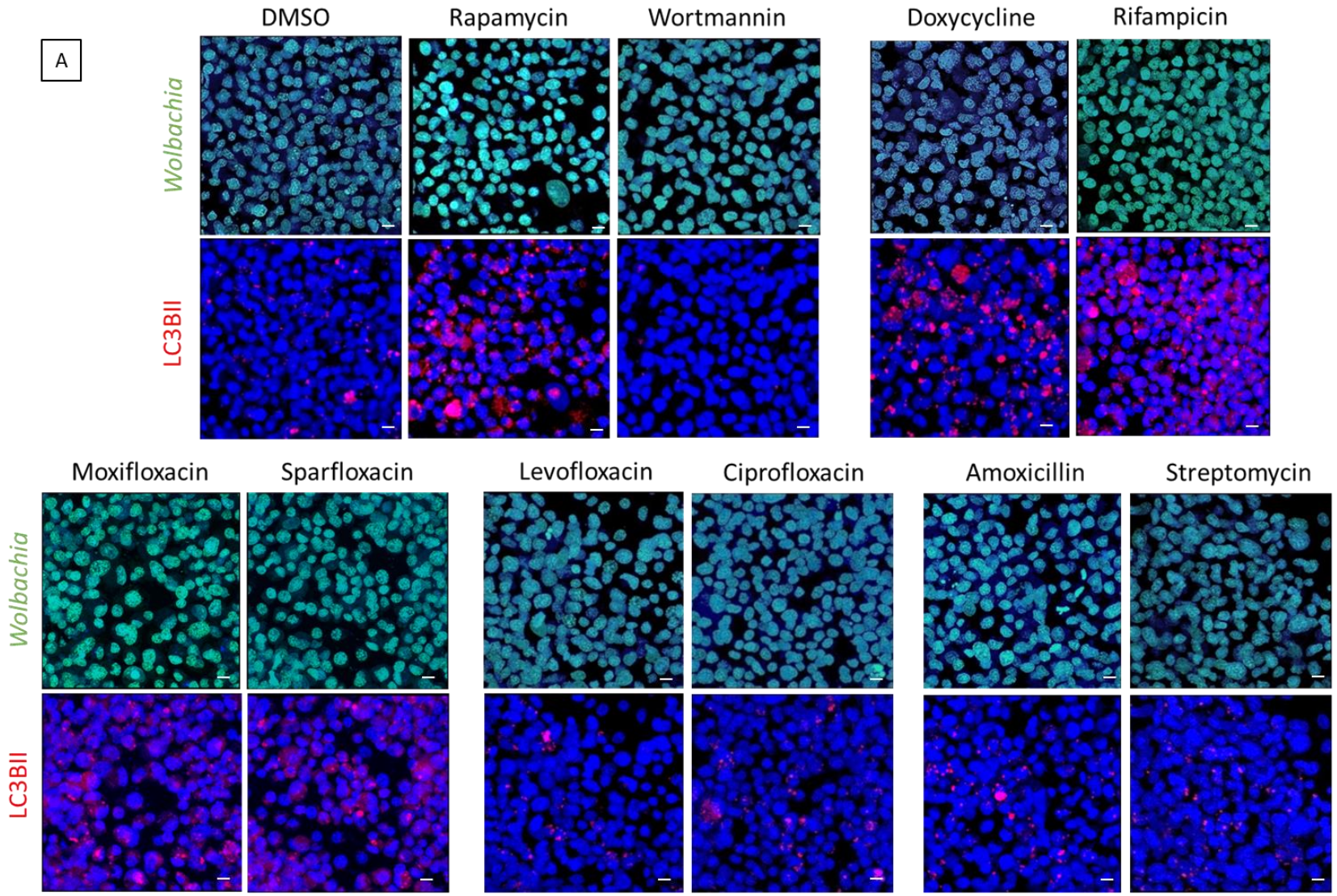
A
DMSO
Rapamycin
Wortmannin
Doxycycline
Rifampicin
Wolbachia
LC3BII
Moxifloxacin
Sparfloxacin
Levofloxacin
Ciprofloxacin
Amoxicillin
Streptomycin
Wolbachia
LC3BII

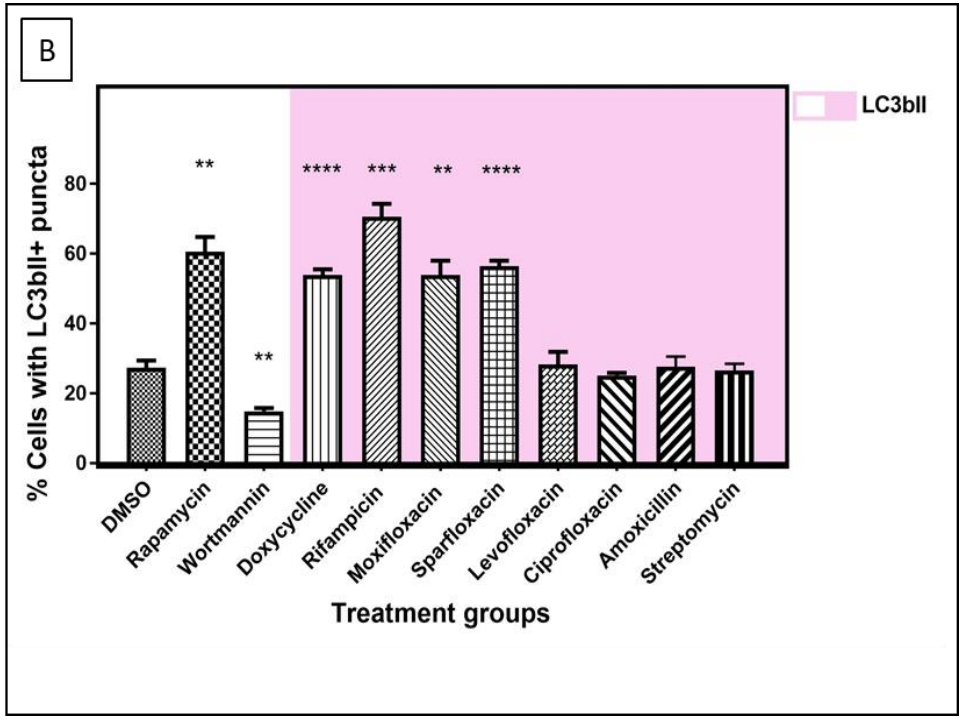


Figure 3. 7 Immunofluorescence staining in C6/36 cells for different antibiotics using autophagic marker LC3B-II.

*Wolbachia*-free C6/36 cells were treated with DMSO (vehicle control representing basal autophagy), rapamycin at 5 µM (positive control), wortmannin at 10 µM (negative control), four anti-*Wolbachia* agents: doxycycline, rifampicin, moxifloxacin and sparfloxacin, and four other antibiotics: levofloxacin, ciprofloxacin, amoxicillin and streptomycin, all at 5 µM for 3 days. Cells were fixed, permeabilised and incubated with autophagy primary and secondary antibodies. Syto11 and DAPI were used to stain *Wolbachia* and cell nuclei (green and blue fluorescence), respectively. Autophagy activation is shown by an increase in red puncta (increase in LC3B-II due to autophagosomes formation). Bar graph (mean with SD) represents % cells with LC3BII positive puncta for each treatment group with three different sections were imaged, where each section contained ≥50 cells. Scale bars in A are 10 µm.

Statistical analysis was performed to compare all treatment groups to DMSO. Statistical significance tested using Student's t-test, statistical significance was at $p \leq 0.05$. For p-value * = 0.01 to 0.05, ** = 0.01 to 0.001, *** = 0.001 to 0.0001, and **** ≤ 0.0001.

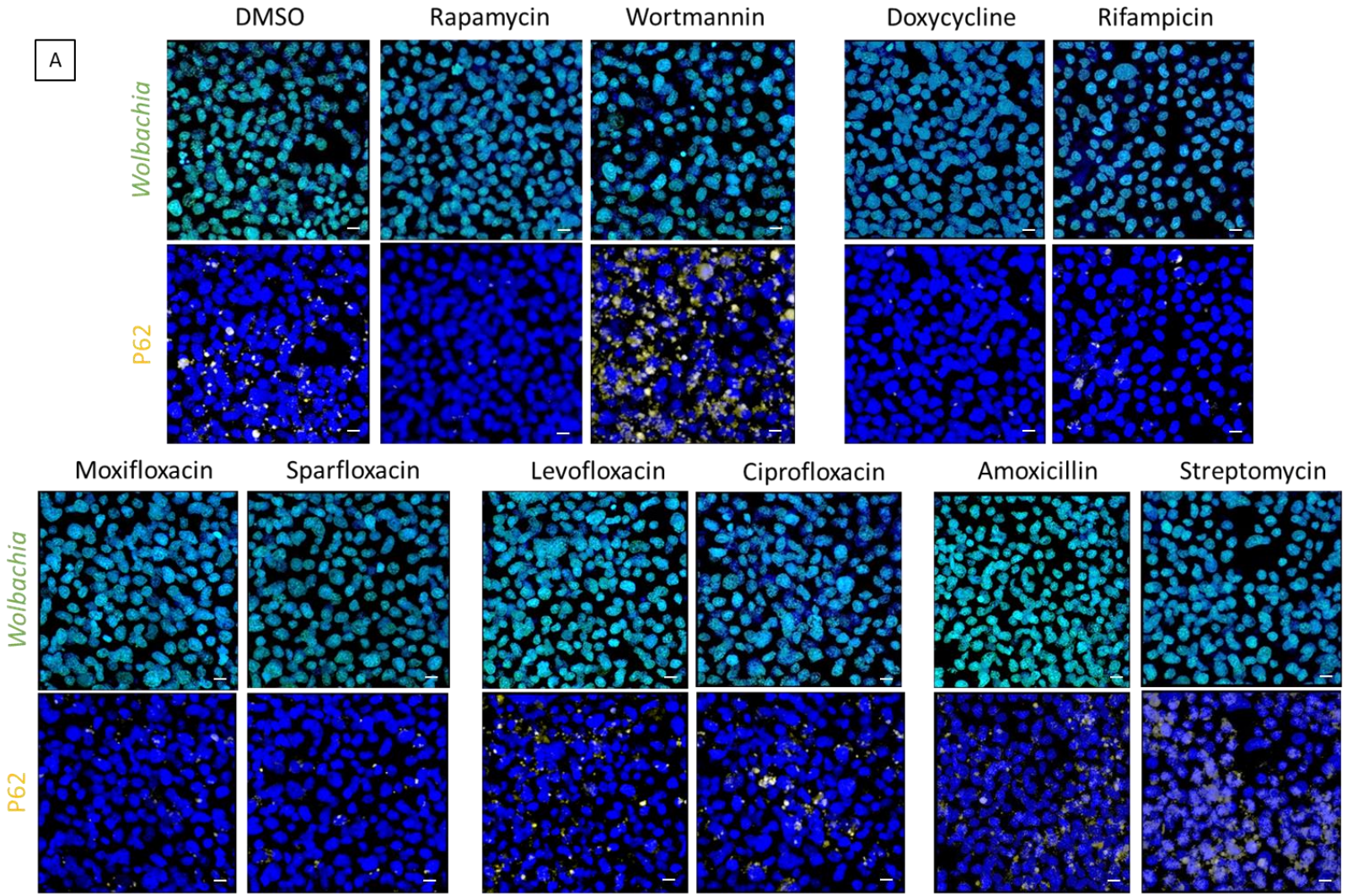
A
DMSO
Rapamycin
Wortmannin
Doxycycline
Rifampicin
Wolbachia
P62
Moxifloxacin
Sparfloxacin
Levofloxacin
Ciprofloxacin
Amoxicillin
Streptomycin
Wolbachia
P62

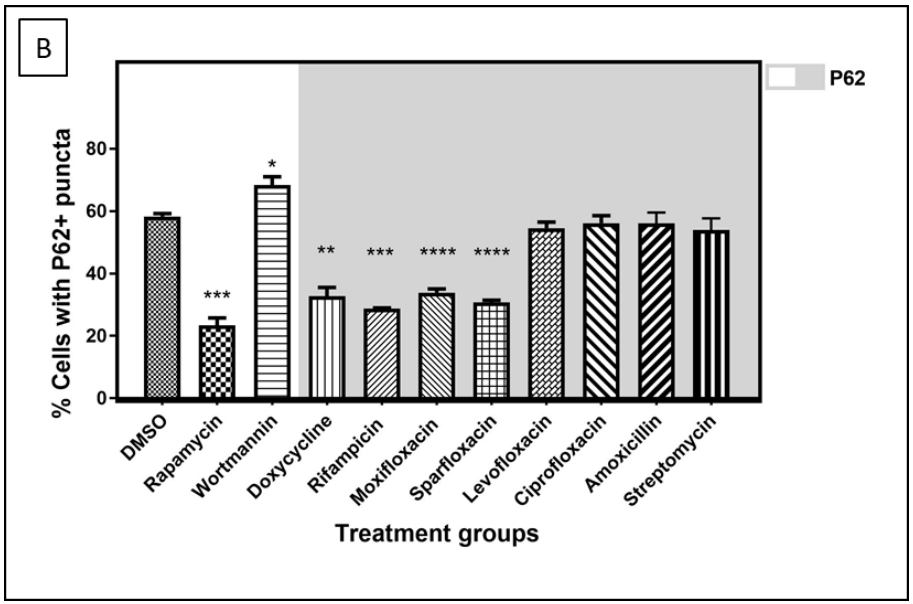


Figure 3. 8 Immunofluorescence staining in C6/36 cells for different antibiotics using autophagic marker p62.

*Wolbachia*-free C6/36 cells were treated with DMSO (vehicle control representing basal autophagy), rapamycin at 5 µM (positive control), wortmannin at 10 µM (negative control), four anti-*Wolbachia* agents: doxycycline, rifampicin, moxifloxacin and sparfloxacin, and four other antibiotics: levofloxacin, ciprofloxacin, amoxicillin and streptomycin, all at 5 µM for 3 days. Cells were fixed, permeabilised and incubated with autophagy primary and secondary antibodies. Syto11 and DAPI were used to stain *Wolbachia* and cell nuclei (green and blue fluorescence), respectively. Autophagy activation is shown by a decrease in yellow puncta (decrease in p62 due to autophagic degradation). Bar graph (mean with SD) represents % cells with p62 positive puncta for each treatment group with three different sections were imaged, where each section contained ≥50 cells. Scale bars in A are 10 µm.

Statistical analysis was performed to compare all treatment groups to DMSO. Statistical significance tested using Student's t-test, statistical significance was at $p \leq 0.05$. For p-value * = 0.01 to 0.05, ** = 0.01 to 0.001, *** = 0.001 to 0.0001, and **** ≤ 0.0001.

### 3.4.3 Measuring concentration-dependency for autophagic induction by antibiotics and the effect on *Wolbachia* load in C6/36*Wp* and C6/36 cells

In this experiment, a range of concentrations from the eight previously tested antibiotics (doxycycline, rifampicin, moxifloxacin, sparfloxacin, levofloxacin, ciprofloxacin, amoxicillin and streptomycin) were examined for their anti-*Wolbachia* activity, as well as their capability to activate autophagy. The rationale for this is to evaluate whether effective antibiotic concentrations against *Wolbachia* also activate autophagy for each tested drug and whether modifying these concentrations would have an impact on the bacteria or the autophagy pathway. This was tested in both *Wolbachia* infected and uninfected C6/36 cells, to examine the effect of antibiotics on activating autophagy in the absence of the bacteria within the same range of concentrations.

As in Section 3.4.2, we quantified the immunofluorescence staining findings based on the percentage of cells with positive LC3B-II and p62 puncta for all tested concentrations of the eight antibiotics to examine their statistical significance compared to the DMSO control. Additionally, *Wolbachia* activity of the tested antibiotics was measured using qPCR to quantify the presence of *Wolbachia* gene copies.

#### 3.4.3.1 Concentration-dependency of antibiotics on autophagy induction - C6/36*Wp*

**i) Anti-*Wolbachia* antibiotics**

Both doxycycline and rifampicin (Figure 3.10 A and B) presented with a significantly higher and lower percentage of LC3B-II and p62, respectively, indicating their autophagic inducing capabilities. This was observed for all tested concentrations of both these antibiotics. Moreover, all tested concentrations of doxycycline and rifampicin significantly reduced *Wolbachia* load irrespective of the concentration (Figure 3.10 C and D).

Conversely, the two anti-*Wolbachia* fluoroquinolone agents (moxifloxacin and sparfloxacin), showed a significant difference in terms of autophagic induction in higher concentrations only (between 5-20 µM) in a concentration-dependent manner (Figure 3.11 A and B).

Interestingly, there also appeared to be a concentration-dependent pattern in terms of anti-*Wolbachia* effect for both moxifloxacin and sparfloxacin. This was observed by the significantly lower *Wolbachia* titre at higher concentrations of cells treated with moxifloxacin and sparfloxacin (Figure 3.11 C and D). Although moxifloxacin at 0.5 µM and sparfloxacin at 1 µM reduced *Wolbachia* significantly, with a 71% and 62% reduction respectively, compared to DMSO, these concentrations did not activate autophagy. On the other hand, the higher concentrations (5-20 µM) of both these fluoroquinolones significantly reduced >90% of *Wolbachia* in cells compared to DMSO and activated autophagy.

A point worth mentioning is that rapamycin at 5 µM (an autophagy inducer), reduced *Wolbachia* titre significantly compared to DMSO control (Figure 3.10-3.12). On the other hand, wortmannin at 10 µM (an autophagy inhibitor) significantly increased *Wolbachia* load compared to control. These findings were also observed in the confocal images of C6/36*Wp* (Figure 3.6 and 7), in which *Wolbachia* stained with syto11 (green fluorescence puncta) were expressed higher and lower in cells treated with wortmannin and rapamycin, respectively, compared to DMSO.

**ii) Other tested antibiotics**

Quantifying the percentage of positive LC3B-II and p62 puncta confirmed our observations of the visual analysis of confocal images for cells treated with levofloxacin, ciprofloxacin, amoxicillin and streptomycin (Figure 3.12 A-D).

For these four antibiotics, all tested concentrations (between 0.125-20 µM) have shown no significant difference in terms of autophagic activity compared to DMSO control. Furthermore, the same concentrations have not influenced any significant change in *Wolbachia* load for all four agents (Figure 3.12 E-H).

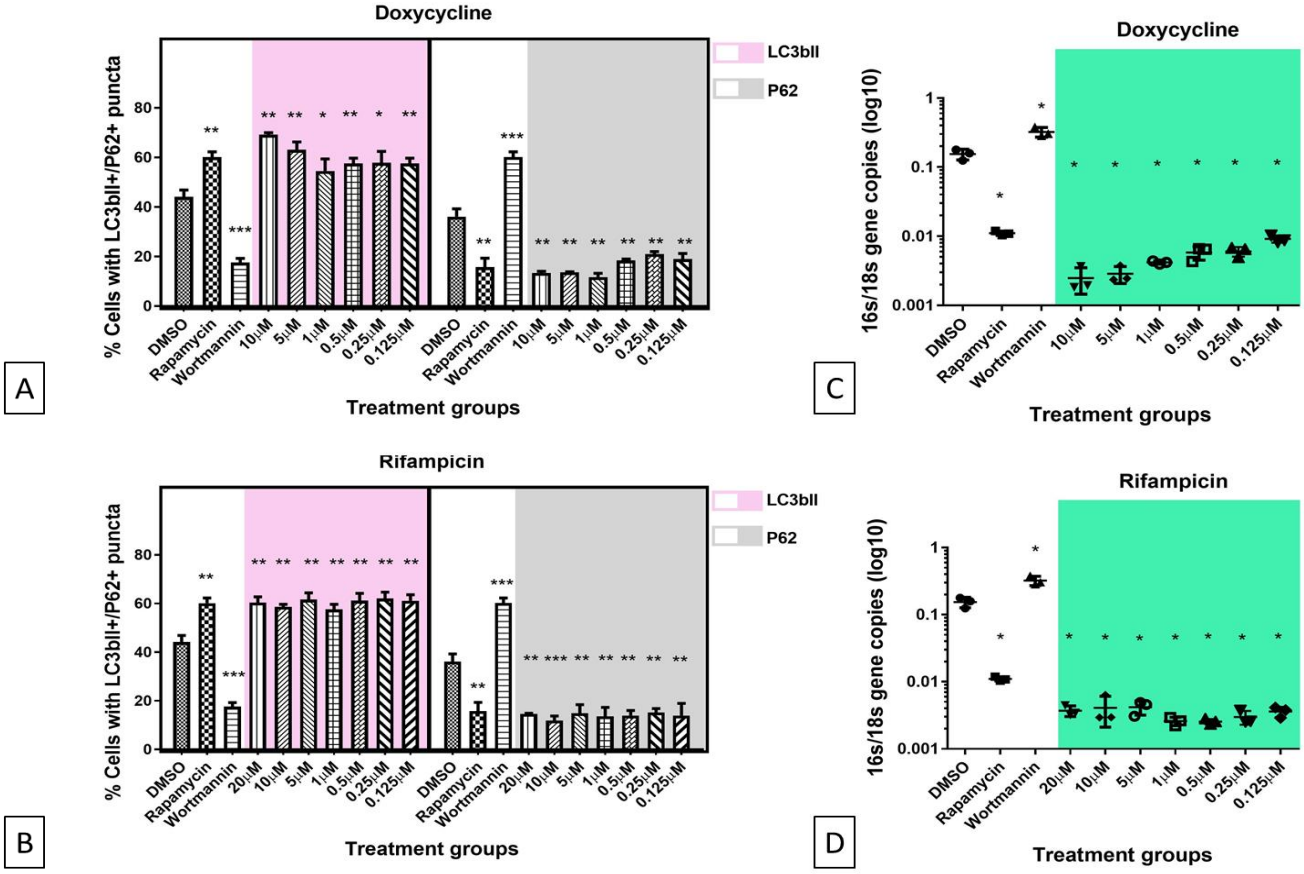


Figure 3. 9 Quantifying antibiotic-induced autophagy and *Wolbachia* load in C6/36*Wp* cells treated with doxycycline and rifampicin.

C6/36 cells infected with *wAlbB* were treated with DMSO (vehicle control representing basal autophagy), rapamycin at 5 µM (positive control), wortmannin at 10 µM (negative control), two anti-*Wolbachia* agents: A and C) doxycycline (between 0.125-10 µM) and B and D) rifampicin (between 0.125-20 µM) for 3 days. For immunofluorescence, A and B) cells were fixed, permeabilised and incubated with autophagy primary and secondary antibodies. For autophagy activation, autophagic markers: LC3B-II and p62 expression increased and decreased, respectively. Graphs (mean with SD) represent % cells with LC3BII or p62 positive puncta for each treatment group with three different sections were imaged, where each section contained ≥50 cells.

In the same treatment groups, qPCR was used to quantify *Wolbachia* C and D) DNA extracted from cells were amplified using *Wolbachia 16s* rRNA gene normalised to *Aedes albopictus 18s* rRNA gene. Graphs (mean with SD) represent *16s:18s* gene copies (log10) in three biological repeats per treatment group.

Statistical analysis was performed to compare all treatment groups to DMSO. Statistical significance tested using Student's t-test, statistical significance was at $p \leq 0.05$. For p-value * = 0.01 to 0.05, ** = 0.01 to 0.001, *** = 0.001 to 0.0001, and **** ≤ 0.0001.

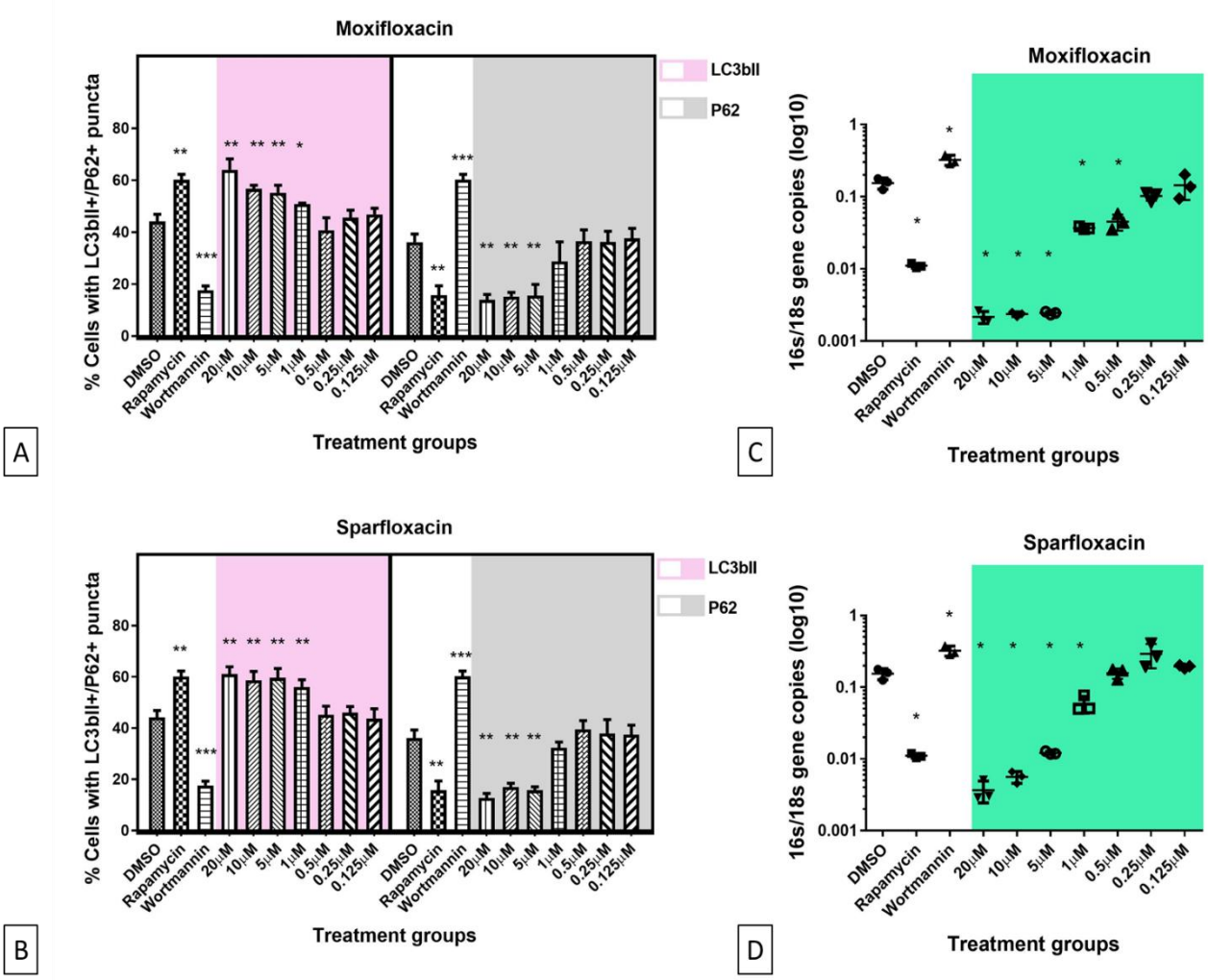


Figure 3. 10 Quantifying antibiotic-induced autophagy and *Wolbachia* load in C6/36*Wp* cells treated with moxifloxacin and sparfloxacin.

C6/36 cells infected with *wAlbB* were treated with DMSO (vehicle control representing basal autophagy), rapamycin at 5 µM (positive control), wortmannin at 10 µM (negative control), two anti-*Wolbachia* agents: A and C) moxifloxacin and B and D) sparfloxacin (both between 0.125-20 µM) for 3 days. For immunofluorescence, A and B) cells were fixed, permeabilised and incubated with autophagy primary and secondary antibodies. For autophagy activation, autophagic markers: LC3B-II and p62 expression increased and decreased, respectively. Graphs (mean with SD) represent % cells with LC3BII or p62 positive puncta for each treatment group with three different sections were imaged, where each section contained ≥50 cells.

In the same treatment groups, qPCR was used to quantify *Wolbachia* C and D) DNA extracted from cells were amplified using *Wolbachia 16s* rRNA gene normalised to *Aedes albopictus 18s* rRNA gene. Graphs (mean with SD) represent *16s:18s* gene copies (log10) in three biological repeats per treatment group.

Statistical analysis was performed to compare all treatment groups to DMSO. Statistical significance tested using Student's t-test, statistical significance was at $p \leq 0.05$. For p-value * = 0.01 to 0.05, ** = 0.01 to 0.001, *** = 0.001 to 0.0001, and **** ≤ 0.0001.

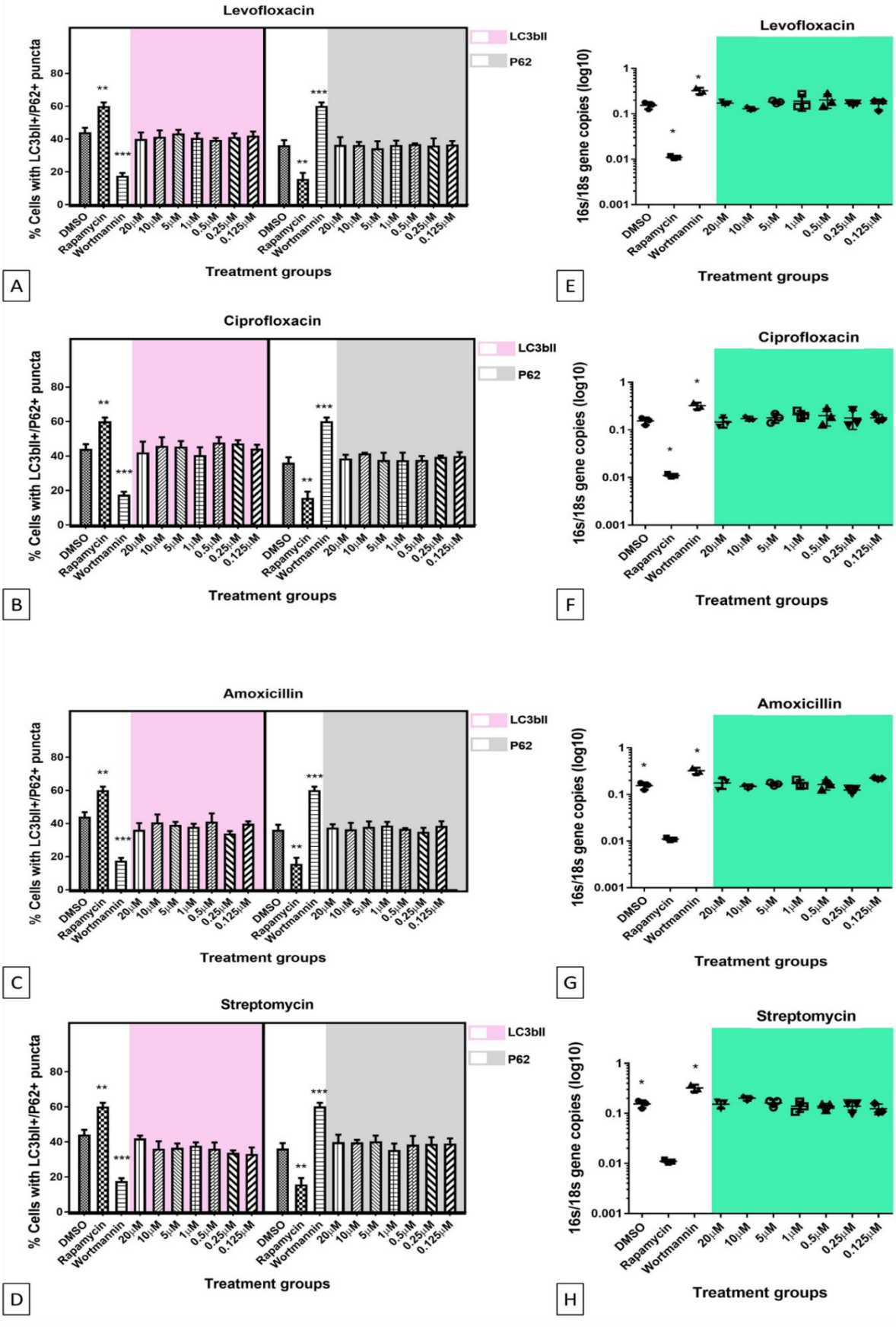
Levofloxacin
% Cells with LC3bII+/P62+ puncta
LC3bII
P62
DMSO
Rapamycin
Wortmannin
20μM
10μM
5μM
1μM
0.5μM
0.25μM
0.125μM
Treatment groups
A
16s/18s gene copies (log10)
E
Ciprofloxacin
B
F
Amoxicillin
C
G
Streptomycin
D
H

Figure 3. 11 Quantifying antibiotic-induced autophagy and *Wolbachia* load in C6/36*Wp* cells treated with levofloxacin, ciprofloxacin, amoxicillin and streptomycin.

C6/36 cells infected with *wAlbB* were treated with DMSO (vehicle control representing basal autophagy), rapamycin at 5 µM (positive control), wortmannin at 10 µM (negative control), and four antibiotics A and E) levofloxacin, B and F) ciprofloxacin, C and G) amoxicillin and D and H) streptomycin all between 0.125-20 µM for 3 days. For immunofluorescence, A, B, C and D) cells were fixed, permeabilised and incubated with autophagy primary and secondary antibodies. For autophagy activation, autophagic markers: LC3B-II and p62 expression increased and decreased, respectively. Graphs (mean with SD) represent % cells with LC3BII or p62 positive puncta for each treatment group with three different sections were imaged, where each section contained ≥50 cells.

In the same treatment groups, qPCR was used to quantify *Wolbachia* E, F, G and H) DNA extracted from cells were amplified using *Wolbachia 16s* rRNA gene normalised to *Aedes albopictus 18s* rRNA gene. Graphs (mean with SD) represent *16s:18s* gene copies (log10) in three biological repeats per treatment group.

Statistical analysis was performed to compare all treatment groups to DMSO. Statistical significance tested using Student's t-test, statistical significance was at $p \leq 0.05$. For p-value * = 0.01 to 0.05, ** = 0.01 to 0.001, *** = 0.001 to 0.0001, and **** ≤ 0.0001.

### 3.4.3.2 Concentration-dependency of antibiotics on autophagy induction – *Wolbachia*-free C6/36

#### i) Anti-*Wolbachia* antibiotics

As in C6/36*Wp*, all four anti-*Wolbachia* agents significantly induced autophagy as expressed by both autophagic markers (Figure 3.13). All tested concentrations showed a significant increase and decrease in LC3B and p62 expression, respectively, compared to DMSO.

#### ii) Other tested antibiotics

C6/36 cells exposed to levofloxacin, ciprofloxacin, amoxicillin and streptomycin demonstrated similar results to those obtained for C6/36*Wp* with the same antibiotics (Figure 3.14). Even at higher concentrations, none of these agents significantly induced autophagy.

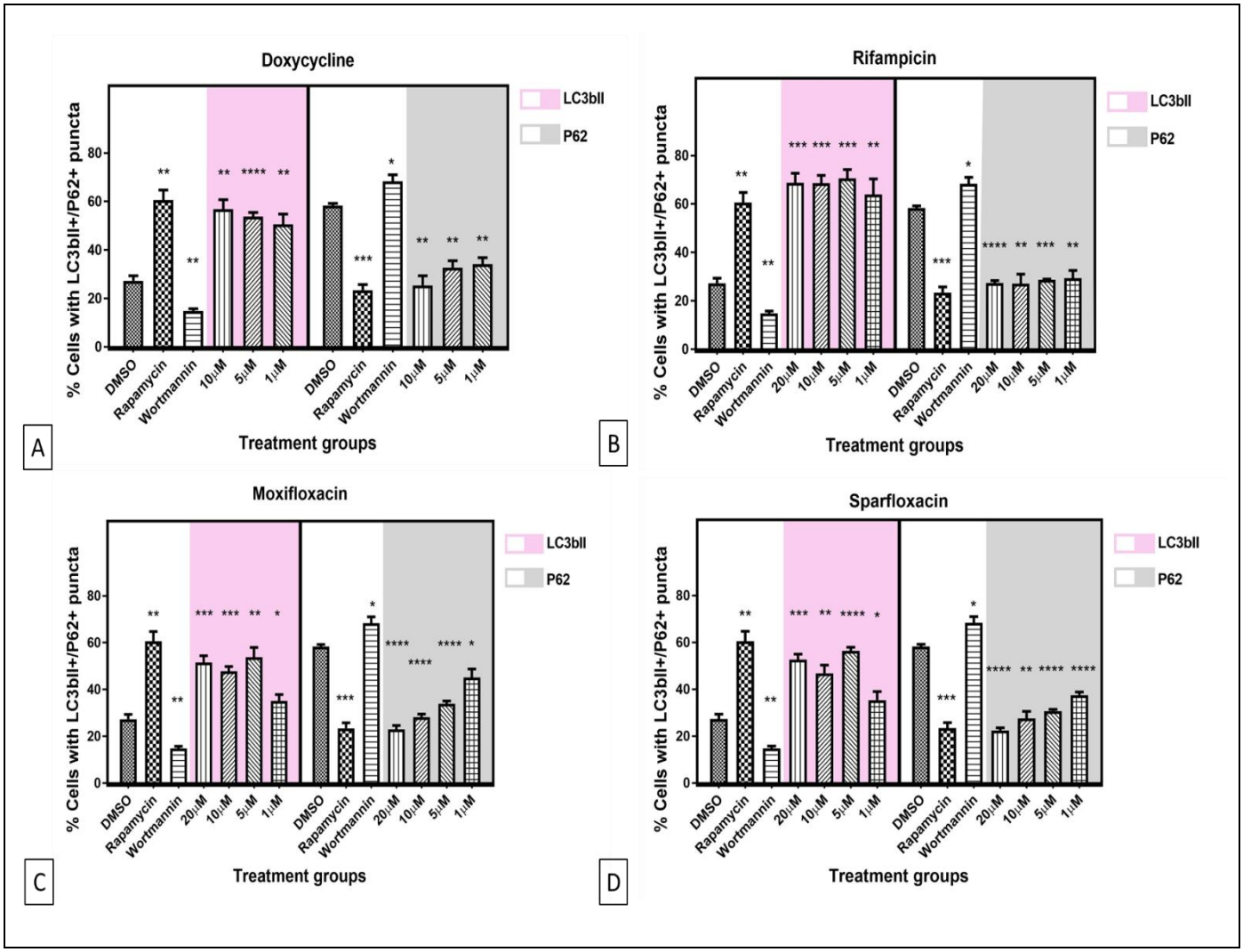


Figure 3. 12 Quantifying antibiotic-induced autophagy in C6/36 cells treated with anti-*Wolbachia* agents.

*Wolbachia*-free C6/36 cells were treated with DMSO (vehicle control representing basal autophagy), rapamycin at 5 µM (positive control), wortmannin at 10 µM (negative control), four anti-*Wolbachia* agents: A) doxycycline (between 1-10 µM) and B) rifampicin C) moxifloxacin and D) sparfloxacin (all between 1-20 µM) for 3 days. Cells were fixed, permeabilised and incubated with autophagy primary and secondary antibodies. For autophagy activation, autophagic markers: LC3B-II and p62 expression increased and decreased, respectively. Graphs (mean with SD) represent % cells with LC3BII or p62 positive puncta for each treatment group with three different sections were imaged, where each section contained ≥50 cells.

Statistical analysis was performed to compare all treatment groups to DMSO. Statistical significance tested using Student's t-test, statistical significance was at $p \leq 0.05$. For p-value * = 0.01 to 0.05, ** = 0.01 to 0.001, *** = 0.001 to 0.0001, and **** ≤ 0.0001.

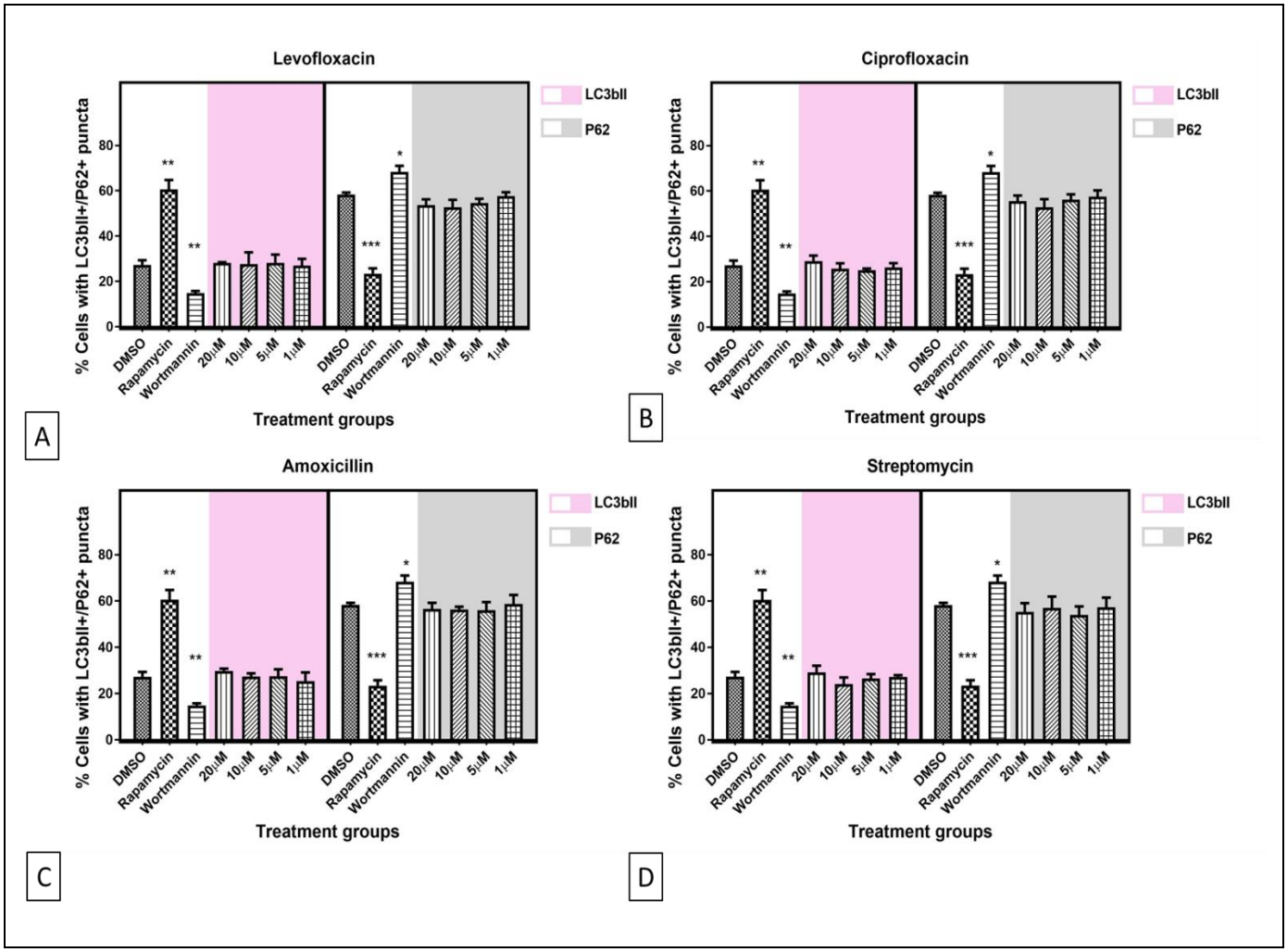


Figure 3. 13 Quantifying antibiotic-induced autophagy in C6/36 cells treated with different antibiotics.

*Wolbachia*-free C6/36 cells were treated with DMSO (vehicle control representing basal autophagy), rapamycin at 5 µM (positive control), wortmannin at 10 µM (negative control), and four antibiotics: A) levofloxacin and B) ciprofloxacin C) amoxicillin and D) streptomycin (all between 1-20 µM) for 3 days. Cells were fixed, permeabilised and incubated with autophagy primary and secondary antibodies. For autophagy activation, autophagic markers: LC3B-II and p62 expression increased and decreased, respectively. Graphs (mean with SD) represent % cells with LC3BII or p62 positive puncta for each treatment group with three different sections were imaged, where each section contained ≥50 cells.

Statistical analysis was performed to compare all treatment groups to DMSO. Statistical significance tested using Student's t-test, statistical significance was at $p \leq 0.05$. For p-value * = 0.01 to 0.05, ** = 0.01 to 0.001, *** = 0.001 to 0.0001, and **** ≤ 0.0001.

### 3.4.4 Time-course assessment of autophagy induction by antibiotics –C6/36*Wp*

The final part of the results section presents our assessment of different time-points (at day 0, 1, 3, 5 and 7) in C6/36 cells infected with *w*AlbB and treated with the eight pre-selected antibiotics: doxycycline, rifampicin, moxifloxacin, sparfloxacin, levofloxacin, ciprofloxacin, amoxicillin and streptomycin at a fixed concentration (5 µM).

We will first present the results for LC3B and p62 immunoblotting expression in C6/36*Wp* to determine autophagic influx at the selected time-points for all tested antibiotics. This will be followed by qPCR analysis to quantify *Wolbachia* elimination at the same time-points.

#### 3.4.4.1 Immunoblotting analysis for autophagy induction at different time-points

The findings for autophagy activation using western blot in the eight pre-selected antibiotics are presented in Figure 3.15 A (for LC3B expression) and Figure 3.15 B (for p62) at different time-points (day 0, 1, 3 ,5 and 7). Autophagic activation was considered present by the expression of two bands for LC3B and the absence of the single band for p62 (as seen for the positive control, rapamycin). As with the previous immunoblotting experiments, DMSO was used to represent basal level of autophagy in C6/36*Wp*.

All four tested anti-*Wolbachia* agents (doxycycline, rifampicin, moxifloxacin, and sparfloxacin) presented evidence of autophagic induction for all treatment periods (day 1, 3, 5 and 7) compared to DMSO, as expressed in the high and low band intensity of LC3B-II and p62, respectively. However, their appeared to be a difference between the anti-*Wolbachia* agents in longer duration of treatment. In the case of doxycycline and rifampicin, expression of a high band intensity of LC3B-II was observed for all treatment periods (from day 1 to day 7). Conversely, both moxifloxacin and sparfloxacin showed a reduced protein expression of LC3B-II after day 1, indicating a possibly lower autophagic influx. The differences in treatment duration between the four anti-*Wolbachia* agents were not observed in terms of p62 expression, where all agents expressed a reduced intensity compared to the DMSO control, and similar to rapamycin.

With regards to other tested antibiotics that lack anti-*Wolbachia* activity (levofloxacin, ciprofloxacin, amoxicillin and streptomycin), a general observation is that different time-points did not appear to impact autophagic induction compared to DMSO, by the low expression and prominent band of LC3B and p62, respectively. Interestingly, an exception of this was observed with two fluoroquinolone agents (levofloxacin and ciprofloxacin) at the beginning of treatment (day1). In the first day of antibiotic treatment, levofloxacin and ciprofloxacin expressed both LC3B bands (indicating possible autophagic activation), however this was not maintained in subsequent treatment days or expressed in p62 immunoblotting interpretation.

#### 3.4.4.2 qPCR analysis of *Wolbachia* load at different time-points

The results for the qPCR analysis to quantify *Wolbachia* load in C6/36*Wp* treated with the eight antibiotics at different time-points are presented in Figure 3.16. A graph presenting the full treatment period (from day 0 to day 7) including all treatment groups in the Appendix A Figure A9.

As seen in Section 3.4.3, rapamycin treated cells reduced *Wolbachia* titre significantly compared to DMSO. The reduction increased with time reaching approximately 50% clearance, compared to the control. Whereas in the case of wortmannin, a significant increase in *Wolbachia* number was recorded at day 3 onwards compared to DMSO.

For all anti-*Wolbachia* agents, there was a significant reduction in *Wolbachia* titre compared to DMSO from day 1 (Figure 3.16). This significant reduction on day 1 (of < 50%) continued in subsequent treatment days for all four agents, reaching over 95% reduction compared to DMSO control at day 7. This reduction was observed earlier for sparfloxacin followed by moxifloxacin, although this was only noticeable for day 1 and 3 of treatment.

Compared to the DMSO control, the remaining four agents (levofloxacin, ciprofloxacin, amoxicillin and streptomycin) did not reduce *Wolbachia* number and this observation remained for the duration of the treatment period (Figure 3.16).

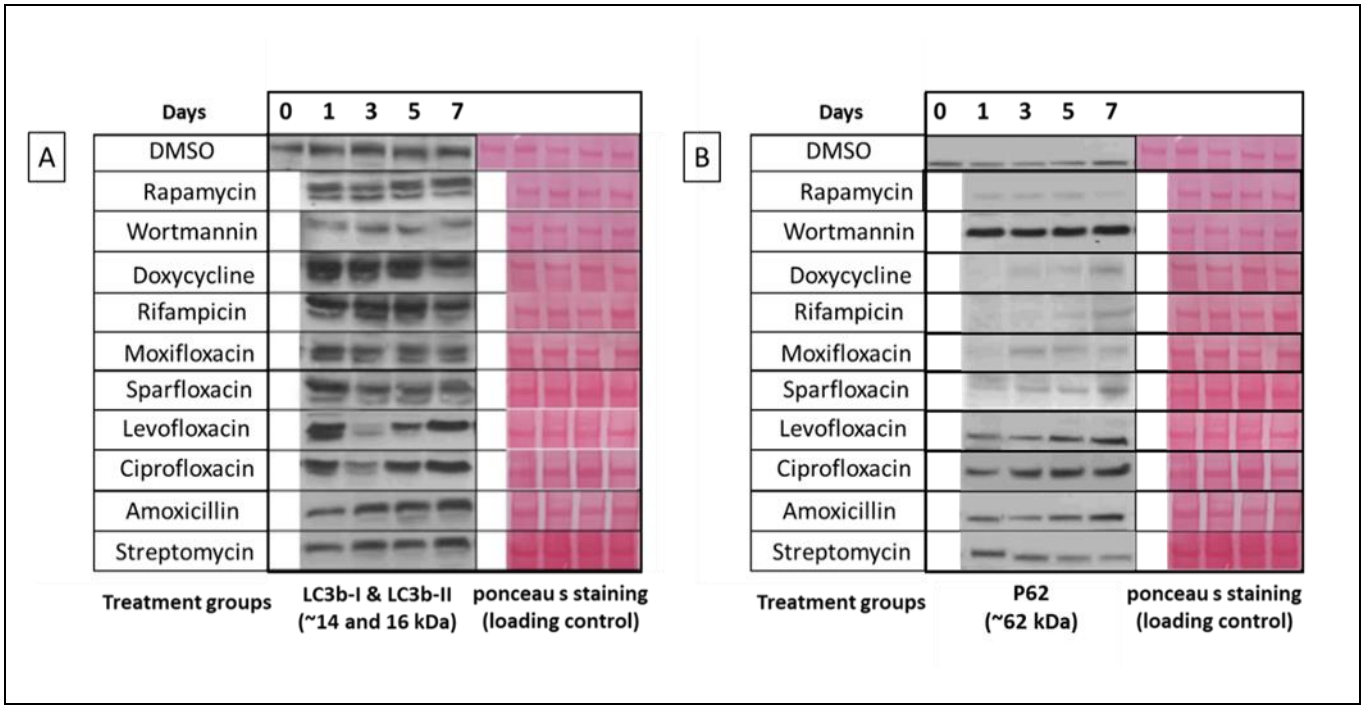


Figure 3. 14 Immunoblotting analysis for autophagy induction at different time-points using diverse antibiotics in C6/36*Wp* cells.

C6/36 mosquito cells infected with *Wolbachia* (*w*AlbB) treated with: DMSO – vehicle control, rapamycin – positive control, wortmannin -autophagy inhibitor, four anti-*Wolbachia* agents: doxycycline, rifampicin, moxifloxacin, sparfloxacin, and four different antibiotics: levofloxacin, ciprofloxacin, amoxicillin, and streptomycin at different time-points: day 0, 1, 3, 5 and 7. Reduced protein extracts of cells were loaded at 50µg/40ul per lane into 4-12% bis tris SDS-PAGE gels. Separated proteins were transferred into nitrocellulose membrane, blocked and incubated with primary and secondary antibodies. Western blot protein expression is presented in **A)** for rabbit anti-LC3B (LC3B-I at 16 kDa and LC3B-II at 14 kDa) and **B)** rabbit anti-p62 (at 80 kDa). Ponceau s staining was used as a loading control.

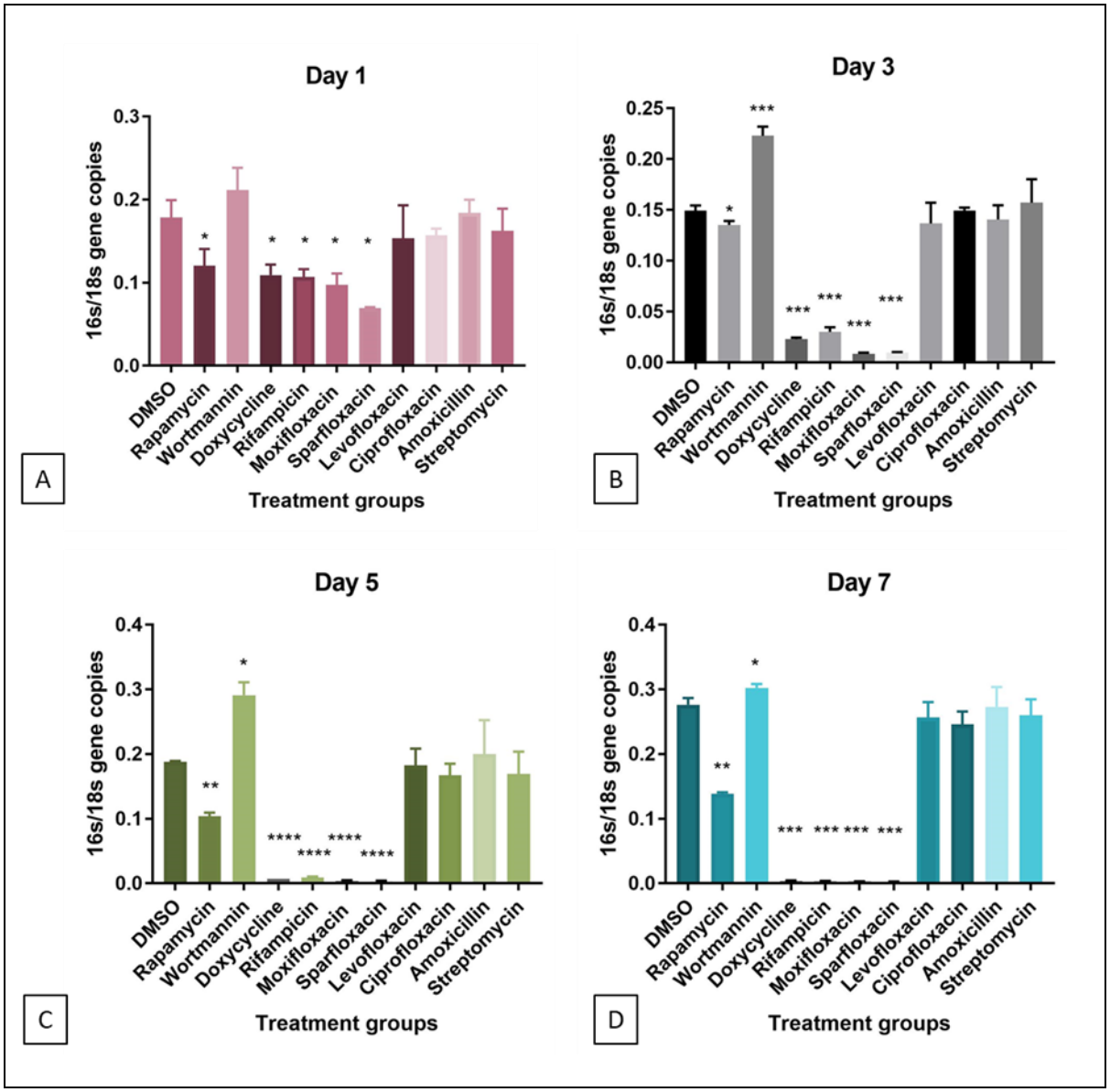


Figure 3. 15 qPCR analysis of *Wolbachia* load in antibiotics at different time-points.

C6/36*Wp* cells were treated at different time-points: **A)** day 1, **B)** day 3, **C)** day 5 and **D)** day 7 with DMSO (vehicle control), rapamycin at 5 µM (autophagy inducer), wortmannin at 10µM (autophagy inhibitor), four anti-*Wolbachia* agents at 5 µM: doxycycline, rifampicin, moxifloxacin and sparfloxacin and four other antibiotics at 5 µM: levofloxacin, ciprofloxacin, amoxicillin and streptomycin. DNA extracted from cells were amplified using *Wolbachia 16s* rRNA gene normalised to *Aedes albopictus 18s* rRNA gene. Graphs (mean with SD) represent *16s:18s* gene copies in three biological repeats per treatment group.

Statistical analysis was performed to compare all treatment groups to DMSO. Statistical significance tested using Student's t-test, statistical significance was at $p \leq 0.05$. For p-value * = 0.01 to 0.05, ** = 0.01 to 0.001, *** = 0.001 to 0.0001, and **** ≤ 0.0001.

## 3.5 Discussion:

Initial experimentation focused on the primary *in vitro* cell-based assay used by the A-WOL consortium of C6/36 infected with *Wolbachia* (*w*AlbB), where all four anti-*Wolbachia* antibiotics (doxycycline, rifampicin, moxifloxacin and sparfloxacin) reduced *Wolbachia* load and induced autophagy. Furthermore, two pre-clinical candidates (TylAMac$^{TM}$ and AWZ1066S) and a re-purposed antibiotic (fusidic acid) from the A-WOL consortium produced similar results to established anti-*Wolbachia* agents, indicating the potential role of autophagy in the efficacy of anti-*Wolbachia* drugs. This observation raised the hypothesis that inhibition of protein synthesis by these antibiotics leads to an inhibition of putative proteins involved in autophagy evasion by *Wolbachia* (87). However, this hypothesis was not supported by experiments on uninfected cells, which also showed a similar pattern of induction of autophagy in the absence of *Wolbachia* infection. To determine if this ability of antibiotics to induce autophagy was restricted to C6/36 cells, another insect cell line that lack *Wolbachia* (SF9 cells) was tested and produced similar results for autophagic activation when treated with the same antibiotics. Importantly this pattern of autophagy induction was replicated in the target organism, *B. malayi* where drugs with efficacy against *Wolbachia* induced autophagy, whereas those lacking efficacy against *Wolbachia* failed to induce autophagy. Next, we screened two mammalian cells lines (THP-1 and MDCK) with the same set of antibiotics, which did not present evidence of autophagic activation, indicating that our observation of antibiotic-induced autophagy was restricted to insect cells and nematodes and not replicated in mammalian cells at the concentrations tested in this research.

Concentration-dependency testing of the antibiotics revealed a close correlation between concentrations of drug that induce autophagy with the elimination of *Wolbachia.* This was particularly apparent with the fluoroquinolones, moxifloxacin and sparfloxacin, where autophagy was only induced by drug concentrations that reduce *Wolbachia* by >90%. This level of *Wolbachia* reduction is the empirical threshold, which has to be achieved to deliver macrofilaricidal activity (65). While all tested concentrations of doxycycline and rifampicin achieved >90% *Wolbachia* reduction, the concentration-dependent manner of reduction was not observed. However, more research is needed in lower concentrations (lower than

0.125 µM) for these two agents to confirm this particular finding. Furthermore, antibiotics without efficacy against *Wolbachia* failed to induce autophagy at any of the concentrations tested. While we have examined different classes of antibiotics in the same concentration it is important to note that differences occur between their EC50 and hence caution is needed when drawing broad conclusions between these drugs.

When examining the effect of antibiotics at different time-points, we observed that induction of autophagy occurs within the first day of exposure and is maintained throughout the seven-day period of culture for all tested anti-*Wolbachia* drugs. This early autophagic activity occurs with only low levels of *Wolbachia* reduction, supporting the notion that autophagy is not only involved in the clearance of dead bacteria, but closely linked with antibacterial activity.

Previous studies have not examined antibiotics of this range of chemical diversity (tetracycline, rifamycin and fluoroquinolone) in insects and nematodes against intracellular bacteria in terms of autophagy activation. However, there is evidence that autophagy is implicated in the efficacy of antimycobacterial drugs. Kim *et al.* (235) examined macrophages infected with *Mycobacterium tuberculosis* (Mtb) treated with anti-tuberculosis (anti-TB) drugs: isoniazid and pyrazinamide, which resulted in autophagy activation only at effective antibacterial concentrations. In the same study, no autophagic activation was observed in the absence of Mtb treated with the same drugs. This observation corresponds with our findings in mammalian cells (lacking *Wolbachia*), where no autophagic activation was observed. Kim *et al.* (235) proposed that autophagy activation in macrophages infected with Mtb was initiated through ROS production, leading to oxidative stress following antimycobacterial treatment. Other researchers have also observed that certain antibiotics may alter cell organelles (such as mitochondria), increase formation of ROS and lower intracellular pH, all of which are factors that may influence autophagic induction (199, 211, 259, 260).

In conclusion, an increase in autophagic activation was consistently observed for all four tested anti-*Wolbachia* drugs (doxycycline, rifampicin, moxifloxacin and sparfloxacin) when exposed to insect cells and *B. malayi* mf, but not for antibiotics without activity against *Wolbachia*. Furthermore, we have successfully observed an increase in autophagic activity

in two pre-clinical candidates and one re-purposed antibiotic from the A-WOL consortium (TylAMac$^{TM}$, AWZ1066S and fusidic acid). Exposure of antibiotics to mammalian cells did not replicate the pattern observed in insect cells and mf, with antibiotics showing no clear evidence of autophagy activation. Through concentration-dependency experimentation on anti-*Wolbachia* antibiotics, we have observed that their anti-*Wolbachia* activity is closely correlates with activating autophagy, which we will examine further in the presence of autophagy inhibitors in Chapter 4 of this thesis.

# Chapter 4 Examining the contribution of autophagy in the activity of anti-*Wolbachia* drugs

## 4.1 Chapter overview

In this third and final results section of this thesis I will present and discuss the experiments performed to examine whether autophagy may play a role in the anti-*Wolbachia* activity of drugs in mosquito cells C6/36*Wp*, microfilariae (mf) and female adult worms of *Brugia malayi*. This was examined using two anti-*Wolbachia* antibiotics, doxycycline and rifampicin, as well as the newly identified drug AWZ1066S, which has been candidate-selected by the A-WOL consortium. These drugs were selected based on known macrofilaricidal properties and their use in clinical trials and pre-clinical development. Furthermore, we have selected these three diverse antibiotics based on their potential different modes of action against *Wolbachia*.

Two sets of experiments were performed in this chapter. In the first group, the impact of autophagy suppression was monitored on doxycycline and rifampicin treated in mosquito cell line C6/36 infected with *w*AlbB (C6/36*Wp*), *B. malayi* mf and female adult worms. In the second set of experiments, the role of autophagy suppression was assessed in *B. malayi* mf and female worms in doxycycline and AWZ1066S induced *Wolbachia* decline after the removal of drugs, in addition to rifampicin in mf. For both sets of experiments, wortmannin and/or l-asparagine, two autophagy inhibitors previously validated in these experimental systems in Chapter 2, were used to suppress autophagy.

## 4.2 Background

### 4.2.1 *Brugia malayi* and *Wolbachia*: a symbiotic relationship

As this chapter will focus on examining anti-*Wolbachia* drugs in the presence of autophagy inhibitors in *B. malayi* mf and female adult worms, this section will briefly discuss the nematode life cycle, including several important biological and structural differences in different developmental stages of *B. malayi*, as well as the symbiotic relationship between it and the intracellular bacteria, *Wolbachia pipientis*. For the full detailed life cycle, the symbiotic relationship as well as the epidemiological relevance of filarial nematodes that cause lymphatic filariasis, please refer to Chapter 1 of this study.

From a general perspective, the life cycle of *B. malayi* is divided into an extrinsic (in the mosquito vector of *Aedes* and *Mansonia* species) and intrinsic life cycle (in the human host). After feeding on an infected human host, mf within the mosquito vector mature into the infective larval stage (L3 larvae) and make their way towards the head and proboscis of the mosquito. Thereafter, a blood meal will transfer the L3 larvae from the mosquito and into a new human host, where it would develop to L4 larvae, and later into the female and male adult stage of the parasite. Adult worms may survive for over ten years in the lymphatic system of humans and female adult worms continue to release mf into the blood stream of the host, thereby continuing the life cycle in subsequent blood meals by mosquito vectors (2, 26, 261).

While the life cycle for *B. malayi* is generally similar to that of *W. bancrofti*, there are several important differences between the two nematode species. First, from a morphological perspective, both the mf and adult stages of *W. bancrofti* are larger in length and diameter than *B. malayi*. In terms of mf, *B. malayi* have distinct lateral indentations of their caudal nuclei, which are not present in *W. bancrofti* (2). Additionally, the cephalic space is larger in *Brugia* species compared to *W. bancrofti* mf (2). The nocturnal periodicity of mf in the blood of human host is observed for both *W. bancrofti* and *B. malayi*, however this periodicity is reversed in *W. bancrofti* in the South Pacific region where the vector is the day biting *Aedes polynesiensis* (2, 9, 10). Finally, it is important to note that the mosquito vectors differ

between *B. malayi* and *W. bancrofti*, with the former transmitted via mosquitoes principally from the *Mansonia* genera only (10, 261).

The symbiotic relationship between filarial nematodes of *B. malayi* and *Wolbachia* has long been documented in the literature and we have previously discussed this issue in Chapter 1 of this thesis. Due to the inability of filarial nematodes to mature, reproduce, and obtain essential nutrients for survival without the presence of *Wolbachia,* their relationship has been described as obligate mutualism (2, 26, 262). While *Wolbachia* can naturally occur in mosquito vectors of filarial nematodes and many other different types of arthropods (including *Aedes albopictus* cell line C6/36*Wp* cells tested in this chapter), their interaction has generally been described as reproductive parasites. On the other hand, Experiments performed on *Aedes albopictus* have also shown that *Wolbachia* infection can increase fecundity, as well as increase the life expectancy of female mosquitoes (26, 263).

For both female and male adult worms, *Wolbachia* are located in the lateral cords of the organism. While *Wolbachia* may occur in certain parts of the reproductive system of female adult worms, such as oocytes, ovaries and the developing embryos of the uterus, the adult male reproductive system of filarial nematodes is devoid of *Wolbachia* (26). Distinct morphological features are present between male and female adult worms of *B. malayi*. Female adult worms are larger in length than their male counterparts, ranging in length between 43-55 mm and 13-23 mm, respectively. Furthermore, female adult worms are on average wider than male worms, generally between 130-170 µm and 70-80 µm, respectively (261).

As previously discussed in Chapter 1, *Wolbachia* are present in all stages of *B. malayi*, however, the population density varies between different worms and life cycle stages (23, 30, 264). Female worms will generally present with a higher number of *Wolbachia* than males due to their larger size and the presence of *Wolbachia* in embryonic stages within the uterus. Mf have the lowest number of *Wolbachia* compared to other developmental stages, which is maintained throughout development to third-stage larvae in the vector, before rapidly expanding during the first week of infection of the mammalian host and throughout development of the fourth-stage larvae (49, 264).

Autophagy (discussed in detail in previous chapters) plays an important role in the regulation of *Wolbachia* populations. Voronin *et al.* (87) observed that autophagy was activated in life stages of *B. malayi* that contain replicating *Wolbachia*. In the same study, the effect of autophagy was assessed, by chemical and genetic manipulation in *B. malayi*, where activation and inhibition of autophagy, decreased and increased *Wolbachia* titres, respectively. Similar results were also observed when inducing or inhibiting autophagy in *Aedes albopictus* cells C6/36 cells and *Drosophila* infected with *Wolbachia*. Moreover, *in vivo* studies performed on jirds infected with *B. malayi* treated with two different autophagy activators (spermidine and rapamycin), decreased *Wolbachia* load compared to non-treated animals (87).

### 4.2.2 Doxycycline, rifampicin and AWZ1066S as anti-*Wolbachia* agents

Due to the documented disadvantages of antiparasitic drugs (for example ivermectin, albendazole, and diethylcarbamazine), which include their ineffectiveness against adult worms (described previously in Chapter 1), as well as the emerging issue of drug resistance, there is a need to consider the possibility of a role for anti-*Wolbachia* agents (26). In light of the obligate symbiotic relationship between filarial nematodes (in all their stages) and *Wolbachia*, the A-WOL consortium has proposed novel approaches in the treatment of filarial infection by targeting *Wolbachia* through anti-*Wolbachia* drugs, including doxycycline, high dose rifampicin and newly developed agent AWZ1066S (52, 64, 82, 265). Details on each of these compounds and their mechanism of action, as well as *in vitro*, *in vivo* and human clinical studies performed using these agents were previously mentioned in Chapter 1.

### 4.2.3 Experimental justification

In the experiments of this chapter, three anti-*Wolbachia* drugs were used: doxycycline, rifampicin and AWZ1066S. The tested drugs were selected based on their proven potency against *Wolbachia,* and potential different modes of action (26, 82), which were described in detail in Chapter 1. Validated *in vitro* assays of *B. malayi* nematodes developed by A-WOL consortium focused on mf and adult worms were used in this chapter.

The first set of experiments were performed to determine whether the pre-selected anti-*Wolbachia* drugs can reduce *Wolbachia* titre when autophagy was inhibited chemically, using wortmannin or l-asparagine during exposure to each antibiotic. This was tested with C6/36*Wp*, *B. malayi* mf and female adult worms. This group of experiments were performed by quantifying *Wolbachia* load (using qPCR).

In the second group of experiments, a post-drug exposure washout assay was conducted to determine whether the continued reduction or rebound in *Wolbachia* load post-exposure to the drug during washout periods were dependent on the autophagy pathway. In this set of experiments, *Wolbachia* load was quantified using qPCR technique in tested *B. malayi* mf and female worms.

## 4.3 Materials and methods:

For more details on the materials used in the experiments conducted in this chapter please refer to the Appendix B Table B.1 section of this thesis.

### 4.3.1 *In vitro* culture of cell lines and worms

**i) Mosquito cell line C6/36*Wp* cells with *w*AlbB:**

The materials and preparation used for mosquito cell line C6/36*Wp* infected with *w*AlbB were the same as those previously described in Chapter 2.3.1.

**ii) *Brugia malayi* microfilariae (mf) and female adult worms:**

The mf and adult stages of the parasite were extracted from the peritoneal cavity of gerbils. This was performed by members of the filariasis laboratory, Mr Andrew Steven and Mr John Archer, Department of Tropical Disease Biology at LSTM, UK, following the same protocol and procedure as described by Griffiths *et al.* (258).

*B. malayi* mf were filtered and cultured following the same steps described in Section 3.3.1.

With regards to adult worms, they were first washed using fresh RPMI media (Gibco, Thermo Fisher Scientific) and later prepared in a similar manner to that of mf culture, described in Section 3.3.1. RPMI 1640 culture media supplemented with 2 mM L-glutamine, 25 mM HEPES, 100 U/ml penicillin-streptomycin, 2.5 mg/ml amphotericin B (Thermo Fisher Scientific) and 10% FBS (Thermo Fisher Scientific), which will be referred to as RPMI media in the rest of this chapter.

### 4.3.2 Analysis of *Wolbachia* load using quantitative polymerase chain reaction (qPCR):

#### 4.3.2.1 C6/36*Wp* cells

C6/36*Wp* cells were seeded in a 96-well plate (Thermo Fisher Scientific) at 10,000 cells/ml in a total volume of 200 µl Leibovits-15 (L-15) media (Gibco, Thermo Fisher Scientific), prepared as described in Section 2.3.1. Cells were treated for 7 and 14 days in the following groups: doxycycline at 5 µM (alone or combined with wortmannin or l-asparagine), rifampicin at 5 µM (alone or combined with wortmannin or l-asparagine), and autophagy inhibitors: wortmannin and l-asparagine, at 10 µM and 10 mM, respectively. DMSO was used as a vehicle control.

Following the preparation of treatment groups, the subsequent steps of DNA extraction and qPCR analysis were performed as previously described in Section 3.3.4. All qPCR findings for this section are presented as a (log10) ratio of *16s:18s* genes, to normalise the results in relation to DNA quantity.

#### 4.3.2.2 *Brugia malayi* mf and female adult worms:

Mf and female adult worms were treated for 6 days in the following groups: doxycycline at 5 µM (alone or combined with wortmannin or l-asparagine), rifampicin at 5 µM (alone or combined with wortmannin or l-asparagine), and autophagy inhibitors: wortmannin and l-asparagine at 10 µM and 10 mM, respectively. DMSO was used as a vehicle control.

8000 mf were cultured in 100 µl RPMI media per well of a 96-well plate. 100 µl of media containing the prepared treatment groups were added to mf suspension in wells for a total volume of 200 µl.

For adult worms, two adult females were cultured into 6-well plates (Thermo Fisher Scientific) in a total of 3 ml RPMI media containing the prepared treatment groups.

**DNA lysis and extraction:**

Genomic DNA was extracted from *B. malayi* worms (mf and adult worms) using QIAmp mini DNA kit from Qiagen. Mf and adult females were transferred from well plates and into microtubes. 35 µl (for mf) and 20 µl (for females) of Proteinase K and 100 µl (for mf) and 180 µl (for females) of ATL tissue lysis buffer (both supplemented with kit) were added to all microtubes and incubated overnight in a water bath set at 56°C. For female adult worms only, prior to the overnight incubation, tubes were incubated for 30 minutes at 56°C and mixed using vortex mixer.

After 20 hours, 200 µl of AL buffer (supplemented with kit) was added and returned to the water bath at 70°C for 10 minutes, to allow adequate cell lysis. 200 µl of absolute ethanol (Sigma Aldrich) was added to tubes and incubated for 5 minutes at room temperature for DNA precipitation. All cell lysates were transferred to mini-spin columns (provided by the DNA kit) and centrifuged at 5000 g for 1 minute. Following centrifugation, two washing steps were performed by adding 500 µl of AW1 followed by 500 µl of AW2 washing buffer (both supplemented with the kit). 100 µl (for mf) and 62 µl (for females) of AE elution buffer (supplemented with kit) was added into each mini-spin column. Columns were centrifuged at 13,000 g for 5 minutes and purified eluted DNA was collected and stored at -20°C for qPCR analysis.

**qPCR analysis:**

The protocol reported by McGarry *et al*. (49) was followed with slight modification, as detailed below. Extracted genomic DNA of *B. malayi* mf and female adults were amplified using *Wolbachia* Surface Protein (w*Bm wsp*) and glutathione S-transferase (*Bm gst)* genes (designed by Integrated DNA Technologies, UK), and gene copy numbers were quantified by qPCR, using CFX384 Real-Time System with C1000 Thermal Cycler (Biorad). The final volume of all reaction wells was 20 µl of SYBR green master mix containing a pair of primers specific for w*Bm wsp* and *Bm gst* (the exact nucleotide sequence of each primer provided in the Appendix B Table B.3).

For *wsp* and *gst,* 2 µl and 1 µl of DNA were added to the reaction mix, respectively. A standard curve of w*Bm wsp* and *gst* plasmid stock serial dilution was performed in duplicates. The following cycling conditions were applied for qPCR: 15 minutes at 95°C, 40 cycles for 15 seconds at 94°C, 30 seconds at 60°C (for *wsp*) and at 55°C (for *gst*), 30 seconds at 72°C, and a melting curve between 60-97°C. Gene copy numbers were normalised and expressed as *wsp:gst* ratio. Five and eight biological replicates were performed for mf and female adult worms, accordingly. Three qPCR reaction technical repeats were performed for each biological sample. All qPCR findings for this section are presented as a (log10) ratio of *wsp:gst* genes to normalise the results in relation to DNA quantity.

### 4.3.3 Viability of *Brugia malayi* microfilariae and adult worms:

Three different methods were used to assess mf and adult worms to determine if the added chemical compounds (anti-*Wolbachia* and/or autophagy inhibitors) previously mentioned in Section 4.3.2 had a negative impact on their viability during the experimental period. These methods are described below.

**i) Motility scoring**

The motility of *B. malayi* mf and female adult worms in all treatment groups was scored daily during the treatment period of 6 days (or 12 days). Following the methodology described by Rao *et al.* (58) , mf and adults were graded from 4 (highly motile) to 0 (stationary), using a light microscope.

**ii) MTT assay**

A colourimetric assay used to quantify the metabolic activity of *B. malayi* mf and adult worms through the detection of formazan colour transformation (blue to purple). This colour change occurred only in live mf and adult worms through the reduction of the tetrazolium salt MTT (3-(4,5 dimethylthiazol-2-yl)-2,5-diphenyl tetrazolium bromide). Heat-killed worms, DMSO treated worms, and blank wells (DMSO only) were used as controls.

A protocol used by Johnston *et al.* (266) for mf, with slight modification for adult worms was followed for MTT assay, these are described below (60, 267, 268).

MTT assay for microfilariae (mf): At day 6, mf were transferred into 1.5 ml microtubes and centrifuged at 1300 g for 5 minutes at 4°C. Supernatants were removed and pellets were resuspended in 400 µl RPMI media. 100 µl MTT (0.5 mg/ml in PBS, Sigma Aldrich) was added to all tubes and incubated for 90 minutes at 37°C in 5% $CO_2$ in the dark. Tubes were centrifuged at 400 g for 5 minutes and pellets were washed with PBS, centrifuged and pellets were resuspended in 200 µl DMSO. The contents were then transferred into 96-well plate and incubated for 1 hour at room temperature to allow formazan crystal solubilisation. All plates were measured at 490 nm using Varioskan plate reader (Thermo Fisher Scientific) and the absorbance readings were subtracted from blank values (DMSO only). Dead mf (heat killed at 56°C followed by freezing ≥ 1 hour) were used as a negative control.

MTT assay for female adult worms: For female adult worms, slight modifications were made for their MTT assay. Adult worms were washed by full immersion of worms into PBS and placed in a 96-well plate, containing 200 µl MTT solution (0.5 mg/ml in PBS). This was followed by an incubation of 2 hours at 37°C in 5% $CO_2$ in the dark. After incubation, all worms were transferred into wells containing 200 µl DMSO for 1 hour at room temperature. Following this procedure, all plates were measured at 490 nm using Varioskan plate reader (Thermo Fisher Scientific) and the absorbance reading were subtracted from blank values (DMSO only). Dead adult worms (heat killed at 56°C followed by freezing ≥ 1 hour) were used as a negative control.

**iii) Mf release count from *Brugia malayi* female adult worms**

Mf release was assessed in female adult worms cultured in 6-well plates with the same treatment groups mentioned in Section 4.3.2.2 (prepared for qPCR analysis) using microscopy. This assessment was performed every two days in the 6-day period of treatment.

10 µl of RMPI media containing two worms in each well was placed onto a slide (in triplicate) and assessed using light microscopy to count the number of mf/10 µl. The estimated total number of mf was calculated in a final volume of 2 ml/well.

### 4.3.4 RNA gene expression of *Wolbachia* – in *B. malayi* mf

Following the preparation described in Section 4.3.2.2 for mf in the same treatment groups, *Wolbachia* viability of *B. malayi* mf was assessed using RNA gene expression analysis.

**RNA extraction**

At day 6 for the treatment groups mentioned above, total RNA was isolated from all samples using MiRCURY RNA Isolation kit (Exiqon). Following the instructions provided by the kit, mf samples were centrifuged at 300 g for 5 minutes to pellet them. 600 µl lysis solution (provided by the kit) was added to all tubes containing mf pellets and resuspended. Samples were homogenised using Pellet Pestle Motor (Kimble) with sterilised RNase and DNase free disposable pellet pestles (Thermo Scientific Fisher) twice for 30 seconds, keeping samples on ice after each rotation. Samples were centrifuged again at 13,000 g for 1 minute to remove cell debris. All sample supernatants were collected, and an equal amount of 70% ethanol was added to each tube.

Mf lysates were transferred into columns (at a maximum of 600 µl/column) and centrifuged at 1300 g for 1 minute. The remaining lysates were added to columns and centrifuged again until all samples were eluted. A volume of 400 µl wash solution (provided by the kit) was added to columns and centrifuged at 13,000 g for 2 minutes. All lysates at this point were treated with 100 µl 0.25 Kunitz unit/µl RNAse-free DNAse I (Qiagen), in order to remove any genomic DNA contamination from samples. Following this, columns were centrifuged at 300 g for 2 minutes and incubated for 15 minutes at room temperature. A second 400 µl of wash solution was added to columns and centrifuged at 13,000 g for 2 minutes. Eluted samples were later transferred into microtubes and 50 µl of elution buffer (provided with the kit) was added and incubated for 3 minutes at room temperature. RNA integrity and purity were recorded using Nanodrop 1000 (Thermo Fisher Scientific).

**Reverse transcription RT-PCR**

After the RNA extraction steps, ~0.25 µg of purified RNA samples were used in reverse transcriptase polymerase chain reaction (RT-PCR) to synthesise complementary DNA (cDNA) using Superscript III RT (Invitrogen, Thermo Fisher scientific). RT-PCR steps in this experiment were optimised by Dr Louise Ford and Mr Shannon Quek, Department of Tropical Disease Biology, LSTM (UK).

Purified RNA samples were added to 1.4 µl (50 ng/µl) random hexamers and 1.4 µl (10 mM) dNTP mix (provided by the kit). This mixture was incubated at 65°C for 5 minutes and placed on ice for 1 minute. The following compounds (all provided by the kit) were added to the mixture: 2.76 µl 10x buffer, 5.52 µl (25 mM) $Mgcl_2$, 2.76 µl (0.1 M) DTT, 1.38 µl (40 U/µl) RNAse OUT and 1.38 µl (200 U/µl) superscript II. Under the following PCR conditions: 10 minutes at 25°C, 50 minutes at 50°C and 5 min at 85°C, cDNA was synthesised.

**qPCR**

In the qPCR reaction, cycle threshold (Ct) values of the targeted and reference genes were quantified using primers targeting *Brugia malayi Wolbachia wsp* gene and nematode *gst* (reference gene). The specificity of primers to target the mRNA of the selected genes was determined using Primer Blast software (National Center for Biotechnology Information - NCBI). These forward and reverse primers were diluted at a final concentration of 0.5 µM. 1.2 µl of each primer was added to 10 µl SYBR green mix with 1 µl of amplified cDNA and 0.4 µl $MgCl_2$ diluted in RNAse-free water (Thermo Fisher Scientific) to provide a total volume of 20 µl in each reaction well. The PCR cycles were set as follows: at 95°C for 15 minutes, 40 cycles at 94°C for 30 seconds, 62°C for 30 seconds and at last 72°C for 1 minute per kb. ΔΔCt values were calculated against a reference gene (*gst*), following the formula used by Ghedin *et al.* (87, 269, 270). This was achieved by comparative quantification of the obtained Ct values through qPCR. ΔCt values were calculated by subtracting the *gst* gene from the *wsp* gene and ΔΔCt values were measured by subtracting treated groups from untreated mf. Using the 2- ΔΔ Ct analysis, the fold changes of gene expression were obtained.

### 4.3.5 Post-drug exposure washout assay in *B. malayi* mf and female adult worms

This experiment was designed to determine the effect of autophagy inhibition (using autophagy inhibitor wortmannin) on *Wolbachia* clearance dynamics post-drug exposure during a washout period without drug, when autophagy was inhibited in *B. malayi* mf and female adult worms. This was designed to test the role of autophagy in either the continued decline in *Wolbachia* loads during washout or the rebound in *Wolbachia* populations. Hence, an increase in *Wolbachia* load following the addition of an autophagy inhibitor after the washout process would indicate a possible role of autophagy.

*B. malayi* mf and female adult worms were incubated with the following treatment groups: DMSO (as a vehicle control), anti-*Wolbachia* agents at 10x $EC_{50}$ (previously determined by A-WOL) (82, 271): doxycycline (1.2 µM) and AWZ1066S (2.4 µM) for two different time-points (6 and 12 days). In addition, rifampicin (0.2 µM) was used for mf only. Mf and adult worms were assessed for their motility throughout the treatment period to monitor viability.

Washout was performed at two different set points for mf (at day 2, sub-optimal exposure or day 6, optimal exposure) and once for adult worms (at day 6, optimal exposure) in a total experimental period of 6 (for mf only) or 12 days (for both life stages). qPCR was done at different pre-set time-points to quantify *Wolbachia* load.

Figure 4.1 and 4.2 present the treatment period (in days) for the availability of tested drugs, their washout, addition of wortmannin and performing qPCR for mf and adult worms.

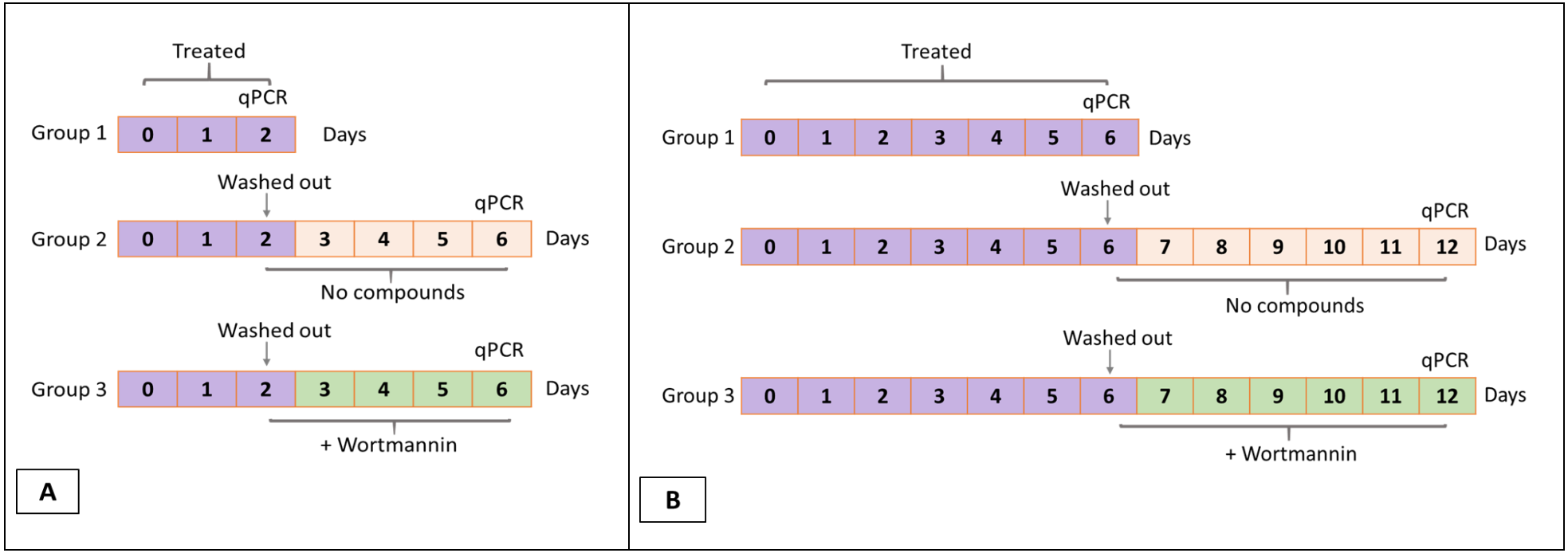


Figure 4. 1 Plan for the post-drug exposure washout experiment with *B. malayi* mf.

To assess the dynamics of *Wolbachia* decline or rebound following the removal of anti-*Wolbachia* drugs with the addition of wortmannin at different set time points. Three different treatment groups were used in *Brugia malayi* mf for a treatment duration of **A)** 6 days and **B)** 12 days.

In **A** and **B)** mf were treated with anti-*Wolbachia* antibiotics: doxycycline, rifampicin and AWZ1066S for different duration (in days) depending on group. In selected treatment groups (group 3), wortmannin was added following washout on **A)** day 2 and **B)** day 6 onwards. qPCR of *Wolbachia wsp* normalised to the nematode *gst* was performed at the end of every treatment cycle for each group in **A** and **B**.

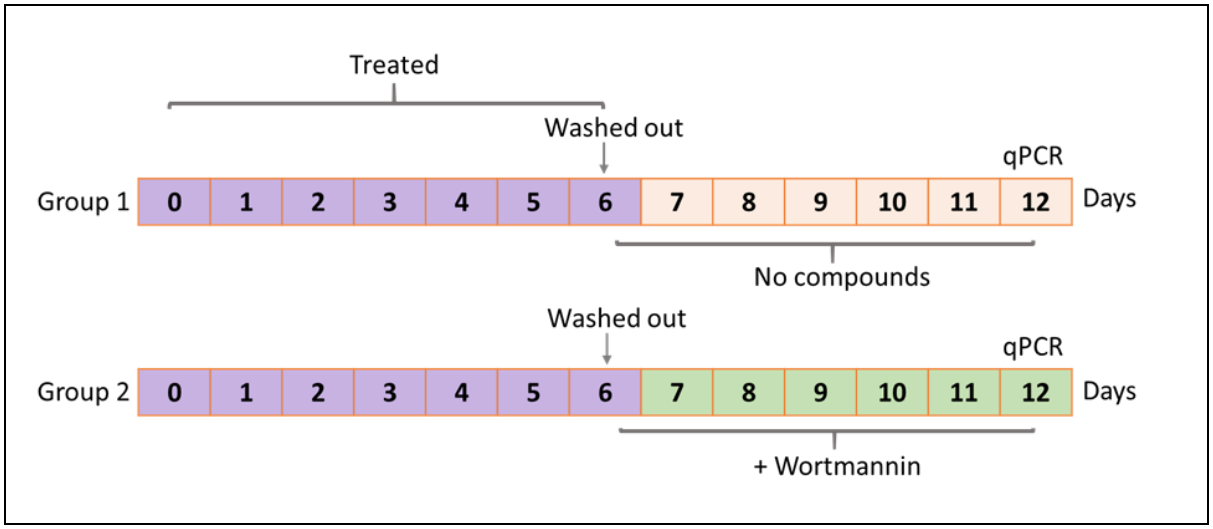


Figure 4. 2 Plan for the post-drug exposure washout experiment with *B. malayi* female adult worms.

To assess the dynamics of *Wolbachia* decline or rebound following the removal of anti-*Wolbachia* drugs with the addition of wortmannin at different set time points. Two different treatment groups were used in *Brugia malayi* adult worms for a treatment duration of 12 days.

Adult worms were treated with anti-*Wolbachia* agents: doxycycline and AWZ1066S for different duration (in days) depending on group. In selected treatment groups (group 2), wortmannin was added following washout on day 6 onwards. qPCR of *Wolbachia wsp* normalised to the nematode *gst* was performed at day 12 for all groups.

### ***B. malayi*** **mf washout technique**

Mf were maintained and cultured as described in Section 4.3.2.2 in the previously mentioned treatment groups. The washout technique was performed as described in Hong *et al.* and Clare *et al.* (82, 271).

The washout procedure was performed by transferring all mf content into sterile 96-deep well plates (Abgene, Thermo Fisher Scientific). 550 µl RPMI media was added to all wells and plates were centrifuged at 200 g for 5 minutes. After centrifugation, 150 µl of supernatant was removed and discarded, and the same amount was taken from the bottom of the wells containing mf pellets and transferred into a new 96-deep well plate, and the same amount of RPMI media was added again to make a total of 700 µl per well. This washing step was repeated 5 times to remove treatment compounds from samples (see Table 4.1 below for further details of the achieved dilution per washout).

For experimental groups with washout of treatment compounds, no anti-*Wolbachia* drugs were added after the pre-selected washout day (at day 2 or 6). Wortmannin was added after washout (for selective groups) at 10 µM.

Following washout, qPCR was performed to quantify *Wolbachia* load in mf, as previously described in Section 4.3.2.2.

| Wash | Mf stock | Diluent (Media) | Dilution factor | Final dilution concentration | | |
|---|---|---|---|---|---|---|
| | | | | Doxycycline (1.2 µM)* | Rifampicin (0.2 µM)* | AWZ1066S (2.4 µM)* |
| 1 | 200 µl | 550 µl | 1: 3.75 | 322.7 nM | 53.3 nM | 637.3 nM |
| 2 | 150 µl | 550 µl | 1: 4.67 | 69.1 nM | 11.4 nM | 136.5 nM |
| 3 | 150 µl | 550 µl | 1: 4.67 | 14.8 nM | 2.4 nM | 29.2 nM |
| 4 | 150µl | 550 µl | 1: 4.67 | 3.2 nM | 0.52 nM | 6.3 nM |
| 5 | 150 µl | 550 µl | 1: 4.67 | 0.68 nM | 0.11 nM | 1.3 nM |

Table 4. 1 Post-drug exposure washout experimental procedure.

This protocol was designed and optimised by Clare *et al.* (271). * Starting from the original concentrations added for anti-*Wolbachia* drugs: doxycycline 1.2 µM, rifampicin 0.2 µM and AWZ1066S 2.4 µM, the following 5 steps of washout were performed to reach 0.68 nM, 0.11 nM and 1.3 nM, respectively. These final concentrations after the washout steps have been previously shown to exhibit no effect in reducing *Wolbachia* titre in *B. malayi* mf by A-WOL team at LSTM, UK.

### *B. malayi* female adult worms washout technique

Adult worms were maintained and cultured as described in Section 4.3.2.2 in the previously mentioned treatment groups with modifications as described below.

Worms were co-cultured with monolayered primary human lymphatic endothelial cells (LECs) to maintain their viability and survival during the 2 weeks treatment. LECs (ECACC) were provided by Miss Amy Marriott and Dr Stephen Cross at Department of Tropical Disease Biology, LSTM, UK. The methodology of co-culturing female adult worms with LECs was developed by Marriott *et al.* (unpublished methodology) (272).

Two adult female worms were placed per well on monolayers of LECs and a total number of 12 worms were cultured for each treatment group. The media used to co-culture *B. malayi* worms and LECs was supplemented with the following, all from Microvascular Endothelial

Cell Growth Medium SingleQuots™ kit (EGM-2 MV singleQuots kit): 25 ml heat-inactivated FBS, 0.2 ml hydrocortisone, 2 ml hF-GF-B, 0.5 ml VEGF, 0.5 ml R3-IGF-1, 0.5 ml ascorbic acid, 0.5 ml hEGF, and 0.5 ml GA-1000.

LECs were pre-attached to the 6-well plate surfaces a day prior to the addition of worms. Transwell plate (6-well plate with inserts) were used for the co-culture of LECs and worms. In each well, a total of 6 ml EGM-2 MV media was added: 4 ml at the bottom of the well (containing LECs and worms with treatment compounds) and 2 ml of EGM-2 MV media (without treatment compounds) in the inserts.

Media in all wells were changed every 2 days during the 12-day treatment. For treatment groups with washout of compounds, no anti-*Wolbachia* drugs were added after the pre-selected washout day (at day 6). Wortmannin was added after washout (for selective groups) with the fresh media (every 2 days).

Following washout, qPCR was performed to quantify *Wolbachia* load in adult worms as previously described in section 4.3.2.2. All qPCR findings for this section are presented as a (log10) ratio of *wsp:gst* genes to normalise the results in relation to DNA quantity.

### 4.3.6 Statistical analysis

In this chapter, statistical analysis was performed using GraphPad Prism version 7. Continuous variables for MTT assay and qPCR were analysed using independent sample for Student's t-test. One-way analysis of variance (ANOVA) was used for continuous variables with two or more independent variables, also analysed using GraphPad Prism version 7. Statistical significance was at $p \leq 0.05$ for all the statistical analysis performed in this chapter.

## 4.4 Results

In the first group of experiments, we explore the effect of autophagy inhibition during drug exposure, using chemical autophagy inhibitors (wortmannin: an early autophagy inhibitor and l-asparagine: late autophagy inhibitor) on the activity of anti-*Wolbachia* drugs (doxycycline and rifampicin, both at 5 µM) in mosquito cell line C6/36*Wp* infected with *Wolbachia w*AlbB and *Brugia malayi* mf and female adult worms. The second set of experiments will examine the effect of autophagy inhibition on the decline or rebound of *Wolbachia* post-exposure to anti-*Wolbachia* drugs.

### 4.4.1 Examining autophagy inhibition in anti-*Wolbachia* activity of drugs during drug exposure – in C6/36*Wp*, *B. malayi* mf and adult female worms

**i) Mosquito cell line C6/36*Wp***

C6/36*Wp* cells exposed to anti-*Wolbachia* drugs (doxycycline and rifampicin) for 7 days in the presence of autophagy inhibitors failed to increase *Wolbachia* titre (Figure 4.3 A). As in shorter treatment periods (7 days), cells exposed to the same anti-*Wolbachia* antibiotics for a longer treatment period of 14 days significantly reduced *Wolbachia* titre by approximately 99% compared to the vehicle control (DMSO) for both antibiotics (Figure 4.3 A and B). The addition of autophagy inhibitors for 14 days significantly reduced the anti-*Wolbachia* properties of doxycycline and rifampicin, but only partially and not to the same extent observed in *B. malayi*, which will be discussed in the following section.

An observation worth mentioning is that when both autophagy inhibitors were tested in the absence of anti-*Wolbachia* drugs, they significantly increased *Wolbachia* titre by approximately 2-fold and 3.5-fold following 7 and 14 days of treatment, respectively, compared to the DMSO. Due to this observation, we compared the percentage in reduction of *Wolbachia* between anti-*Wolbachia* drugs and DMSO with autophagy inhibitors alone and combined with antibiotics, where all comparisons showed an approximate 99% reduction in *Wolbachia* indicating no difference between the groups.

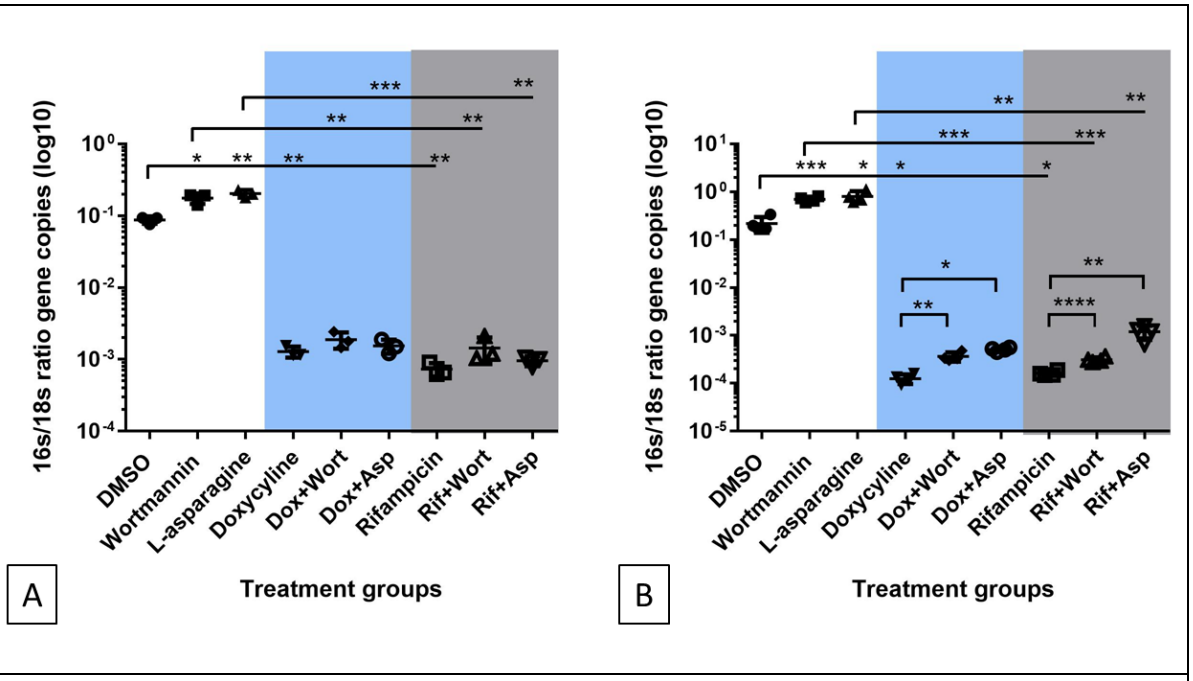


| % *Wolbachia* Reduction compared to DMSO | | | | |
|---|---|---|---|---|
| **Treatment groups** | **7 days** | **Statistical Significance** | **14 days** | **Statistical Significance** |
| Doxycycline | 99% | Yes | 99.9% | Yes |
| Rifampicin | 99% | Yes | 99.9% | Yes |
| % *Wolbachia* Reduction compared to Wortmannin or L-asparagine | | | | |
| Doxycycline + wortmannin | 99% | Yes | >99% | Yes |
| Doxycycline + l-asparagine | 99% | Yes | >99% | Yes |
| Rifampicin + wortmannin | 99% | Yes | >99 % | Yes |
| Rifampicin + l-asparagine | 99.5% | Yes | >99% | Yes |

Figure 4. 3 qPCR analysis of *Wolbachia* load of autophagy inhibition during drug exposure in C6/36*Wp* cells.

C6/36 cells Infected with *w*AlbB were treated with doxycycline or rifampicin at 5 µM alone or combined with wortmannin (at 10 µM) or l-asparagine (at 10 mM) for **A)** 7 and **B)** 14 days. In addition, treatment groups containing only wortmannin or l-asparagine were included. DMSO was used as vehicle control. DNA extracted from cells were amplified using *Wolbachia 16s* rRNA gene normalised to the *A. albopictus 18s* rRNA gene, expressed as ratios *16s:18s* (for actual values: please refer to the Appendix A Figure A10). Graphs (mean with SD) represent *16s:18s* gene copies (log10).

Statistical analysis to compare all treatment groups to DMSO was tested using Student's t-test. One-way ANOVA was used to determine the significant difference in percentage reduction of *Wolbachia* when comparing antibiotics alone and DMSO with autophagy inhibitors combined with antibiotics and autophagy inhibitors alone. Statistical significance was at $p \leq 0.05$. For p-value * = 0.01 to 0.05, ** = 0.01 to 0.001, *** = 0.001 to 0.0001, and **** ≤ 0.0001.

**ii) *B. malayi* mf and female adult worms**

Using either wortmannin or l-asparagine to suppress autophagy in worms exposed to doxycycline or rifampicin (both at 5 µM) significantly reduced the ability of these anti-*Wolbachia* drugs to eliminate the bacteria, compared to worms treated with only anti-*Wolbachia* drugs. This reduction in anti-*Wolbachia* activity was not significant when compared to DMSO control. Similar findings were observed for both mf (Figure 4.4 A) and female adult worms (Figure 4.4 B).

As observed in C6/36*Wp* cells, both autophagy inhibitors in the absence of anti-*Wolbachia* drugs significantly increased *Wolbachia* titre compared to the DMSO in mf (wortmannin 20%, l-asparagine 23% increase) and female adult worms (wortmannin 53%, l-asparagine 58% increase). To further examine the effect of autophagy inhibitors on doxycycline and rifampicin activity against *Wolbachia*, the percentage (%) reduction of *Wolbachia* was calculated between control groups. In mf, the % reduction in *Wolbachia* compared to DMSO for doxycycline (84%) and rifampicin (82%) was significantly higher than the reduction measured for the combination of antibiotics and wortmannin compared with wortmannin alone (for doxycycline + wortmannin= 26%, for rifampicin + wortmannin= 30%). This significant % reduction in *Wolbachia* was also observed for doxycycline and rifampicin combined with l-asparagine in mf.

As in mf, the significant reduction in % of *Wolbachia* load was also seen in female adult worms. The reduction in *Wolbachia* load achieved by doxycycline (71%) and rifampicin (67%) alone compared to DMSO was significantly higher than the reduction observed when comparing the combination of autophagy inhibitors with both anti-*Wolbachia* agents (doxycycline + wortmannin/l-asparagine= 28-43%; rifampicin + wortmannin/l-asparagine= 35-42%). Based on these observations in mf and adult worms, inhibiting autophagy using either wortmannin or l-asparagine during antibiotic exposure reduced the ability of these antibiotics to eliminate *Wolbachia*.

With regards to the viability assessment, the results of the MTT assay have indicated that tested chemicals in all treatment groups did not hinder the metabolic activity of mf (Figure 4.4 C) and female adult worms (Figure 4.4 D). Similar observations were also seen in

visualising worms for motility scoring (Figure 4.4), with the highest motility score (4) recorded in all treatment groups. For female adult worms only, our findings for manual counting mf release reached similar levels for treatment groups compared to DMSO control at day 6, indicating their viability at all tested concentrations.

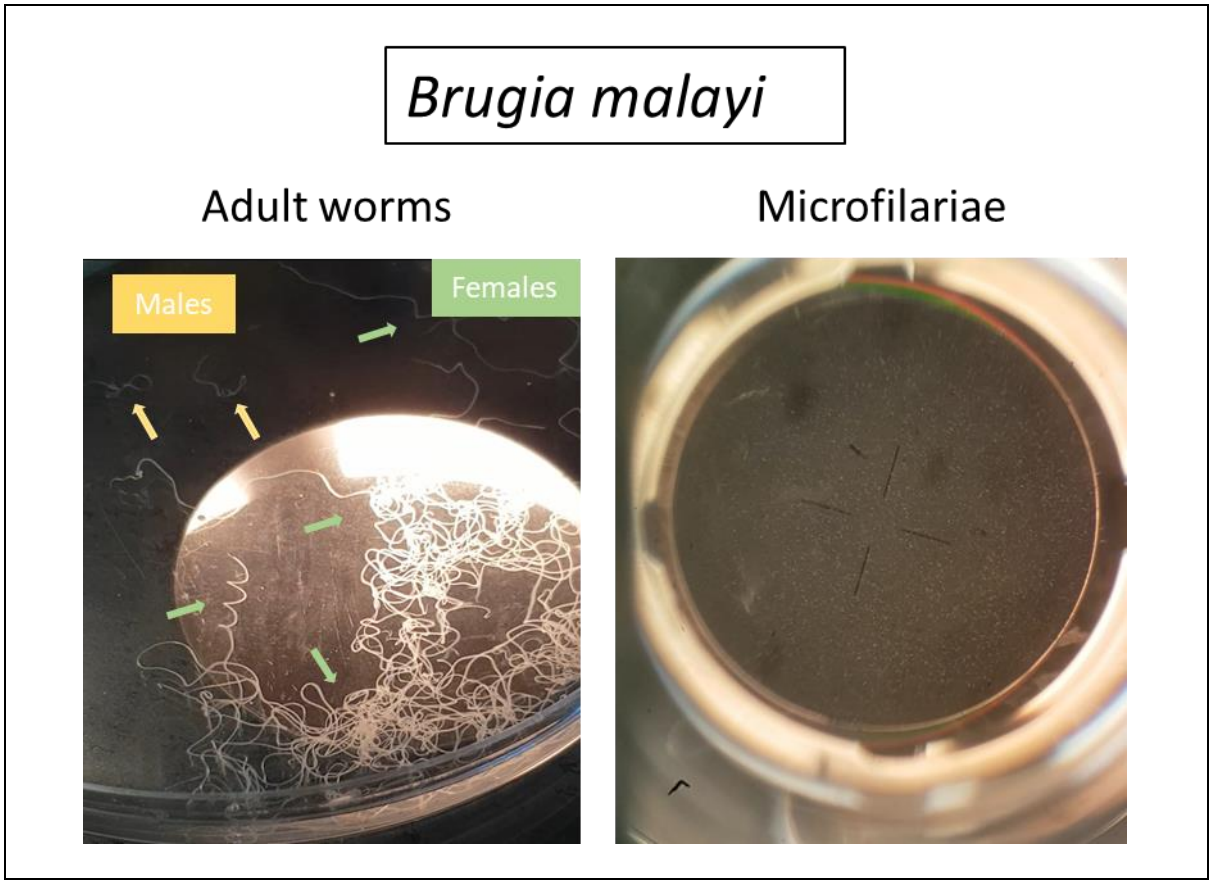


Figure 4. 4 Microscopic images of *B. malayi* adult worms and microfilariae in RPMI media during motility scoring (taken from video feed).

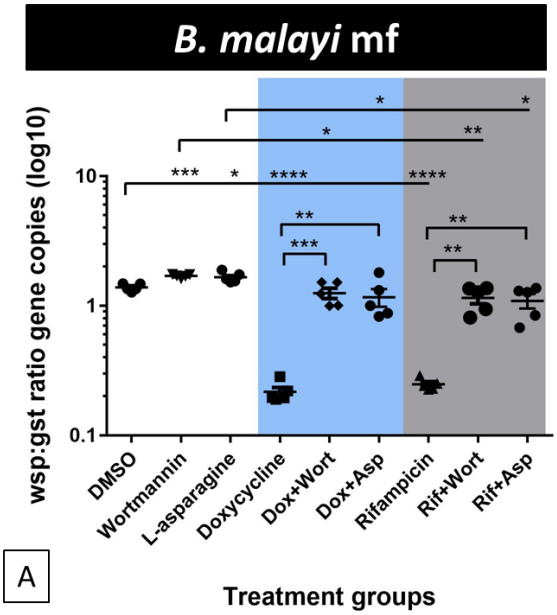


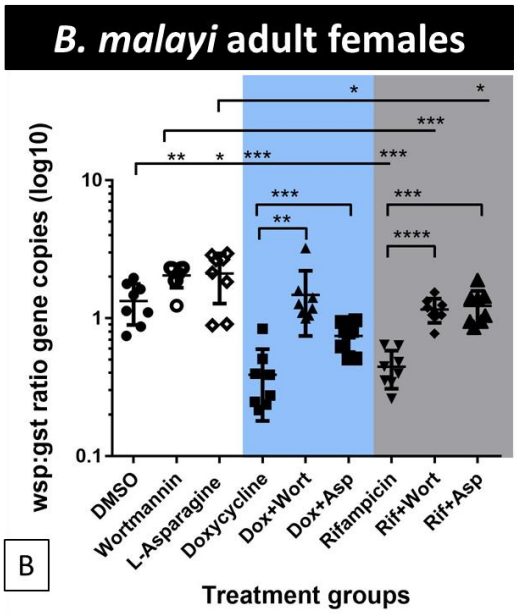


| % *Wolbachia* Reduction compared to DMSO | | |
|---|---|---|
| **Treatment groups** | **% in *B. malayi* mf** | **Statistical Significance** |
| Doxycycline | 84% | Yes |
| Rifampicin | 82% | Yes |
| % *Wolbachia* Reduction compared to Wortmannin or L-asparagine | | |
| Doxycycline + wortmannin | 26% | Yes |
| Doxycycline + l-asparagine | 32% | Yes |
| Rifampicin + wortmannin | 30% | Yes |
| Rifampicin + l-asparagine | 34% | Yes |

| % *Wolbachia* Reduction compared to DMSO | | |
|---|---|---|
| **Treatment groups** | **% in *B. malayi* adults** | **Statistical Significance** |
| Doxycycline | 71% | Yes |
| Rifampicin | 67% | Yes |
| % *Wolbachia* Reduction compared to Wortmannin or L-asparagine | | |
| Doxycycline + wortmannin | 28% | Yes |
| Doxycycline + l-asparagine | 43% | Yes |
| Rifampicin + wortmannin | 35% | Yes |
| Rifampicin + l-asparagine | 42% | Yes |

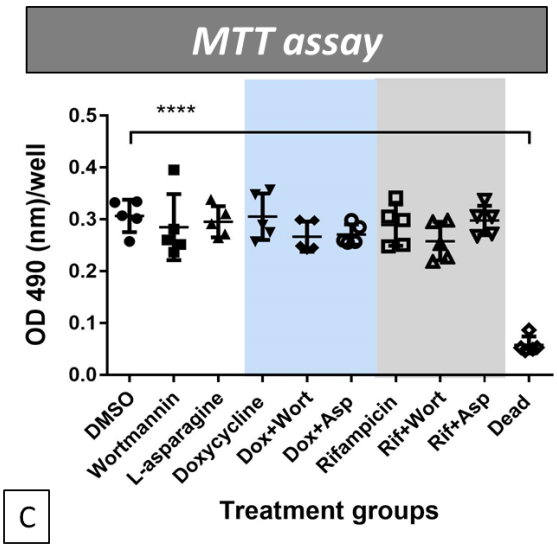


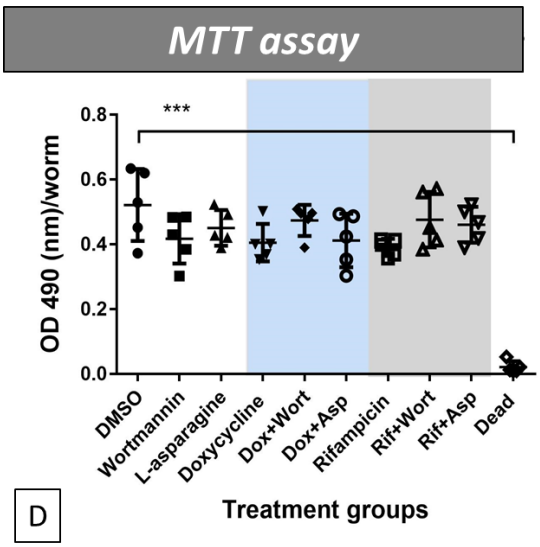

Figure 4. 5 qPCR analysis of *Wolbachia* load of autophagy inhibition during drug exposure in *B. malayi* mf and female adult worms.

*Brugia malayi* A) mf and B) female worms were treated with doxycycline (dox) or rifampicin (Rif) at 5 µM alone or combined with wortmannin (wort) (at 10 µM) or l-asparagine (Asp) (at 10 mM) for 6 days. In addition, treatment groups containing only wortmannin or l-asparagine were included. DMSO was used as vehicle control. DNA extracted from worms were amplified using *Wolbachia wsp* gene normalised to the nematode *gst* gene. Graphs (mean with SD) represent *wsp:gst* gene copies (log10) in five and eight biological repeats per treatment group, for mf and female worms, respectively.

MTT assay for C) mf and D) female worms: Formazan colour transformation of viable worms treated with the same treatment groups mentioned above were measured at an optical density of 490 nm using VarioSkan plate reader. Graphs (mean with SD) represent optical density at 490 nm in five biological repeats per treatment group for MTT assay.

Statistical analysis to compare all treatment groups to DMSO was tested using Student's t-test. One-way ANOVA was used to determine the significant difference in percentage reduction of *Wolbachia* when comparing antibiotics alone and DMSO with autophagy inhibitors combined with antibiotics and autophagy inhibitors alone. Statistical significance was at $p \leq 0.05$. For p-value * = 0.01 to 0.05, ** = 0.01 to 0.001, *** = 0.001 to 0.0001, and **** ≤ 0.0001.

### 4.4.2 *Wolbachia* RNA gene expression in *B. malayi* mf

In order to determine the viability of *Wolbachia* following exposure to anti-*Wolbachia* drugs alone or with the inhibition of autophagy, I measured the RNA expression of *wsp* in the different experimental groups (Figure 4.5). Our rationale of quantifying mRNA is that its expression indicates viable bacteria only, whereas genomic DNA expression may detect both viable and dead bacteria. Hence, mRNA expression was taken as a confirmatory step for viable *Wolbachia* to further solidify our findings (58, 74).

*Wolbachia* RNA expression in mf after exposure to doxycycline and rifampicin indicated no expression of *wsp* in the treated groups, suggesting the absence of any viable bacteria remaining. In the groups exposed to drug and inhibitors of autophagy, *wsp* expression was observed at levels similar to DMSO controls. However, as in mf gDNA qPCR analysis, it is important to note that exposure to autophagy inhibitors in DMSO controls lead to significant elevation in *wsp* expression. Further analysis comparing these groups to drug-exposed mf with autophagy inhibitors showed a 51-56% reduction in the level of gene expression compared to autophagy inhibitors alone. This reduction in gene expression was significantly lower than the ≥ 98% reduction for drug-exposed mf compared to DMSO in the absence of autophagy inhibitors.

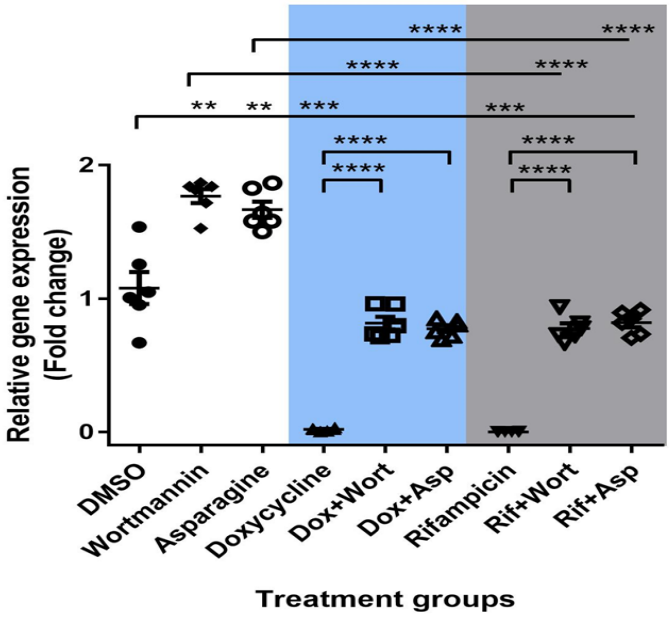


| % *wsp* gene expression reduction compared to DMSO | | |
|---|---|---|
| **Treatment groups** | **% in *B. malayi* mf** | **Statistical Significance** |
| Doxycycline | 98% | Yes |
| Rifampicin | 99.9% | Yes |
| % *wsp* gene expression reduction compared to Wortmannin or L-asparagine | | |
| Doxycycline + wortmannin | 54% | Yes |
| Doxycycline + l-asparagine | 54% | Yes |
| Rifampicin + wortmannin | 56% | Yes |
| Rifampicin + l-asparagine | 51% | Yes |

Figure 4. 6 *Wolbachia* RNA gene expression of autophagy inhibition during drug exposure in *B. malayi* mf.

The relative change in *B. malayi Wolbachia wsp* gene expression levels between untreated mf and different mf groups exposed to the following treatment for 6 days: doxycycline (dox) or rifampicin (Rif) at 5 µM alone or combined with wortmannin (wort) (at 10 µM) or l-asparagine (Asp) (at 10 mM). In addition, treatment groups containing only wortmannin or l-asparagine were included. Graph (mean with SD) represents fold change of gene expression in six biological repeats per treatment group.

Statistical analysis to compare all treatment groups to DMSO was tested using Student's t-test. One-way ANOVA was used to determine the significant difference in percentage reduction of *Wolbachia* when comparing antibiotics alone and DMSO with autophagy inhibitors combined with antibiotics and autophagy inhibitors alone. Statistical significance was at $p \leq 0.05$. For p-value * = 0.01 to 0.05, ** = 0.01 to 0.001, *** = 0.001 to 0.0001, and **** ≤ 0.0001.

### 4.4.3 Post-drug exposure washout assay in *B. malayi* mf and female adult worms

As we have observed a reduction in anti-*Wolbachia* activity through inhibiting autophagy in drug-exposed mf and adult worms, we examined whether autophagy plays a role in the continued decline or rebound of *Wolbachia* post-drug washout. As previously discussed in the method section, antibiotics at the concentration of 10x EC50 were tested in this experiment: for doxycycline (1.2 µM), AWZ1066S (2.4 µM) and rifampicin (0.2 µM).

In this section, I will first present the results for the post-drug exposure washout experiment in *B. malayi* mf in two different treatment durations (2 day exposure and 4 day washout [sub-optimal exposure] and 6 day exposure and 6 day washout [optimal exposure]) (Figure 4.6 and 4.7), followed by 6 day exposure and 6 day washout [optimal exposure] in female adult worms (Figure 4.8). For all treatment groups, mf and female adult worms were confirmed to be highly motile (with a motility score of 4), indicating their viability throughout the 6-day or 12-day treatment period.

**i) *B. malayi* mf – 2-day exposure with 4-day washout period (sub-optimal exposure)**

After only two days of anti-*Wolbachia* treatment (group 1), all three drugs: doxycycline, rifampicin and AWZ1066S, significantly reduced *Wolbachia* by 39% compared to control (DMSO) in mf. Washout of drugs (at day 2) with a quantification measurement of *Wolbachia* genes performed on day 6, appeared to record a higher clearance of the bacteria achieved by AWZ1066S (88%) compared to the other two tested antibiotics (doxycycline 64%, rifampicin 54%). Following sub-optimal exposure with day 4 washout (group 2), a continued significant reduction of *Wolbachia* titre was recorded for all three drugs with the highest reduction observed for AWZ1066S. When autophagy was inhibited by wortmannin (group 3) in the washout period, a significant rebound in *Wolbachia* load was observed for all anti-*Wolbachia* drugs.

**ii) *B. malayi* mf – 6-day exposure and 6-day washout period (optimal exposure)**

Following optimal drug exposure (group 1), the three antibiotics achieved > 90% reduction in *Wolbachia*. A continued reduction in *Wolbachia* load was observed for the tested anti-*Wolbachia* drugs in optimal drug exposure with day 6 washout (group 2) compared to optimal exposure without washout (group 1). However, autophagy inhibition (group 3) resulted in a slight rebound in doxycycline treatment only.

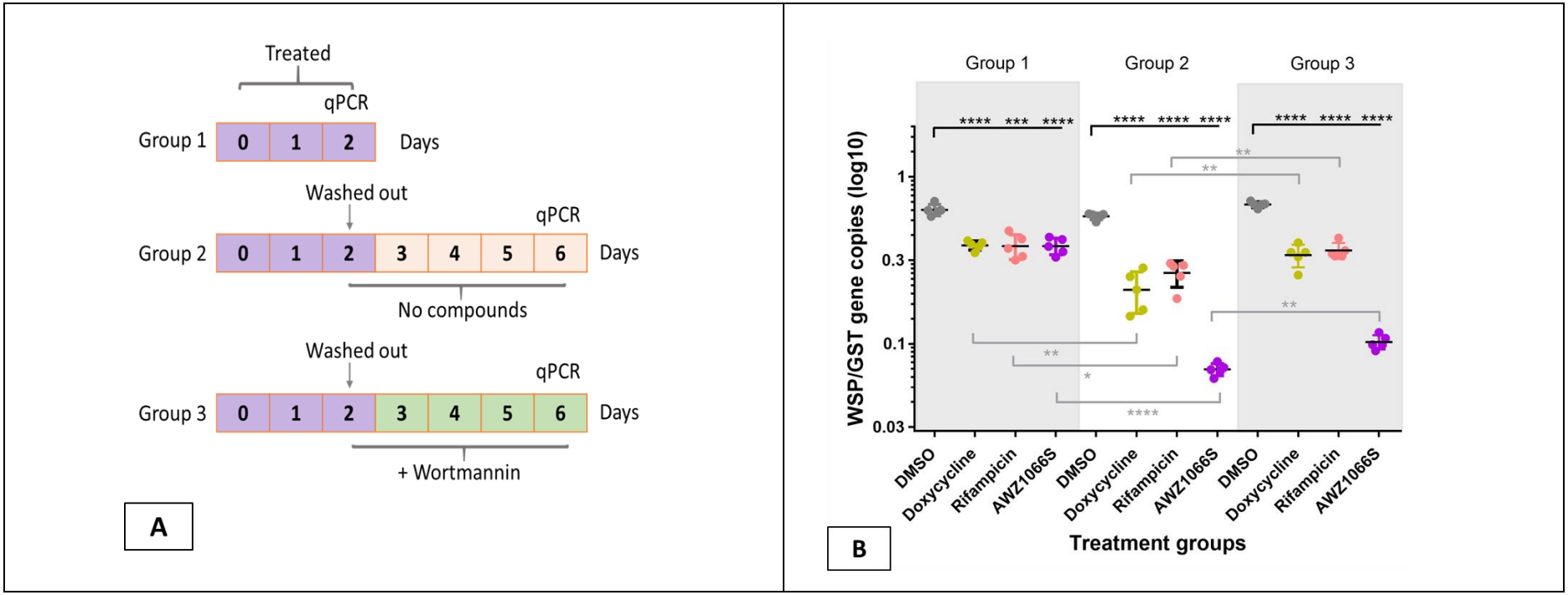


Figure 4. 7 Post-drug exposure washout assay in *B. malayi* mf for 2-day sub-optimal exposure with 4-day washout period.

Mf were treated as shown in A) with anti-*Wolbachia* agents: doxycycline (1.2 µM), rifampicin (0.2 µM) and AWZ1066S (2.4 µM) for 2 days. Washout of drugs was performed at day 2, followed by the addition of wortmannin in group 3 only. qPCR was performed at day 2 for group 1 and day 6 for all other groups. DNA extracted from mf were amplified using *Wolbachia wsp* gene normalised to the nematode *gst* gene as a ratio representing *Wolbachia* load for each treatment group. Graph (mean with SD) represents *wsp:gst* gene copies (log10) in five biological repeats per treatment group.

Statistical analysis was performed to compare all treatment groups to DMSO and other selected subgroups. Statistical significance tested using Student's t-test, statistical significance was at $p \leq 0.05$. For p-value * = 0.01 to 0.05, ** = 0.01 to 0.001, *** = 0.001 to 0.0001, and **** ≤ 0.0001.

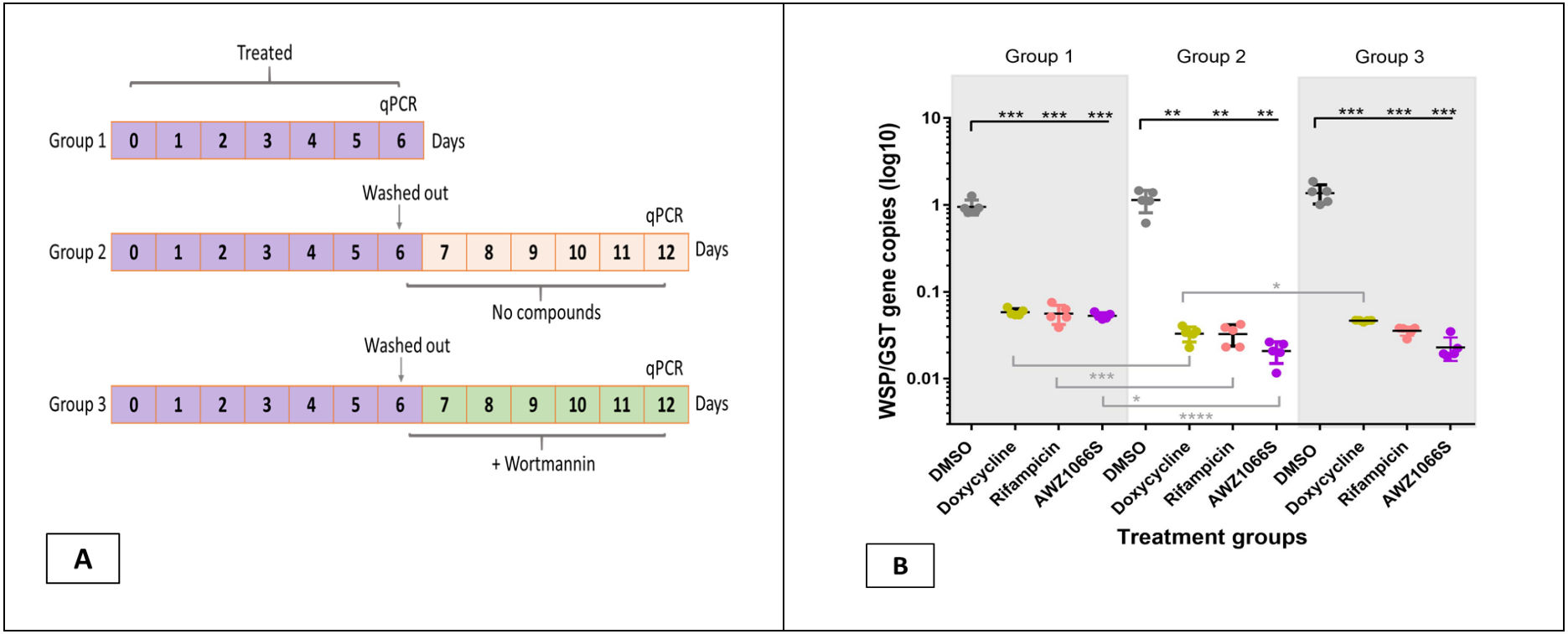


Figure 4. 8 Post-drug exposure washout assay in *B. malayi* mf for 6-day optimal exposure with 6-day washout period.

Mf were treated as shown in A) with anti-*Wolbachia* agents: doxycycline (1.2 µM), rifampicin (0.2 µM) and AWZ1066S (2.4 µM) for 6 days. Washout of drugs was performed at day 6 in group 2 and 3, followed by the addition of wortmannin in group 3 only. qPCR was performed at day 6 for group 1 and day 12 for all other groups. DNA extracted from mf were amplified using *Wolbachia wsp* gene normalised to the nematode *gst* gene as a ratio representing *Wolbachia* load for each treatment group. Graph (mean with SD) represents *wsp:gst* gene copies (log10) in five biological repeats per treatment group.

Statistical analysis was performed to compare all treatment groups to DMSO and other selected subgroups. Statistical significance tested using Student's t-test, statistical significance was at $p \leq 0.05$. For p-value * = 0.01 to 0.05, ** = 0.01 to 0.001, *** = 0.001 to 0.0001, and **** ≤ 0.0001.

### iii) *B. malayi* female adult worms – 6-day exposure and 6-day washout (optimal exposure)

The results for the post-drug exposure washout assay in female adult worms are presented in Figure 4.8. When quantifying *Wolbachia* gene ratio at day 12, optimal exposure of worms with both doxycycline and AWZ1066S has shown significantly higher *Wolbachia* clearance with a 67% and 86% reduction of *Wolbachia* respectively, compared to worms treated with DMSO (control), following the washout of drugs at day 6 (group 1). The anti-*Wolbachia* properties post-washout appeared to be higher in AWZ1066S, compared to doxycycline. As we previously observed in *B. malayi* mf, inhibiting autophagy with wortmannin (group 2) following optimal exposure with day 6 washout resulted in a significant *Wolbachia* rebound for both antibiotics.

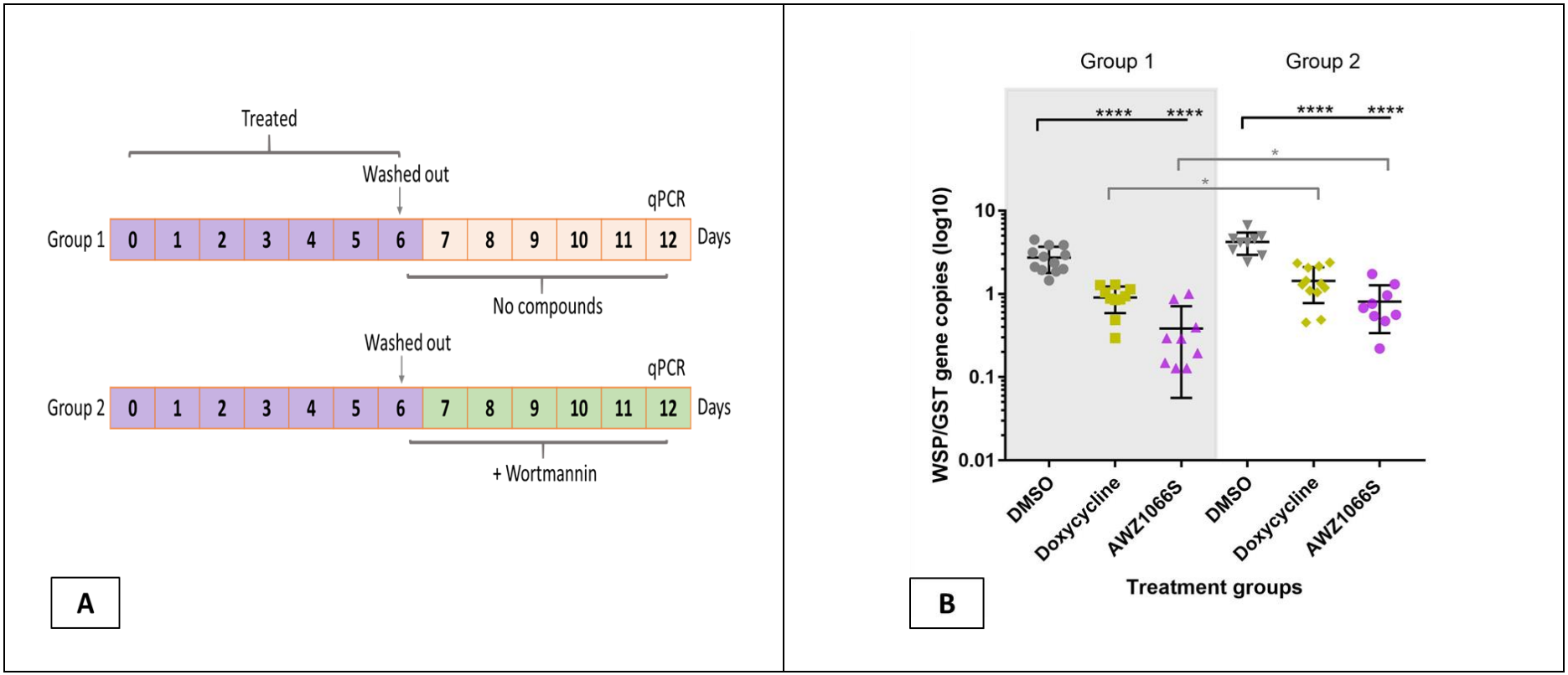


Figure 4. 9 Post-drug exposure washout assay in *B. malayi* female adult worms for 6-day optimal exposure with 6-day washout period.

Female adult worms were treated as shown in A) with anti-*Wolbachia* agents: doxycycline (1.2 µM) and AWZ1066S (2.4 µM) for 6 days. Washout of drugs was performed at day 6, followed by the addition of wortmannin in group 2 only. qPCR was performed at day 12 for all groups. DNA extracted from adult worms were amplified using *Wolbachia wsp* gene normalised to the nematode *gst* gene as a ratio, representing *Wolbachia* load for each treatment group. Graph (mean with SD) represents *wsp:gst* gene copies (log10) in twelve biological repeats per treatment group.

Statistical analysis was performed to compare all treatment groups to DMSO and other selected subgroups. Statistical significance tested using Student's t-test, statistical significance was at $p \leq 0.05$. For p-value * = 0.01 to 0.05, ** = 0.01 to 0.001, *** = 0.001 to 0.0001, and **** ≤ 0.0001.

## 4.5 Discussion

In the experiments of this chapter, we have used validated *in vitro* screening assays developed by the A-WOL consortium to examine the role of autophagy in the depletion of *Wolbachia* in *B. malayi* mf and female adult worms. The rationale for our approach is to determine whether autophagy has a role that is dependent or independent of different classes of anti-*Wolbachia* antibiotics with different modes of action. Hence, we chose doxycycline and rifampicin for their known and established anti-*Wolbachia* properties, as well as AWZ1066S, a candidate-selected by the A-WOL consortium.

In insect cells (C6/36*Wp*) exposed to anti-*Wolbachia* antibiotics, inhibition of autophagy using two different inhibitors (wortmannin: an early autophagy inhibitor and l-asparagine: late inhibitor) over a 7 and 14 day period did not present a significant difference in terms of percentage *Wolbachia* reduction compared to antibiotics alone. Even though these antibiotics can induce autophagy in this cell line (as observed in Chapter 3), this induction did not appear to be linked to the efficacy of these drugs in this experiment design. Conversely, clear evidence was observed in mf that inhibiting autophagy during drug exposure decreases the antibiotics' ability to reduce the bacterial population and loss of *Wolbachia* viability. Furthermore, drug exposure to female adult worms while inhibiting autophagy presented similar findings to mf in terms of reducing the ability of drugs to eliminate *Wolbachia*.

Due to the observed reduction in anti-*Wolbachia* activity in drug-exposed nematodes when autophagy is inhibited, we have examined whether autophagy plays a role in the continued decline or rebound of *Wolbachia* following drug washout. In both mf and female adult worms, the inhibition of autophagy post-drug washout resulted in a rebound of *Wolbachia*, despite the continued decline in *Wolbachia* following drug washout. Therefore, the decline of *Wolbachia* following washout is dependent on autophagy. In contrast to sub-optimal drug exposure, autophagy inhibition in optimal exposure in mf did not show a rebound of *Wolbachia* post-washout. This finding raises the possibility that beyond 90% *Wolbachia* reduction recorded following optimal drug exposure in mf, autophagy does not appear to have a role in the anti-*Wolbachia* activity of drugs.

The apparent difference between the requirement for autophagy in elimination of *Wolbachia* between C6/36 cells and *B. malayi* may relate to the differences in *Wolbachia* in both systems, being parasitic and mutualistic respectively, or may relate to a differential potency of autophagy inhibition between insect cells and *B. malayi*. Further experiments are needed to monitor the inhibition of autophagy under these experimental conditions in C6/36*Wp* cells. For example, shorter treatment periods (of less than 7 days) using the same antibiotics combined with autophagy inhibitors have to be assessed. Furthermore, future work will benefit from examining lower concentrations of doxycycline and rifampicin as these might yield different results in terms of *Wolbachia* load in insect cells compared to nematodes in the presence of autophagy inhibitors. With regards to anti-*Wolbachia* drug susceptibility, Johnston *et al.* (251) have proposed that the penetration of antibiotics into the nematode cuticle differs from cell membrane of insects. Moreover, differences between *Wolbachia* in insects and nematodes have to be considered and whether this also impacts drug susceptibility (32, 251, 262).

In *B. malayi*, inhibiting autophagy during the period of drug exposure lead to a complete inhibition of *Wolbachia* elimination, with bacterial numbers in inhibited groups showing no significant difference to controls. This complete inhibition was not observed in the experiments testing the role of autophagy following drug wash-out, where although a significant rebound was observed following inhibition of autophagy, this was only a partial rebound. This observation suggests a more profound role for autophagy in the early mode-of-action/efficacy against *Wolbachia* and argues against it simply being a mechanism required for the removal of the bacteria from the cell. This was further supported by an analysis of the viability of the bacteria, which significantly increased in the presence of autophagy inhibition. Together these results support a role for autophagy in the direct killing of *Wolbachia* during drug treatment and independent of the mode-of-action of different antibiotic classes.

Further experiments are required to test whether AWZ1066S with a more rapid clearance of *Wolbachia*, compared to existing anti-*Wolbachia* drugs (82) is dependent on autophagy in *B. malayi* mf and adult females. This can be examined further by directly measuring autophagic activity (through autophagic markers, including LC3B and p62) or factors associated with autophagy activation, such as ROS formation. Other researchers have found AWZ1066S to

be a fast-acting drug in terms of *Wolbachia* elimination (82), and this could potentially play a future role in further improving the efficacy and macrofilaricidal properties, as well as shorten the duration (≤ 7 days) of current treatment modalities against LF and onchocerciasis.

The challenges of *in vitro* culturing adult worms for longer treatment periods are well documented (60, 262, 273, 274). However, in the methodology performed in this chapter of co-culturing female adult worms with LECs supplemented with specific growth factors and nutrients, developed at LSTM, UK (unpublished methodology) (272), we have successfully prolonged the duration of culturing adult worms for 12 days. An important limitation was faced with regards to adult worms. Due to the time constraints of this project and the efforts required to obtain large numbers of adult worms from animal hosts, the decision was made to limit the number of treatment groups. Therefore, certain anti-*Wolbachia* drugs were prioritised over others in our assessment of adult worms compared to mf, where all the desired groups were analysed. This limitation was also considered in testing of female adult worms in optimal drug exposure (longer treatment duration) as opposed to both optimal and suboptimal drug exposure in mf.

Finally, it is worth noting that while we have examined the possible role of autophagy inhibition using two chemical inhibitors acting on different stages of the autophagic pathway, we have not assessed the pathway through genetic inhibition due to time limitations of this project. While there are currently no efforts of successfully inhibiting autophagy in C6/36 cells through gene silencing, this method of autophagic suppression has been examined in previous work in nematodes (*B. malayi* female adult worms) and insect cells (*Drosophila* cells) (87).

In conclusion, we have demonstrated the importance of autophagy as a pathway responsible for delivering the efficacy of anti-*Wolbachia* antibiotics and their reduction of bacterial viability in *B. malayi* mf and adult worms. Furthermore, the decline of *Wolbachia* population during the washout period post-drug exposure is partially dependent on autophagy in nematodes.

# Chapter 5 Summary and Conclusions

Through the series of experiments we have performed in this research, we were able to determine a role for autophagy in the activity of antibiotics against *Wolbachia* in the target organism, *B. malayi*. This role could potentially be used to improve the efficacy and shorten current treatment regimens, of new anti-wolbachial macrofilaricidal drugs. In this final chapter, we will summarise our main findings and provide recommendations for future experimental work.

**Wortmannin and l-asparagine: safe and effective autophagy inhibitors**

In the experiments in Chapter 2, we were able to identify two autophagy inhibitors, wortmannin and l-asparagine, that suppressed autophagy and did not negatively impact cell growth, viability and toxicity in mosquito C6/36 cells. This was successfully achieved between the concentrations of 5-20μM and 10-20mM for wortmannin and l-asparagine, respectively. Furthermore, we have detected the range of their autophagic inhibitory capabilities using two methods, immunoblotting and immunofluorescence staining (IF) assays. Our results will aid future research as we have examined both an early (wortmannin) and late (l-asparagine) autophagy inhibitor.

Although we have observed the safety and effectiveness of l-asparagine as an autophagy inhibitor between 10 and 20 mM, there are considerable gaps in understanding how amino acids inhibit the autophagic pathway. Future experimental work is needed to understand whether amino acids, used as chemical autophagy inhibitors, may interfere with other pathways not associated with autophagy in insect cells and other cell lines, such as in protein synthesis and cell proliferation (275, 276). This has to be taken into consideration given the high concentration of l-asparagine needed in our experiments to successfully inhibit autophagy in C6/36 cells. Moreover, high amino acid supplementation can activate AKT phosphorylation through mTORC2 activation, which in turn can affect autophagy and other cellular process (129, 275).

In our experimentation using 3-ma and ly294002, both inhibitors were not suitable to chemically suppress autophagy in C6/36 cells, due to their toxicity when used in autophagic inhibiting concentrations. Furthermore, the conditions set in our experiments, such as the

long treatment duration and full nutrient culture media, must also be considered in future assessments of determining suitable autophagy inhibitors. Despite only testing four chemical autophagy inhibitors in our experiments, two of which were deemed suitable in C6/36 cells, several widely used agents have not been fully examined in insect cells, for example bafilomycin A1 and chloroquine, and could be considered in the future research (118, 124).

**Antibiotic-induced autophagy: A restricted role in insect cells and nematodes, independent of *Wolbachia***

In Chapter 3, we have successfully demonstrated an increase in autophagic activation, which was consistently observed in four broad-spectrum anti-*Wolbachia* antibiotics from different classes (doxycycline, rifampicin, moxifloxacin and sparfloxacin) exposed to two different insect cell lines (C6/36 and SF9 cells), as well as in *B. malayi* mf. Moreover, this autophagic activation was also observed for selected-candidates from the A-WOL consortium (TylAMac$^{TM}$, AWZ1066S and fusidic acid). The chemical structures of antibiotics and compounds examined in the series of experiments performed in this thesis for their activity against *Wolbachia* and autophagy are presented in Figure 5.1. Interestingly, the antibiotic-induced autophagy was observed both in the presence and absence of *Wolbachia* in insect cells, indicating a direct effect of anti-*Wolbachia* antibiotics on autophagy that is independent of the bacteria. With regards to mammalian cells (THP-1 and MDCK), it is important to note that all tested anti-*Wolbachia* drugs did not activate autophagy, highlighting their restricted role in insect cells and nematodes in activating the pathway. This particular observation is of importance due to that fact that if an activation of autophagy by these antibiotics occurred in mammalian cells, it could lead to adverse events.

Through concentration-dependency testing of anti-*Wolbachia* antibiotics, we have demonstrated that only concentrations that induced autophagy resulted in effective *Wolbachia* depletion (of >90%), the empirical threshold of delivering the desired macrofilaricidal activity (65). This observation was more apparent for the two anti-*Wolbachia* fluoroquinolones (moxifloxacin and sparfloxacin). Hence, the efficacy of anti-*Wolbachia* drugs against the bacteria is closely linked with their ability to induce autophagy. Additionally, we have found evidence that this autophagic induction starts early (within the

first day of drug exposure), even before the effective clearance of *Wolbachia*. This observation supports the notion that the role of autophagy is not limited to the clearance of dead bacteria but plays an important part in the activity of these antibiotics. In contrast, the four tested antibiotics that lack anti-*Wolbachia* properties (ciprofloxacin, levofloxacin, amoxicillin and streptomycin) (Figure 5.1) did not activate autophagy or deplete *Wolbachia,* in different cell lines and when changing experimental variables, including concentrations and time.

Future research can examine the four diverse anti-*Wolbachia* drugs used in this thesis, or antibiotic-induced autophagy as a concept, in other insect cell lines in the presence and absence of *Wolbachia*. Examples of these include *Anopheles*, as well as other *Aedes* and insect cell lines. Also, there is potential for examining our observations in *Drosophila* and *Caenorhabditis elegans* due to their widespread use in autophagic evaluation and genetic and experimental tractability. It would be worth extending our observations to other intracellular bacteria, as well as in parasitic organisms such as *Plasmodium* species (95, 277-282). Moreover, more research is needed to assess other types of mammalian cells from the ones examined in Chapter 3 or mammalian cells transfected with *Wolbachia*, in order to further confirm our findings in terms of autophagic induction (283). Although as a cautionary note, due to the inconsistency observed when using the autophagic marker LC3B in mammalian cells, alternative autophagic markers should be considered (131, 284). These include p62 (which provided consistent findings in this research irrespective of tested antibiotics, cell line and experimental approach), as well as potential candidates that have gained recent prominence as selective autophagic markers, for example NBR1, NDP52 and OPTN (131, 143, 145, 146).

As we only tested *B. malayi* mf that was naturally infected with *Wolbachia*, future work is needed to examine autophagic induction in similar experimental settings on other nematodes lacking *Wolbachia,* for example *Loa loa* and *Acanthocheilonema viteae*. Examining drug exposed *Wolbachia*-free nematodes will confirm our findings in uninfected insect cells, where autophagy was independently activated in the absence of *Wolbachia*.

Further studies are needed to evaluate our observations with regards to the tested fluoroquinolones, where two drugs showed anti-*Wolbachia* activity and autophagy

induction (moxifloxacin and sparfloxacin) in a concentration-dependent pattern, while ciprofloxacin and levofloxacin presented with neither of these properties. This class of antibiotics could be examined in similar experimental settings in other insect and mammalian cell lines, using IF assay as it provided more robust results compared to western blot in this research. The differential induction of autophagy by fluoroquinolones may be useful to determine any molecular structures associated with the induction of autophagy and efficacy against *Wolbachia.*

Future work can benefit from implementing other imaging techniques not assessed in this thesis, including electron and confocal microscopy. Through these methods, *Wolbachia* can be located within the tested cells and in situations where autophagy is inhibited or activated, autophagy associated structures such as autophagosomes and autophagolysosomes or cellular structures, including mitochondria, can be visualised (285, 286).

It is important to note that while we have monitored an increase in autophagic influx for the four tested anti-*Wolbachia* drugs, we have not examined other factors associated with these antibiotics that may influence autophagy. Examples of these factors include, oxidative stress (ROS production), pH and mitochondrial damage (199, 211, 235, 244, 259, 260). Moreover, research is needed to assess the autophagic activity of anti-*Wolbachia* drugs, through autophagy-related gene expression.

As recent studies have presented the superior efficacy and potency of AWZ1066S (82), TylAMac$^{TM}$ (81) and fusidic acid (86) as anti-*Wolbachia* drugs compared to established antibiotics (doxycycline, rifampicin and moxifloxacin), there is a need to examine if the A-WOL selected candidates have higher autophagic inducing capabilities. This will aid in our understanding of whether the potency of drugs against *Wolbachia* is linked to their autophagic promoting activity.

Figure has been removed due to third party copyrighted material.

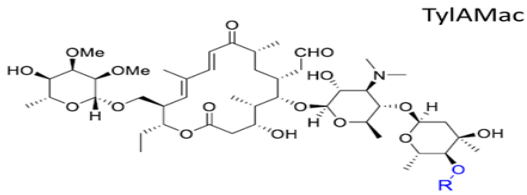


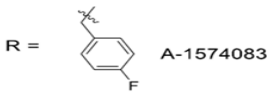


AWZ1066S

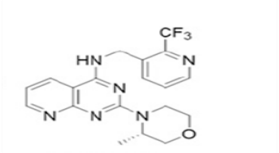


Fusidic acid

Figure has been removed due to third party copyrighted material.

Figure 5. 1 Chemical structures of selected compounds of diverse classes.

Data source: (81, 82, 287).

**The contribution of autophagy in the efficacy of anti-*Wolbachia* antibiotics**

Using validated *in vitro* screening assays developed by the A-WOL consortium in Chapter 4, we have successfully demonstrated the contribution of autophagy in the efficacy of anti-*Wolbachia* drugs and their ability to reduce bacterial viability in *B. malayi* mf and adult worms. This was examined by inhibiting autophagy using wortmannin and l-asparagine during anti-*Wolbachia* drug exposure in nematodes, resulting in an inhibition of *Wolbachia* reduction when compared to antibiotic exposure alone. Furthermore, we have demonstrated in both mf and female adult worms, a continued decline in *Wolbachia* load post-exposure washout of antibiotics, which was reversed following autophagy suppression during the washout period. This indicate that bacterial decline is dependent on autophagy in nematodes both during exposure to anti-wolbachial drugs and post drug exposure.

In contrast to our observations in *B. malayi*, the inhibition of autophagy in insect cells (C6/36*Wp*) during drug exposure did not impact the ability of these antibiotics to reduce *Wolbachia*. Future work is required to confirm whether this observation in insect cells is due to experimental conditions or if it demonstrates that autophagy is not linked to the efficacy of these drugs in insect cells. As we have examined drug exposure in C6/36*Wp* cells in a 7 and 14-day period, with an over 90% reduction in *Wolbachia* for both periods, future studies can examine these cells in shorter periods or with sub-optimal concentrations of antibiotics.

Several recommendations could be made for future experimentation in investigating anti-*Wolbachia* antibiotic-induced autophagy. To complement our chemical induced suppression we could use genetic suppression of autophagy-related genes using gene silencing (RNA interference). Additionally, it is worth examining anti-*Wolbachia* antibiotics and autophagy inhibition in *Onchocerca* species, in order to confirm our findings in other filarial nematodes that are relevant to human filariasis. In the future, *in vivo* studies are needed to determine if they will yield similar findings to my thesis when examining anti-*Wolbachia* activity during autophagic inhibition. An example of how this can be performed is through generating transgenic mice with autophagy-related genes and locating autophagic markers (such as LC3 with green fluorescent protein GFP, monomeric red fluorescent protein mFRP or mCHERRY) using immunofluorescence microscopy (288-291). From these *in vivo* experiments, future

studies can evaluate the role of antibiotic-induced autophagy in mf, as well as different life stages of *B. malayi* within infected transgenic mice.

The promising results of my thesis highlight the role of autophagy in the anti-*Wolbachia* properties of antibiotics. While there are considerable gaps with regards to our understanding of autophagy as a target for anti-*Wolbachia* drug therapy, we have to consider the role it may play when selecting future macrofilaricidal drugs for the treatment of lymphatic filariasis, as well as onchocerciasis. In particular the induction of autophagy could be used in developing high-throughput screening of additional drug libraries and in the lead optimisation of existing 'hits' identified by the A-WOL consortium (271). Despite only evaluating autophagy in anti-*Wolbachia* drugs in my thesis, the findings we have obtained may help future work in improving the understanding of selective autophagy, particularly in developing treatments for other intracellular microorganisms, including *Mycobacterium tuberculosis* (292, 293) and *Chlamydia trachomatis* (294, 295). Moreover, research has highlighted the role of modulating autophagy in future treatment of intracellular parasites, for example Intrahepatic stages of *Plasmodium* spp. (281, 296, 297), *Toxoplasma gondii* (222, 297-299) and *Leishmania* (297, 300, 301). Recently, significant breakthroughs have been made with the discovery of new potent anti-*Wolbachia* agents, such as TylAMac$^{TM}$ and AWZ1066S, and chemically inducing autophagy can potentially play a future role in further improving their efficacy and macrofilaricidal properties.

There is future potential of combining the anti-*Wolbachia* drugs used in this research with other drugs that form part of the current MDA treatment in endemic areas against filarial diseases. While several examples have successfully been implemented by combining MDA agents, such as albendazole or DEC with doxycycline in clinical trials (70, 73, 75) (and rifampicin in pre-clinical models (61)), there is potential of examining this further using autophagy inducers. As current trends of effective treatment modalities against LF and onchocerciasis aim for shorter oral treatment periods (of ≤ 7 days) with macrofilaricidal properties of over 90% (empirical threshold), autophagy can become an important target for anti-*Wolbachia* drug research and provide future solutions in drug therapy. Autophagy as a concept and its induction may play a future role by shortening treatment periods, thereby reducing the cost and burden of filarial diseases in order to reach the targets of global MDA treatments.

# References


1. World Health Organisation. Lymphatic filariasis 2018 [Available from: https://www.who.int/news-room/fact-sheets/detail/lymphatic-filariasis (accessed on 24 March 2019).

2. Paily KP, Hoti SL, Das PK. A review of the complexity of biology of lymphatic filarial parasites. J Parasit Dis. 2009;33(1-2):3-12.

3. Centres for Disease Control and Prevention. Parasites - lymphatic filariasis, epidemiology and risk factors 2019 [Available from: https://www.cdc.gov/parasites/lymphaticfilariasis/epi.html (accessed on 13 April 2019).

4. World Health Organisation. Global Health Observatory (GHO) data 2019 [Available from: https://www.who.int/gho/neglected_diseases/lymphatic_filariasis/en/ (accessed on 13 April 2019).

5. World Health Organisation. What is lymphatic filariasis 2019 [Available from: https://www.who.int/lymphatic_filariasis/disease/en/ (accessed on 13 April 2019).

6. James SL, Abate D, Abate KH, Abay SM, Abbafati C, Abbasi N, et al. Global, regional, and national incidence, prevalence, and years lived with disability for 354 diseases and injuries for 195 countries and territories, 1990-2017: a systematic analysis for the Global Burden of Disease Study 2017. Lancet. 2018:1789.

7. World Health Organisation. Lymphatic filariasis - Morbidity management and disability prevention (MMDP) 2019 [Available from: https://www.who.int/lymphatic_filariasis/managing-morbidity/en/ (accessed on 13 April 2019).

8. World Health Organisation. Lymphatic filariasis - Status of mass drug administration 2018 [Available from: http://apps.who.int/neglected_diseases/ntddata/lf/lf.html (accessed on 19 Sep 2019).

9. Black SJ, Seed JR. World Class Parasites: The Filaria. Klei TR, Rajan TV, editors. U.S.A: Springer Science and Business Media, LLC; 2002.

10. Centres for Disease Control and Prevention. Biology - Life Cycle of Wuchereria bancrofti 2018 [Available from: https://www.cdc.gov/parasites/lymphaticfilariasis/biology_w_bancrofti.html (accessed on 14 April 2019).

11. Eddleston M, Davidson R, Brent A, Wilkinson R. Oxford Handbook of Tropical Medicine New York: Oxford University Press; 2011.

12. Tamarozzi F, Halliday A, Gentil K, Hoerauf A, Pearlman E, Taylor MJ. Onchocerciasis: the role of Wolbachia bacterial endosymbionts in parasite biology, disease pathogenesis, and treatment. Clin Microbiol Rev. 2011;24(3):459-68.

13. World Health Organisation. Onchocerciasis 2018 [Available from: https://www.who.int/news-room/fact-sheets/detail/onchocerciasis (accessed on 15 April 2019).

14. Centres for Disease Control and Prevention. Onchocerciasis FAQs 2013 [Available from: https://www.cdc.gov/parasites/onchocerciasis/gen_info/faqs.html (accessed on 15 April 2019).

15. World Health Organisation. Onchocerciasis - Status of endemicity of onchocerciasis 2018 [Available from: http://apps.who.int/neglected_diseases/ntddata/oncho/onchocerciasis.html (accessed on 19 Sep 2019).

16. Centres for Disease Control and Prevention. Parasites - Onchocerciasis (also known as River Blindness) Biology 2013 [Available from: https://www.cdc.gov/parasites/onchocerciasis/biology.html# (accessed on 15 April 2019).

17. World Health Organisation. Guideline – Alternative mass drug administration regimens to eliminate lymphatic filariasis 2017 [Available from: https://apps.who.int/iris/bitstream/handle/10665/259381/9789241550161-eng.pdf;jsessionid=FC5D829808617F6001004EE71DB22F35?sequence=1 (accessed on 16 April 2019).

18. World Health Organisation. Global programme to eliminate lymphatic filariasis: progress report, 2017 2018 [Available from: https://apps.who.int/iris/bitstream/handle/10665/275719/WER9344.pdf?ua=1 (accessed on 16 April 2019).

19. Taylor MJ, Awadzi K, Basáñez M-G, Biritwum N, Boakye D, Boatin B, et al. Onchocerciasis Control: Vision for the Future from a Ghanian perspective. Parasit Vectors. 2009;2(1):7.

20. Osei-Atweneboana MY, Awadzi K, Attah SK, Boakye DA, Gyapong JO, Prichard RK. Phenotypic Evidence of Emerging Ivermectin Resistance in Onchocerca volvulus. PLoS Negl Trop Dis. 2011;5(3):e998.

21. Taylor MJ, Bordenstein SR, Slatko B. Microbe Profile: Wolbachia: a sex selector, a viral protector and a target to treat filarial nematodes. Microbiology. 2018;164(11):1345-7.

22. Bouchery T, Lefoulon E, Karadjian G, Nieguitsila A, Martin C. The symbiotic role of Wolbachia in Onchocercidae and its impact on filariasis. Clin Microbiol Infect. 2013;19(2):131-40.

23. Taylor MJ, Bandi C, Hoerauf A. Wolbachia bacterial endosymbionts of filarial nematodes. Adv Parasitol. 2005;60:245-84.

24. Newton ILG, Savytskyy O, Sheehan KB. Wolbachia Utilize Host Actin for Efficient Maternal Transmission in Drosophila melanogaster. PLoS Pathog. 2015;11(4):e1004798.

25. Zug R, Hammerstein P. Still a Host of Hosts for Wolbachia: Analysis of Recent Data Suggests That 40% of Terrestrial Arthropod Species Are Infected. PLoS One. 2012;7(6):e38544.

26. Slatko BE, Taylor MJ, Foster JM. The Wolbachia endosymbiont as an anti-filarial nematode target. Symbiosis. 2010;51(1):55-65.

27. Glowska E, Dragun-Damian A, Dabert M, Gerth M. New Wolbachia supergroups detected in quill mites (Acari: Syringophilidae). Infect Genet Evol. 2015;30:140-6.

28. Kozek WJ, Marroquin HF. Intracytoplasmic bacteria in Onchocerca volvulus. Am J Trop Med Hyg. 1977;26(4):663-78.

29. McLaren DJ, Worms MJ, Laurence BR, Simpson MG. Micro-organisms in filarial larvae (Nematoda). Trans R Soc Trop Med Hyg. 1975;69(5-6):509-14.

30. Kozek WJ. Transovarially-transmitted intracellular microorganisms in adult and larval stages of Brugia malayi. J Parasitol. 1977;63(6):992-1000.

31. Sironi M, Bandi C, Sacchi L, Di Sacco B, Damiani G, Genchi C. Molecular evidence for a close relative of the arthropod endosymbiont Wolbachia in a filarial worm. Mol Biochem Parasitol. 1995;74(2):223-7.

32. Taylor MJ, Hoerauf A. Wolbachia bacteria of filarial nematodes. Parasitol Today. 1999;15(11):437-42.

33. Williams SA, Lizotte-Waniewski MR, Foster J, Guiliano D, Daub J, Scott AL, et al. The filarial genome project: analysis of the nuclear, mitochondrial and endosymbiont genomes of Brugia malayi. Int J Parasitol. 2000;30(4):411-9.

34. Büttner DW, Wanji S, Bazzocchi C, Bain O, Fischer P. Obligatory symbiotic Wolbachia endobacteria are absent from Loa loa. Filaria J. 2003;2(1):10.

35. Ferri E, Bain O, Barbuto M, Martin C, Lo N, Uni S, et al. New Insights into the Evolution of Wolbachia Infections in Filarial Nematodes Inferred from a Large Range of Screened Species. PLoS One. 2011;6(6):e20843.

36. Ta-Tang T-H, Crainey JL, Post RJ, Luz SL, Rubio JM. Mansonellosis: current perspectives. Res Rep Trop Med. 2018;9:9-24.

37. Fenn K, Blaxter M. Are filarial nematode Wolbachia obligate mutualist symbionts? Trends Ecol Evol. 2004;19(4):163-6.

38. McNulty SN, Foster JM, Mitreva M, Dunning Hotopp JC, Martin J, Fischer K, et al. Endosymbiont DNA in Endobacteria-Free Filarial Nematodes Indicates Ancient Horizontal Genetic Transfer. PLoS One. 2010;5(6):e11029.

39. Choi Y-J, Ghedin E, Berriman M, McQuillan J, Holroyd N, Mayhew GF, et al. A Deep Sequencing Approach to Comparatively Analyze the Transcriptome of Lifecycle Stages of the Filarial Worm, Brugia malayi. PLoS Negl Trop Dis. 2011;5(12):e1409.

40. Scott AL, Ghedin E. The genome of Brugia malayi - all worms are not created equal. Parasitol Int. 2009;58(1):6-11.

41. Foster J, Ganatra M, Kamal I, Ware J, Makarova K, Ivanova N, et al. The Wolbachia genome of Brugia malayi: endosymbiont evolution within a human pathogenic nematode. PLoS Biol. 2005;3(4):e121.

42. Wu B, Novelli J, Foster J, Vaisvila R, Conway L, Ingram J, et al. The heme biosynthetic pathway of the obligate Wolbachia endosymbiont of Brugia malayi as a potential anti-filarial drug target. PLoS Negl Trop Dis. 2009;3(7):e475-e.

43. Wu B, Novelli J, Jiang D, Dailey HA, Landmann F, Ford L, et al. Interdomain lateral gene transfer of an essential ferrochelatase gene in human parasitic nematodes. PNAS. 2013;110(19):7748-53.

44. Lustigman S, Melnikow E, Anand SB, Contreras A, Nandi V, Liu J, et al. Potential involvement of Brugia malayi cysteine proteases in the maintenance of the endosymbiotic relationship with Wolbachia. Int J Parasitol Drugs Drug Resist. 2014;4(3):267-77.

45. Luck AN, Anderson KG, McClung CM, VerBerkmoes NC, Foster JM, Michalski ML, et al. Tissue-specific transcriptomics and proteomics of a filarial nematode and its Wolbachia endosymbiont. BMC Genomics. 2015;16:920-.

46. Shaikevich EV, Ganushkina LA. Wolbachia Bacteria and Filarial Nematodes: Mutual Benefit and the Parasite's Achilles' Heel. Biol Bull Rev. 2018;8(6):509-17.

47. Landmann F, Foster JM, Slatko B, Sullivan W. Asymmetric Wolbachia Segregation during Early Brugia malayi Embryogenesis Determines Its Distribution in Adult Host Tissues. PLoS Negl Trop Dis. 2010;4(7):e758.

48. Pietri JE, DeBruhl H, Sullivan W. The rich somatic life of Wolbachia. Microbiologyopen. 2016;5(6):923-36.

49. McGarry HF, Egerton GL, Taylor MJ. Population dynamics of Wolbachia bacterial endosymbionts in Brugia malayi. Mol Biochem Parasitol. 2004;135(1):57-67.

50. Landmann F, Voronin D, Sullivan W, Taylor MJ. Anti-filarial Activity of Antibiotic Therapy Is Due to Extensive Apoptosis after Wolbachia Depletion from Filarial Nematodes. PLoS Pathog. 2011;7(11):e1002351.

51. Turner JD, Langley RS, Johnston KL, Gentil K, Ford L, Wu B, et al. Wolbachia Lipoprotein Stimulates Innate and Adaptive Immunity through Toll-like Receptors 2 and 6 to Induce Disease Manifestations of Filariasis. J Biol Chem. 2009(33):22364.

52. Taylor MJ, Hoerauf A, Townson S, Slatko BE, Ward SA. Anti-Wolbachia drug discovery and development: safe macrofilaricides for onchocerciasis and lymphatic filariasis. Parasitol. 2014;141(1):119-27.

53. Walker M, Specht S, Churcher TS, Hoerauf A, Taylor MJ, Basáñez M-G. Therapeutic efficacy and macrofilaricidal activity of doxycycline for the treatment of river blindness. Clin Infect Dis. 2015;60(8):1199-207.

54. Chopra I, Roberts M. Tetracycline antibiotics: mode of action, applications, molecular biology, and epidemiology of bacterial resistance. Microbiol Mol Biol Rev. 2001;65(2):232-60.

55. Hoerauf A, Nissen-Pähle K, Schmetz C, Henkle-Dührsen K, Blaxter ML, Büttner DW, et al. Tetracycline therapy targets intracellular bacteria in the filarial nematode Litomosoides sigmodontis and results in filarial infertility. J Clin Invest. 1999;103(1):11-8.

56. Bandi C, McCall JW, Genchi C, Corona S, Venco L, Sacchi L. Effects of tetracycline on the filarial worms Brugia pahangi and Dirofilaria immitis and their bacterial endosymbionts Wolbachia. Int J Parasitol. 1999;29(2):357-64.

57. Rao RU, Moussa H, Weil GJ. Brugia malayi: effects of antibacterial agents on larval viability and development in vitro. Exp Parasitol. 2002;101(1):77-81.

58. Rao R, Well GJ. In vitro effects of antibiotics on Brugia malayi worm survival and reproduction. J Parasitol. 2002;88(3):605-11.

59. World Health Organisation. WHO Model List of Essential Medicines 2017 [20:[Available from: https://apps.who.int/iris/bitstream/handle/10665/273826/EML-20-eng.pdf?ua=1.

60. Townson S, Tagboto S, McGarry HF, Egerton GL, Taylor MJ. Onchocerca parasites and Wolbachia endosymbionts: evaluation of a spectrum of antibiotic types for activity against Onchocerca gutturosa in vitro. Filaria J. 2006;5:4-.

61. Turner JD, Sharma R, Al Jayoussi G, Tyrer HE, Gamble J, Hayward L, et al. Albendazole and antibiotics synergize to deliver short-course anti-Wolbachia curative treatments in preclinical models of filariasis. PNAS. 2017;114(45):E9712-e21.

62. Volkmann L, Fischer K, Taylor M, Hoerauf A. Antibiotic therapy in murine filariasis (Litomosoides sigmodontis): comparative effects of doxycycline and rifampicin on Wolbachia and filarial viability. Trop Med Int Health. 2003;8(5):392-401.

63. Townson S, Hutton D, Siemienska J, Hollick L, Scanlon T, Tagboto SK, et al. Antibiotics and Wolbachia in filarial nematodes: antifilarial activity of rifampicin, oxytetracycline and chloramphenicol against Onchocerca gutturosa, Onchocerca lienalis and Brugia pahangi. Ann Trop Med Parasitol. 2000;94(8):801-16.

64. Aljayyoussi G, Tyrer HE, Ford L, Sjoberg H, Pionnier N, Waterhouse D, et al. Short-Course, High-Dose Rifampicin Achieves Wolbachia Depletion Predictive of Curative Outcomes in Preclinical Models of Lymphatic Filariasis and Onchocerciasis. Sci Rep. 2017;7(1):210.

65. Taylor MJ, Hoerauf A, Bockarie M. Lymphatic filariasis and onchocerciasis. Lancet. 2010;376(9747):1175-85.

66. Specht S, Mand S, Marfo-Debrekyei Y, Debrah AY, Konadu P, Adjei O, et al. Efficacy of 2- and 4-week rifampicin treatment on the Wolbachia of Onchocerca volvulus. Parasitol Res. 2008;103(6):1303-9.

67. Debrah AY, Mand S, Marfo-Debrekyei Y, Batsa L, Albers A, Specht S, et al. Macrofilaricidal Activity in Wuchereria bancrofti after 2 Weeks Treatment with a Combination of Rifampicin plus Doxycycline. J Parasitol Res. 2011;2011:201617.

68. Hoerauf A, Mand S, Fischer K, Kruppa T, Marfo-Debrekyei Y, Debrah AY, et al. Doxycycline as a novel strategy against bancroftian filariasis-depletion of Wolbachia endosymbionts from Wuchereria bancrofti and stop of microfilaria production. Med Microbiol Immunol. 2003;192(4):211-6.

69. Taylor MJ, Makunde WH, McGarry HF, Turner JD, Mand S, Hoerauf A. Macrofilaricidal activity after doxycycline treatment of Wuchereria bancrofti: a double-blind, randomised placebo-controlled trial. Lancet. 2005;365(9477):2116-21.

70. Supali T, Djuardi Y, Pfarr KM, Wibowo H, Taylor MJ, Hoerauf A, et al. Doxycycline treatment of Brugia malayi-infected persons reduces microfilaremia and adverse reactions after diethylcarbamazine and albendazole treatment. Clin Infect Dis. 2008;46(9):1385-93.

71. Hoerauf A, Specht S, Marfo-Debrekyei Y, Buttner M, Debrah AY, Mand S, et al. Efficacy of 5-week doxycycline treatment on adult Onchocerca volvulus. Parasitol Res. 2009;104(2):437-47.

72. Turner JD, Mand S, Debrah AY, Muehlfeld J, Pfarr K, McGarry HF, et al. A randomized, double-blind clinical trial of a 3-week course of doxycycline plus albendazole and ivermectin for the treatment of Wuchereria bancrofti infection. Clin Infect Dis. 2006;42(8):1081-9.

73. Mand S, Pfarr K, Sahoo PK, Satapathy AK, Specht S, Klarmann U, et al. Macrofilaricidal activity and amelioration of lymphatic pathology in bancroftian filariasis after 3 weeks of doxycycline followed by single-dose diethylcarbamazine. Am J Trop Med Hyg. 2009;81(4):702-11.

74. Hoerauf A, Mand S, Volkmann L, Buttner M, Marfo-Debrekyei Y, Taylor M, et al. Doxycycline in the treatment of human onchocerciasis: Kinetics of Wolbachia endobacteria reduction and of inhibition of embryogenesis in female Onchocerca worms. Microbes Infect. 2003;5(4):261-73.

75. Tamarozzi F, Tendongfor N, Enyong PA, Esum M, Faragher B, Wanji S, et al. Long term impact of large scale community-directed delivery of doxycycline for the treatment of onchocerciasis. Parasit Vectors. 2012;5:53.

76. Klarmann-Schulz U, Specht S, Debrah AY, Batsa L, Ayisi-Boateng NK, Osei-Mensah J, et al. Comparison of Doxycycline, Minocycline, Doxycycline plus Albendazole and

Albendazole Alone in Their Efficacy against Onchocerciasis in a Randomized, Open-Label, Pilot Trial. PLoS Negl Trop Dis. 2017;11(1):e0005156.

77. Anti-Wolbachia consortium. The A.WOL Approach 2019 [Available from: https://awol.lstmed.ac.uk/why-a%E2%88%99wol/the-a%E2%88%99wol-approach (accessed on 29 April 2019).

78. Anti-Wolbachia consortium. Why Anti-Wolbachia 2019 [Available from: https://awol.lstmed.ac.uk/why-anti-wolbachia (accessed on 12 March 2019).

79. Johnston KL, Ford L, Taylor MJ. Overcoming the challenges of drug discovery for neglected tropical diseases: the A.WOL experience. J Biomol Screen. 2014;19(3):335-43.

80. Clare RH, Cook DA, Johnston KL, Ford L, Ward SA, Taylor MJ. Development and validation of a high-throughput anti-Wolbachia whole-cell screen: a route to macrofilaricidal drugs against onchocerciasis and lymphatic filariasis. J Biomol Screen. 2015;20(1):64-9.

81. Taylor MJ, von Geldern TW, Ford L, Hübner MP, Marsh K, Johnston KL, et al. Preclinical development of an oral anti-Wolbachia macrolide drug for the treatment of lymphatic filariasis and onchocerciasis. Sci Transl Med. 2019;11(483):eaau2086.

82. Hong WD, Benayoud F, Nixon GL, Ford L, Johnston KL, Clare RH, et al. AWZ1066S, a highly specific anti-Wolbachia drug candidate for a short-course treatment of filariasis. PNAS. 2019;116(4):1414-9.

83. Still JG, Clark K, Degenhardt TP, Scott D, Fernandes P, Gutierrez MJ. Pharmacokinetics and safety of single, multiple, and loading doses of fusidic acid in healthy subjects. Clin Infect Dis. 2011;52 Suppl 7:S504-12.

84. Craft JC, Moriarty SR, Clark K, Scott D, Degenhardt TP, Still JG, et al. A randomized, double-blind phase 2 study comparing the efficacy and safety of an oral fusidic acid loading-dose regimen to oral linezolid for the treatment of acute bacterial skin and skin structure infections. Clin Infect Dis. 2011;52 Suppl 7:S520-6.

85. National Institute for Health and Care Excellence. Fusidic Acid 2019 [Available from: https://bnf.nice.org.uk/drug/fusidic-acid.html (Accessed on 29 April 2019).

86. Aljayyoussi G, Taylor M. Repurposing fusidic acid for the rapid treatment of lymphatic filariasis and onchocerciasis in humans: Evidence from in-vivo studies 2019 [unpublished].

87. Voronin D, Cook DA, Steven A, Taylor MJ. Autophagy regulates Wolbachia populations across diverse symbiotic associations. PNAS. 2012;109(25):E1638-46.

88. Mizushima N, Komatsu M. Autophagy: renovation of cells and tissues. Cell. 2011;147(4):728-41.

89. Levine B, Kroemer G. Biological Functions of Autophagy Genes: A Disease Perspective. Cell. 2019;176(1-2):11-42.

90. Levine B, Kroemer G. Autophagy in the pathogenesis of disease. Cell. 2008;132(1):27-42.

91. Codogno P, Meijer AJ. Autophagy and signaling: their role in cell survival and cell death. Cell Death Differ. 2005;12 Suppl 2:1509-18.

92. Mizushima N. Autophagy: process and function. Genes Dev. 2007;21(22):2861-73.

93. Parzych KR, Klionsky DJ. An overview of autophagy: morphology, mechanism, and regulation. Antioxid Redox Signal. 2014;20(3):460-73.

94. Glick D, Barth S, Macleod KF. Autophagy: cellular and molecular mechanisms. J Pathol. 2010;221(1):3-12.

95. Lőrincz P, Mauvezin C, Juhász G. Exploring Autophagy in Drosophila. Cells. 2017;6(3):22.

96. Wesselborg S, Stork B. Autophagy signal transduction by ATG proteins: from hierarchies to networks. Cell Mol Life Sci. 2015;72(24):4721-57.

97. Jung CH, Ro SH, Cao J, Otto NM, Kim DH. mTOR regulation of autophagy. FEBS Lett. 2010;584(7):1287-95.

98. Nagy P, Varga A, Kovacs AL, Takats S, Juhasz G. How and why to study autophagy in Drosophila: it's more than just a garbage chute. Methods. 2015;75:151-61.

99. He C, Klionsky DJ. Regulation mechanisms and signaling pathways of autophagy. Annu Rev Genet. 2009;43:67-93.

100. Sarkar S. Regulation of autophagy by mTOR-dependent and mTOR-independent pathways: autophagy dysfunction in neurodegenerative diseases and therapeutic application of autophagy enhancers. Biochem Soc Trans. 2013;41(5):1103-30.

101. Gatica D, Lahiri V, Klionsky DJ. Cargo recognition and degradation by selective autophagy. Nat Cell Biol. 2018;20(3):233-42.

102. Dengjel J, Abeliovich H. Musical chairs during mitophagy. Autophagy. 2014;10(4):706-7.

103. Sharma V, Verma S, Seranova E, Sarkar S, Kumar D. Selective Autophagy and Xenophagy in Infection and Disease. Front Cell Dev Biol. 2018;6(147).

104. Steele S, Brunton J, Kawula T. The role of autophagy in intracellular pathogen nutrient acquisition. Front Cell Infect Microbiol. 2015;5:51.

105. Taylor MJ, Voronin D, Johnston KL, Ford L. Wolbachia filarial interactions. Cell Microbiol. 2013;15(4):520-6.

106. Mizushima N, Yoshimori T, Levine B. Methods in mammalian autophagy research. Cell. 2010;140(3):313-26.

107. Huang J, Brumell JH. Bacteria-autophagy interplay: a battle for survival. Nat Rev Microbiol. 2014;12(2):101-14.

108. Tattoli I, Sorbara MT, Philpott DJ, Girardin SE. Bacterial autophagy: the trigger, the target and the timing. Autophagy. 2012;8(12):1848-50.

109. Choy A, Dancourt J, Mugo B, O'Connor TJ, Isberg RR, Melia TJ, et al. The Legionella effector RavZ inhibits host autophagy through irreversible Atg8 deconjugation. Science. 2012;338(6110):1072-6.

110. Choy A, Roy CR. Autophagy and bacterial infection: an evolving arms race. Trends Microbiol. 2013;21(9):451-6.

111. Ogawa M, Yoshimori T, Suzuki T, Sagara H, Mizushima N, Sasakawa C. Escape of Intracellular Shigella from Autophagy. Science. 2005;307(5710):727-31.

112. Schnaith A, Kashkar H, Leggio SA, Addicks K, Kronke M, Krut O. Staphylococcus aureus subvert autophagy for induction of caspase-independent host cell death. J Biol Chem. 2007;282(4):2695-706.

113. Niu H, Yamaguchi M, Rikihisa Y. Subversion of cellular autophagy by Anaplasma phagocytophilum. Cell Microbiol. 2008;10(3):593-605.

114. Romano PS, Gutierrez MG, Beron W, Rabinovitch M, Colombo MI. The autophagic pathway is actively modulated by phase II Coxiella burnetii to efficiently replicate in the host cell. Cell Microbiol. 2007;9(4):891-909.

115. Beare PA, Gilk SD, Larson CL, Hill J, Stead CM, Omsland A, et al. Dot/Icm Type IVB Secretion System Requirements for Coxiella burnetii Growth in Human Macrophages. MBio. 2011;2(4):e00175-11.

116. Petiot A, Ogier-Denis E, Blommaart EF, Meijer AJ, Codogno P. Distinct classes of phosphatidylinositol 3'-kinases are involved in signaling pathways that control macroautophagy in HT-29 cells. J Biol Chem. 2000;275(2):992-8.

117. Wu YT, Tan HL, Shui G, Bauvy C, Huang Q, Wenk MR, et al. Dual role of 3-methyladenine in modulation of autophagy via different temporal patterns of inhibition on class I and III phosphoinositide 3-kinase. J Biol Chem. 2010;285(14):10850-61.

118. Yang YP, Hu LF, Zheng HF, Mao CJ, Hu WD, Xiong KP, et al. Application and interpretation of current autophagy inhibitors and activators. Acta Pharmacol Sin. 2013;34(5):625-35.

119. Seglen PO, Gordon PB. 3-Methyladenine: specific inhibitor of autophagic/lysosomal protein degradation in isolated rat hepatocytes. Proc Natl Acad Sci U S A. 1982;79(6):1889-92.

120. Powis G, Bonjouklian R, Berggren MM, Gallegos A, Abraham R, Ashendel C, et al. Wortmannin, a potent and selective inhibitor of phosphatidylinositol-3-kinase. Cancer Res. 1994;54(9):2419-23.

121. Vlahos CJ, Matter WF, Hui KY, Brown RF. A specific inhibitor of phosphatidylinositol 3-kinase, 2-(4-morpholinyl)-8-phenyl-4H-1-benzopyran-4-one (LY294002). J Biol Chem. 1994;269(7):5241-8.

122. Jahreiss L, Menzies FM, Rubinsztein DC. The itinerary of autophagosomes: from peripheral formation to kiss-and-run fusion with lysosomes. Traffic. 2008;9(4):574-87.

123. Hoyvik H, Gordon PB, Berg TO, Stromhaug PE, Seglen PO. Inhibition of autophagic-lysosomal delivery and autophagic lactolysis by asparagine. J Cell Biol. 1991;113(6):1305-12.

124. Redmann M, Benavides GA, Berryhill TF, Wani WY, Ouyang X, Johnson MS, et al. Inhibition of autophagy with bafilomycin and chloroquine decreases mitochondrial quality and bioenergetic function in primary neurons. Redox Biol. 2017;11:73-81.

125. Seglen PO, Gordon PB, Poli A. Amino acid inhibition of the autophagic/lysosomal pathway of protein degradation in isolated rat hepatocytes. Biochim Biophys Acta. 1980;630(1):103-18.

126. Gordon PB, Seglen PO. Prelysosomal convergence of autophagic and endocytic pathways. Biochem Biophys Res Commun. 1988;151(1):40-7.

127. Klionsky DJ, Cuervo AM, Seglen PO. Methods for Monitoring Autophagy from Yeast to Human. Autophagy. 2014;3(3):181-206.

128. Meijer AJ, Lorin S, Blommaart EF, Codogno P. Regulation of autophagy by amino acids and MTOR-dependent signal transduction. Amino Acids. 2015;47(10):2037-63.

129. Hu CA, Wu Z, Wang J. Amino acids and autophagy: their crosstalk, interplay and interlock. Amino Acids. 2015;47(10):2035-6.

130. Barth S, Glick D, Macleod KF. Autophagy: assays and artifacts. J Pathol. 2010;221(2):117-24.

131. Klionsky DJ, Abdelmohsen K, Abe A, Abedin MJ, Abeliovich H, Acevedo Arozena A, et al. Guidelines for the use and interpretation of assays for monitoring autophagy (3rd edition). Autophagy. 2016;12(1):1-222.

132. Bauckman KA, Owusu-Boaitey N, Mysorekar IU. Selective autophagy: xenophagy. Methods. 2015;75:120-7.

133. Orhon I, Reggiori F. Assays to Monitor Autophagy Progression in Cell Cultures. Cells. 2017;6(3).

134. Ambrosio. LC3-I conversion to LC3-II does not necessarily result in complete autophagy. Int J Mol Med. 1998.

135. Lee S, Hiradate Y, Hoshino Y, Tanemura K, Sato E. Quantitative analysis in LC3-II protein in vitro maturation of porcine oocyte. Zygote. 2014;22(3):404-10.

136. Kabeya Y, Mizushima N, Ueno T, Yamamoto A, Kirisako T, Noda T, et al. LC3, a mammalian homologue of yeast Apg8p, is localized in autophagosome membranes after processing. EMBO J. 2000;19(21):5720-8.

137. Lee Y-K, Lee J-A. Role of the mammalian ATG8/LC3 family in autophagy: differential and compensatory roles in the spatiotemporal regulation of autophagy. BMB Reports. 2016;49(8):424-30.

138. Bjørkøy G, Lamark T, Pankiv S, Øvervatn A, Brech A, Johansen T. Monitoring Autophagic Degradation of p62/SQSTM1. Methods Enzymol2009. p. 181-97.

139. Moy RH, Cherry S. Antimicrobial autophagy: a conserved innate immune response in Drosophila. J Innate Immun. 2013;5(5):444-55.

140. Bartlett BJ, Isakson P, Lewerenz J, Sanchez H, Kotzebue RW, Cumming RC, et al. p62, Ref(2)P and ubiquitinated proteins are conserved markers of neuronal aging, aggregate formation and progressive autophagic defects. Autophagy. 2011;7(6):572-83.

141. Zaffagnini G, Martens S. Mechanisms of Selective Autophagy. J Mol Biol. 2016;428(9 Pt A):1714-24.

142. Pankiv S, Clausen TH, Lamark T, Brech A, Bruun JA, Outzen H, et al. p62/SQSTM1 binds directly to Atg8/LC3 to facilitate degradation of ubiquitinated protein aggregates by autophagy. J Biol Chem. 2007;282(33):24131-45.

143. Lippai M, Low P. The role of the selective adaptor p62 and ubiquitin-like proteins in autophagy. Biomed Res Int. 2014;2014:832704.

144. Ying H, Yue BY. Optineurin: The autophagy connection. Exp Eye Res. 2016;144:73-80.

145. Verlhac P, Gregoire IP, Azocar O, Petkova DS, Baguet J, Viret C, et al. Autophagy receptor NDP52 regulates pathogen-containing autophagosome maturation. Cell Host Microbe. 2015;17(4):515-25.

146. Kirkin V, Lamark T, Sou YS, Bjorkoy G, Nunn JL, Bruun JA, et al. A role for NBR1 in autophagosomal degradation of ubiquitinated substrates. Mol Cell. 2009;33(4):505-16.

147. Mizushima N, Yoshimori T. How to Interpret LC3 Immunoblotting. Autophagy. 2014;3(6):542-5.

148. Blommaart EF, Krause U, Schellens JP, Vreeling-Sindelarova H, Meijer AJ. The phosphatidylinositol 3-kinase inhibitors wortmannin and LY294002 inhibit autophagy in isolated rat hepatocytes. Eur J Biochem. 1997;243(1-2):240-6.

149. O'Neill SL, Pettigrew MM, Sinkins SP, Braig HR, Andreadis TG, Tesh RB. In vitro cultivation of Wolbachia pipientis in an Aedes albopictus cell line. Insect Mol Biol. 1997;6(1):33-9.

150. Turner JD, Langley RS, Johnston KL, Egerton G, Wanji S, Taylor MJ. Wolbachia endosymbiotic bacteria of Brugia malayi mediate macrophage tolerance to TLR- and CD40-specific stimuli in a MyD88/TLR2-dependent manner. J Immunol. 2006;177(2):1240-9.

151. Johnston KL, Cook DAN, Berry NG, David Hong W, Clare RH, Goddard M, et al. Identification and prioritization of novel anti-Wolbachia chemotypes from screening a 10,000-compound diversity library. Sci Adv. 2017;3(9):eaao1551.

152. Klionsky DJ, Abeliovich H, Agostinis P, Agrawal DK, Aliev G, Askew DS, et al. Guidelines for the use and interpretation of assays for monitoring autophagy in higher eukaryotes. Autophagy. 2008;4(2):151-75.

153. Yoshii SR, Mizushima N. Monitoring and Measuring Autophagy. Int J Mol Sci. 2017;18(9).

154. Gomez-Sanchez R, Pizarro-Estrella E, Yakhine-Diop SM, Rodriguez-Arribas M, Bravo-San Pedro JM, Fuentes JM, et al. Routine Western blot to check autophagic flux: cautions and recommendations. Anal Biochem. 2015;477:13-20.

155. Pircs K, Nagy P, Varga A, Venkei Z, Erdi B, Hegedus K, et al. Advantages and limitations of different p62-based assays for estimating autophagic activity in Drosophila. PLoS One. 2012;7(8):e44214.

156. Nezis IP, Simonsen A, Sagona AP, Finley K, Gaumer S, Contamine D, et al. Ref(2)P, the Drosophila melanogaster homologue of mammalian p62, is required for the formation of protein aggregates in adult brain. J Cell Biol. 2008;180(6):1065-71.

157. Tanida I, Minematsu-Ikeguchi N, Ueno T, Kominami E. Lysosomal turnover, but not a cellular level, of endogenous LC3 is a marker for autophagy. Autophagy. 2005;1(2):84-91.

158. Slavin SA, Leonard A, Grose V, Fazal F, Rahman A. Autophagy inhibitor 3-methyladenine protects against endothelial cell barrier dysfunction in acute lung injury. Am J Physiol Lung Cell Mol Physiol. 2018;314(3):L388-L96.

159. Stroikin Y, Dalen H, Loof S, Terman A. Inhibition of autophagy with 3-methyladenine results in impaired turnover of lysosomes and accumulation of lipofuscin-like material. Eur J Cell Biol. 2004;83(10):583-90.

160. Punnonen EL, Marjomaki VS, Reunanen H. 3-Methyladenine inhibits transport from late endosomes to lysosomes in cultured rat and mouse fibroblasts. Eur J Cell Biol. 1994;65(1):14-25.

161. Mizushima N, Yamamoto A, Hatano M, Kobayashi Y, Kabeya Y, Suzuki K, et al. Dissection of autophagosome formation using Apg5-deficient mouse embryonic stem cells. J Cell Biol. 2001;152(4):657-68.

162. Hou H, Zhang Y, Huang Y, Yi Q, Lv L, Zhang T, et al. Inhibitors of phosphatidylinositol 3'-kinases promote mitotic cell death in HeLa cells. PLoS One. 2012;7(4):e35665.

163. Gui MC, Chen B, Yu SS, Bu BT. Effects of suppressed autophagy on mitochondrial dynamics and cell cycle of N2a cells. J Huazhong Univ Sci Technolog Med Sci. 2014;34(2):157-60.

164. Sheng Y, Sun B, Guo WT, Zhang YH, Liu X, Xing Y, et al. 3-Methyladenine induces cell death and its interaction with chemotherapeutic drugs is independent of autophagy. Biochem Biophys Res Commun. 2013;432(1):5-9.

165. Caro LH, Plomp PJ, Wolvetang EJ, Kerkhof C, Meijer AJ. 3-Methyladenine, an inhibitor of autophagy, has multiple effects on metabolism. Eur J Biochem. 1988;175(2):325-9.

166. Xue L, Borutaite V, Tolkovsky AM. Inhibition of mitochondrial permeability transition and release of cytochrome c by anti-apoptotic nucleoside analogues. Biochem Pharmacol. 2002;64(3):441-9.

167. Wu Y, Wang X, Guo H, Zhang B, Zhang XB, Shi ZJ, et al. Synthesis and screening of 3-MA derivatives for autophagy inhibitors. Autophagy. 2013;9(4):595-603.

168. Moon EK, Kim SH, Hong Y, Chung DI, Goo YK, Kong HH. Autophagy inhibitors as a potential antiamoebic treatment for Acanthamoeba keratitis. Antimicrob Agents Chemother. 2015;59(7):4020-5.

169. Brunn GJ WJ, Sabers C, Wiederrecht G, Lawrence JC, Abraham RT. Direct inhibition of the signaling functions of the mammalian target of rapamycin by the phosphoinositide 3-kinase inhibitors, wortmannin and LY294002.EMBO J. 1996;15(19):5256-67. .

170. Christian F, Anthony DF, Vadrevu S, Riddell T, Day JP, McLeod R, et al. p62 (SQSTM1) and cyclic AMP phosphodiesterase-4A4 (PDE4A4) locate to a novel, reversible protein aggregate with links to autophagy and proteasome degradation pathways. Cell Signal. 2010;22(10):1576-96.

171. Collado M, Medema RH, Garcia-Cao I, Dubuisson ML, Barradas M, Glassford J, et al. Inhibition of the phosphoinositide 3-kinase pathway induces a senescence-like arrest mediated by p27Kip1. J Biol Chem. 2000;275(29):21960-8.

172. Feldman ME, Apsel B, Uotila A, Loewith R, Knight ZA, Ruggero D, et al. Active-site inhibitors of mTOR target rapamycin-resistant outputs of mTORC1 and mTORC2. PLoS Biol. 2009;7(2):e38.

173. Brunn GJ, Williams J, Sabers C, Wiederrecht G, Lawrence JC, Jr., Abraham RT. Direct inhibition of the signaling functions of the mammalian target of rapamycin by the phosphoinositide 3-kinase inhibitors, wortmannin and LY294002. EMBO J. 1996;15(19):5256-67.

174. Vanrell MC, Losinno AD, Cueto JA, Balcazar D, Fraccaroli LV, Carrillo C, et al. The regulation of autophagy differentially affects Trypanosoma cruzi metacyclogenesis. PLoS Negl Trop Dis. 2017;11(11):e0006049.

175. Schmidt RS, Butikofer P. Autophagy in Trypanosoma brucei: amino acid requirement and regulation during different growth phases. PLoS One. 2014;9(4):e93875.

176. Seglen PO, Berg TO, Blankson H, Fengsrud M, Holen I, Strømhaug PE. Structural Aspects of Autophagy. Adv Exp Med Biol. 1996:103-11.

177. Seglen PO. Amino acid control of autophagic sequestration and protein degradation in isolated rat hepatocytes. J Cell Biol. 1984;99(2):435-44.

178. Swer PB, Lohia R, Saran S. Analysis of rapamycin induced autophagy in Dictyostelium discoideum. Indian J Exp Biol. 2014(4):295.

179. Jiang RY, Pei HL, Gu WD, Huang J, Wang ZG. Autophagic inhibitor attenuates rapamycin-induced inhibition of proliferation in cultured A549 lung cancer cells. Eur Rev Med Pharmacol Sci. 2014;18(6):806-10.

180. Ravikumar B, Vacher C, Berger Z, Davies JE, Luo S, Oroz LG, et al. Inhibition of mTOR induces autophagy and reduces toxicity of polyglutamine expansions in fly and mouse models of Huntington disease. Nat Genet. 2004;36(6):585-95.

181. Tanemura M, Ohmura Y, Deguchi T, Machida T, Tsukamoto R, Wada H, et al. Rapamycin causes upregulation of autophagy and impairs islets function both in vitro and in vivo. Am J Transplant. 2012;12(1):102-14.

182. Musiwaro P, Smith M, Manifava M, Walker SA, Ktistakis NT. Characteristics and requirements of basal autophagy in HEK 293 cells. Autophagy. 2013;9(9):1407-17.

183. Karanasios E, Ktistakis NT. Signalling in autophagy. Autophagy at the Cell, Tissue and Organismal Level. United Kingdom SpringerBriefs in Cell Biology; 2016. p. 17.

184. Levine B, Klionsky DJ. Development by self-digestion: molecular mechanisms and biological functions of autophagy. Dev Cell. 2004;6(4):463-77.

185. Bergamini E, Cavallini G, Donati A, Gori Z. The role of macroautophagy in the ageing process, anti-ageing intervention and age-associated diseases. Int J Biochem Cell Biol. 2004;36(12):2392-404.

186. Rutkowski DT, Hegde RS. Regulation of basal cellular physiology by the homeostatic unfolded protein response. J Cell Biol. 2010;189(5):783-94.

187. Lee JJ, Sanchez-Martinez A, Zarate AM, Benincá C, Mayor U, Clague MJ, et al. Basal mitophagy is widespread in Drosophila but minimally affected by loss of Pink1 or parkin. J Cell Biol. 2018;217(5):1613-22.

188. Escoll P, Rolando M, Buchrieser C. Modulation of Host Autophagy during Bacterial Infection: Sabotaging Host Munitions for Pathogen Nutrition. Front Immunol. 2016;7:81.

189. Russell RC, Yuan HX, Guan KL. Autophagy regulation by nutrient signaling. Cell Res. 2014;24(1):42-57.

190. Kroemer G, Marino G, Levine B. Autophagy and the integrated stress response. Mol Cell. 2010;40(2):280-93.

191. Vabulas RM, Hartl FU. Protein synthesis upon acute nutrient restriction relies on proteasome function. Science. 2005;310(5756):1960-3.

192. Takeshige K, Baba M, Tsuboi S, Noda T, Ohsumi Y. Autophagy in yeast demonstrated with proteinase-deficient mutants and conditions for its induction. J Cell Biol. 1992;119(2):301-11.

193. Wu W, Wei W, Ablimit M, Ma Y, Fu T, Liu K, et al. Responses of two insect cell lines to starvation: autophagy prevents them from undergoing apoptosis and necrosis, respectively. J Insect Physiol. 2011;57(6):723-34.

194. Scott RC, Schuldiner O, Neufeld TP. Role and regulation of starvation-induced autophagy in the Drosophila fat body. Dev Cell. 2004;7(2):167-78.

195. Kanazawa T, Taneike I, Akaishi R, Yoshizawa F, Furuya N, Fujimura S, et al. Amino acids and insulin control autophagic proteolysis through different signaling pathways in relation to mTOR in isolated rat hepatocytes. J Biol Chem. 2004;279(9):8452-9.

196. Mordier S, Deval C, Bechet D, Tassa A, Ferrara M. Leucine limitation induces autophagy and activation of lysosome-dependent proteolysis in C2C12 myotubes through a mammalian target of rapamycin-independent signaling pathway. J Biol Chem. 2000;275(38):29900-6.

197. Shang L, Chen S, Du F, Li S, Zhao L, Wang X. Nutrient starvation elicits an acute autophagic response mediated by Ulk1 dephosphorylation and its subsequent dissociation from AMPK. PNAS. 2011;108(12):4788-93.

198. Scherz-Shouval R, Elazar Z. Regulation of autophagy by ROS: physiology and pathology. Trends Biochem Sci. 2011;36(1):30-8.

199. Fang C, Gu L, Smerin D, Mao S, Xiong X. The Interrelation between Reactive Oxygen Species and Autophagy in Neurological Disorders. Oxid Med Cell Longev. 2017;2017:8495160.

200. Filomeni G, De Zio D, Cecconi F. Oxidative stress and autophagy: the clash between damage and metabolic needs. Cell Death Differ. 2015;22(3):377-88.

201. Xiao B, Goh JY, Xiao L, Xian H, Lim KL, Liou YC. Reactive oxygen species trigger Parkin/PINK1 pathway-dependent mitophagy by inducing mitochondrial recruitment of Parkin. J Biol Chem. 2017;292(40):16697-708.

202. Huang J, Canadien V, Lam GY, Steinberg BE, Dinauer MC, Magalhaes MAO, et al. Activation of antibacterial autophagy by NADPH oxidases. PNAS. 2009;106(15):6226-31.

203. Azad MB, Chen Y, Gibson SB. Regulation of autophagy by reactive oxygen species (ROS): implications for cancer progression and treatment. Antioxid Redox Signal. 2009;11(4):777-90.

204. Lee Y, Jung J, Cho KJ, Lee SK, Park JW, Oh IH, et al. Increased SCF/c-kit by hypoxia promotes autophagy of human placental chorionic plate-derived mesenchymal stem cells via regulating the phosphorylation of mTOR. J Cell Biochem. 2013;114(1):79-88.

205. Degenhardt K, Mathew R, Beaudoin B, Bray K, Anderson D, Chen G, et al. Autophagy promotes tumor cell survival and restricts necrosis, inflammation, and tumorigenesis. Cancer Cell. 2006;10(1):51-64.

206. White E. The role for autophagy in cancer. J Clin Invest. 2015;125(1):42-6.

207. Jiang P, Mizushima N. Autophagy and human diseases. Cell Res. 2014;24(1):69-79.

208. Bednarczyk M, Zmarzły N, Grabarek B, Mazurek U, Muc-Wierzgoń M. Genes involved in the regulation of different types of autophagy and their participation in cancer pathogenesis. Oncotarget. 2018;9(76):34413-28.

209. Zhang Z, Lai Q, Li Y, Xu C, Tang X, Ci J, et al. Acidic pH environment induces autophagy in osteoblasts. Sci Rep. 2017;7:46161-.

210. Marino ML, Pellegrini P, Di Lernia G, Djavaheri-Mergny M, Brnjic S, Zhang X, et al. Autophagy is a protective mechanism for human melanoma cells under acidic stress. J Biol Chem. 2012;287(36):30664-76.

211. Berezhnov AV, Soutar MP, Fedotova EI, Frolova MS, Plun-Favreau H, Zinchenko VP, et al. Intracellular pH Modulates Autophagy and Mitophagy. J Biol Chem. 2016;291(16):8701-8.

212. Niu H, Xiong Q, Yamamoto A, Hayashi-Nishino M, Rikihisa Y. Autophagosomes induced by a bacterial Beclin 1 binding protein facilitate obligatory intracellular infection. PNAS. 2012;109(51):20800-7.

213. Moreau K, Lacas-Gervais S, Fujita N, Sebbane F, Yoshimori T, Simonet M, et al. Autophagosomes can support Yersinia pseudotuberculosis replication in macrophages. Cell Microbiol. 2010;12(8):1108-23.

214. Gutierrez MG, Vazquez CL, Munafo DB, Zoppino FC, Beron W, Rabinovitch M, et al. Autophagy induction favours the generation and maturation of the Coxiella-replicative vacuoles. Cell Microbiol. 2005;7(7):981-93.

215. Vazquez CL, Colombo MI. Coxiella burnetii modulates Beclin 1 and Bcl-2, preventing host cell apoptosis to generate a persistent bacterial infection. Cell Death Differ. 2010;17(3):421-38.

216. Pujol C, Klein KA, Romanov GA, Palmer LE, Cirota C, Zhao Z, et al. Yersinia pestis can reside in autophagosomes and avoid xenophagy in murine macrophages by preventing vacuole acidification. Infect Immun. 2009;77(6):2251-61.

217. Starr T, Child R, Wehrly TD, Hansen B, Hwang S, Lopez-Otin C, et al. Selective subversion of autophagy complexes facilitates completion of the Brucella intracellular cycle. Cell Host Microbe. 2012;11(1):33-45.

218. Amer AO, Swanson MS. Autophagy is an immediate macrophage response to Legionella pneumophila. Cell Microbiol. 2005;7(6):765-78.

219. Kagan JC, Roy CR. Legionella phagosomes intercept vesicular traffic from endoplasmic reticulum exit sites. Nat Cell Biol. 2002;4(12):945-54.

220. Mestre MB, Fader CM, Sola C, Colombo MI. Alpha-hemolysin is required for the activation of the autophagic pathway in Staphylococcus aureus-infected cells. Autophagy. 2010;6(1):110-25.

221. Mestre MB, Colombo MI. cAMP and EPAC Are Key Players in the Regulation of the Signal Transduction Pathway Involved in the α-Hemolysin Autophagic Response. PLoS Pathog. 2012;8(5):e1002664.

222. Wang Y, Weiss LM, Orlofsky A. Host cell autophagy is induced by Toxoplasma gondii and contributes to parasite growth. J Biol Chem. 2009;284(3):1694-701.

223. Lee YR, Lei HY, Liu MT, Wang JR, Chen SH, Jiang-Shieh YF, et al. Autophagic machinery activated by dengue virus enhances virus replication. Virology. 2008;374(2):240-8.

224. Prentice E, Jerome WG, Yoshimori T, Mizushima N, Denison MR. Coronavirus replication complex formation utilizes components of cellular autophagy. J Biol Chem. 2004;279(11):10136-41.

225. Jackson WT, Giddings TH, Jr., Taylor MP, Mulinyawe S, Rabinovitch M, Kopito RR, et al. Subversion of Cellular Autophagosomal Machinery by RNA Viruses. PLoS Biol. 2005;3(5):e156.

226. Le Clec'h W, Braquart-Varnier C, Raimond M, Ferdy J-B, Bouchon D, Sicard M. High Virulence of Wolbachia after Host Switching: When Autophagy Hurts. PLoS Pathog. 2012;8(8):e1002844.

227. Fleming A, Noda T, Yoshimori T, Rubinsztein DC. Chemical modulators of autophagy as biological probes and potential therapeutics. Nat Chem Biol. 2011;7(1):9-17.

228. Thoreen CC, Kang SA, Chang JW, Liu Q, Zhang J, Gao Y, et al. An ATP-competitive mammalian target of rapamycin inhibitor reveals rapamycin-resistant functions of mTORC1. J Biol Chem. 2009;284(12):8023-32.

229. Renna M, Jimenez-Sanchez M, Sarkar S, Rubinsztein DC. Chemical inducers of autophagy that enhance the clearance of mutant proteins in neurodegenerative diseases. J Biol Chem. 2010;285(15):11061-7.

230. Balgi AD, Fonseca BD, Donohue E, Tsang TC, Lajoie P, Proud CG, et al. Screen for chemical modulators of autophagy reveals novel therapeutic inhibitors of mTORC1 signaling. PLoS One. 2009;4(9):e7124.

231. Williams RS, Cheng L, Mudge AW, Harwood AJ. A common mechanism of action for three mood-stabilizing drugs. Nature. 2002;417(6886):292-5.

232. Sarkar S, Floto RA, Berger Z, Imarisio S, Cordenier A, Pasco M, et al. Lithium induces autophagy by inhibiting inositol monophosphatase. J Cell Biol. 2005;170(7):1101-11.

233. Shaltiel G, Shamir A, Shapiro J, Ding D, Dalton E, Bialer M, et al. Valproate decreases inositol biosynthesis. Biol Psychiatry. 2004;56(11):868-74.

234. Williams A, Sarkar S, Cuddon P, Ttofi EK, Saiki S, Siddiqi FH, et al. Novel targets for Huntington's disease in an mTOR-independent autophagy pathway. Nat Chem Biol. 2008;4(5):295-305.

235. Kim JJ, Lee HM, Shin DM, Kim W, Yuk JM, Jin HS, et al. Host cell autophagy activated by antibiotics is required for their effective antimycobacterial drug action. Cell Host Microbe. 2012;11(5):457-68.

236. Liang Y, Zhou T, Chen Y, Lin D, Jing X, Peng S, et al. Rifampicin inhibits rotenone-induced microglial inflammation via enhancement of autophagy. Neurotoxicology. 2017;63:137-45.

237. Piccaro G, Pietraforte D, Giannoni F, Mustazzolu A, Fattorini L. Rifampin induces hydroxyl radical formation in Mycobacterium tuberculosis. Antimicrob Agents Chemother. 2014;58(12):7527-33.

238. Tang C, Yang L, Jiang X, Xu C, Wang M, Wang Q, et al. Antibiotic drug tigecycline inhibited cell proliferation and induced autophagy in gastric cancer cells. Biochem Biophys Res Commun. 2014;446(1):105-12.

239. Zhang E, Zhao X, Zhang L, Li N, Yan J, Tu K, et al. Minocycline promotes cardiomyocyte mitochondrial autophagy and cardiomyocyte autophagy to prevent sepsis-induced cardiac dysfunction by Akt/mTOR signaling. Apoptosis. 2019;24(3-4):369-81.

240. Zhang L, Huang P, Chen H, Tan W, Lu J, Liu W, et al. The inhibitory effect of minocycline on radiation-induced neuronal apoptosis via AMPKα1 signaling-mediated autophagy. Sci Rep. 2017;7(1):16373-.

241. Dong W, Xiao S, Cheng M, Ye X, Zheng G. Minocycline induces protective autophagy in vascular endothelial cells exposed to an in vitro model of ischemia/reperfusion-induced injury. Biomed Rep. 2016;4(2):173-7.

242. Wu Z, Zou X, Zhu W, Mao Y, Chen L, Zhao F. Minocycline is effective in intracerebral hemorrhage by inhibition of apoptosis and autophagy. J Neurol Sci. 2016;371:88-95.

243. Desjarlais M, Pratt J, Lounis A, Mounier C, Haidara K, Annabi B. Tetracycline derivative minocycline inhibits autophagy and inflammation in concanavalin-a-activated human hepatoma cells. Gene Regul Syst Bio. 2014;8:63-73.

244. Xing Y, Liqi Z, Jian L, Qinghua Y, Qian Y. Doxycycline Induces Mitophagy and Suppresses Production of Interferon-beta in IPEC-J2 Cells. Front Cell Infect Microbiol. 2017;7:21.

245. Bruning A, Brem GJ, Vogel M, Mylonas I. Tetracyclines cause cell stress-dependent ATF4 activation and mTOR inhibition. Exp Cell Res. 2014;320(2):281-9.

246. Kim TS, Shin Y-H, Lee H-M, Kim JK, Choe JH, Jang J-C, et al. Ohmyungsamycins promote antimicrobial responses through autophagy activation via AMP-activated protein kinase pathway. Sci Rep. 2017;7(1):3431-.

247. Li J, Kim SG, Blenis J. Rapamycin: one drug, many effects. Cell Metab. 2014;19(3):373-9.

248. Shor B, Zhang W-G, Toral-Barza L, Lucas J, Abraham RT, Gibbons JJ, et al. A New Pharmacologic Action of CCI-779 Involves FKBP12-Independent Inhibition of mTOR Kinase Activity and Profound Repression of Global Protein Synthesis. Cancer Res. 2008;68(8):2934-43.

249. Floto RA, Sarkar S, Perlstein EO, Kampmann B, Schreiber SL, Rubinsztein DC. Small molecule enhancers of rapamycin-induced TOR inhibition promote autophagy, reduce toxicity in Huntington's disease models and enhance killing of mycobacteria by macrophages. Autophagy. 2007;3(6):620-2.

250. Hermans PG, Hart CA, Trees AJ. In vitro activity of antimicrobial agents against the endosymbiont Wolbachia pipientis. J Antimicrob Chemother. 2001;47(5):659-63.

251. Johnston KL, Ford L, Umareddy I, Townson S, Specht S, Pfarr K, et al. Repurposing of approved drugs from the human pharmacopoeia to target Wolbachia endosymbionts of onchocerciasis and lymphatic filariasis. Int J Parasitol Drugs Drug Resist. 2014;4(3):278-86.

252. Hoerauf A, Volkmann L, Nissen-Paehle K, Schmetz C, Autenrieth I, Buttner DW, et al. Targeting of Wolbachia endobacteria in Litomosoides sigmodontis: comparison of tetracyclines with chloramphenicol, macrolides and ciprofloxacin. Trop Med Int Health. 2000;5(4):275-9.

253. Fenollar F, Maurin M, Raoult D. Wolbachia pipientis growth kinetics and susceptibilities to 13 antibiotics determined by immunofluorescence staining and real-time PCR. Antimicrob Agents Chemother. 2003;47(5):1665-71.

254. Nighot PK, Hu CA, Ma TY. Autophagy enhances intestinal epithelial tight junction barrier function by targeting claudin-2 protein degradation. J Biol Chem. 2015;290(11):7234-46.

255. Gerszten RE, Friedrich EB, Matsui T, Hung RR, Li L, Force T, et al. Role of phosphoinositide 3-kinase in monocyte recruitment under flow conditions. J Biol Chem. 2001;276(29):26846-51.

256. Jiang Y, Kou J, Han X, Li X, Zhong Z, Liu Z, et al. ROS-Dependent Activation of Autophagy through the PI3K/Akt/mTOR Pathway Is Induced by Hydroxysafflor Yellow A-Sonodynamic Therapy in THP-1 Macrophages. Oxid Med Cell Longev. 2017;2017:8519169.

257. Yang M, Hao Y, Gao J, Zhang Y, Xu W, Tao L. Spinosad induces autophagy of Spodoptera frugiperda Sf9 cells and the activation of AMPK/mTOR signaling pathway. Comp Biochem Physiol C Toxicol Pharmacol. 2017;195:52-9.

258. Griffiths KG, Alworth LC, Harvey SB, Michalski ML. Using an intravenous catheter to carry out abdominal lavage in the gerbil. Lab Anim (NY). 2010;39(5):143-8.

259. Xiao Y, Xiong T, Meng X, Yu D, Xiao Z, Song L. Different influences on mitochondrial function, oxidative stress and cytotoxicity of antibiotics on primary human neuron and cell lines. J Biochem Mol Toxicol. 2018:e22277.

260. Kohanski MA, Dwyer DJ, Collins JJ. How antibiotics kill bacteria: from targets to networks. Nat Rev Microbiol. 2010;8(6):423-35.

261. Centres for Disease Control and Prevention. Biology - Life Cycle of Brugia malayi 2018 [Available from: https://www.cdc.gov/parasites/lymphaticfilariasis/biology_b_malayi.html (accessed on 14 April 2019).

262. Slatko BE, Luck AN, Dobson SL, Foster JM. Wolbachia endosymbionts and human disease control. Mol Biochem Parasitol. 2014;195(2):88-95.

263. Dobson SL, Marsland EJ, Rattanadechakul W. Mutualistic Wolbachia infection in Aedes albopictus: accelerating cytoplasmic drive. Genetics. 2002;160(3):1087-94.

264. Fenn K, Blaxter M. Quantification of Wolbachia bacteria in Brugia malayi through the nematode lifecycle. Mol Biochem Parasitol. 2004;137(2):361-4.

265. Anti-Wolbachia consortium. Why anti-Wolbachia 2019 [Available from: https://awol.lstmed.ac.uk/why-anti-wolbachia (accessed on 29 April 2019).

266. Johnston KL, Wu B, Guimaraes A, Ford L, Slatko BE, Taylor MJ. Lipoprotein biosynthesis as a target for anti-Wolbachia treatment of filarial nematodes. Parasit Vectors. 2010;3:99.

267. Comley JC, Rees MJ, Turner CH, Jenkins DC. Colorimetric quantitation of filarial viability. Int J Parasitol. 1989;19(1):77-83.

268. Comley JC, Townson S, Rees MJ, Dobinson A. The further application of MTT-formazan colorimetry to studies on filarial worm viability. Trop Med Parasitol. 1989;40(3):311-6.

269. Ghedin E, Hailemariam T, DePasse JV, Zhang X, Oksov Y, Unnasch TR, et al. Brugia malayi gene expression in response to the targeting of the Wolbachia endosymbiont by tetracycline treatment. PLoS Negl Trop Dis. 2009;3(10):e525.

270. Livak KJ, Schmittgen TD. Analysis of relative gene expression data using real-time quantitative PCR and the 2(-Delta Delta C(T)) Method. Methods. 2001;25(4):402-8.

271. Clare RH, Bardelle C, Harper P, Hong WD, Börjesson U, Johnston KL, et al. Industrial scale high-throughput screening delivers multiple fast acting macrofilaricides. Nat Commun. 2019;10(1):11.

272. Marriott A. The reduction, refinement and replacement of animals in anti-filarial drug research. Supervised by Joseph Turner and Mark Taylor [PhD Dissertation - Unpublished]. UK: Liverpool School of Tropical Medicine 2019.

273. Ballesteros C, Tritten L, O'Neill M, Burkman E, Zaky WI, Xia J, et al. The Effect of In Vitro Cultivation on the Transcriptome of Adult Brugia malayi. PLoS Negl Trop Dis. 2016;10(1):e0004311.

274. Njouendou AJ, Ritter M, Ndongmo WPC, Kien CA, Narcisse GTV, Fombad FF, et al. Successful long-term maintenance of Mansonella perstans in an in vitro culture system. Parasit Vectors. 2017;10(1):563.

275. Tato I, Bartrons R, Ventura F, Rosa JL. Amino acids activate mammalian target of rapamycin complex 2 (mTORC2) via PI3K/Akt signaling. J Biol Chem. 2011;286(8):6128-42.

276. Nicklin P, Bergman P, Zhang B, Triantafellow E, Wang H, Nyfeler B, et al. Bidirectional transport of amino acids regulates mTOR and autophagy. Cell. 2009;136(3):521-34.

277. Chen Y, Scarcelli V, Legouis R. Approaches for Studying Autophagy in Caenorhabditis elegans. Cells. 2017;6(3):27.

278. Palmisano NJ, Meléndez A. Autophagy in C. elegans development. Dev Biol. 2019;447(1):103-25.

279. Zhang H, Chang JT, Guo B, Hansen M, Jia K, Kovács AL, et al. Guidelines for monitoring autophagy in Caenorhabditis elegans. Autophagy. 2015;11(1):9-27.

280. Coppens I. Metamorphoses of malaria: the role of autophagy in parasite differentiation. Essays Biochem. 2011;51:127-36.

281. Cervantes S, Bunnik EM, Saraf A, Conner CM, Escalante A, Sardiu ME, et al. The multifunctional autophagy pathway in the human malaria parasite, Plasmodium falciparum. Autophagy. 2014;10(1):80-92.

282. Nezis IP. Selective Autophagy in Drosophila. Int J Cell Biol. 2012;2012:9.

283. Noda H, Miyoshi T, Koizumi Y. In Vitro Cultivation of Wolbachia in Insect and Mammalian Cell Lines. In Vitro Cell Dev Biol Anim. 2002(7):423.

284. Subramani S, Malhotra V. Non-autophagic roles of autophagy-related proteins. EMBO reports. 2013;14(2):143-51.

285. Eskelinen E-L, Reggiori F, Baba M, Kovács AL, Seglen PO. Seeing is believing: The impact of electron microscopy on autophagy research. Autophagy. 2011;7(9):935-56.

286. Biazik J, Vihinen H, Jokitalo E, Eskelinen EL. Ultrastructural Characterization of Phagophores Using Electron Tomography on Cryoimmobilized and Freeze Substituted Samples. Methods Enzymol. 2017;587:331-49.

287. National Center for Biotechnology Information. PubChem - Compound summary 2019 [Available from: https://pubchem.ncbi.nlm.nih.gov/ (accessed on 19 Sep 2019).

288. Vodicka P, Lim J, Williams DT, Kegel KB, Chase K, Park H, et al. Assessment of chloroquine treatment for modulating autophagy flux in brain of WT and HD mice. J Huntingtons Dis. 2014;3(2):159-74.

289. Esteban-Martinez L, Boya P. Autophagic flux determination in vivo and ex vivo. Methods. 2015;75:79-86.

290. Moulis M, Vindis C. Methods for Measuring Autophagy in Mice. Cells. 2017;6(2):14.

291. Mizushima N. Methods for monitoring autophagy using GFP-LC3 transgenic mice. Methods Enzymol. 2009;452:13-23.

292. Deretic V. Autophagy in tuberculosis. Cold Spring Harb Perspect Med. 2014;4(11):a018481.

293. Jo EK. Autophagy as an innate defense against mycobacteria. Pathog Dis. 2013;67(2):108-18.

294. Al-Zeer MA, Al-Younes HM, Lauster D, Abu Lubad M, Meyer TF. Autophagy restricts Chlamydia trachomatis growth in human macrophages via IFNG-inducible guanylate binding proteins. Autophagy. 2013;9(1):50-62.

295. Yang S, Traore Y, Jimenez C, Ho EA. Autophagy induction and PDGFR-β knockdown by siRNA-encapsulated nanoparticles reduce chlamydia trachomatis infection. Sci Rep. 2019;9(1):1306.

296. Schmuckli-Maurer J, Reber V, Wacker R, Bindschedler A, Zakher A, Heussler VT. Inverted recruitment of autophagy proteins to the Plasmodium berghei parasitophorous vacuole membrane. PLoS One. 2017;12(8):e0183797.

297. Evans RJ, Sundaramurthy V, Frickel E-M. The Interplay of Host Autophagy and Eukaryotic Pathogens. Front Cell Dev Biol. 2018;6:118-.

298. Subauste CS. Interplay Between Toxoplasma gondii, Autophagy, and Autophagy Proteins. Front Cell Infect Microbiol. 2019;9(139).

299. Sébastien B. The role of host autophagy machinery in controlling Toxoplasma infection. Virulence. 2018(0):1.

300. Dias BRS, de Souza CS, Almeida NdJ, Lima JGB, Fukutani KF, dos Santos TBS, et al. Autophagic Induction Greatly Enhances Leishmania major Intracellular Survival Compared to Leishmania amazonensis in CBA/j-Infected Macrophages. Front Microbiol. 2018;9(1890).

301. Pitale DM, Gendalur NS, Descoteaux A, Shaha C. Leishmania donovani Induces Autophagy in Human Blood–Derived Neutrophils. J Immunol. 2019:ji1801053.

# Appendix A

| Chemical compound | Dose | Day 0 (%) | Day 2 (%) | Day 4 (%) | Day 6 (%) | Day 8 (%) | Growth effect |
|---|---|---|---|---|---|---|---|
| 3-MA | 1mM | 8.3 | 2.8 (↑) | 5.3 (↑) | 15.6 | 37.6 | |
| | 2mM | 0.3 | 16.9 | 0.4 (↑) | 41.7 | 58.8 | |
| | 3mM | 15.6 | 8.8 | 0.7 | 43.7 | 59.7 | |
| | 4mM | 2.6 (↑) | 27.5 | 3.6 | 52.5 | 65.1 | |
| | 5mM | 24 | 36.4 | 9.5 | 51.8 | 64.8 | |
| LY294002 | 1µM | 9.1 (↑) | 30.6 | 0. 8 | 1.0 (↑) | 16.6 | |
| | 2µM | 8.8 (↑) | 50 | 4.8 | 3.7 | 17 | |
| | 3µM | 7.98 | 46.1 | 7.9 | 39.7 | 54.4 | |
| | 4µM | 11.97 (↑) | 47.7 | 8 | 41.8 | 54.4 | |
| | 5µM | 4.4 (↑) | 26.9 | 16.1 | 38.9 | 56.5 | |
| | 10µM | 7.98 | 3.5 (↑) | 27.4 | 46.5 | 63 | |
| | 15µM | 11.97 (↑) | 7.2 (↑) | 36.7 | 54.5 | 65.8 | |
| | 20µM | 17.1 | 58.5 | 52.1 | 63.3 | 69 | |
| Wortmannin | 1µM | 4.15 | 1.8 | 13.9 (↑) | 4.6 (↑) | 10 | |
| | 5µM | 8.2 | 3.8 | 4.5 | 33.1 | 10.9 | |
| | 10µM | 8.3 | 15.2 | 19.4 | 4.7 | 10.3 | |
| | 15µM | 1.6 | 2.8 | 4.1 | 2.5 (↑) | 13.1 | |
| | 20µM | 27.2 | 2.9 | 6.4 | 3.1 (↑) | 13.5 | |
| L-Asparagine | 1mM | 5.5 | 23.2 | 27.8 | 6 | 5.2 | |
| | 5mM | 6 | 31.2 | 20.4 | 9.7 | 14 | |
| | 10mM | 8.3 | 26.7 | 19.4 | 4.7 | 10 | |
| | 15mM | 0.8 (↑) | 17.8 | 21.2 | 9.4 | 17.2 | |
| | 20mM | 7.6 | 16.3 | 25.3 | 12.1 | 12.7 | |

**Table A 1 Impact of selected autophagy inhibitors on C6/36*Wp* cell growth inhibition.** C6/36 mosquito cell line infected with *Wolbachia* (*w*AlbB) dynamic growth profile after treatment with chemical autophagy inhibitors at selected concentrations for set-time points (at day 0, 2, 4, 6 and 8) expressed as percentages in reduction of cell growth to DMSO treated cells. An upward arrow indicates an increase in percentage. For cell growth effect, green represents compounds with no measurable effect on cell growth and red indicates compounds with an effect of more than 50% reduction of cell growth compared to DMSO control.

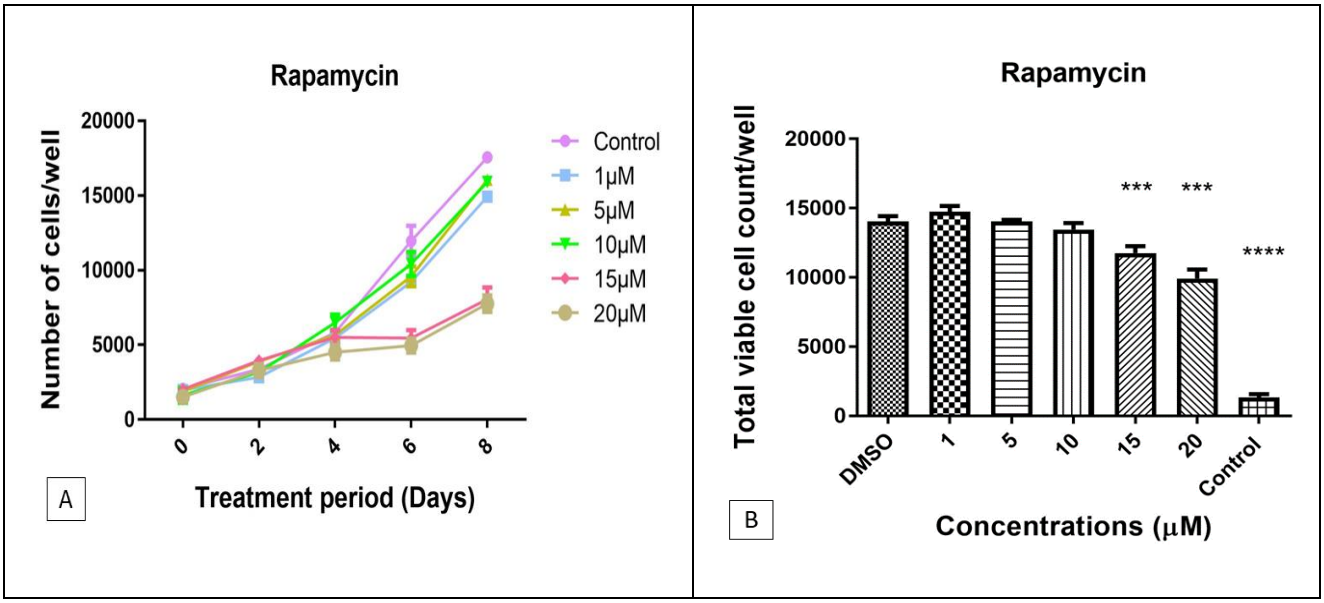


**Figure A 1 Rapamycin safety profile testing on C6/36*Wp* cell line.** Infected C6/36 cells with *w*AlbB were treated with rapamycin at different concentrations (1-20 µM) for 8 days. **A)** Total number of cells/well were measured every two days (at day 0, 2, 4, 6 and 8) using Operetta. Suitability of rapamycin concentration was considered if its effect on cell proliferation was less than 50% reduction compared to control (DMSO treated cells). Rapamycin between 1-10 µM did not affect cell growth and were found to be suitable. **B)** Total number of viable cells were stained with calcein AM and measured at day 8 using Operetta. Saponin was used as a control, expressing the presence of dead cells. Rapamycin between 1-10 µM were found to be viable and no difference was observed compared to the control.

Graphs (mean with SD) represent **A)** total number of cells and **B)** total viable cell count in four biological repeats for every treatment group. Cell viability/cytotoxicity was assessed by comparing with DMSO control using Student's t-test, where statistical significance was $p \leq 0.05$. For p-value * = 0.01 to 0.05, ** = 0.01 to 0.001, *** = 0.001 to 0.0001, and **** ≤ 0.0001.

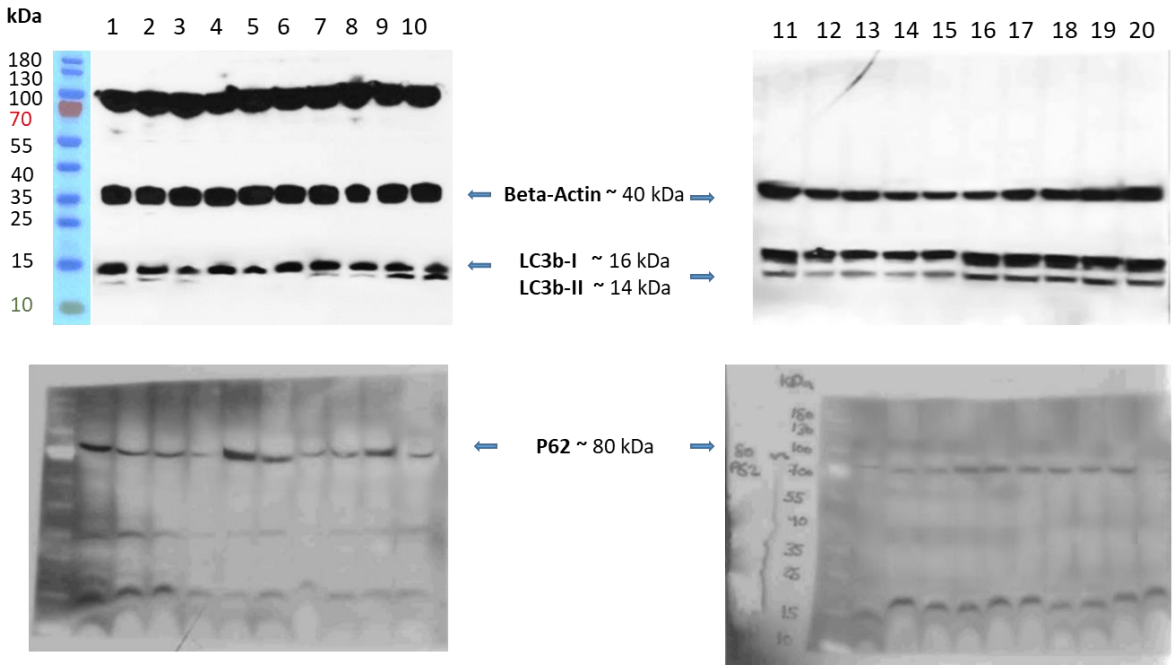


**Figure A 2 Full membrane blots for C6/36*Wp* against LC3B and p62 markers of autophagy.** C6/36 cells infected with *w*AlbB treated with selected autophagy inhibitors at different concentrations alone or combined with rapamycin. **Lane 1:** DMSO, **lane 2:** ly294002 at 1 µM, **lane 3-6:** wortmannin from 1-20 µM, **lane 7-10:** l-asparagine from 1-20 mM, a combination of rapamycin and **lane 11:** ly294002 at 1 µM, **lane 12-15:** wortmannin from 1-20 µM, **lane 16-19:** l-asparagine from 1-20 mM, and **lane 20:** rapamycin alone.

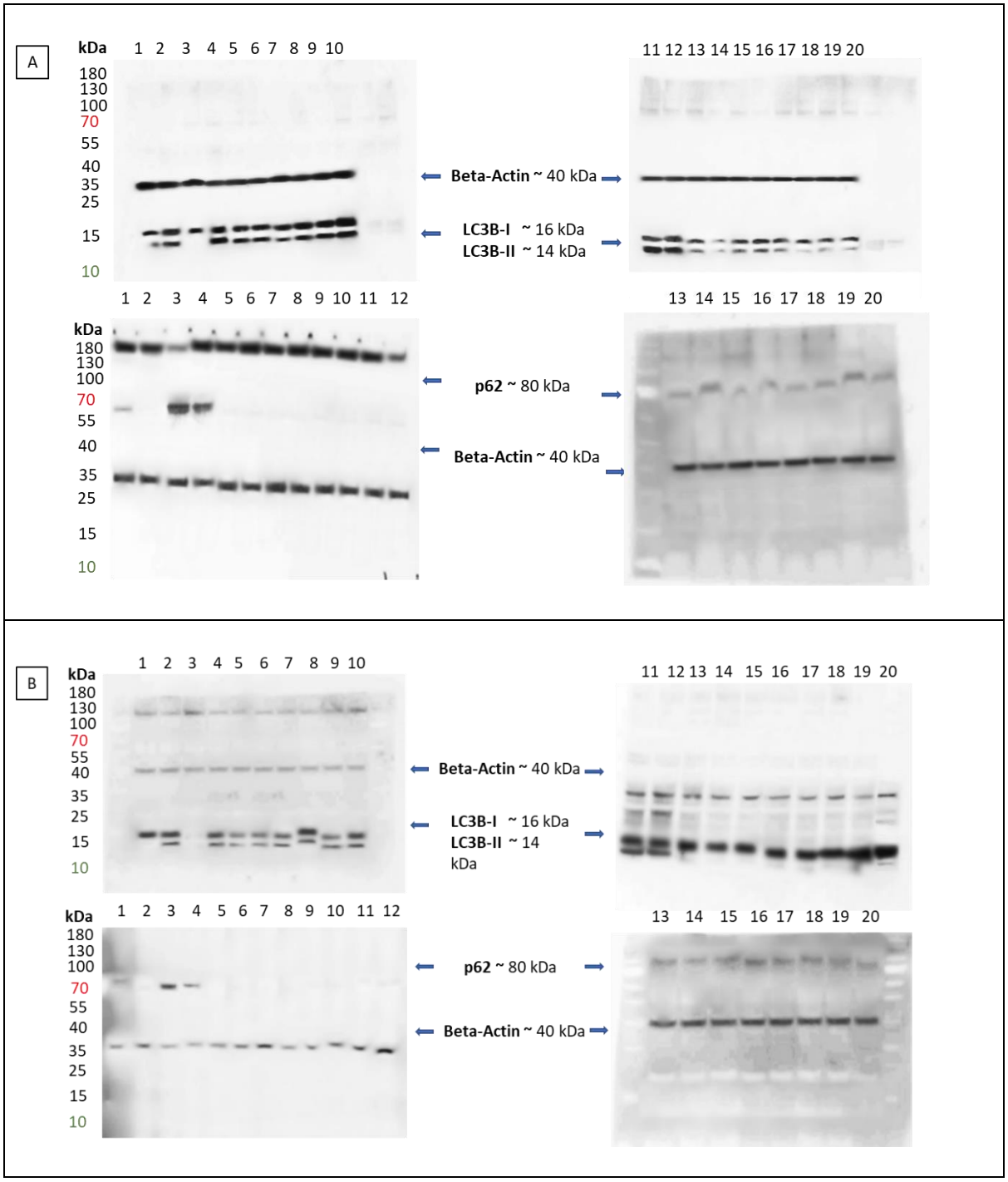


**Figure A 3 Full membrane blots for C6/36*Wp* against LC3B and p62 markers of autophagy in different antibiotics.** C6/36 **A)** infected with wAlbB and **B)** *Wolbachia*-free cells treated with DMSO – vehicle control (lane 1), rapamycin – positive control (lane 2), wortmannin – early autophagy inhibitor (lane 3), l-asparagine – late autophagy inhibitor (lane 4), four anti-*Wolbachia* agents: doxycycline (lane 5-6), rifampicin (lane 7-8), moxifloxacin (lane 9-10), sparfloxacin (lane 11-12), and four different antibiotics: levofloxacin (lane 13-14), ciprofloxacin (lane 15-16), amoxicillin (lane 17-18), and streptomycin (lane 19-20) for 3 days.

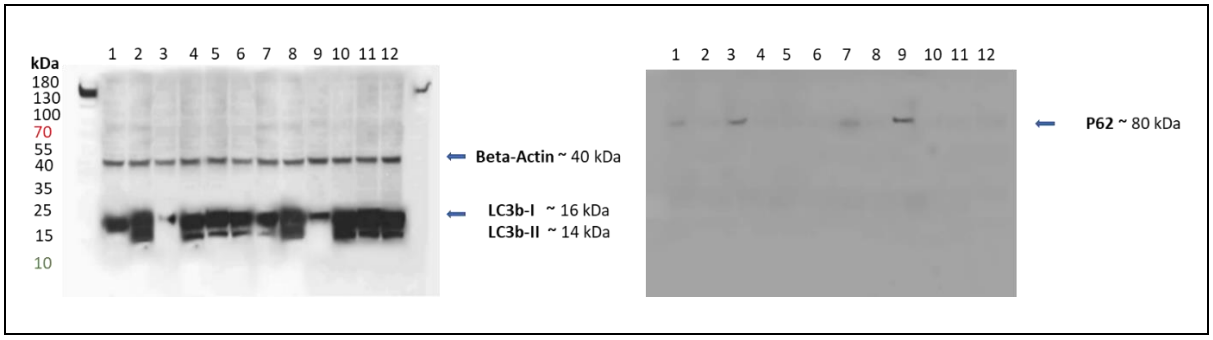


**Figure A 4 Full membrane blots for C6/36 cells against LC3B and p62 markers of autophagy in pre-clinical candidates and re-purposed antibiotic from the A-WOL consortium.** *Wolbachia*-free C6/36 (lane 1-6) and infected C6/36*Wp* cells (lane 7-12) were treated with: DMSO – vehicle control (lane 1 and 7), rapamycin – positive control (lane 2 and 8), wortmannin – autophagy inhibitor (lane 3 and 9), TylAMac$^{TM}$ (lane 4 and 10), fusidic acid (lane 5 and 11), and AWZ1066S (lane 6 and 12) for 3 days.

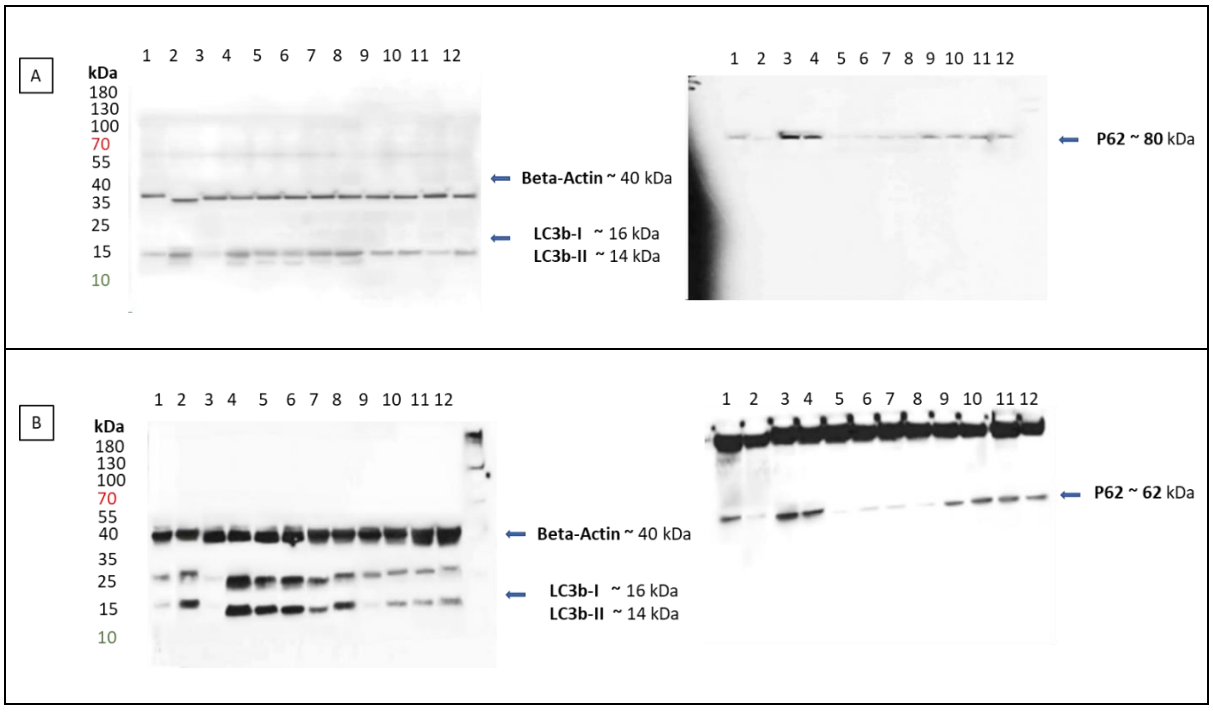


**Figure A 5 Full membrane blots for SF9 and *B.malayi* worms against LC3B and p62 markers of autophagy in different antibiotics. A)** SF9 insect cells and **B)** *B. malayi* mf worms were treated with: DMSO – vehicle control (lane 1), rapamycin – positive control (lane 2), wortmannin – early autophagy inhibitor (lane 3), l-asparagine – late autophagy inhibitor (lane 4), four anti-*Wolbachia* agents: doxycycline (lane 5), rifampicin (lane 6), moxifloxacin (lane 7), sparfloxacin (lane 8), and four different antibiotics: levofloxacin (lane 9), ciprofloxacin (lane 10), amoxicillin (lane 11), and streptomycin (lane 12) for 3 days.

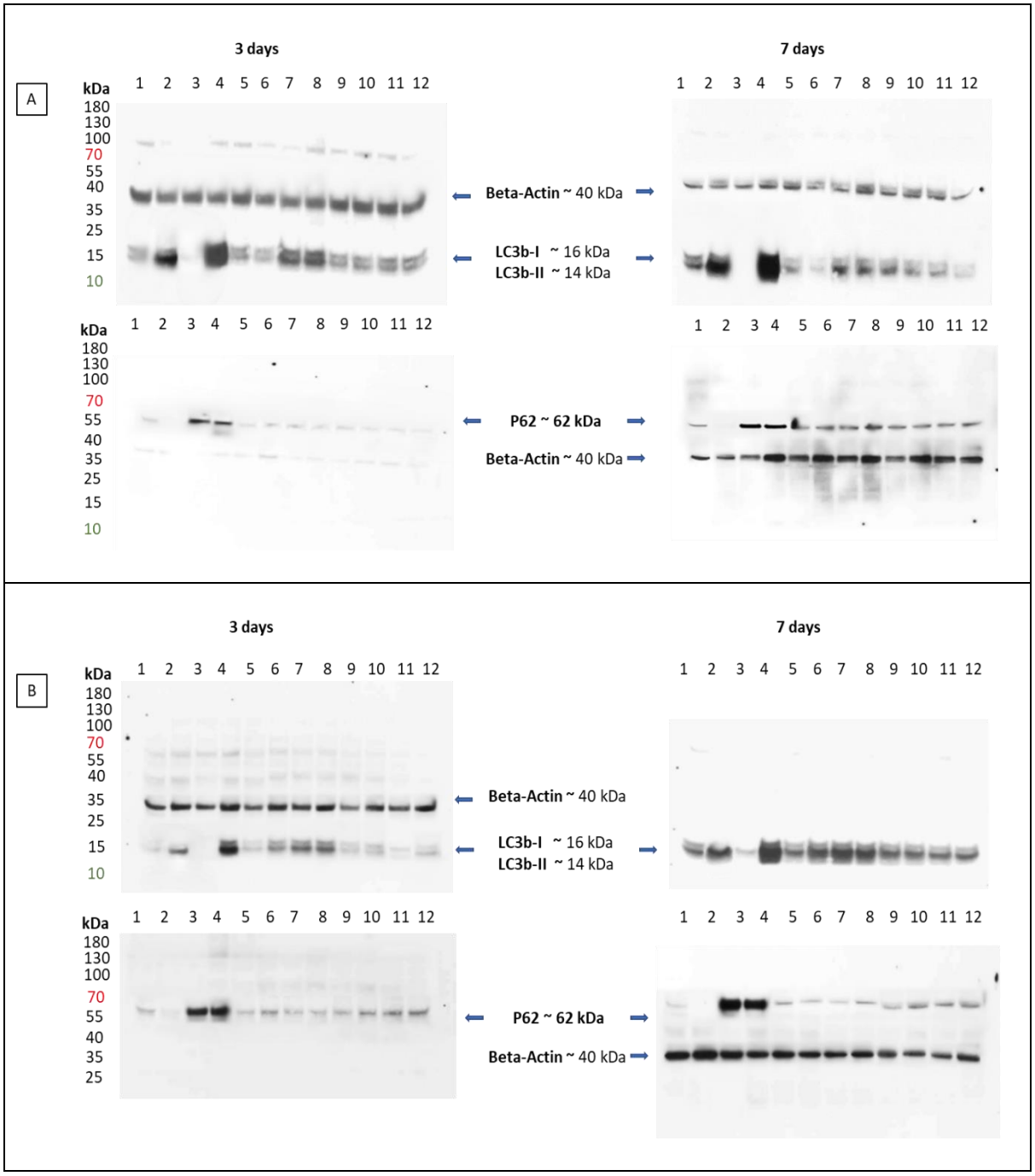


**Figure A 6 Full membrane blots for THP-1 and MDCK cells against LC3B and p62/SQSTM-1 markers of autophagy in different antibiotics. A)** THP-1 and **B)** MDCK cells were treated with: DMSO – vehicle control (lane 1), rapamycin – positive control (lane 2), wortmannin – early autophagy inhibitor (lane 3), l-asparagine – late autophagy inhibitor (lane 4), four anti-*Wolbachia* agents: doxycycline (lane 5), rifampicin (lane 6), moxifloxacin (lane 7), sparfloxacin (lane 8), and four different antibiotics: levofloxacin (lane 9), ciprofloxacin (lane 10), amoxicillin (lane 11), and streptomycin (lane 12) for 3 and 7 days.

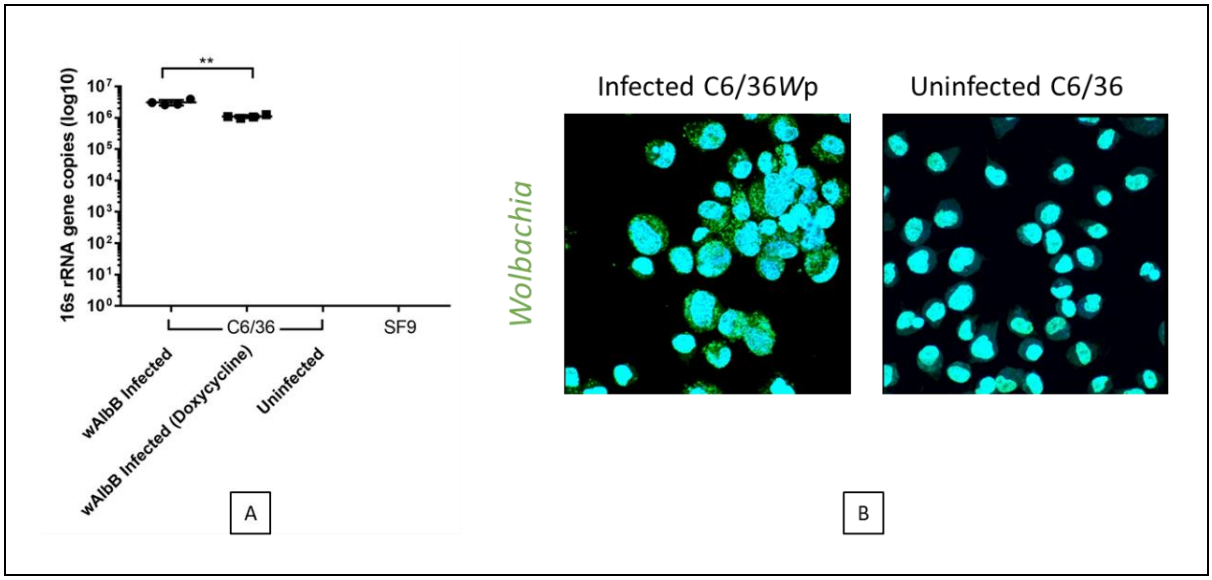


**Figure A 7 Detection of *Wolbachia* in insect cells. A)** using qPCR analysis, DNA extracted from C6/36 (infected and uninfected with *w*AlbB) and SF9 cells were amplified using *Wolbachia 16s* rRNA gene using the following thermal cycling conditions: 15 minutes at 95˚C, 35 cycles, for 15 seconds at 94˚C, 30 seconds at 55˚C, 15 seconds at 72˚C and a melting curve between 50-95˚C. Four biological repeats per treatment group were analysed. Statistical significance tested using Student's t-test, statistical significance was at $p \leq 0.05$. For p-value * = 0.01 to 0.05, ** = 0.01 to 0.001, *** = 0.001 to 0.0001, and **** ≤ 0.0001.

**B)** Confocal images of C6/36 cells (infected and uninfected with *w*AlbB) stained with syto11 (green fluorescence puncta) to detect *Wolbachia* infection.

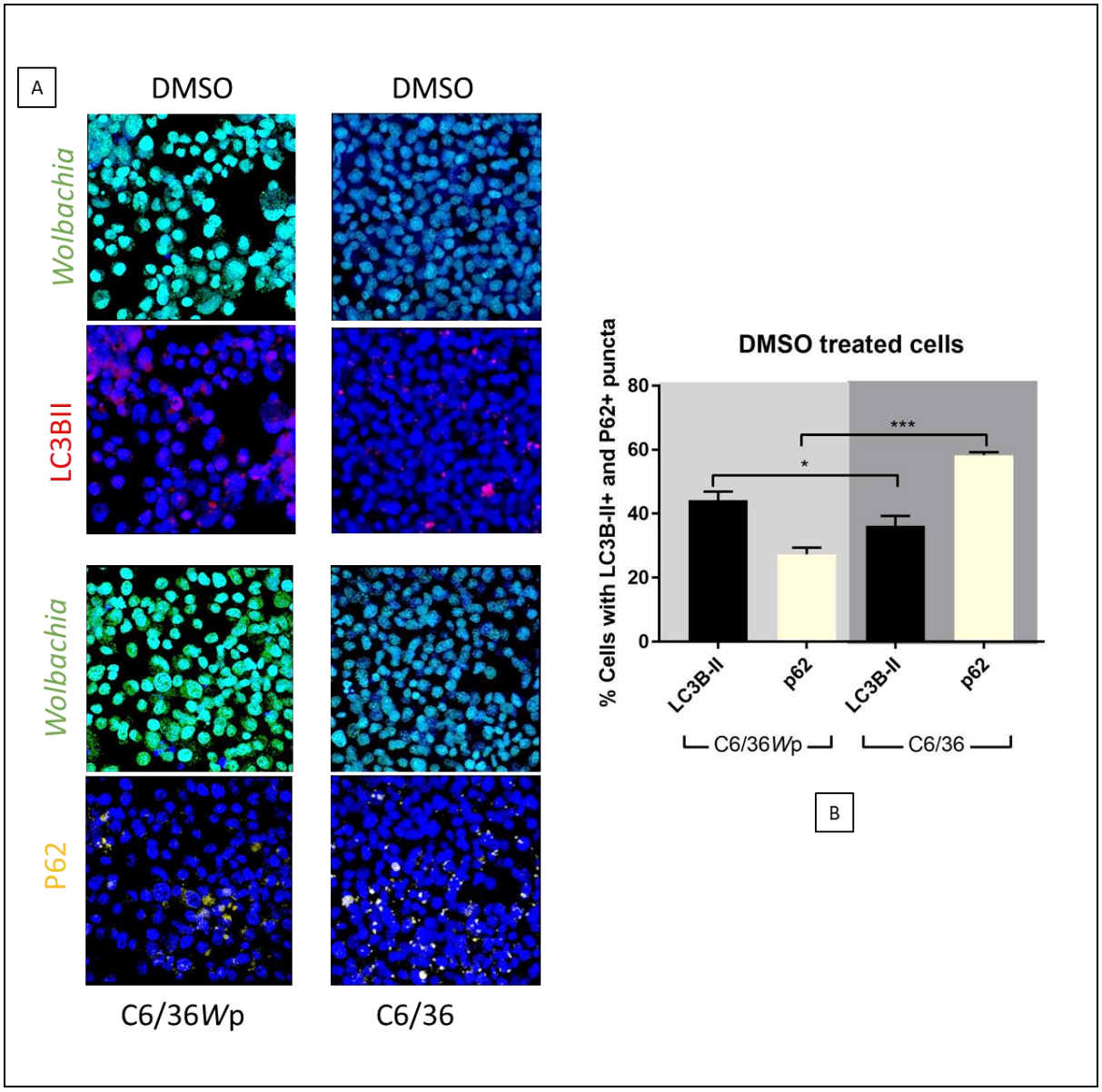


**Figure A 8 Comparison in autophagic induction of C6/36 cells uninfected and infected with *w*AlbB using two autophagic markers LC3B-II and p62.** Using immunofluorescence staining assay **A)** confocal images of LC3B-II and p62 expression in cells treated with DMSO. **B)** Quantification analysis of the two autophagic markers expressed in percentages of LC3B-II and p62 puncta/cell. For each treatment group, three different sections were imaged, where each section contained ≥50 cells.

Statistical significance tested using Student's t-test, statistical significance was at $p \leq 0.05$. For p-value * = 0.01 to 0.05, ** = 0.01 to 0.001, *** = 0.001 to 0.0001, and **** ≤ 0.0001.

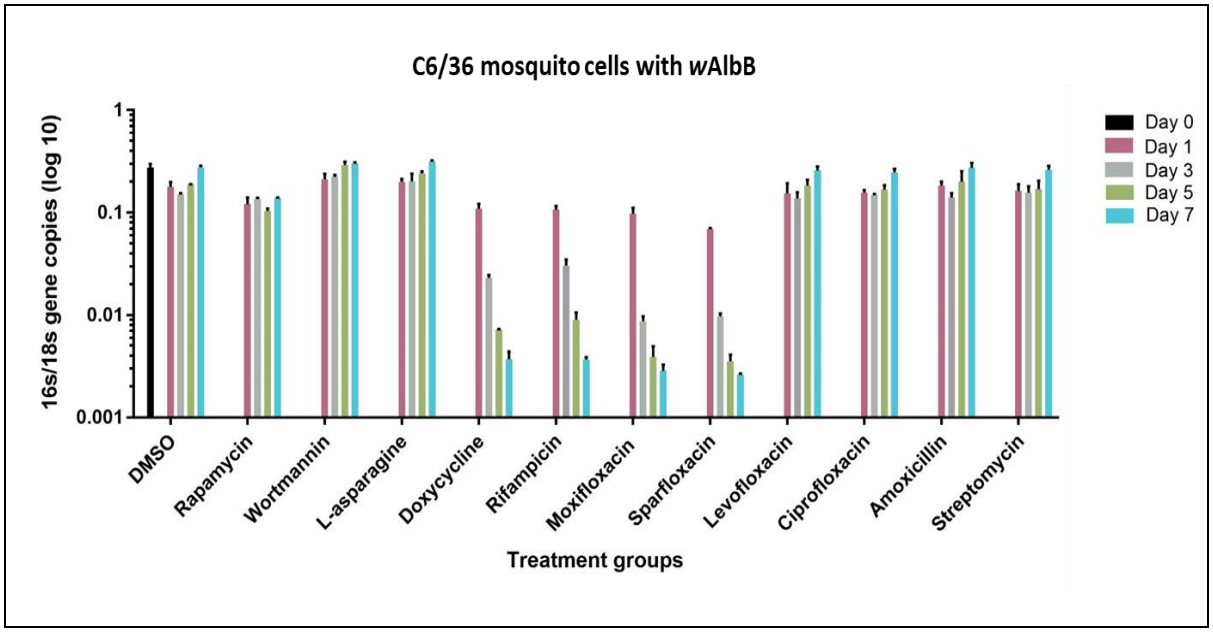


**Figure A 9 qPCR analysis of *Wolbachia* load in antibiotics at different time-points.** C6/36*Wp* cells were treated at different time-points: day 0, 1, 3, 5 and 7 with DMSO (vehicle control), rapamycin at 5 µM (autophagy inducer), wortmannin at 10 µM (autophagy inhibitor), four anti-*Wolbachia* agents at 5 µM: doxycycline, rifampicin, moxifloxacin and sparfloxacin and four other antibiotics at 5 µM: levofloxacin, ciprofloxacin, amoxicillin and streptomycin. *Wolbachia* load is expressed as a ratio of *16s:18s* rRNA gene in log10. Three biological repeats per treatment group were analysed.

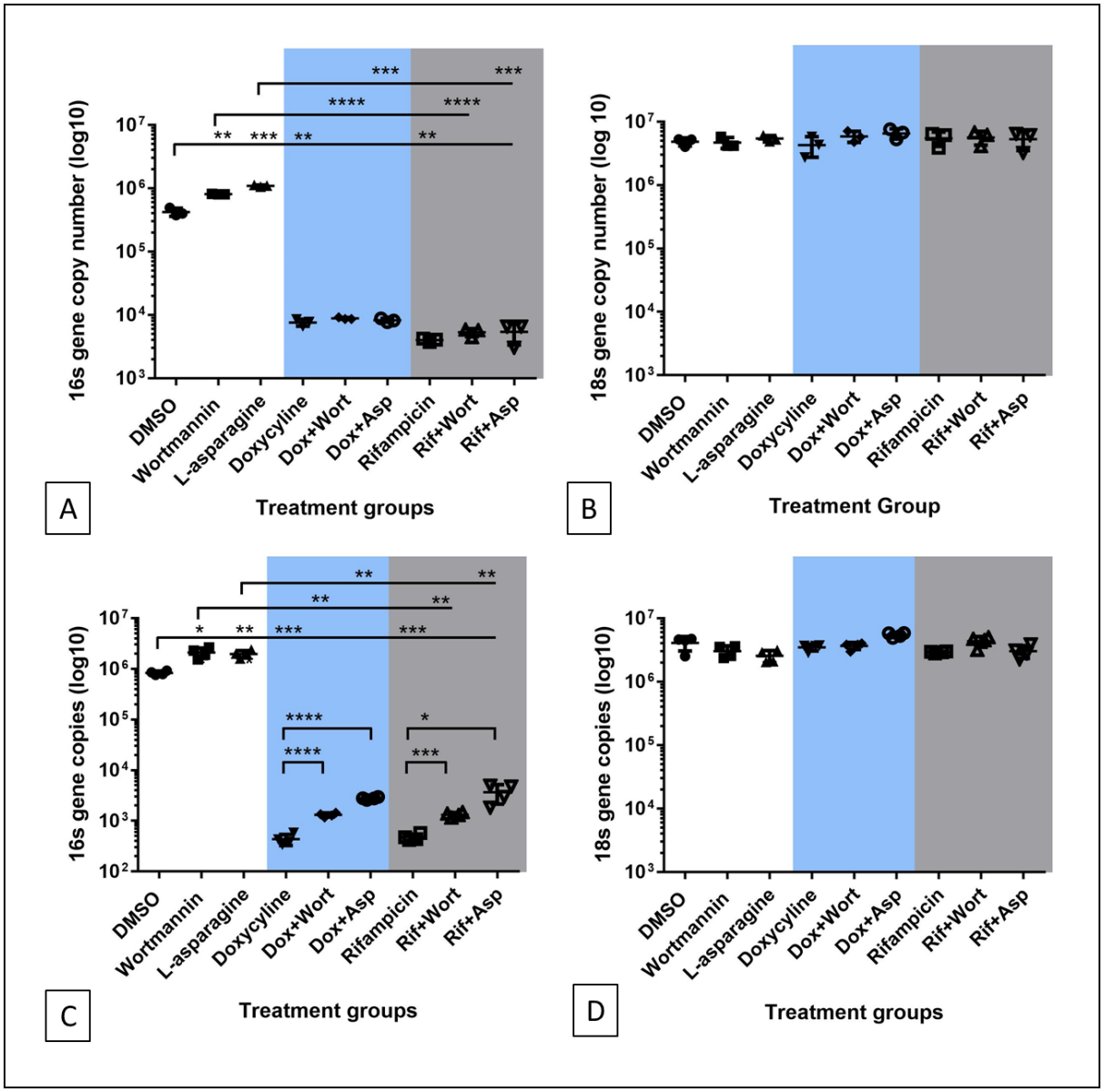


**Figure A 10 qPCR analysis of *16s* and *18s* rRNA genes of autophagy inhibition during drug exposure in C6/36*Wp* cells.** Infected C6/36 cells with *w*AlbB were treated with doxycycline (Dox) or rifampicin (Rif) at 5 µM alone or combined with wortmannin (Wort) at 10 µM or l-asparagine (Asp) at 10 mM for **A** and **B)** 7 days and **C** and **D)** for 14 days. In addition, treatment groups containing only wortmannin or l-asparagine were included. DMSO was used as vehicle control. DNA extracted from cells were amplified using **A** and **C)** *Wolbachia 16s* rRNA gene and the **B** and **D)** *Aedes albopictus 18s* rRNA gene.

Statistical analysis was performed to compare all treatment groups to DMSO and other selected subgroups. Statistical significance tested using Student's t-test, statistical significance was at $p \leq 0.05$. For p-value *= 0.01 to 0.05, ** = 0.01 to 0.001, *** = 0.001 to 0.0001, and **** ≤ 0.0001.

# Appendix B: list of materials

| Product type | Product name | Supplier |
|---|---|---|
| **Solution/Liquid** | Amphotericin B | Gibco, Thermo Fisher Scientific |
| | DAPI mounting medium | Vectashield, Vector laboratories |
| | Dimethyl sulfoxide (DMSO) Hybri-Max™, sterile-filtered (ampules) | Sigma Aldrich |
| | Eagle's Minimum Essential Medium (EMEM) | |
| | Endothelial cell basal medium-2 (EBM-2) | Lonza-Clonetics |
| | Ethanol | Sigma Aldrich |
| | Foetal bovine serum FBS | Thermo Fisher Scientific |
| | Formaldehyde solution 16% | Pierce, Thermo Fisher Scientific |
| | Leibovitz's 15 (L-15) medium | Gibco, Thermo Fisher Scientific |
| | MEM non-essential amino acids | Sigma Aldrich |
| | Methanol | |
| | Nuclease free water | Thermo Fisher Scientific |
| | NuPAGE MES SDS Running Buffer (20x) | |
| | NuPAGE antioxidant | |
| | NuPAGE sample reducing agent | |
| | NuPAGE LDS sample buffer (4x) | |
| | PageRuler™ Prestained Protein Ladder, 10 to 180 kDa | |
| | Penicillin-Streptomycin (10,000 U/ml) | |
| | Phosphate-buffered saline PBS | Sigma Aldrich |
| | Protease inhibitor mix | GE Healthcare |
| | Rapamycin ready-made solution 2.47mM | Sigma Aldrich |
| | Restore™ Plus Western Blot Stripping Buffer | Thermo Fisher Scientific |
| | RIPA lysis buffer | |
| | RPMI 1640 culture media | Gibco, Thermo Fisher Scientific |
| | SF-900 II Serum free medium | |
| | Ssofast EvaGreen Supermix | Biorad |
| | Syto 11 stain | Life Technologies, Thermo Fisher Scientific |
| | Tissue Extraction Reagent | Invitrogen, Thermo Fisher Scientific |
| | TRITC goat anti-rabbit (whole molecule) | Sigma Aldrich |
| | Trypan blue solution 0.4% | Thermo Fisher Scientific |
| | Trypsin/EDTA solution 0.25% | Sigma Aldrich |
| | Tryptone phosphate broth | |
| | Triton x100 | |
| | Tween 20 | |

| | | |
|---|---|---|
| | Wortmannin ready-made solution 10mM | |
| **Antibodies** | Beta actin antibody (mouse) | Cell signaling |
| | FITC Ds grade, goat anti-rabbit | Invitrogen, Thermo Fisher Scientific |
| | Goat anti-rabbit HRP conjugated secondary antibody | New England Bio Labs, Cell Signaling |
| | Hoechst 34442 | Life Technologies, Thermo Fisher Scientific |
| | LC3B antibody, rabbit | Invitrogen, Thermo Fisher Scientific |
| | LC3B antibody, rabbit | Cell signaling |
| | LC3B antibody, rabbit | Novus |
| | Monkey anti-rabbit HRP IgG secondary antibody | GE Healthcare |
| | P62/Sequestosome 1, rabbit | Cell signaling |
| | Rabbit anti-mouse HRP linked secondary antibody | Sigma Aldrich |
| **Powder** | Amoxicillin | |
| | Bovine serum albumin BSA | |
| | Ciprofloxacin | |
| | Doxycycline hyclate | |
| | Rifampicin | |
| | Glycine | |
| | L-asparagine | |
| | Ly294002 | |
| | MTT formazan | |
| | Moxifloxacin hydrochloride | |
| | Saponin | |
| | Sparfloxacin | |
| | Streptomycin sulfate salt | |
| | Sodium Chloride NaCl | |
| | Thiazolyl Blue Tetrazolium Bromide | |
| | Trizma base | |
| | 3-Methyladenine (3-MA) | |
| **Kits** | Baseline-ZERO™ DNase | Epicentre |
| | Bicinchoninic acid protein assay BCA kit | Pierce, Thermo Fisher Scientific |
| | Chemilluminscent substrate super signal system | |
| | EGM-2 MV singleQuots | Lonza-Clonetics |
| | Live/Dead Viability/Cytotoxicity kit | Life Technologies, Thermo Fisher Scientific |
| | MiRCURY RNA Isolation kit | Exiqon |
| | QIAmp mini DNA kit | Qiagen |
| | SuperScript™ III Reverse Transcriptase | Invitrogen, Thermo Fisher scientific |
| **Miscellaneous** | Bis Tris Bolt plus 6-12% gel | Thermo Fisher Scientific |
| | CORDLESS PELLET PESTLE | Kimble |

| | | |
|---|---|---|
| | Corning™ Disposable Vacuum Filter/Storage Systems | Thermo Fisher Scientific |
| | Nitrocellulose Membrane Hybond ECL (pore size 0.22µM) | Amersham, GE Healthcare |
| | Nunc cell scrapers | Thermo Fisher Scientific |
| | RNase free disposable pellet pestles | |
| | Sephadex G-25 in PD-10 Desalting Columns | GE Healthcare |
| | Sterilin™ 7mL Polystyrene Bijou Containers with cover slips | Thermo Fisher Scientific |
| | X-ray films CL xsposure | |
| | 384 well PCR plate | Biorad |
| | 96 Well 0.8mL Polypropylene Deepwell Storage Plate | Abgene, Thermo Fisher Scientific |

Table B. 1 Materials and products used throughout the thesis.

| Buffer/solution | Components |
|---|---|
| NuPAGE MES SDS Running Buffer (1x) | 50 ml of MES running buffer<br>950 ml distilled water |
| Tris Buffered Saline TBS washing buffer (10x) | 2 M Tris base (pH 8.5) – 12.1 g in 50 ml<br>5 M Sodium Chloride NaCl (pH 7.6 with HCl) – 87.8 g in 300 ml<br>640 ml distilled water<br>10 ml Tween 20 |
| Tris Glycin transfer buffer (10x) | Tris Base 30.3 g (pH 8.3)<br>Glycine 144 g<br>distilled water to adjust volume to 1 L<br>Diluted to 1x by adding 700 distilled water, 100 ml of the 10x prepared buffer and 200 ml methanol (20%) |
| Ponceau S staining | 0.2% (w/v) Ponceau S<br>5% glacial acetic acid |

Table B. 2 Buffers/solutions and components

| Primers | Sequences |
|---|---|
| *16s* forward | 5'-TTGCTATTAGATGAGCCTATATTAG-3' |
| *16s* reversed | 5'-GTGTGGCTGATCATCCTCT-3' |
| *18s* forward | 5'-CCGTGATGCCCTTAGATGTT-3' |
| *16s* reversed | 5'-ATGCGCATTTAAGCGATTTC-3' |
| *BMWSP forward* | 5' CCC TGC AAA GGC ACA AGT TAT TG 3' |
| *BMWSP Reversed* | 5' CGA GCT CCA GCA AAG AGT TTA ATT 3' |
| *GST 1368* | 5' GAG ACA TCT TGC TCG CAA AC 3' |
| *GST 1632* | 5' ATC ACG GAC GCC TTC ACA G 3' |

Table B. 3 Complete List of primer pairs used. The table represents a complete list of all primers and their sequences used in qPCR reactions of this thesis. All were designed and purchased by Integrated DNA Technologies (UK).